Springer Transactions in Civil
and Environmental Engineering

Ashish Pandey
Sanjay Kumar
Arun Kumar *Editors*

Hydrological Aspects of Climate Change

Springer

Springer Transactions in Civil and Environmental Engineering

Editor-in-Chief

T. G. Sitharam, Indian Institute of Technology Guwahati, Guwahati, Assam, India

Springer Transactions in Civil and Environmental Engineering (STICEE) publishes the latest developments in Civil and Environmental Engineering. The intent is to cover all the main branches of Civil and Environmental Engineering, both theoretical and applied, including, but not limited to: Structural Mechanics, Steel Structures, Concrete Structures, Reinforced Cement Concrete, Civil Engineering Materials, Soil Mechanics, Ground Improvement, Geotechnical Engineering, Foundation Engineering, Earthquake Engineering, Structural Health and Monitoring, Water Resources Engineering, Engineering Hydrology, Solid Waste Engineering, Environmental Engineering, Wastewater Management, Transportation Engineering, Sustainable Civil Infrastructure, Fluid Mechanics, Pavement Engineering, Soil Dynamics, Rock Mechanics, Timber Engineering, Hazardous Waste Disposal Instrumentation and Monitoring, Construction Management, Civil Engineering Construction, Surveying and GIS Strength of Materials (Mechanics of Materials), Environmental Geotechnics, Concrete Engineering, Timber Structures.

Within the scopes of the series are monographs, professional books, graduate and undergraduate textbooks, edited volumes and handbooks devoted to the above subject areas.

More information about this series at http://www.springer.com/series/13593

Ashish Pandey · Sanjay Kumar · Arun Kumar
Editors

Hydrological Aspects of Climate Change

Springer

Editors
Ashish Pandey
Department of Water Resources Development and Management
Indian Institute of Technology Roorkee
Roorkee, India

Arun Kumar
Department of Hydro and Renewable Energy
Indian Institute of Technology Roorkee
Roorkee, India

Sanjay Kumar
Surface Water Hydrology Division
National Institute of Hydrology
Roorkee, India

ISSN 2363-7633 ISSN 2363-7641 (electronic)
Springer Transactions in Civil and Environmental Engineering
ISBN 978-981-16-0393-8 ISBN 978-981-16-0394-5 (eBook)
https://doi.org/10.1007/978-981-16-0394-5

© The Editor(s) (if applicable) and The Author(s), under exclusive license to Springer Nature Singapore Pte Ltd. 2021
This work is subject to copyright. All rights are solely and exclusively licensed by the Publisher, whether the whole or part of the material is concerned, specifically the rights of translation, reprinting, reuse of illustrations, recitation, broadcasting, reproduction on microfilms or in any other physical way, and transmission or information storage and retrieval, electronic adaptation, computer software, or by similar or dissimilar methodology now known or hereafter developed.
The use of general descriptive names, registered names, trademarks, service marks, etc. in this publication does not imply, even in the absence of a specific statement, that such names are exempt from the relevant protective laws and regulations and therefore free for general use.
The publisher, the authors and the editors are safe to assume that the advice and information in this book are believed to be true and accurate at the date of publication. Neither the publisher nor the authors or the editors give a warranty, expressed or implied, with respect to the material contained herein or for any errors or omissions that may have been made. The publisher remains neutral with regard to jurisdictional claims in published maps and institutional affiliations.

This Springer imprint is published by the registered company Springer Nature Singapore Pte Ltd.
The registered company address is: 152 Beach Road, #21-01/04 Gateway East, Singapore 189721, Singapore

Foreword

Climate change is one of the most critical global challenges likely to cause considerable changes in the spatial and temporal distribution of water resources in the coming decades. Unfortunately, these changes are likely to be unfavorable in many countries which already suffer from pressures on water resources and water scarcity. This may prove to be the case in India which is still largely dependent upon rain-fed agriculture. In the context of anticipated global warming due to increasing atmospheric greenhouse gases, it is necessary to evaluate the possible impact on freshwater resources of the country as climate change can have important implications for freshwater supply for drinking water, rain-fed agriculture, groundwater supply, forestry, biodiversity, and sea level. Climate change affects the hydrologic cycle by directly increasing the evaporation of available surface water and vegetation transpiration and snow and glacier melts. Consequently, these changes can influence precipitation amounts, timings, and intensity rates and indirectly impact the flux and storage of water in surface and subsurface reservoirs (i.e., lakes, soil moisture, and groundwater). In addition, there may be other associated impacts, such as sea water intrusion, water quality deterioration, and potable water shortage. The impact of future climatic change is expected to be more severe in developing countries such as India whose majority of the rural population is dependent on agriculture. Water sector in India is under stress due to many reasons including population increase and rising demands for energy, fresh water, and food.

In order to minimize the adverse impacts of climate change on country's water resources and attaining its sustainable development and management, there is a need for developing the rational adaptation strategies and enhancing the capacity to adapt those strategies after carrying out the risk, reliability, and uncertainty analysis. Accordingly, the present practices being followed in the water resources sector are required to be reviewed and revised considering climate change, which would provide the means for alleviating the negative impacts of climate change.

The Roorkee Water Conclave 2020, broadly focusing on "Hydrological Aspects of Climate Change," provided an opportunity to policy-makers, academicians, researchers, students, and practitioners to share their experiences and knowledge by presenting the fundamental/applied scientific advancements made in the field of

water resources development and management under changing climate for sustainable development. This volume includes full-length papers of 19 keynote papers from India and abroad.

I hope that this book will become useful to researchers and practitioners.

Roorkee, India

Ajit K. Chaturvedi
Director, IIT Roorkee

Preface

This book comprises 16 chapters focusing on the hydrological aspects of climate change. It includes climate change and water–food security and policy issues within water–energy–food nexus and climate risks to water security in Canada's western interior. Moreover, forcing global hydrological changes in the twentieth and twenty-first centuries, Indian summer monsoon system, observed climate change over India and its impact on hydrological sectors, the importance of data in mitigating climate change and real-time monitoring of small reservoir hydrology using ICT and application of deep learning for prediction of water level have been demonstrated.

The book has covered the hydrology problems, challenges and opportunities to provide timeline of significant hydrology developments over the past century and a half; flood modelling, mapping and monitoring of sparsely gauged catchments using remote sensing product study have been presented. A chapter on "Ground and Satellite Observations to Predict Flooding Phenomena" focuses on some crucial questions that may be considered a challenge for the scientific community, Indices for Meteorological and Hydrological Drought.

It broadens an Indian perspective to highlight the various initiatives/steps taken by the Government of India to efficiently manage water to reduce the country's agricultural water footprint, an overview highlighting the importance of water resources management in the Indian context. Adaptation to Climate Change in Agriculture, Improved Agricultural Water Management and Protected Cultivation Technologies and Use of Oxygen-18 and Deuterium to Delineate Groundwater Recharge have also been included.

This book is useful for academicians, water practitioners, scientists, water managers, environmentalists, administrators, NGOs, researchers and students involved in hydrological studies focusing on climate change, etc.

Roorkee, India

Ashish Pandey
Sanjay Kumar
Arun Kumar

Contents

About the Editors

Dr. Ashish Pandey is currently a Professor at the Department of Water Resources Development & Management, IIT Roorkee. He received Ph.D. from IIT Kharagpur. He pursued his B.Tech. in Agricultural Engineering and M.Tech. in Soil and Water Engineering from JNKVV, Jabalpur. He is a Fellow member of Institution of Engineers, the Indian Association of Hydrologists, and Indian Water Resources Society. He published 165 research papers in peer-reviewed and high impact international/national journals/seminars/conferences/ symposia. Prof. Pandey has over 20 years of experience in the field of Irrigation Water Management, Soil and Water Conservation Engineering, Hydrological Modeling of Watershed, Remote sensing and GIS Applications in Water Resources.

Dr. Sanjay Kumar is currently working as Scientist 'E' at National Institute of Hydrology, Roorkee. He received his Ph.D. in Civil Engineering from Delhi Technological University (DTU), India. He pursued his B.E. in Civil Engineering from MNNIT, Allahabad and obtained his M.E. in Hydraulics and Flood Control from DTU, Delhi. He has had more than 21 years of research experience in the field of hydrology. His research interests include surface water hydrology, flood modeling, design flood estimation, flood frequency analysis using L moments, climate change studies, time series modeling and reliability & uncertainty analysis of hydrologic systems.

Prof. Arun Kumar is currently working as Professor of HRED, IIT Roorkee. He pursued his Bachelor's in Civil Engineering from IIT Roorkee, Master's in Civil Engineering from IISc Bengaluru and Ph.D. from IIT Roorkee. He did Hydropower Diploma studies at NTH, Trondheim. His research areas are hydropower development, environmental management of water bodies, energy economics and policy. He was the coordinating lead author for IPCC special report on renewable energy for hydropower. Prof. Kumar has over 39 years of experience in the field of hydropower and environmental management of rivers and lakes.

Chapter 1
Climate Change, and Water and Food Security: Policies Within Water–Food–Energy Nexus

R. S. Kanwar, S. S. Kukal, and P. Kanwar

1.1 Introduction

Climate change is one of the most important challenges facing humanity on the planet, especially water and food security which is affecting almost all continents of the world. Industrialization and population growth in twenty-first century are considered to be the primary reasons for increased annual air temperatures, and highly variable and intense rainstorms around the globe. As a result, enhanced greenhouse effect has exposed us to the adverse effects of global warming (Haris et al. 2013; Hundal and Kaur 2007). The mean surface temperature on the planet has increased by 0.85 °C since 1880 and is likely to increase by another 3.7–4.8 °C by 2100 (IPCC 2014). Climatic change is causing global warming which is affecting every aspect of life. Tropical and sub-tropical regions of the world are facing high temperatures at abnormal scales resulting in huge impacts on agricultural productivity. Some studies have reported that 10–40% loss in Indian food grain production could occur due to increase in temperature by 2080–2100 (Parry et al. 2004; IPCC 2007).

In order to achieve UN's Sustainable Development Goals for 2030 to make the world free of hunger and malnutrition, we must take actions now to develop, strengthen and sustain resilience in water and food production and distribution systems to meet the future demand that will increase demands on water for irrigation,

R. S. Kanwar (✉)
Department of Agricultural and Biosystems Engineering, Iowa State University, Ames, IA, USA
e-mail: rskanwar@iastate.edu

S. S. Kukal
Punjab Water Regulation & Development Authority, Government of Punjab, Chandigarh, India

Punjab Agricultural University, Ludhiana, Punjab, India

P. Kanwar
Division of Ecological and Water Resources, Minnesota Department of Natural Resources, St. Paul, Minnesota, MN, USA

© The Author(s), under exclusive license to Springer Nature Singapore Pte Ltd. 2021

A. Pandey et al. (eds.), *Hydrological Aspects of Climate Change*,
Springer Transactions in Civil and Environmental Engineering,
https://doi.org/10.1007/978-981-16-0394-5_1

particularly in water scarcity areas of the world. An increase in water scarcity under changing climate presents its own challenges, including cross-border water conflicts as well as competing demands for water for agriculture, industry and domestic use.

Groundwater is the primary source of irrigation and drinking water for about 2 billion people in the world, and the impact of climate change on the quantity and quality of groundwater resources is huge. Groundwater has been withdrawn at unsustainable rates in almost every country in the world to meet the drinking water needs of growing population and irrigation demands to grow more food in arid and semi-arid climates of the world.

At the same time, little research has been done to determine the impact of climate change on groundwater recharge rates and quality. Changing weather patterns and more frequent intense rain storms, observed within last 10–15 years, are causing flooding, soil erosion and water pollution. Unless we develop science-driven management systems and incentive-based policies, water quality could become one of the major challenges for the society. Everts and Kanwar (1993) installed 50 piezometers (vertical and angled) at depths of 3–120 m in glacial till shallow and artesian aquifers of Central Iowa and measured groundwater recharge rates. Ella et al. (2002) used the field data on hydraulic conductivities for different soil and aquitard layers to develop hydrologic models to determine groundwater recharge rates to artesian, glacial till aquifers in Iowa. Rekha et al. (2011) and Olson et al (1997) reported that macropore flow was primarily responsible for carrying nitrate from manure and agricultural fertilizers to shallow and deeper groundwater systems in Iowa. Several other studies have been conducted to investigate the long-term effects of climate and agricultural production practices on the leaching of nitrate, phosphorus, bacteria, and pesticides to shallow and deeper groundwater systems (Hruby et al. 2016, 2018; Hoover et al. 2015; Huy et al. 2013; Pappas et al. 2008; Kalita et al. 1997; Kanwar et al. 2005, 1997; and Karlen et al. 1998). These studies have shown clearly that land-applied chemicals and animal waste can pollute groundwater systems of the Midwest in the USA but farmers and producers have become willing partners to adopt innovative best chemical and crop production practices to minimize impacts on water quality, improve soil health and helping mitigate climate change impacts on agriculture.

In certain parts of the world, the availability of good quality groundwater for drinking and irrigation is going to be the greatest threat to humanity in twenty-first century. Therefore, we must invent new governance using innovative incentive-based policies and technological innovations to mitigate the threat of climate change on water and food security for the growing population. For example, 85% of groundwater is used for irrigation in India and farmers have been pumping groundwater at unsustainable rates since the green revolution started in 1960s, resulting in lowering of groundwater tables in many aquifers from about 6 m in 1970 to more than 100 m in 2019 in less than 50 years. In USA, compared to an average year, only 55% of Colorado River water is flowing to Lake Powell due to below-average rainfall and runoff. Reservoirs in the Colorado River Basin are 12% more likely to fall to below the critical low levels by 2025.

The impact of climate change on the faster depletion of groundwater for irrigation and its impact on declining agricultural production in certain parts of the world

has escalated food inflation. Also, acute food shortages in many African and Asian countries, where people cannot afford expensive food, are dying of starvation (Misra 2014). There are water crises all over the world including western USA, India, Africa and Middle East due to depletion of surface and groundwater resources.

The earlier described studies/panel reports are clear evidence that climate change is making huge impact on accelerated loss of biodiversity with major long-term consequences on the global economy. In order to ensure an environmentally and economically sound sustainable future for the growing population of the world, we as a global society must recognize that the climate change is real; and environmental quality and economic development are not mutually exclusive. Therefore, the key question for the global society is "what can be done to reduce the emission of greenhouse gases (carbon dioxide, nitrous oxide and methane)? Greenhouse gases trap heat in the atmosphere and make the planet warmer. To be very honest, the major cause of increased greenhouse gas emissions to atmosphere is the human activities for the past 150 years (IPCC 2007). The largest source of greenhouse gas emissions in the USA is from burning fossil fuels for electricity, residential and commercial buildings, industry and transportation (Fig. 1.1).

Fossil Fuels and Climate Change: Developed countries are the largest consumers of fossil fuels and producing larger share of greenhouse gas emissions. The USA, for example, is just 5% of world population, but contributes 25% of total CO_2 output in the world. Currently, a child born in the USA is likely to produce seven times the carbon emissions of a child born in China and 168 times the child born in Bangladesh. The USA has the largest population in the developed world, and its population may double before the end of the century. Currently, US's 350 M people produce more than double the greenhouse gases than that of Europe, five times the global average

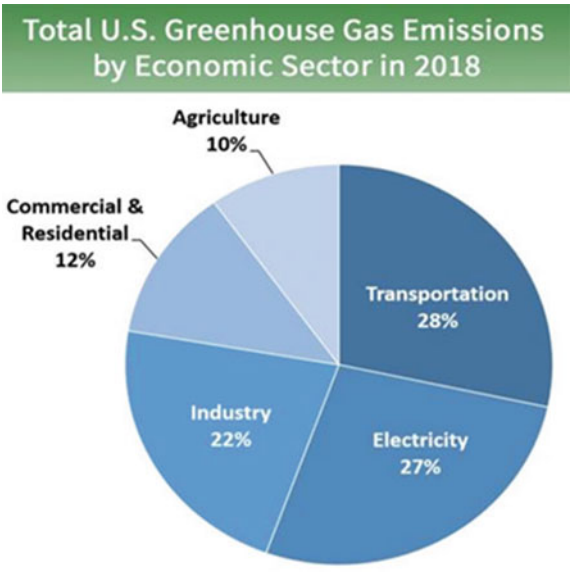

Fig. 1.1 Sources of greenhouse gas emissions in the USA as affected by population growth

and more than 10 times the average of developing nations. The increased greenhouse gas emissions are the result of massive consumption of natural resources and fossil fuels to maintain higher standard of living and lack of political will to end fossil fuel economy. Transportation sector accounts for 28% of all US carbon emissions (Fig. 1.1). About 12% of US carbon emissions come from the residential sector. Due to a dramatic decrease in household size, from 3.1 persons per home in 1970 to 2.6 in 2000, homebuilding is outpacing the population growth. More Americans are driving farther to reach bigger homes with higher heating and cooling bills. These trends are carbon footprint inherent of a burgeoning US population.

Population Growth and Climate Change: Whether we agree or not, there is a direct relationship between population growth and climate change which is one of the focus areas of this chapter. Climate change is affecting the entire world, and different regions are experiencing varying degrees of effects due to faster population growth. Some researchers in the world are making it very clear that one of the best options for the world is to consider controlling population to reduce the burden on earth. The largest single threat to the ecology and biodiversity of the planet is the climate change due to the build-up of human-generated greenhouse gases in the atmosphere.

In just 50 years (1970–2020), the world's population has more than doubled to over 7.5 billion people. That means more than 7.5B bodies that need to be fed, clothed and kept warm, all requiring a large amount of energy, which is largely coming from fossil fuels. Along with this consumption, these 7.5B people are also producing large quantities of waste requiring more energy to treat the waste to keep soil, water and air clean. The demand for energy and the production of waste are among significant producers of greenhouse gas emissions that contribute to climate change.

At the 2015 UN Climate Change Conference in Paris, 196 counties have agreed to limit global warming to 1.5 °C. Several countries around the world are beginning to address the problem by reducing their carbon footprint through less consumption of natural resources and use of better technologies. But unsustainable population growth can overwhelm these efforts, leading us to conclude that we not only need smaller footprints, but fewer feet on the planet. A successful example is from the city of Portland, Oregon, in the USA where city decreased its combined per-capita residential energy and car driving carbon footprint by 5% between 2000 and 2005. During this period, however, its population grew by 8%. Second successful example is from the city of Stockholm in Sweden which has become the first fossil-fuel free city in the world. Stockholm uses nearly 100% energy from clean energy sources such as biofuels produced from city's food waste and municipality wastewater. Sweden has also decided to become the world's first fossil-fuel free nation as part of their commitment under Roadmap 2050. To do this, Sweden must reduce greenhouse gas emissions by 40% by the year 2020 compared with 1990 levels, and completely rid of vehicles using fossil fuels by 2030.

Global human population is growing by 83 million or 1.1% annually, although growth rates among countries vary from 0.1% to more than 3%. The global population has grown from one billion in 1800 to 7.8 billion in 2020. It is expected to keep growing, and estimates have put the total population at 8.6 billion by mid-2030,

Table 1.1 Global population growth rate from 1800 to 2050

Year	Population (10^9)
A&E → Malthus	0.9
1800	1
1900	1.6
2000	6
2010	6.9
2020	7.5
2030	8.2
2050	9.2
2100	11.2

9.8 billion by mid-2050 and 11.2 billion by 2100 (Table 1.1). Many nations with rapid population growth have low standards of living, whereas many nations with low population growth rates have higher standards of living. Table 1.1 gives data on population growth in the world in recent history (1800–2020) and projected growth in 2030, 2050 and 2100. Table 1.1 shows that population grew from 1 billion to 1.6 billion (1.6 times) in 100 years from 1800 to 1900, whereas population grew from 1.6 billion to 6 billion (3.75 times) in next 100 years. Other way to look at the population data in Table 1.1 is that in 100 years between 1800 and 1900, world population grew by only 600 million, whereas in next 100 years (1900–2000), the world population grew by 4400 million and the world added another billion people on earth in just 10 years (from 2000 to 2010) on the planet. Therefore, the question for the global community would be to see if we can sustain this level of population growth without deteriorating biodiversity and the environment around us where we live and our children will thrive for years to come. Haris et al. (2013) have clearly shown that increased population growth on the planet is resulting in deforestation, industrialization, urbanization and consumption of natural resources at alarming rates.

Climate change researchers have warned that we must reduce atmospheric CO_2 to 350 ppm in order to avoid global catastrophe (Solomon et al. 2007). A 2009 study of the relationship between population growth and global warming determined that the "carbon legacy" of just one child can produce 20 times more greenhouse gas than a person will save by driving a high-mileage car, recycling, using energy-efficient appliances and light bulbs, etc. Each child born in the USA will add about 9441 metric tons of carbon dioxide to the carbon legacy of an average parent. The study concludes that the potential for savings from reduced population growth are huge compared to the savings that can be achieved by changes in lifestyle.

The year 2020 is likely to be one of the five hottest years in the USA. Climate disasters are devastating the USA with record forest fires on the Pacific coast and Brazil with forest fires engulfing the Amazon; repeated floods and storms hitting the Atlantic and Gulf states in the USA; unknown earlier derecho-type rain storms with 80 plus miles an hour wind speeds in Iowa; frequent tornadoes in Midwest; the

precipitous decline in Arctic sea ice; and the accelerating threats to Greenland's and Antarctica's ice sheets that could trigger a catastrophic rise in the sea level. Therefore, countries like USA and Canada and rest of the western world need to do its part to achieve global climate safety. The entire world needs a massive shift in industry from fossil fuels to renewable energy; from internal combustion engines to electric vehicles powered by the renewable energy; and from heating oil and natural gas to electric heat pumps in homes and commercial buildings. Oil-producing countries and the vested interests of the fossil-fuel industry will fight these changes but global society needs to develop legal framework and incentive-based policies to move away from fossil-fuel economy to bio- and clean energy economy for climate safety and enhancing biodiversity on the planet.

Other environmental consequences of global warming are the rise in seas water levels. There is plenty of evidence that the sea water levels are rising with temperature rise, threatening low-lying areas, coastal populations and ecosystems around the world. With rising sea levels, water is encroaching on agricultural lands resulting in soil salinity and other environmental hazards by making freshwater polluted that people may rely on for their drinking purposes. Many plants and animals live in areas with specific climate conditions, enabling them to survive and flourish. Extreme weather events, increase in temperature and rising seas are beginning to affect plants and animals, altering their habitat and bringing life-threatening stresses and diseases. Temperature increase of 2–3 °C would increase the number of people living in malarial climates by 3–5%, putting hundreds of millions of people at risk. Tremendous progress has been made in eradicating the mosquito and reducing malarial cases and deaths. Nonetheless, low rates of agricultural productivity growth and high rates of malaria infection often coincide, particularly in sub-Saharan Africa. For poor countries with limited resources, treating malaria can seem out of reach economically, especially in rural areas. Changes in land-use patterns, specifically the control of water pollution and deforestation can reduce malarial transmission. Reduction of greenhouse gas emissions to a level that brings atmospheric CO_2 back from 386 parts per million to 350 or less, lesser consumption of natural resources and long-term population reduction to ecologically sustainable levels will help solve the global warming crisis and move us towards a healthier and sustainable society.

Agriculture and Climate Change: Farmers are impacted by extreme weather conditions, which include drought, severe heat, flooding and shifting climatic trends. To meet the food security needs of the global society, we must increase food production by about 50% by 2030 and reduce greenhouse gas emissions by 30%. Nitrous oxide from agriculture is one of the primary source of greenhouse gas emissions (IPCC 2007). Agriculture has contributed about 70% of gas emissions from 2007 to 2016 from fertilizers in China, India and the USA (IPCC 2007). Agriculture uses about 100 million tons of nitrogen fertilizers in croplands around the world and about 100 million tons of nitrogen from animal manure cycles through pasturelands. The highest growth rates in gas emissions are found in emerging economies, particularly Brazil, China and India, where acres under crops and livestock numbers have increased significantly. Though agriculture is a contributor to climate change, the industry is playing a positive role in curbing greenhouse gas emissions like carbon

dioxide, methane and nitrogen oxide. Farmers too are adopting carbon sequestration farming practices and cutting-edge tools to reduce greenhouse gases to atmosphere. The development of climate-smart solutions like digital farming, improved plant breeding technologies, innovative irrigation methods like drip irrigation, reduced tillage and good nutrient management practices for crop production will reduce agriculture's impact on climate change. Digital tools and new agriculture techniques have enabled farmers to make on-site decisions to grow more food on less acreage, offering to feed a growing population. In addition, effective crop protection solutions are helping farmers to manage their crops in response to threats of weeds, insects or disease.

Another area where the global agricultural community needs to pay attention is area of food waste. An estimated 1/3 of all food produced is wasted or damaged in storage or lack of storage. Food wastage, a food security issue, apart from releasing about 6% of global greenhouse gas emissions from agriculture is also a serious issue to address for the agricultural community.

1.2 US Midwest Case Studies on Climate Change Effects on Water and Food Security

Iowa, USA Case Study: Iowa's climate is typically cold in winter and hot and humid in summer. More recently, Iowa has been experiencing extreme weather patterns, more frequent rains and warmer winters. Although several studies have been conducted in Iowa to observe the long-term effects of climate change on crop production and water quality, we have decided to include the following study in this chapter to make a point on how weather patterns are affecting Iowa agriculture. Impacts of agriculture on water quality is the major issue facing Iowa's water security, and most of the research efforts are designed to develop innovative technologies, cropping systems and policies to minimize the impact of agriculture on water quality. Two field hydrology laboratories were established in 1980s to collect long-term data on Iowa's tillage and crop rotation systems to investigate the impact of different farming systems on production, soil health and water quality. This allowed us to collect weather data on rainfall patterns and its impact on groundwater recharge rates and chemical leaching into groundwater (Ella et al. 2002; Everts and Kanwar 1993; Rekha et al. 2011; and Olson et al. 1997; Hruby et al. 2016, 2018; Huy et al. 2013; Pappas et al. 2008; Kalita et al. 1997; Kanwar et al. 2005, 1997).

Experiments and Data Analysis: Experiments were collected at the Glacial-Till Field Hydrology Laboratory near Ames, Iowa. Eleven field plots were used in this experiment with corn and soybeans on half of each plot (Huy et al. 2013). Data on weather, crop production, and shallow groundwater quality was collected for 12 years (1998–2009) using state-of-the-art instrumentation to monitor subsurface drain flows and collect water samples for water quality analyses. The experimental treatments

were arranged in a completely randomized design with three replications of each treatment.

Daily rainfall data was collected at the Iowa State University Agricultural Engineering Farm weather station, and the monthly precipitation values are presented in Table 1.2. The long-term average precipitation for Ames, Iowa (1961–1990), was 740 mm during the major rainy season and most of growing season (between March and October). During the 12-year study period (1998–2009), the average precipitation at the experimental site was 798 mm, which was about 8% above the long-term average. For four years (1999, 2007, 2008 and 2009), the average precipitation measurements of 949, 915, 1145 and 829 mm, respectively, were higher than the normal precipitation. Seven of the 12 years had precipitation within 10% of the normal precipitation. Comparison of monthly average precipitation data revealed that in the months of April, May and August, the monthly precipitation amounts were higher than the long-term average. The higher than normal amounts of rainfall measured in April and May likely resulted in higher tile flow volumes and nitrate losses with tile drain water, which may require innovative crop and nutrient management practices to protect the quality of surface and groundwater resources. In addition, data in Table 1.2 also indicates that almost every three years, Iowa is facing either flooding conditions due to more than normal rainfalls or drought conditions due to less than normal rainfall. This weather phenomenon in Iowa is more recent, and Iowa is seeing more extreme events of flooding causing several economic losses in agriculture and other property.

Table 1.2 Precipitation (mm) at Ames, Iowa during the study period, 1998–2009 (Huy et al. 2013)

	Month								Growing season	Drainage season
Year	March	April	May	June	July	August	Sept	Oct	(May–Sept)	(March–Oct)
1998	71	81	92	274	68	94	24	102	552	806
1999	25	207	150	185	162	151	61	9	709	949
2000	11	21	120	104	72	34	26	50	356	437
2001	28	96	190	50	48	74	149	65	511	700
2002	10	95	130	81	150	209	38	79	606	790
2003	29	112	122	150	168	25	100	24	565	730
2004	96	61	208	91	50	132	34	45	515	717
2005	35	82	111	124	104	172	111	9	622	748
2006	74	109	55	21	141	156	191	63	564	811
2007	81	153	169	52	75	200	48	137	545	915
2008	71	130	216	271	234	53	78	92	852	1145
2009	103	116	102	104	70	123	24	186	424	829
Average	**53**	**105**	**139**	**125**	**112**	**119**	**74**	**72**	**568**	**798**
Normal	54	89	108	129	106	102	87	65	532	740

Table 1.3 gives data subsurface drainage volumes from shallow groundwater from the field plots. As expected, the variation in precipitation patterns considerably affected the variation in subsurface drain flows at both yearly and monthly levels (Table 1.3). Figure 1.2 presents the effects of precipitation on subsurface drain

Table 1.3 Average monthly and yearly subsurface drainage flow volumes (mm) (Huy et al. 2013)

Year	Mar	Apr	May	Jun	Jul	Aug	Sep	Oct	Total
1998	2	33	31	96	41	0	0	0	203
1999	0	44	46	55	6	3	0	0	154
2000	0	0	1	4	0	0	0	0	5
2001	0	3	41	22	2	0	0	0	69
2002	0	0	46	19	10	6	0	0	81
2003	0	0	84	10	46	0	0	0	141
2004	15	47	39	52	1	0	0	0	153
2005	0	24	42	10	7	9	0	0	93
2006	0	23	52	3	1	0	72	75	226
2007	0	0	14	59	10	0	0	0	83
2008	0	63	77	167	50	48	0	0	405
2009	0	51	83	27	3	0	0	10	174
Average	1	24	46	44	15	6	6	7	149

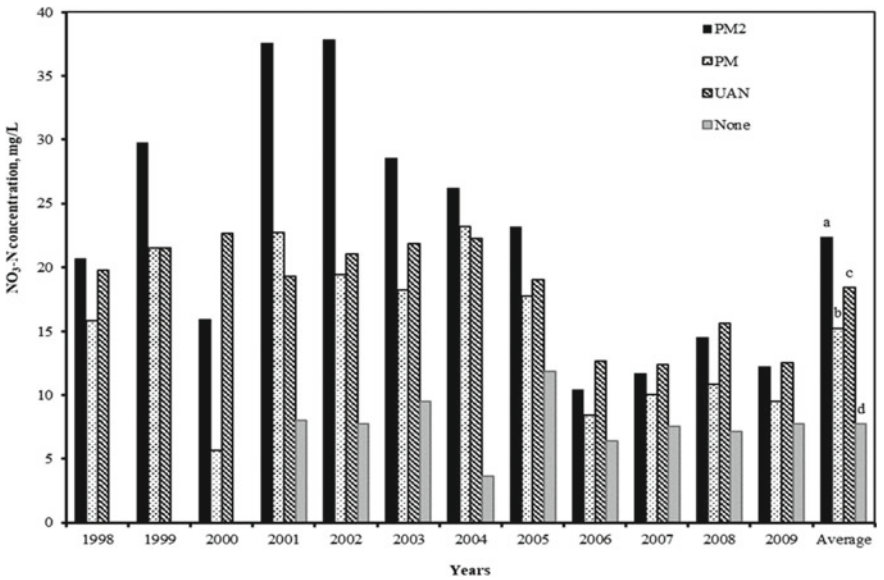

Fig. 1.2 Subsurface drainage (mm) as response to annual precipitation by different N treatments and years (Huy et al. 2013)

flow over the 12-year study period. Subsurface drain flows were lowest in 2000, the driest rainfall year and highest in 2008, the wettest year. The control treatment yielded the highest annual average tile flow (13.3 cm year^{-1}), which is likely due to reduced evapotranspiration caused by reduced crop development and yields from reduced nutrient application.

High monthly subsurface drain flow variability was observed for all treatments. Similar spatial variability in subsurface drain flow was observed in previous studies, with this variability attributed to changes in soil characteristics following long-term cultivation with different crop rotations and N sources. This study found that there was no difference in subsurface drain flow volumes between corn and soybean years during a six-year study period because each year had a different combination of rainfall timing, intensity and amounts. The timing of precipitation had a larger impact on subsurface drainage volume and NO_3–N export in subsurface drainage, especially due to the cycle of wet–dry–normal weather conditions in the Midwestern US. This study and several other studies conducted at this research site on nitrate leaching concluded that variation in NO_3–N concentration and losses may not be closely associated with daily subsurface drain flows but rather with seasonal variation in rainfall patterns due to climate change. Rainfall patterns during the growing season were the main factors contributing to NO_3–N export to subsurface drainage and eventually to Iowa's rivers and deeper groundwater systems.

Wet and dry cycles of weather conditions, and the seasonal effects of rainfall distribution during the growing season, resulted in significant effects on subsurface drain flows, groundwater recharge and the NO_3–N concentration and NO_3–N losses with subsurface drain water. Currently, approximately 9.5 million ha of Iowa farmland were planted to corn and soybean, with 5.7 million ha designated to corn only. This study results suggest that with nitrogen application at a rate of 168 kg N ha^{-1} to corn fields, significant amounts of nitrogen could be transported to Iowa's water bodies resulting in water quality impairments. Therefore, it can be concluded that the land application of N-fertilizers may be an environmentally sound option if timings of fertilizer application in response to weather patterns can be managed well using concepts of precision farming to maintain NO_3–N concentrations measured in subsurface drain water not exceeding the EPA standard of 10 mg/l for safe drinking water. Additional research on agricultural production systems and climate change needs to be continued so that farmers can be educated on how to keep their farm economically viable in meeting food security needs of growing world population.

Minnesota, USA Study: Just like Iowa, Minnesota is accustomed to cold and snowy winters, along with warm and humid summers. In addition, Minnesota's agriculture is very similar to Iowa growing corn and soybeans as primary two crops. It is relatively common for any season to be far warmer, colder, wetter or drier than normal. This variability in climate can make it difficult to notice where, when and how climatic conditions change in the state; however, over 125 years of consistent climate data makes it clear that widespread changes outside the normal variations are clearly underway in Minnesota. Minnesota has experienced wetter and warmer weather in the past several decades. All but two years since 1970 have been some combination of wetter and/or warmer than historic averages, and compared to twentieth-century

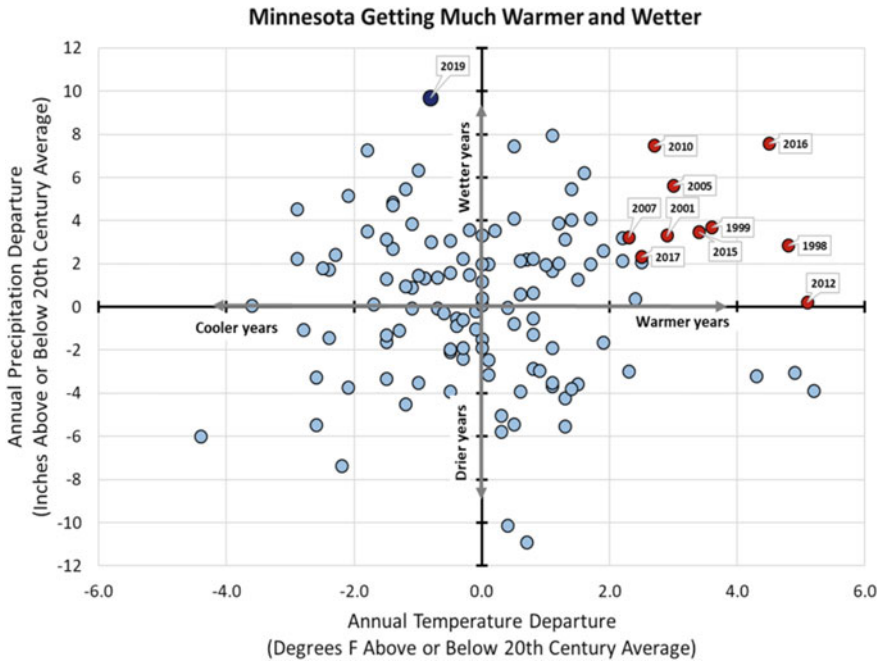

Fig. 1.3 Plot of annual temperature and precipitation in Minnesota (Kanwar et al. 2020)

averages, all of the ten wettest and warmest years on record occurred after 1998 (Kanwar et al. 2020), see Fig. 1.3. Just recently, in 2019, Minnesota experienced the wettest year on record, see Fig. 1.3.

Minnesota's climate swings naturally from relatively dry to relatively wet periods; however, the wetter conditions have dominated recent decades. Precipitation above historical averages have become increasingly frequent, and departures from those averages have grown as well, leading to sustained precipitation surpluses never before documented in the state (Kanwar et al. 2020), see Fig. 1.4.

Minnesota is also becoming warmer during nights and winter. Annual temperatures have climbed nearly 3° since 1895, but 80% of that warming has only been since 1970. During those five decades, winters have warmed by 5 °F, winter nights have warmed by 6 °F, but summers have warmed by just a half a degree F, and summer daytime high temperatures have decreased slightly in southern Minnesota (Kanwar et al. 2020), see Fig. 1.5. Water is a defining resource for Minnesota, central to our economy, communities and identity; and the state will always be sensitive to dry conditions and drought. While Minnesota continues to experience periodic drought in specific regions, those periods have not increased in severity or length. Recent surges in precipitation have meant the state has not seen any increases in drought severity, duration or areal coverage over the past few decades. However, the extremely wet cycle the state is in will end eventually. A shift towards a dry regime should be expected, as climate change will not eliminate wet and dry periods in Minnesota.

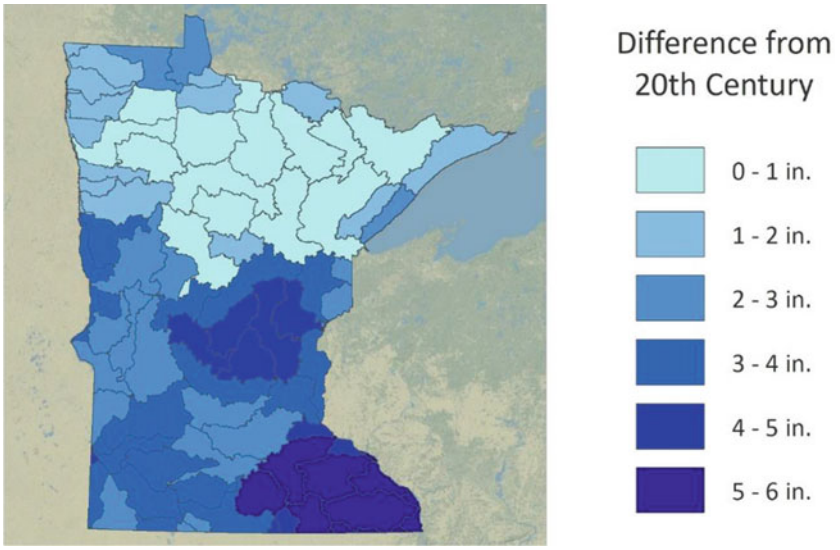

Fig. 1.4 Annual precipitation increase since the twentieth century (Kanwar et al. 2020)

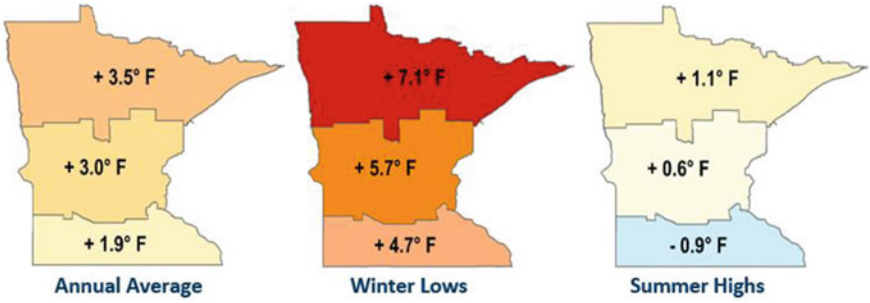

Fig. 1.5 Temperature change by region (Kanwar et al. 2020)

Even with a generally wetter climate, climatologists predict that Minnesota should expect occasional episodes of severe drought, and these drought events could happen immediately following, or may even occur in specific areas of the state during, a wet period affecting agricultural productivity of the state of Minnesota severely (Kanwar et al. 2020).

1.3 India Case Study on Climate Change Effects on Food and Water Security in South Asia

India Case Study at PAU Ludhiana: The state of Punjab in India is the largest irrigated, wheat and rice growing, area of India. The average crop yields in Punjab are close to some of the most advanced agricultural economies of the world such as USA, Canada and Australia. This is due to the contributions of Punjab Agricultural University at Ludhiana, Punjab (PAU), in educating the farmers of Punjab on the use of best agricultural and water management practices. This university was established in 1961 by the Ohio State University on the Land Grant pattern under a USAID grant of $70 million. The PAU recruited some of the best trained faculty in the world in 1960s who developed new plant varieties and helped Punjab farmers to adopt best agricultural practices to fully mechanize crop production methods. Climate change is now affecting India's agriculture. Therefore, it was decided to include the climate data collected from a weather station in Ludhiana in this chapter to provide evidence of climate change in South Asia. The city of Ludhiana in Punjab, India, is situated at 30°54′33″ N latitude, 75°48′22″ E longitude and 247 m altitude above mean sea level. This part of South Asia experiences semi-arid type of climatic conditions resulting in distinct spring, winter and summer seasons. The climatic data on maximum temperature (Tmax), minimum temperature (Tmin), relative humidity (RH), wind speed (WS), sunshine hours (SSH) and open-pan evaporation (PE) was collected from the Agrometeorological Center at PAU for 47 years from 1970 to 2016 and are given in Figs. 1.6, 1.7, 1.8, 1.9, 1.10 and 1.11 (Kingra 2017). Temporal variability depicted increase in minimum temperature at 0.05 °C analysis using Mann–Kendall and Sen's slope per year both during rabi and kharif seasons (Kingra et al. 2017) as well as annually (Kingra et al. 2018a; b, c). In this chapter, we are using these data to show the impacts of climatic change on crop yields of Punjab and future directions for research at PAU to make sure that farming systems in South Asia stay sustainable and farmers' incomes are protected.

Climate change is posing a serious threat to the food security for the growing population growth of India. This has attracted the attention of scientists and policy-makers in the recent decades to focus their energies in addressing this serious global issue. Under the present environmental conditions and circumstances, there is an urgent need to manage climate variability and its adverse effects to attain food security and agricultural sustainability in future. Keeping this in view, the climatic records of central Punjab (Ludhiana) have been analysed to quantify the climatic changes and their likely impacts on agricultural productivity. Lower minimum temperature, relative humidity, rainfall and number of rainy days during the reproductive growth period of wheat covering the months of February and March have been found favourable for higher grain yield (Kingra 2016a). Minimum temperature explained 44% variability in wheat yield (Kingra et al. 2018a). Higher daytime temperature, sunshine hours and lower afternoon relative humidity during vegetative growth and lower daytime temperature, sunshine hours and higher afternoon relative humidity are favourable

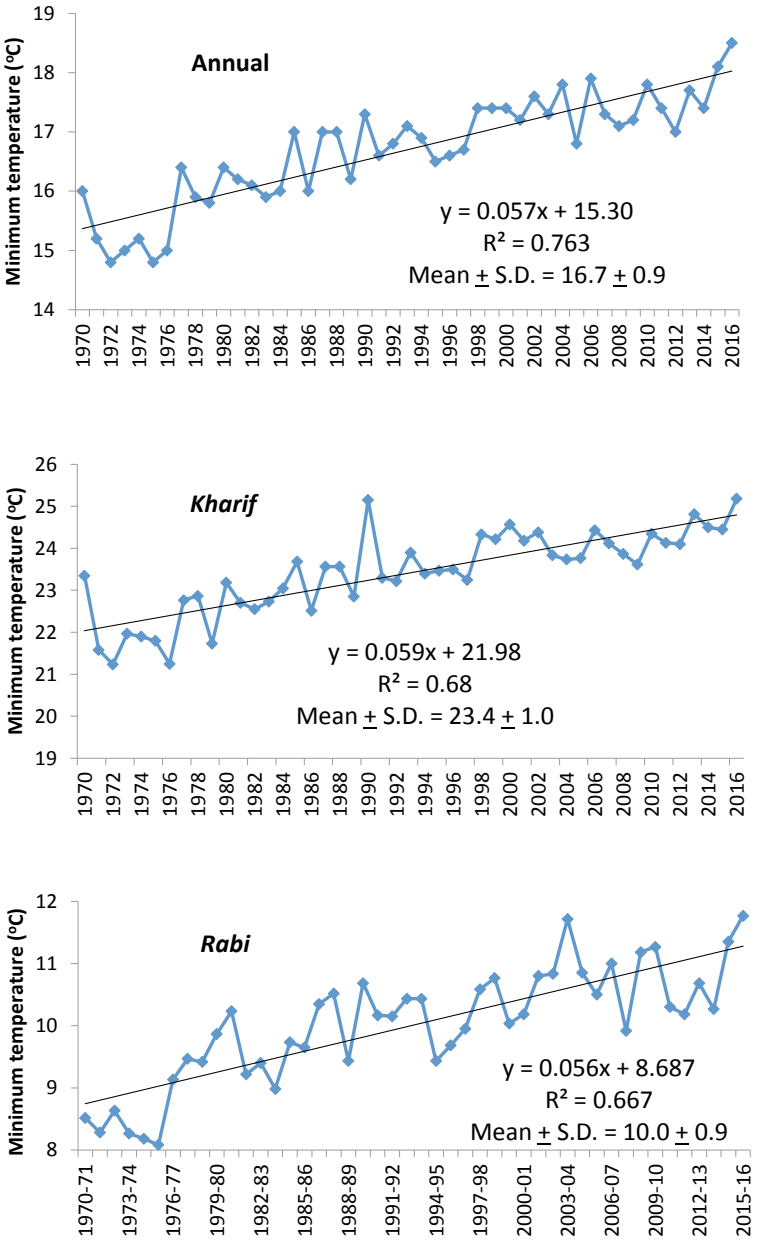

Fig. 1.6 Temporal variability in annual and seasonal (during rabi and kharif seasons) average minimum temperature in central Punjab (Kingra 2017)

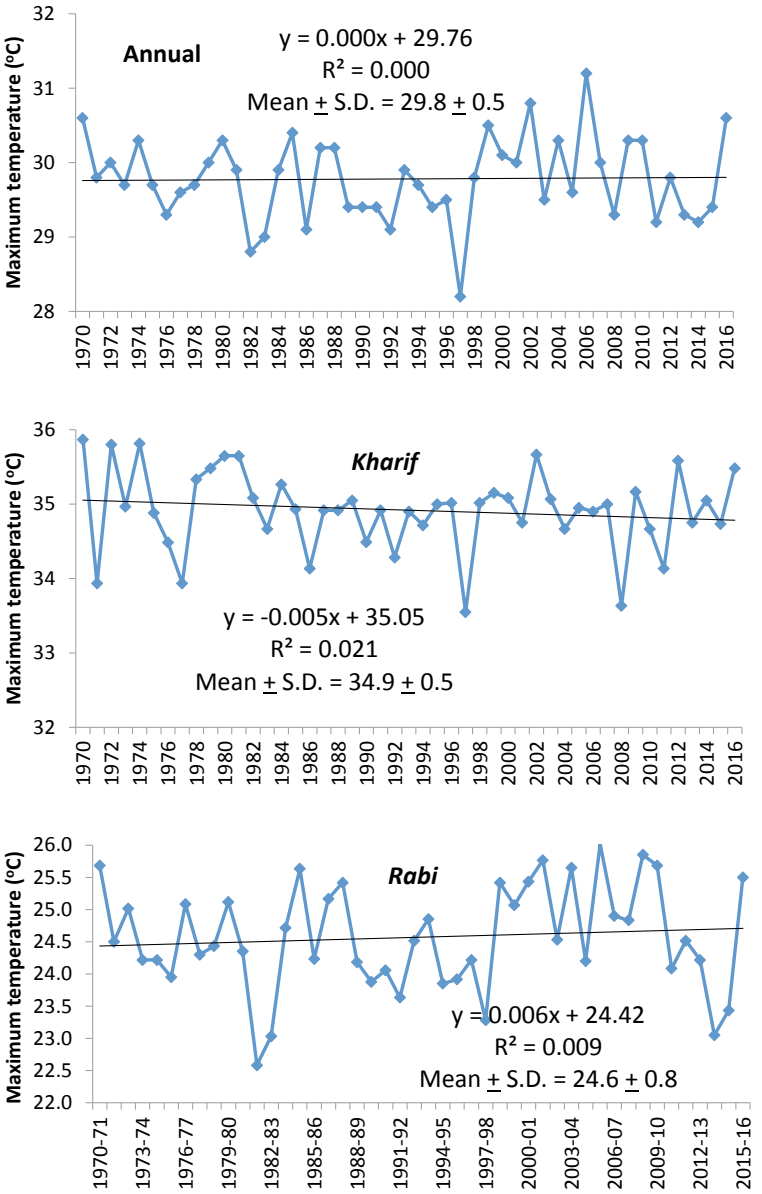

Fig. 1.7 Temporal variability in annual and seasonal average maximum temperature in central Punjab (Kingra 2017)

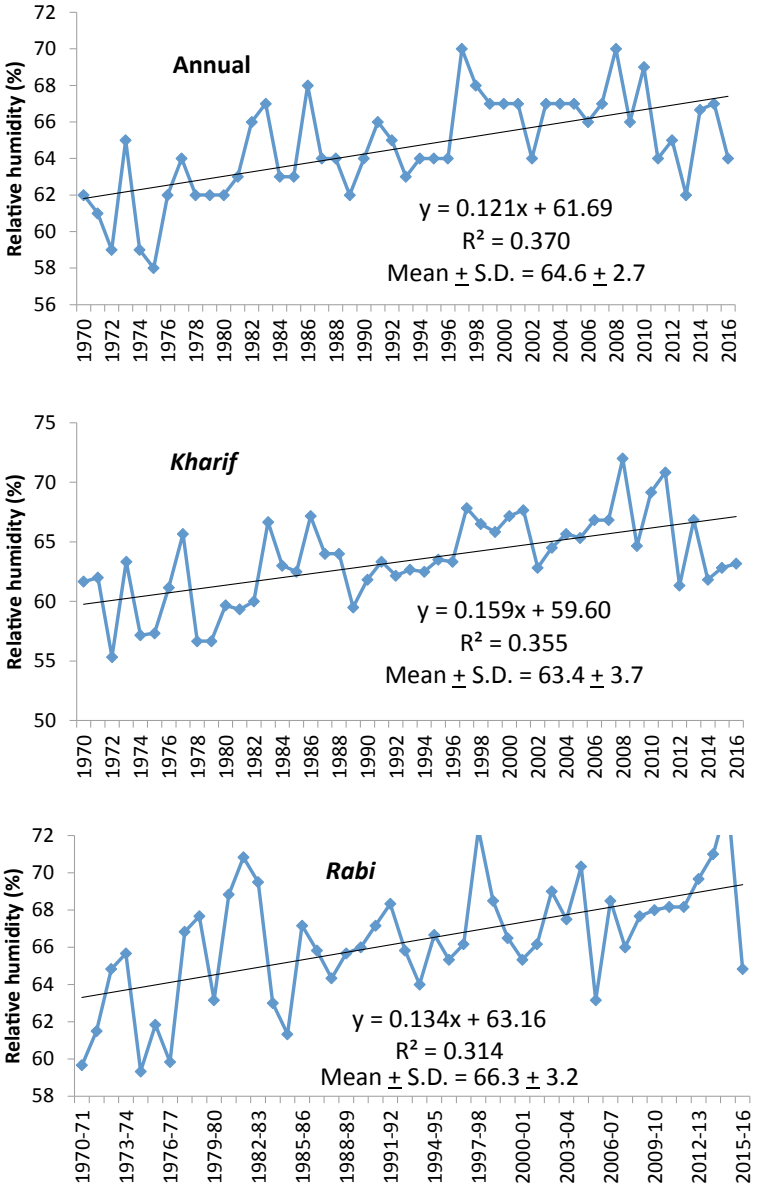

Fig. 1.8 Temporal variability in annual and seasonal average relative humidity in central Punjab (Kingra 2017)

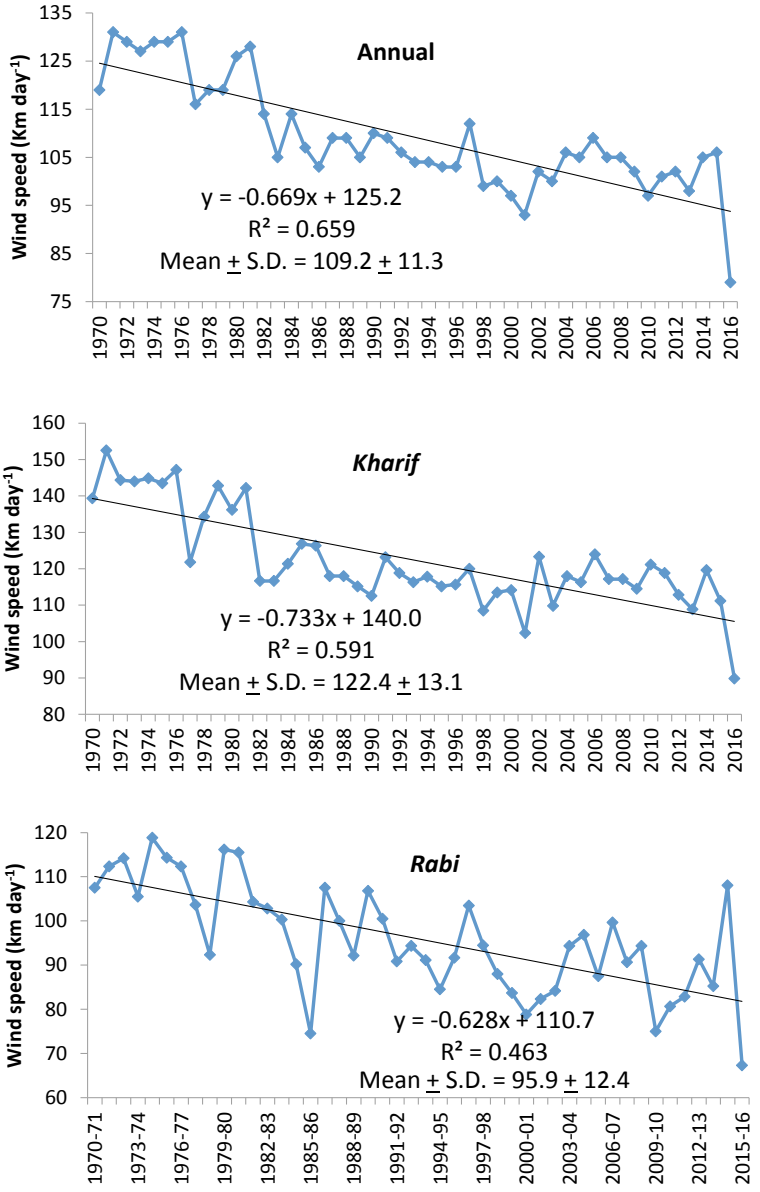

Fig. 1.9 Temporal variability in annual and seasonal average wind speed in central Punjab (Kingra 2017)

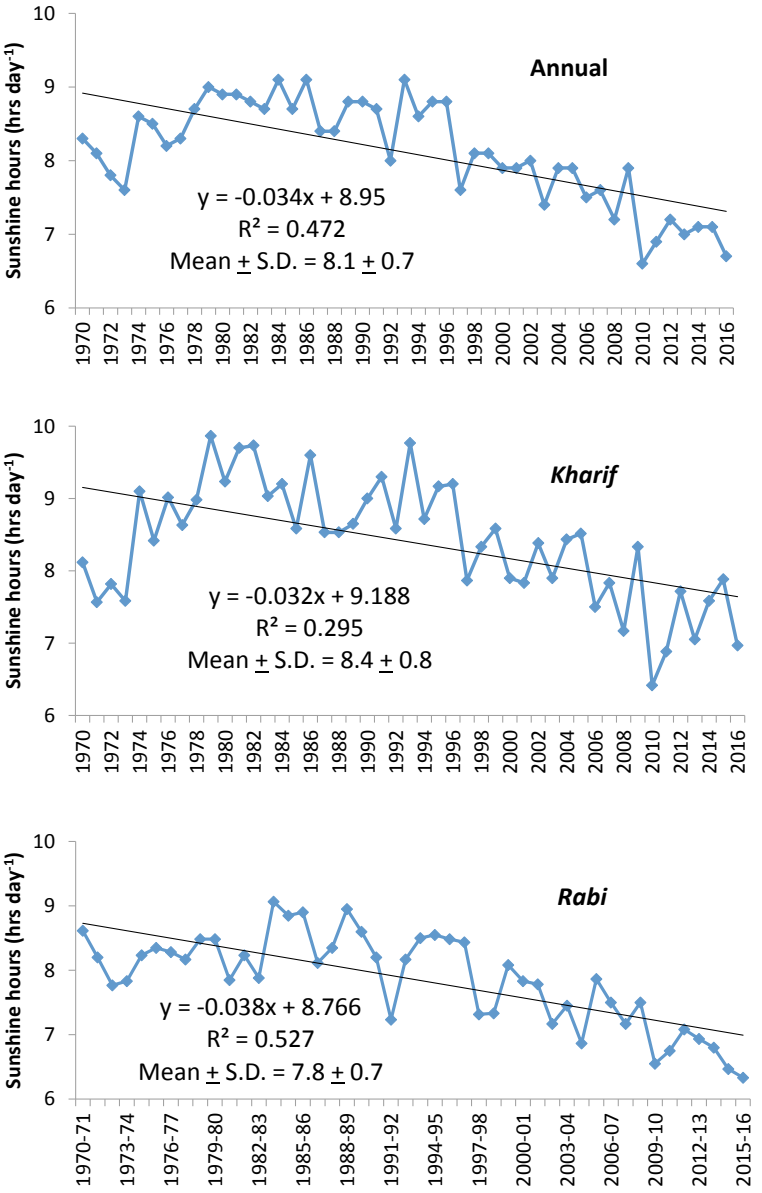

Fig. 1.10 Variability in annual/seasonal average sunshine hours in central Punjab (Kingra 2017)

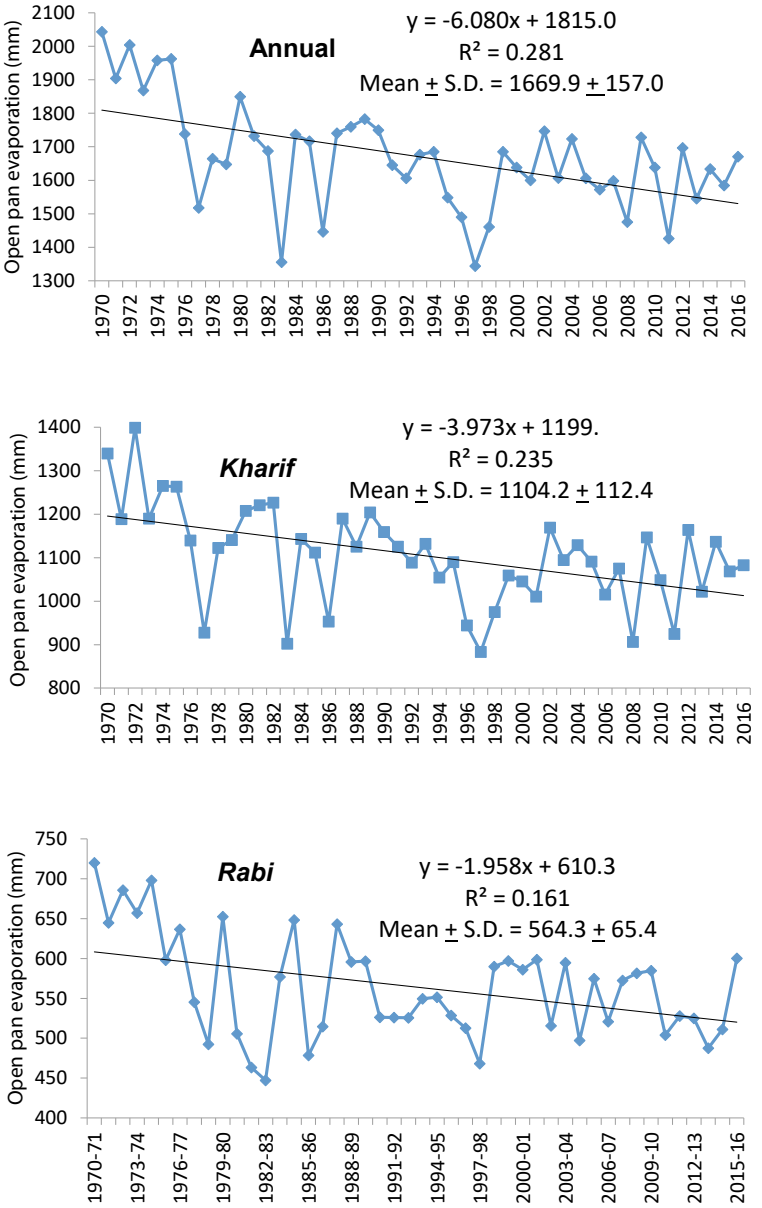

Fig. 1.11 Temporal variability in annual and seasonal open pan evaporation in central Punjab (Kingra 2017)

for obtaining higher rice yields (Kingra 2016b). Spatial variations in yield, rainfall and temperature are substantial, and these have important consequences for food security by indicating the need for region-specific technologies (Kingra et al. 2018b).

Data given in Figs. 1.6 and 1.7 clearly shows that minimum and maximum temperatures in Punjab are increasing and effects on climate change on agriculture are real. Increased temperatures will affect the water requirements of crops and directly affecting water security needs of India because 85% of India's water is used for agriculture. Significant increase in minimum temperature has been observed on monthly as well as yearly basis for both growing seasons (rabi and kharif). The rate of increase in minimum temperature is being highest during the months of February, March, September and October (0.07 °C) and lowest during the months of January and June (0.03 °C). As the four months with the highest rate of increase coincide with the reproductive growth period of rabi (February and March) and kharif (September and October) crops, climate change poses a serious threat to crop productivity in the region of Punjab because seasonal minimum temperature variability of 16.7 ± 0.9 °C, 23.4 ± 1.0 °C and 10.0 ± 0.9 °C, respectively, along with year-to-year variations (Fig. 1.6), puts Punjab in high risk zone for heat stress risks in future. The studies have shown that higher minimum temperatures during tillering (late November to early December) and during grain formation stage (late February to early March) have resulted in reduction in wheat yield to the extent of 3–8% (Dr KK Gill, Personal Communication).

Mean monthly relative humidity data has also been observed to increase during different months except March, April, May and August, during which no significant trends. The period from April to June has been observed to be the driest with mean relative humidity ranging from 40.4 to 52.8%, whereas during the period from July to September during monsoon rains, humid conditions ranged from 73.0 to 78.0%. In addition to this, the cold months of January, February and December also experienced humid conditions with relative humidity ranging from 72.0 to 75.5 per cent, whereas the months of March, October and November experienced moderate humidity ranging from 62.6 to 66.5% (Fig. 1.8). Similarly, trends in wind speed (Fig. 1.9) were observed. Higher wind speeds were observed in the months of April to July affecting transmission of plant diseases and water requirements. The data on wind speed shows a significant decrease in wind speed during all the months except during the month of March.

Data on sunshine hours and open pan evaporation for the Punjab region is given in Figs. 1.10 and 1.11, respectively. There is a decreasing trend in sunshine hours. Sunshine hours have a significant effect on the process of photosynthesis, and the decreasing daily sunshine hours will have severe impacts on the rate of photosynthesis and hence crop productivity. This could be one reason that the crop yields have remained static over the last decade or so despite of better crop cultivars and cultural practices being recommended by PAU. Data on open pan evaporation (Fig. 1.11) shows that monthly open pan evaporation at Ludhiana, Punjab, ranged from 46.2 ± 9.5 mm in January to 305.6 ± 51.0 mm in May. Due to hot and dry conditions during the months of April, May and June, highest rate of evaporation was observed during these three months. This analysis indicates that the decrease in evaporation at a rate

of 6.0 mm annually with seasonal decrease of 4.0 mm during *kharif* and 2.0 mm during *rabi* season due to climatic variations might have resulted in increased relative humidity and decreased wind speed over time.

These climatic shifts in Punjab can have great implications on agricultural productivity of India. This study clearly indicates that climate change effects in Indian sub-continent are real, and policy-makers and researchers must prepare themselves for the future course of action. Minimum temperature during crop reproductive and maturity period is very critical. Increase in minimum daily temperatures during this crop-growing period increases the evapotranspiration losses and reduces crop yields significantly. This can lead to terminal heat stress in both *rabi* and *kharif* crops affecting productivity of these crops.

Table 1.4 gives data on the effect of yearly rainfall amounts and distribution in rainfall on wheat yields for four years (2009–2013). The year 2012–2013 was extremely wet, and fields were waterlogged for extended periods of time affecting crop yields severely. During the years, when rainfall was close to normal, the wheat yields showed an increasing trend. Again, these data shows that extremely wet years can significantly decrease crop yields due to excessive wetness in the field. Table 1.5 gives the per cent decrease in crop yields with increase in temperatures. Rising temperatures could reduce wheat yields by 10–28% because of insect damage or heat stress.

All these climatic variations are likely to have severe implications on crop productivity in the region. Improved cultivation systems like zero tillage, bed planting and conventional tillage with mulch produce higher grain yield and improve water productivity of wheat than conventional planting. Irrigation management and retaining crop residue in field are other measures to manage terminal heat stress and

Table 1.4 Effect of rainfall amount and distribution on wheat yield in Punjab

Year	Rainfall amount (mm)	Rain distribution (Number of rainy days)	Average wheat yield (Mg/ha)	
			Ludhiana	Punjab
2009–10	49.7	4	4.63	4.31
2010–11	74.2	7	4.96	4.69
2011–12	65.6	6	5.38	5.10
2012–13	157.6	13	4.84	4.53

Table 1.5 Response of different wheat varieties to increase in temperature

Wheat variety	Decrease in yield (%) as a function of temperature increment (°C)				
	+0.5 °C	+1.0 °C	+1.5 °C	+2.0 °C	+2.5 °C
PBW 343	−3.0	−8.0	−16.0	−23.5	−23.0
PBW 621	−7.0	−11.0	−15.5	−22.0	−24.5
PBW 550	−5.0	−9.0	−14.0	−23.0	−27.0
DBW 17	−10.0	−13.0	−19.5	−26.5	−28.0

improve water productivity in wheat (Kingra et al. 2019a). Kingra and Mahey (2013) reported higher soil moisture extraction by wheat under flat planting as compared to bed planting in wheat. Kingra et al. (2011) also observed increase in heat use efficiency of wheat under adequate water supply indicating irrigation management as effective strategy to beat water and heat stress in wheat. Similarly, to overcome the adverse effects of climate change on rice productivity, agronomic management practices like cultivation system, irrigation management and fertilizer management, etc., can play a significant role either by leading to reduction in greenhouse gas (GHG) emission or by reduction of climate change impact on rice productivity (Kingra et al. 2019b).

1.4 Conclusions

Three examples of fields studies reported in this chapter from three difference regions of the world clearly indicate that climate change is likely to affect the food and water security for the growing global population. Therefore, we as a global community of researchers and policy makers, need to work together to develop innovative technologies, best management systems, and adaptable policies to mitigate the effects of climate change by reducing greenhouse gas emmisions to the atmosphere. Since agriculture is one of the contributors of greenhouse gas emissions to the atmosphere, agricultural community and food industry need to play a positive and supportive role in curbing carbon dioxide, methane and nitrogen oxide emissions from animal and crop production systems in agricultural watersheds. Farmers are already adopting carbon sequestration farming practices, and cutting-edge and proven technologies to reduce greenhouse gases to atmosphere. The development and implementation of climate-smart best agricultural practices including conservation tillage, precision and digital farming, improved plant breeding technologies, innovative irrigation and water management methods like drip irrigation, and good manure/nutrient management practices will help reduce agriculture's impact on climate change. Digital tools and precision agriculture techniques have already enabled farmers to make on-site decisions to grow more food with less inputs and on less acreage, offering the potential to reduce the energy use and the number of acres needed to feed a growing global population.

Another area where the global agricultural community needs to pay attention is in the area of post-harvest food losses. An estimated 1/3 of all food produced is more or less wasted or damaged in storage or during transportation. Wet and dry cycles, and extreme weather events, and the seasonal effects of rainfall distribution during the growing season on groundwater recharge and water quality need further studies. In addition, additional research on efficient animal and crop production systems in response to climate change are needed in different parts of the world so that farmers can be educated on how to best manage their farming activities in environmentally sound manner and keeping their farms economically viable to meet the food security needs. Studies conducted in India on climate change effect on

crop productivity, and water security indicates that future research need to focus on optimizing input use efficiency and developing incentive-based adaptive policies to sustain natural resources for attaining food security. Elevated CO_2 emission from agriculture and increasing temperatures should become the focus of future studies to mitigate climate change. On-farm management systems (timely planting of crops, reduced dependance on groundwater for irrigation, integrated nutrient and pest management, minimum tillage and crop rotations practices for carbon sequestration and improving soil health) and resource conservation technologies should be part and parcel of future farming system.

References

Ella VB, Melvin SW, Kanwar RS, Jones L, Horton R (2002) Inverse three-dimensional groundwater modeling using finite difference method for recharge estimation in a glacial till aquitard. Trans Am Soc Agric Eng 45(3):703–715

Everts CJ, Kanwar RS (1993) Effect of purging on hydraulic conductivity measured in monitoring piezometers installed in an aquitard. Hydrol Sci J 38(2):89–101

Haris AVA, Biswas S, Chhabra V, Elanchezhian R, Bhatt BP (2013) Impact of climate change on wheat and winter maize over a sub-humid climatic environment. Curr Sci 104(2):206–214

Hoover NL, Kanwar RS, Soupir M, Pederson C (2015) Effects of poultry manure application on phosphorus in soil and tile drain water under a corn-soybean rotation. Water Air Soil Pollut 226(5):138–150

Hruby CE, Soupir ML, Moorman TB, Shelley M, Kanwar RS (2016) Effects of tillage and poultry manure application rates on Salmonella and fecal indicator bacteria concentrations in tiles draining Des Moines Lobe soils. J Environ Manage 171:60–69

Hruby CE, Soupir ML, Moorman TB, Pederson C, Kanwar RS (2018) Salmonella and fecal indicator bacteria survival in soils amended with poultry manure. Water, Air, Soil Pollut 229(2) https://doi.org/10.1007/s11270-017-3667-z

Hundal SS, Kaur P (2007) Climatic variability and impact on cereal productivity in Indian Punjab. Curr Sci 92(4):506–512

Huy NQ, Kanwar RS, Hoover NL, Dixon P, Hobbs J, Pederson C, Soupir ML (2013) Long-term effects of poultry manure application on nitrate leaching in tile drain water. Trans Am Soc Agric Biol Eng 56(1):91–101

IPCC (2007) Climate change mitigation: intergovernmental panel on climate change; Metz OR, Davidson PR, Bosch R, Dave LA. Meyer, Cambridge University Press, Cambridge, United Kingdom and New York, NY, USA

IPCC (2014) Climate change 2014: synthesis report. In: Pachauri RK, Meyer LA (eds) Contribution of working groups I, II and III to the fifth assessment report of the intergovernmental panel on climate change. IPCC, Geneva, Switzerland, pp 151

Kalita PK, Kanwar RS, Baker JL, Melvin SW (1997) Groundwater residues of atrazine and alachlor under water quality table management practices. Trans Am Soc Agric Eng 40(3):605–614

Kanwar RS, Colvin TS, Karlen DL (1997) Subsurface drain water quality under ridge and three other tillage systems. J Prod Agric 10(2):227–234

Kanwar RS, Cruse R, Ghaffarzadeh M, Bakhsh A, Karlen D, Bailey T (2005) Corn-soybean and alternate farming systems effects on water quality. Appl Eng Agric 21(2):181–188

Kanwar P, Considine E, Stenquist B, Moeckel JA, Blumenfeld K, Chisholm I, Frischman J, Hovey T, Hunt S, Kloiber S, Loughry J, Miller D, Moore Z, Nelson C, O'Shea D, Putzier P, Radomski P, Sorenson J (2020) Water availability and assessment report. Appendix C to the 2020 EQB water plan. Minnesota Department of Natural Resources

Karlen DL, Kumar A, Kanwar RS, Cambardella CA, Colvin TS (1998) Tillage system effects on 15-year carbon-based and simulated N budgets in a tile-drained Iowa field. Soil Tillage Res 48(3):155–165

Kingra PK (2016a) Climate variability impacts on wheat productivity in central Punjab. J Agro-Meteorol 18(1):97–99

Kingra PK (2016b) Climate variability and impact on productivity of rice in central Punjab. J Agro-Meteorol 18(1):146–148

Kingra PK (2017) Climatic variability and its implications on agricultural productivity in central Punjab. Indian J Econ Agric Dev 13(3):442–453. https://doi.org/10.5958/2322-0430.2017.00201.3

Kingra PK, Mahey RK (2013) Moisture extraction pattern and ET-yield models in wheat under different management practices in central Punjab. J Agro-Meteorol 15(1):51–57

Kingra PK, Mahey RK, Gill KK, Singh S (2011) Thermal requirement and heat use efficiency of wheat under different irrigation levels in central Punjab. Indian J Ecol 79:18–23

Kingra PK, Setia R, Singh S, Kaur J, Kaur S, Singh SP, Kukal SS, Pateriya B (2017) Climatic variability and its characterization over Punjab India. J Agro-Meteorol 19(3):246–250

Kingra PK, Setia R, Kaur S, Kaur J, Singh S, Singh SP, Kukal SS, Pateriya B (2018a) Mausan 69(1):147–160

Kingra PK, Setia R, Kaur S, Kaur J, Singh S, Singh SP, Kukal SS, Pateriya B (2018b) Assessing the impact of climate variations on wheat yield in north-west India using GIS. Spat Inf Res. https://doi.org/10.1007/s41324-018-0174-2

Kingra PK, Setia R, Kaur S, Kaur J, Singh S, Singh SP, Kukal SS, Pateriya B (2018c) Spatio-temporal analysis of the climate impact on rice yield in north-west India. Spat Inf Res. https://doi.org/10.1007/s41324-018-0182-2

Kingra PK, Kaur J, Kaur R (2019a) Managing strategies for sustainable wheat (*Triticum aestivum* L.) production under climate change in south Asia—a review. J Agric Phys 19(1):1–15

Kingra PK, Kaur R, Kaur S (2019b) Climate change impacts on rice productivity and strategies for its sustainable management. Indian J Agric Sci 89(2):171–180

Misra AK (2014) Climate change and challenges of water and food security. Int J Sustain Built Environ 3(1):153–165

Olson DI, Kanwar RS, Bischoff JH (1997) Construction and testing of a field facility for measuring water and agrichemical transport through the Vadose Zone. Trans Am Soc Agric Eng 40(4):961–969

Pappas EA, Kanwar RS, Baker JL, Lorimor JC, Mickelson S (2008) Fecal indicator bacteria in subsurface drain water following swine manure application. Trans Am Soc Agric Biol Eng 51(5):1567–1573

Parry ML, Rosenzweig C, Iglesias A, Livermore AM, Fischer G (2004) Effects of climate change on global food production under SRES emissions and socio-economic-scenarios. Glob Environ Change 14:53–67

Rekha PN, Kanwar RS, Nayak AK, Hoang CK, Pederson CH (2011) Nitrate leaching to shallow groundwater systems from agricultural fields with different management practices. J Environ Monit 13:2550–2558

Solomon S, Qin D, Manning M, Chen Z, Marquis M, Avery K (2007) Climate change: the physical science basis contributions of working group I to the fourth assessment report of the intergovernmental panel on climate change. Cambridge University Press, Cambridge

Chapter 2
Climate Change Risks to Water Security in Canada's Western Interior

M. Rehan Anis, Yuliya Andreichuk, Samantha A. Kerr, and David J. Sauchyn

2.1 Introduction

Much of the impact of anthropogenic climate change on social and natural systems results from changes to regional hydrological regimes including shifts in the seasonal water balances and increases in the frequency and severity of hydroclimatic extremes (Abbott et al. 2019; Jiménez Cisneros et al. 2014; Marvel et al. 2019). Climate change impacts on water resources affect food security and economic prosperity, especially in dry climates where aridity (a negative water balance in normal years) and drought are economically and ecological limiting. The semiarid to sub-humid plains of western Canada have more than 80% of the country's agricultural land. In this region, melting snow accounts for most of the runoff and surface water supplies. A warming climate will result in decreases in the depth of the snowpack, length of the snow cover season and the proportion of precipitation falling as snow (Mudryk et al. 2018), with a corresponding reduction in end-of-season snowpack and summer water levels and streamflow (Bonsal et al. 2019).

The potential impacts of a warming climate on water availability in snow-dominated mid- and high-latitude river basins are a serious concern given that, over the past several decades, these regions have experienced some of the most rapid warming on earth (Bonsal et al. 2019). In western Canada, declining streamflow has been observed in rivers draining the eastern slopes of the central/southern Rocky Mountains, (Burn et al. 2004; Rood et al. 2005; Schindler and Donahue 2006; St. Jacques et al. 2010; Bawden et al. 2015). Snow in the Rocky Mountains is the backbone of the industrial water supply, including the source of water for irrigation of agricultural land. The bank of surplus water from wasting alpine glaciers has been mostly spent, and mass balance is shrinking quickly (Marshall et al. 2011).

M. R. Anis · Y. Andreichuk · S. A. Kerr · D. J. Sauchyn (✉)
Prairie Adaptation Research Collaborative (PARC), University of Regina, Regina, Canada
e-mail: sauchyn@uregina.ca

© The Author(s), under exclusive license to Springer Nature Singapore Pte Ltd. 2021

A. Pandey et al. (eds.), *Hydrological Aspects of Climate Change*,
Springer Transactions in Civil and Environmental Engineering,
https://doi.org/10.1007/978-981-16-0394-5_2

This paper describes research on the impact of climate change on water security in western Canada using as a case study the North Saskatchewan River Basin (NSRB). The tributaries of the Saskatchewan River flow from the Rocky Mountains across a vast area of interior plains that represents the largest area of drylands in Canada. We present an analysis of past and future climate and hydrology. We compare pre-industrial paleohydrology to model simulations of future climate and river flow. Research on the extent to which anthropogenic climate change departs from natural variability informs an assessment of the resilience of water resource policy and infrastructure, which were designed to operate under historical climatic variability. Human-induced climate trends are superimposed on natural multi-decadal climate variability, which is more evident and impactful at regional scales. Our case study of climate change and water security in the NSRB begins with a discussion of the drivers of hydroclimatic variability in this region.

2.1.1 Natural Variability of the Regional Hydroclimatic

Future projections of regional changes in precipitation and water resources are constrained by an incomplete understanding and simulation of the climate system, by making assumptions about anthropogenic forcing, and by a significant component of stochastic internal variability (Hawkins and Sutton 2009; Deser et al. 2012). Natural variability can dampen, mask or enhance human-induced trends with a larger influence at regional scales and for variables related to the water cycle. Barrow and Sauchyn (2019) found that in western Canada natural variability is the dominant source of uncertainty for the projection of future precipitation, accounting for more uncertainty than discrepancies among climate models and choice of greenhouse emission scenarios. These findings indicate that any attempts to project the climate of future decades require an understanding of natural variability in the regional hydroclimate and how well numerical models simulate this internal variability of the climate system.

Canada's western interior has a typical mid-latitude continental climate with large seasonal and inter-annual variability. Water allocation, and the design of storage and conveyance structures, is based primarily on average seasonal water levels, but otherwise water resources are managed to prevent the adverse impacts of flooding and drought. While these hydrological extremes are difficult to predict, their probability is strongly linked to periodic fluctuations in sea surface temperatures (Bonsal et al. 2019). Strong teleconnections between the regional hydroclimate and Pacific basin atmosphere–ocean oscillations drive much of the hydroclimatic variability at annual to decadal time scales, in some cases obscuring signals of climate change (Fye et al. 2006; Moore et al. 2007). Indices that describe the dynamics of these large-scale climate systems include the Pacific Decadal Oscillation (PDO), the Pacific North American (PNA) pattern and the El Niño Southern Oscillation (ENSO). The extreme phases of ENSO are inversely related to precipitation during the cold season: El Niño (La Niña) is associated with below (above) average precipitation in our region. There

is a strong negative relationship between the PDO and streamflow in western Canada; thus, water levels are higher when the PDO is in its negative phase and drier when the PDO is positive (St. Jacques et al. 2010). Gurrapu et al. (2016) demonstrated the strong influence of the PDO on peak river flows in western Canada. They found two distinct flood frequency curves for the negative and positive phases of the PDO. The curves diverge at higher return periods, indicating that flood flows are much more likely during the negative (cool) phase of the PDO.

Recent flooding and drought in the Prairie Provinces have been some of the most costly natural disasters in Canadian history. Studies of the drought in 2015 (Szeto et al. 2016) and floods in 2013 and 2014 (Teufel et al. 2017; Pomeroy et al. 2015) concluded that these naturally occurring events were intensified by human-caused climate change. One of the most robust climate projections, globally (IPCC 2014), nationally (Zhang et al. 2019) and regionally (Gizaw and Gan 2015), is an increase in rainfall intensity. This excess water will occur as the warmer climate converges with the wet phase of the PDO and ENSO. Similarly, the dry phase also will be amplified, when there is an absence of rain but also higher temperatures than in the past (Tam et al. 2018). Climate model projections suggest increasing exposure of the Prairies to drought, especially in summer and fall (Bonsal et al. 2019). The worst-case scenario for the Prairie Provinces is the reoccurrence of consecutive years of severe drought, such as occurred in the 1930s and in preceding centuries (Sauchyn et al. 2015). The warmer climate will amplify the impacts of a future prolonged drought. Meteorological drought (lack of rain) immediately affects dryland farming, while hydrological drought (low water levels) impacts irrigation, municipal and industrial water supplies.

2.2 Climate and Hydrology of the Upper North Saskatchewan River Basin

The North Saskatchewan River Basin (NSRB) is a headwater sub-basin of the larger Nelson River Basin, extending from the Rocky Mountains to Hudson Bay. Above Edmonton, Alberta, the NSRB has a drainage area of 28,100 km^2 and elevations that range between 611 and 3543 m above sea level (Fig. 2.1). The North Saskatchewan River (NSR) begins at the toe of the Saskatchewan Glacier in the Columbia Icefields, which have experienced dramatic changes, losing 22.5% of their total area between 1919 and 2009 (Tennant and Menounos 2013). The Saskatchewan Glacier and perpetual snows in the Rocky Mountain maintain river flow through the late spring and summer months. Land cover in the NSRB ranges from the alpine and montane ecosystems of the Rocky Mountains, to foothills forest, and the grassland, aspen parkland and agricultural landscape of the northern Great Plains. Even though the plains landscape comprises about 60 per cent of the drainage area, it yields a small proportion of the annual runoff given the sub-humid climate.

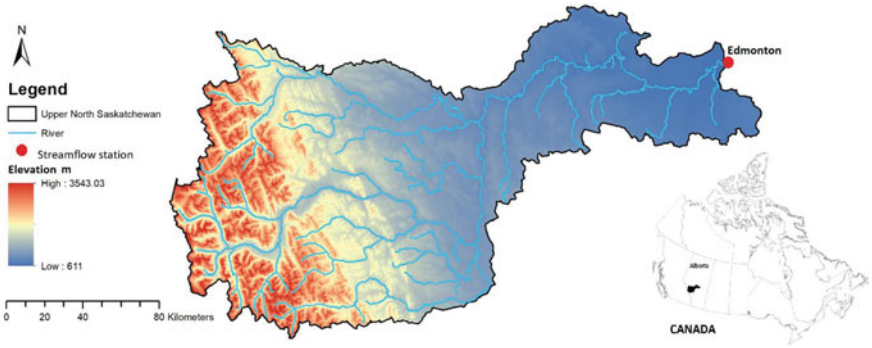

Fig. 2.1 Location, river network and elevations of the drainage basin of the North Saskatchewan River above Edmonton, Alberta

2.2.1 Climate

Environment and Climate Change Canada (ECCC) and its predecessors have monitored water and weather across a national network of gauges since the 1880s. Historical water and weather data are readily available from the websites of the Water Survey of Canada (https://wateroffice.ec.gc.ca) and the Meteorological Service of Canada (https://climate.weather.gc.ca/historical_data/), respectively. These monitoring networks were first installed in western Canada to locate reliable sources of water for irrigation, transportation and crop production. Thus, the location of the gauges on local streams, and of weather stations at agricultural research stations and airports, was initially the most important consideration when establishing these networks. Fortunately, the continuity of some of these hydrometric and meteorological stations has been maintained, because long records are vital for understanding the variability and change in our hydroclimate.

ECCC's database of Adjusted and Homogenized Canadian Climate Data (https://ec.gc.ca/dccha-ahccd/) (AHCCD) was created for use in climate research including climate change studies (Vincent et al. 2012; AHCCD 2017). It incorporates a number of adjustments applied to the original weather station data to address shifts due to changes in instruments and in observing procedures (Vincent et al. 2012; AHCCD 2017). During the period 1979–2016, the average minimum temperature for the NSRB was −12.3 °C and the average maximum temperature was 13.6 °C. Total annual precipitation averages 620 mm. The Rocky Mountain ranges of western Canada block much of the moisture brought by westerly winds from the Pacific. As a result, the annual precipitation is as high as 2000 mm at high elevations and as low as 300 mm in the plains (Environment Canada 1995).

Figure 2.2 is a time series of the mean annual temperature recorded at Edmonton since 1880. The annual average temperatures have ranged between −1 and 5 °C. Not only are there large differences in temperature between years, but there are also consecutive years of warmer (e.g. mid 80s to early 90s) and cooler (e.g. mid 60s to

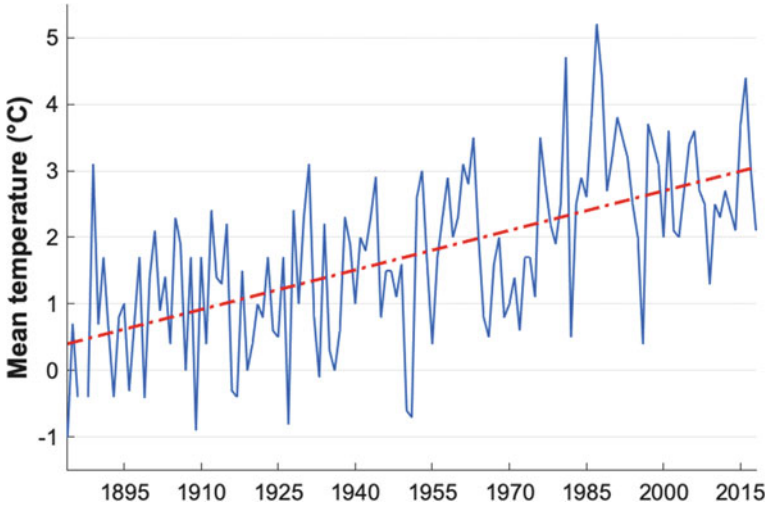

Fig. 2.2 Mean annual temperature at Edmonton since 1884 and the linear upward trend in red

mid 70s) weather. This variability from year-to-year and decade-to-decade tends to obscure a statistically significant upward trend. Nevertheless, the region is getting warmer; mean annual temperature has risen by more than 2 °C. Similar results were found by Jiang et al. (2017), when they analysed the seasonal trends in precipitation and temperature across Alberta using the Canadian Gridded Temperature and Precipitation Anomalies (CANGRD) dataset and found a consistent regional pattern of increasing temperature over all seasons.

While Fig. 2.2 illustrates a statistically significant ($p < 0.001$) rise of 2.7 °C in mean annual temperature, these data averaged for the whole year hide an important fact; most of the warming is occurring in winter to the lowest temperatures. Thus, western Canada is not getting hotter; it is getting much less cold. Figure 2.3 is a plot of mean daily minimum winter (DJF) temperature at Edmonton from 1884 to 2018. The statistically significant ($p < 0.001$) increase is 6.5 °C. There is large natural variability around this upward trend. The warmest winter was in 1931 during a very strong El Niño. Over the past three decades, the two coldest winters had a mean daily minimum temperature of approximately −20 °C. These would have been average winters for most of the twentieth century.

Total annual precipitation at Edmonton since 1884 is plotted in Fig. 2.4. It ranges from 250 to 800 mm from dry to wet years. The red dashed line indicates a linear upward trend; however, the increase is small relative to the range of values and large inter-annual and decadal variability. Even though most of the precipitation occurs in spring and early summer, winter precipitation (mostly snow) is more effective in producing soil moisture and runoff, since much of the summer rainfall is lost by evapotranspiration.

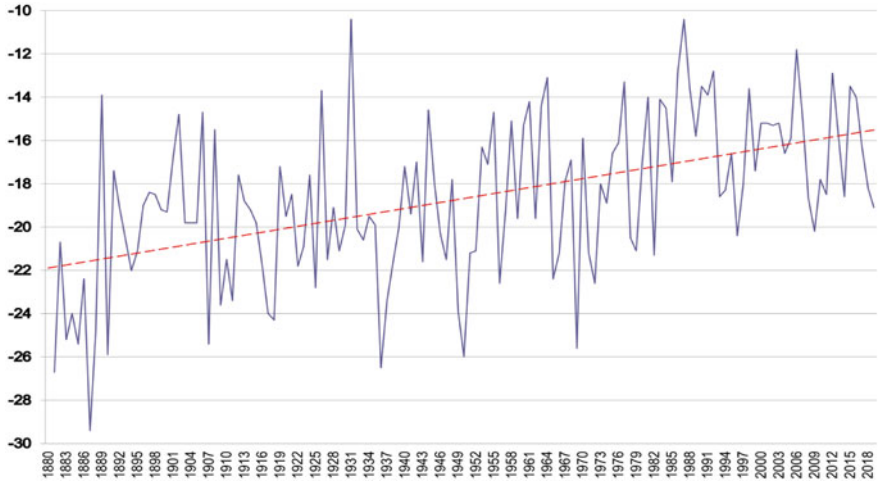

Fig. 2.3 Mean daily minimum winter (DJF) temperature (°C) at Edmonton, 1884–2019

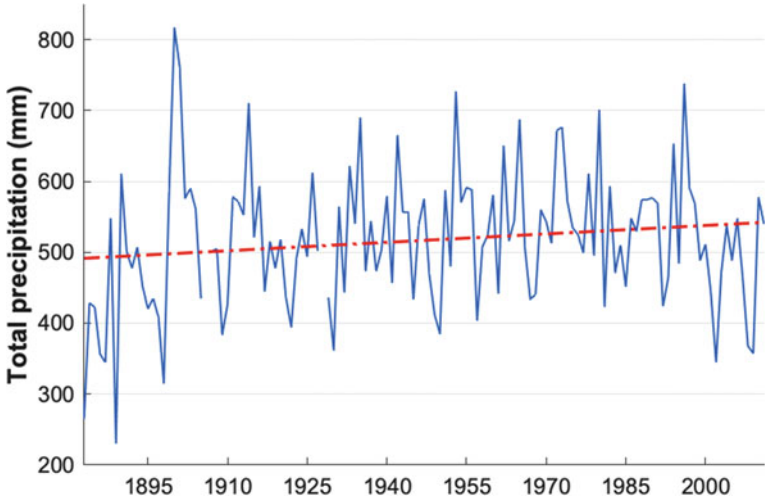

Fig. 2.4 Total annual precipitation at Edmonton since 1884, with an upward trend in red

2.2.2 Hydrology

The climate of the mountainous region of the NSRB (Fig. 2.1) is characterized by high precipitation and low evapotranspiration, resulting in high water yield. The mean annual discharge of the NSR at Edmonton is 215 m^3/s. In Alberta, the NSRB drains an area of about 57,000 km^2 (Fig. 2.5; NSWA 2014). It is sub-divided into

Fig. 2.5 Sub-basins of the North Saskatchewan River Basin (NSWA 2012)

12 sub-basins. The Cline, Brazeau, Ram and Clearwater rivers, which are headwater tributaries in the Rocky Mountains, generate 88% of the total annual runoff (NSWA 2012).

2.2.2.1 Historical Streamflow Records

The streamflow gauge at Edmonton (05DF001) was recording natural flows of the North Saskatchewan River from 1911 until the mid 1960s when the Brazeau and Bighorn dams were built. Water is released from these reservoirs throughout the year for power generation, and there is little capacity to control or mitigate flooding of the NSR (EPCOR 2017). The River Forecast Centre of Alberta Environment and Parks has reconstructed naturalized flows by computing unregulated flows at the reservoir sites and routing these flows to Edmonton. While operation of the dams has little overall effect on mean annual flows, it increases flows in the cold season (Oct–Apr) and decreases them in the warm season (May–Sep). This is illustrated in Fig. 2.6, which is plot of mean monthly flow of the NSR at Edmonton from 1912–1971 prior to the Bighorn Dam, and from 1972–2015, after the construction of the Dam. The natural flow (the blue bars) is characteristic of mid-latitude mountain watersheds with a snow-dominated hydrologic regime, where approximately 40% of the annual discharge occurs in June and July from rainfall and melt of the mountain snowpack.

Figure 2.6 shows that relatively high flows are maintained throughout the summer from the melt of snow and glaciers at high elevations. MacDonald et al. (2012)

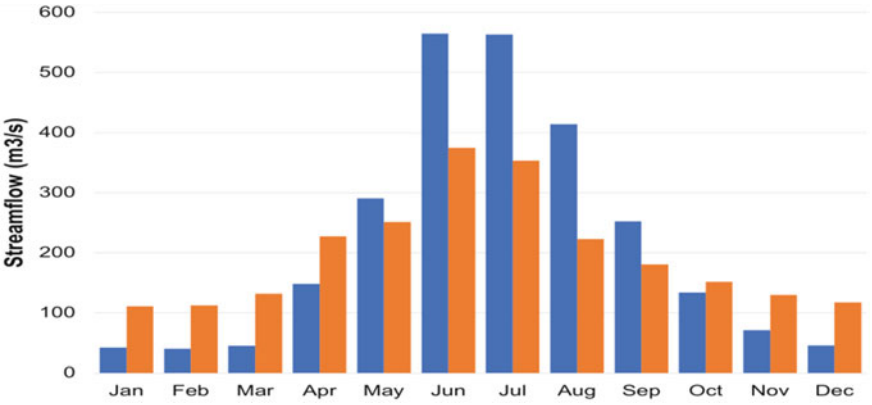

Fig. 2.6 Mean monthly flow (m^3/s) of the North Saskatchewan River (NSR) at Edmonton from 1912–1971 (blue) and 1972–2015 (orange), before and after construction of the Bighorn Dam

modelled the future snowpack of the NSRB, quantifying potential changes in snow water equivalent. They found that there may be little change in the annual maximum snow accumulation; however, spring snow melt likely will occur earlier as the climate warms and with an increase in the proportion of rain versus snow. The accelerated retreat of mountain glaciers in recent decades is an indication of repeated years of negative mass balance, where melt of glacier ice in summer exceeds the contribution of new ice converted from the winter snowpack. Among the five major rivers that flow from the eastern slopes of the Rocky Mountains, the North Saskatchewan is fed by the largest ice volume and area of glaciers (about 1% of the watershed above Edmonton; Marshall et al. 2011). Recent trends and modelling of glacier mass balance suggest that glaciers on the eastern slopes of the Rockies will lose 80–90% of their volume by 2100, with a corresponding decline in glacier contributions to streamflow (Marshall et al. 2011). The contribution of glacier meltwater to the NSR is less than 3% of the regulated flow at Edmonton during July through September (Comeau et al. 2009). While the loss of glacier ice has generated extra runoff from the larger glaciers, the number of glaciers is declining as the smaller ice masses disappear. Figure 2.7, a time series of annual flow of the NSR at Edmonton, shows a downward trend, but also considerable interannual and decadal variability reflecting the influence ENSO and the PDO on the regional hydroclimate (St. Jacques et al. 2010, 2014; Gurrapu et al. 2016; Sauchyn et al. 2011, 2015). It should be noted that this gauge station is located downstream of two water treatment plant intakes and does not account for the portion of withdrawals that are returned to the NSR (EPCOR 2017).

In Fig. 2.8, naturalized streamflow from 1912–2010 is plotted for each season: winter (DJF), spring (MAM), summer (JJA) and fall (SON). The linear trends (red lines) are not statistically significant in spring and fall; however, they are significant ($p < 0.05$) in winter and summer, with an increase of 8.5 m^3/s and a decrease of 113.7 m^3/s, respectively. These streamflow trends are consistent with climate changes over the past century. Warming has led to winter snowmelt, and less snow and ice

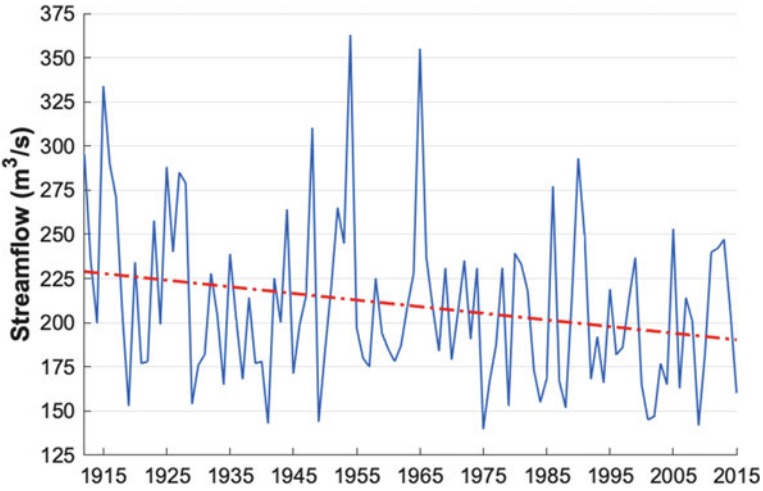

Fig. 2.7 Mean annual flow (m^3/s) of the North Saskatchewan River (NSR) at Edmonton, 1912–2015. The red line represents a downward linear trend

remain at high headwater elevations to sustain summer flow. These flow series are also marked by large differences between years and decades, such that short-term trends can reflect natural variability rather than climate change.

In Fig. 2.9, water-year hydrographs are plotted for three time periods. This comparison of observed natural flows of the North Saskatchewan River at Edmonton shows a decrease in spring/summer flows in the past 30 years and an increase in winter flows. This is consistent with the trends in the time series of annual flows by season (Fig. 2.8), which show an upward trend in winter and a downward trend in summer flows. The total annual flows increased 3.5% for the period of 1950–1979 and decreased 5.3% for the period of 1950–1979 compared to the base period of 1912–1941.

Detection and attribution of climate cycles is necessary to distinguish natural climate variability from trends imposed by global climate change. The wavelet transformation of climate time series assigns power to the spectrum of frequencies across the time domain. Figure 2.10 is a continuous wavelet plot for natural NSR flow at Edmonton from 1912–2010. The power at low frequencies corresponds to the decadal variability of the PDO and, at two to four years, the continuous effect of ENSO.

2.2.2.2 Groundwater

Further growth in Alberta's population and economy could place increasing demands on groundwater systems (Grasby et al. 2009; Worley Parsons 2009; Hughes et al. 2017). The Paskapoo Formation in west-central Alberta is an important aquifer and source of groundwater for industrial use, primarily in the oil and gas industry (Hughes et al. 2017). Data on groundwater levels is available from the Alberta Groundwater

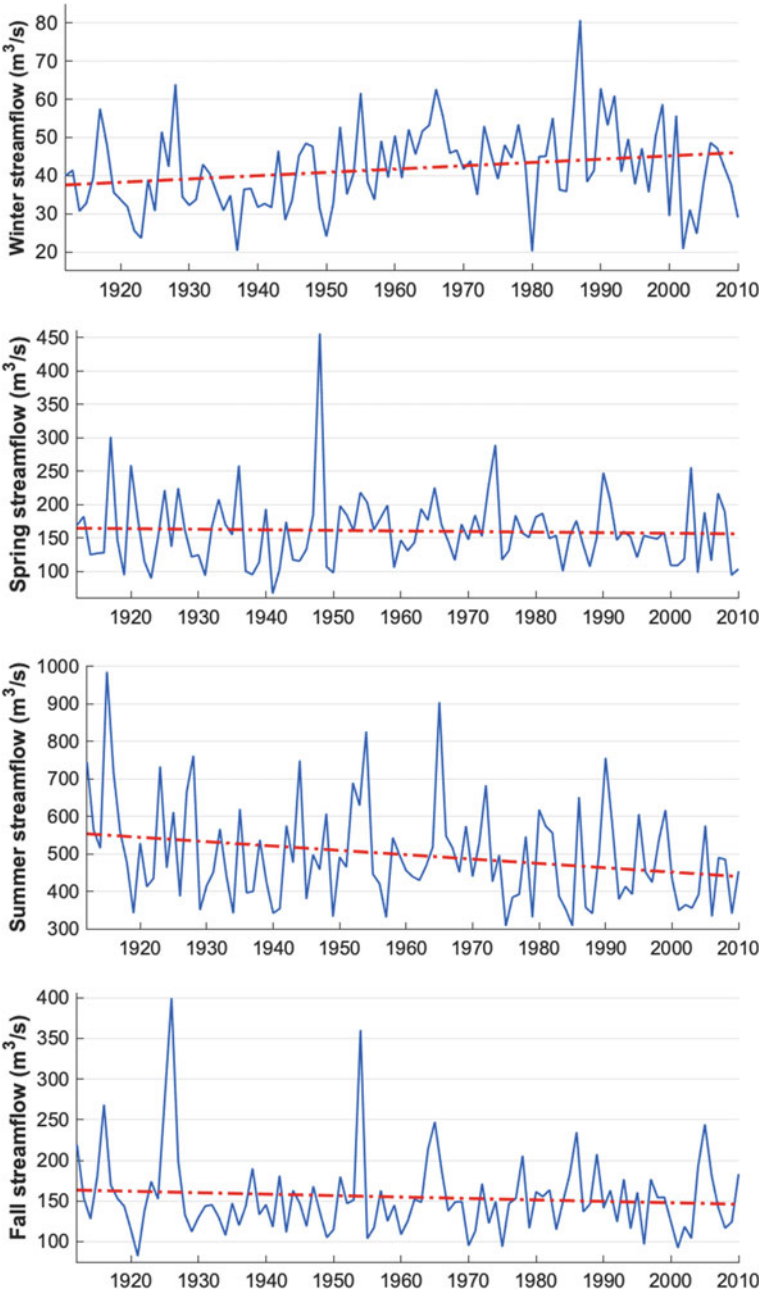

Fig. 2.8 Naturalized flow (m^3/s) of the North Saskatchewan River (NSR) from 1912 to 2010 at Edmonton by season

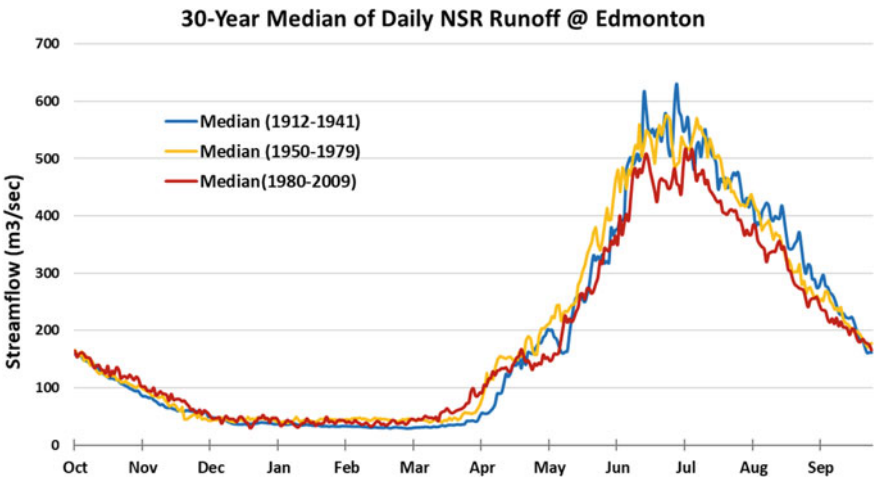

Fig. 2.9 Comparison of median of 30-year daily natural streamflow for North Saskatchewan River at Edmonton for three different time periods

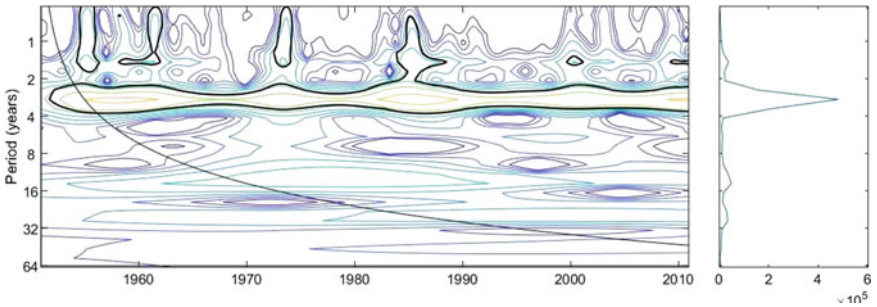

Fig. 2.10 Continuous wavelet plot for NSR natural streamflow at Edmonton from 1911–2010

Observation Well Network (https://aep.alberta.ca/water/programs-andservices/groundwater/groundwater-observation-well-network/). Data from these observation wells demonstrates the influence of climatic variability on groundwater table elevation, but as yet there is no evidence of the impact of a warming climate on groundwater recharge (Perez-Valdivia and Sauchyn 2012). Research has shown that when ENSO and PDO are in their respective positive phases, groundwater levels reflect the resulting warmer and drier winters and reduced groundwater recharge (Hayashi and Farrow 2014; Perez-Valdivia and Sauchyn 2012).

2.2.3 The Paleohydrology of the NSRB

Understanding the long-term natural variability of the regional hydroclimate is an important precursor to research on the impacts of climate change. Natural proxy records of hydroclimate, such as tree-ring chronologies, provide knowledge of past climate-driven non-stationarities in hydrologic variables. Ring-width data from long-lived trees growing at dry sites are a proxy of seasonal and annual water levels. The growth of these trees is limited by the availability of soil moisture, and the same weather variables (precipitation, temperature, evapotranspiration) that determine river flow also control tree growth. As a result, there is a similar integrating and lagged response of tree growth and streamflow to inputs of precipitation (Kerr et al. In review; Sauchyn and Ilich 2017).

We reconstructed estimates of warm (May–September) and cool (October–April) season streamflow for the NSR at Edmonton from multi-species measurements of annual ring width (RW), earlywood width (EW) and latewood width (LW) using standard methods in dendrohydrology (Meko et al. 2012). Multiple linear regression (MLR) using a forward stepwise procedure with a cross-validation stopping rule (leave n-out) was used to model and reconstruct warm and cool season streamflow from 1200 to 2015. The tree-ring models were calibrated over the full instrumental naturalized streamflow record (1912–2010) using a nested approach, where shorter tree-ring chronologies are dropped from the pool of predictors and the procedure is repeated using the remaining longer series. No more than five chronologies were used for each reconstruction nest, in order to avoid multi-collinearity and an over-fit model, while achieving maximum reduction of the residual variance not accounted for by predictors already in the model. Predictors included lagged (±two years) chronologies to account for any differences in the timing of the response of streamflow and tree growth to inputs of precipitation and snow meltwater.

Following the methods of Kerr et al. (In review), each nest of estimated streamflow is a discrete independent reconstruction (i.e. for each season), using tree-ring chronologies that positively correlate with either warm or cool season streamflow, or both. None of the same chronologies was used as potential predictors in the other reconstruction. This procedure was applied to minimize inter-seasonal correlation in the tree-ring reconstructed estimates of streamflow, which can be seen in sub-annual chronologies (i.e. EW and LW) from the same tree (Stahle et al. 2020; Kerr et al. In review). Calibration and verification statistics indicate skilful reconstructions of warm and cool season streamflow from robust models with considerable predictive power. The models accounted for up to 65% of the naturalized streamflow instrumental variance. As illustrated in Fig. 2.11, the reconstructions replicated the inter-annual variability in historical streamflow, but are better at capturing low flows, while underestimating high flows, throughout the calibration period. Underestimation of peak flows is a common limitation of dendrohydrology, as there is a biological limit to the response of tree growth to high precipitation and low evapotranspiration during wet years. Nested models were discarded after approximately

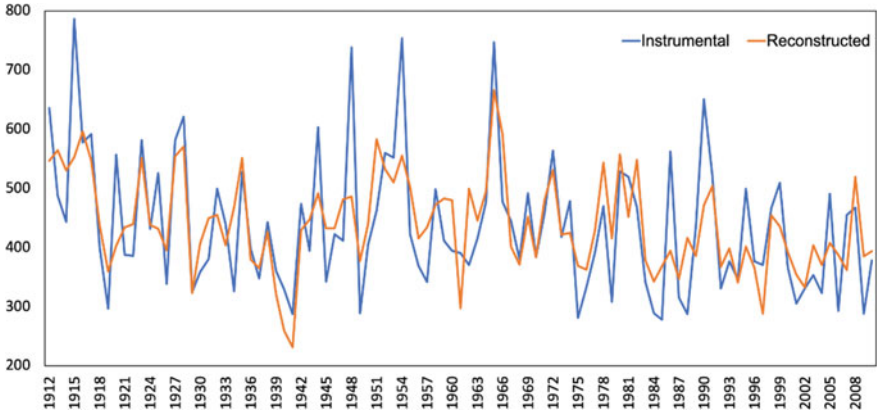

Fig. 2.11 NSR at Edmonton instrumental and tree-ring reconstructed warm season streamflow (m^3/s) for the calibration period, 1912–2010

1200, as R^2_{adj} values began to decline to below 35%, and other descriptive statistics indicated the model prediction was declining, due to a lack of sample depth of statistically significant chronologies.

In Figs. 2.12 and 2.13, the reconstructions (1200–2015) of the warm and cool seasonal flow of the NSR at Edmonton are shown as anomalies (departure from the mean). The seasonal paleohydrology reflects the natural variability of the climate recorded in the tree-rings. The low flow years of the instrumental record (i.e. 1930s,

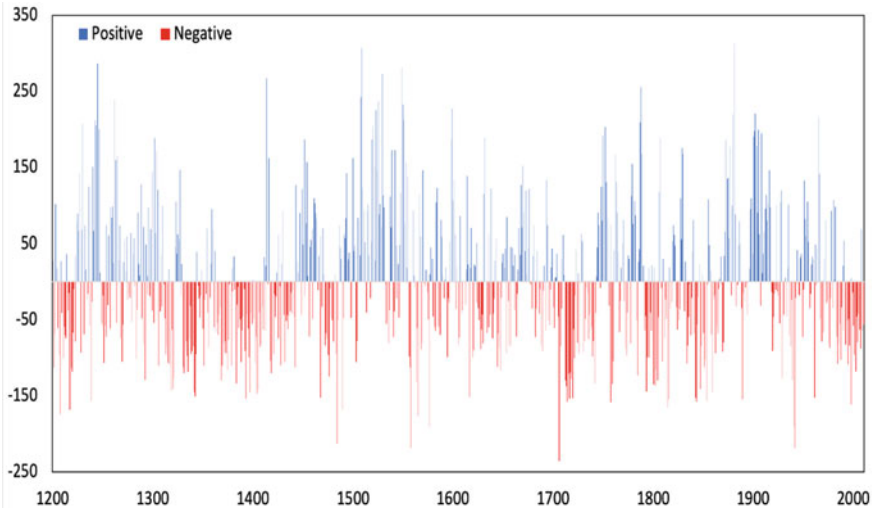

Fig. 2.12 Tree-ring reconstructed warm season (May through August) streamflow (m^3/s) plotted as positive (blue) and negative (red) departures from the mean warm season flow for the NSR at Edmonton, 1200–2015

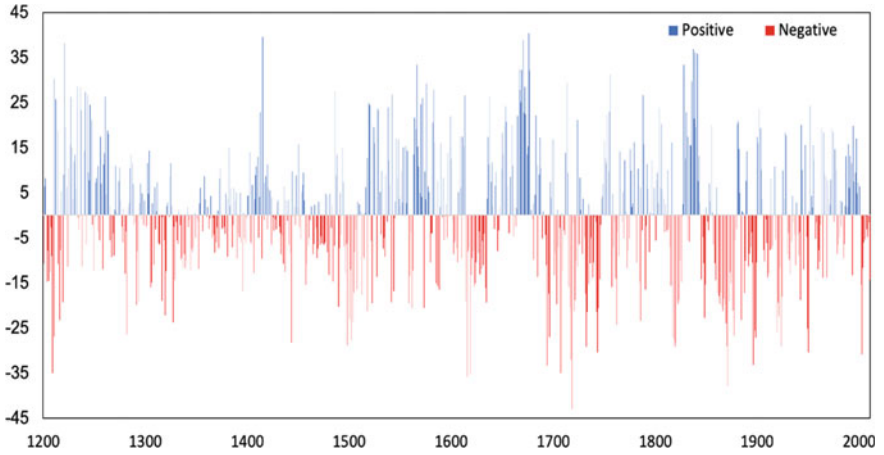

Fig. 2.13 Tree-ring reconstructed cool season (December through April) streamflow (m^3/s) plotted as positive (blue) and negative (red) departures from the mean cool season flow for the NSR at Edmonton, 1200–2015

1980s and early 2000s) are clearly visible. Even more noticeable are periods of low flow that exceed the historical worst-case scenario in terms of severity and duration (i.e. fourteenth and fifteenth centuries in the warm season record). Decadal scale variability is also evident in these plots, in terms of successive years of high and low flows, which last one to three decades. In both seasons, low- and high-water levels reoccur at more or less regular intervals.

We further explored the reconstructed time series of warm and cool season streamflow for a better understanding of the global drivers of the natural variability in the regional hydroclimate. The long-term seasonal impacts of slowly varying modes of sea surface temperature (SST) variability are realized in their decadal-to-multidecadal effects on other teleconnections and large-scale atmospheric circulation (Howard et al. 2019). We identified the main oscillatory modes of variability in the NSRB paleohydrology using continuous wavelet transform (Grinsted et al. 2004) of the reconstructed warm and cool seasonal flows of the NSR at Edmonton. The wavelet plots in Figs. 2.14 and 2.15 show significant multi-decadal and inter-annual modes of variability, which can be linked to the influence of the PDO and ENSO on the hydroclimate of western North America (St. Jacques et al. 2010; Sauchyn et al. 2015; Gurrapu et al. 2016; Sauchyn and Ilich 2017).

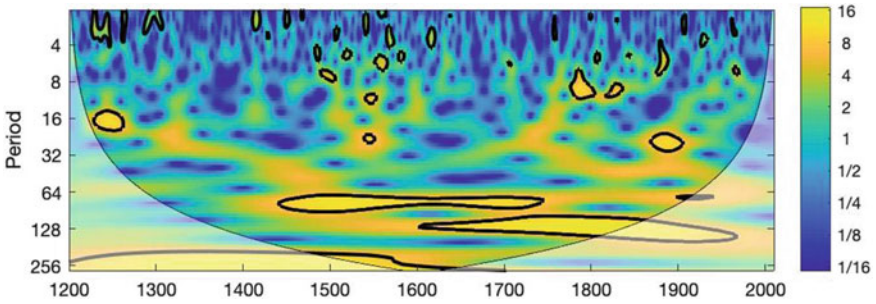

Fig. 2.14 Continuous wavelet power spectrum for warm season tree-ring reconstructed streamflow (1200–2015) of the NSR at Edmonton. Thick black contour lines indicate significance at 95% level

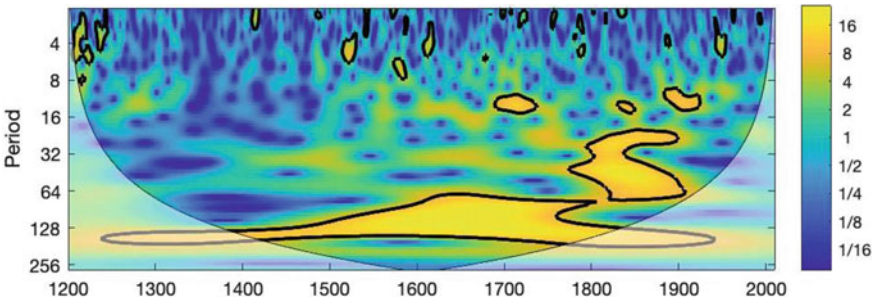

Fig. 2.15 Continuous wavelet power spectrum for cool season tree-ring reconstructed streamflow (1200–2015) of the NSR at Edmonton. Thick black contour lines indicate significance at 95% level

2.3 Water Use and Demand

2.3.1 Historical Water Use

The security of water supplies is function of not only supply, but also the demands placed on these supplies for industrial and residential use. Information on the use and consumption of water in the Edmonton region is available from the annual reports compiled by EPCOR Water Canada and from studies for the North Saskatchewan Watershed Alliance (NWSA) by AMEC (2007) and Thompson (2016). Additional province-wide data from the Alberta Water Use Reporting System (https://aep.alberta.ca/water/reports-data/water-use-reporting-system/default.aspx) indicate that 70% of licenced surface water use in the NSRB occurs within the Capital Region (Strawberry, Sturgeon, Beaverhill sub-basins; Fig. 2.5). This region had a slight increase in water allocations and use in 2016 compared to 2006, with a large increase in commercial water use and decrease in industrial water use. About 20% of the licenced surface water use occurs within the Headwaters Region (Cline, Brazeau, Ram, Clearwater, Modeste sub-basins). Water allocations and use within

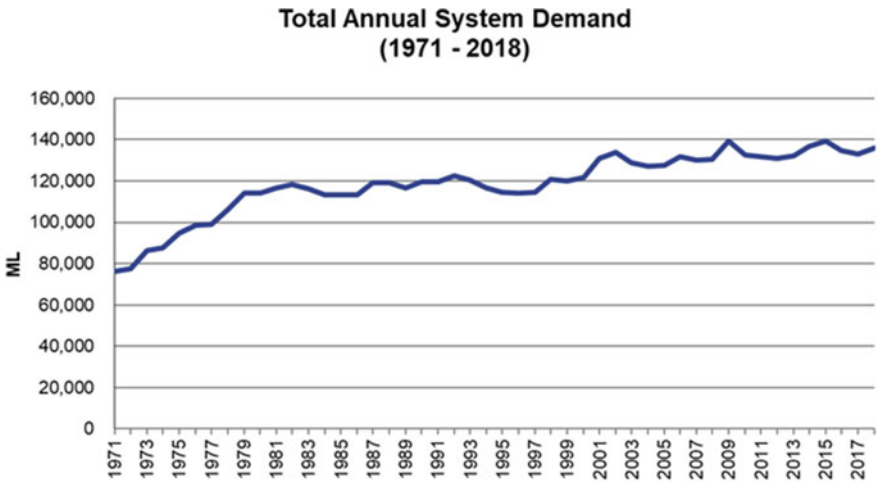

Fig. 2.16 Total annual demand, from 1971 to 2018, for the Edmonton regional water system. *Source* EPCOR Water Canada

the basin had changed slightly by 2016 compared to 2006: 2% increase for licenced withdrawals and 7% increase for licenced use (Thompson 2016).

Unlike the closed sub-basins (Bow, Oldman and SSR) in southern Alberta, Alberta Environment and Parks continues to grant water licences in the NSRB. About 20% of the NSR is allocated, while much less water is extracted. That is, full allocations are not being used and much of the water that is extracted is returned to the NSR. The amount of water in the NSR is large relative to the volume of water withdrawn by the Water Treatment Plants (WTPs) for drinking water purposes, which is less than 3% of the total daily flow (EPCOR 2017). Figure 2.16 is a plot of the total annual demand, from 1971–2018, for the Edmonton regional water system. There are two notable inflections in this demand curve. Demand rose through the 1970s and then levelled off until 2000 when there was another rise in demand to a slightly higher level. The mean average daily demand for 2001–2018 was 363 ML/d, and mean peak hour demand was 741 ML/d.

Figure 2.17 of average daily demand from 1971–2018 makes a distinction between the City of Edmonton, which accounts for most of the demand, and the larger metropolitan region. Regional water use has increased at a faster rate than in the city; it was almost 5 times higher in 2018 than in 1971, while in-city water use was only 1.5 times higher. By 2018, raw water intake increased by 24% compared to 1983. Data for in-city commercial total water consumption are available for 1991–2018 only; consumption decreased by 31% over this period.

While total consumption (residential, multi-residential, commercial and regional) in 2018 was 78% higher than in 1971, per capita Edmonton water consumption decreased. Total per capita water use in 2018 was 42% lower than the 1971–1980 average (31% lower than 2001), at 289 L/capita/d, while the city's population increased by 2.1 times, from 462,572 (1971–1980 average) to 951,000 (2018).

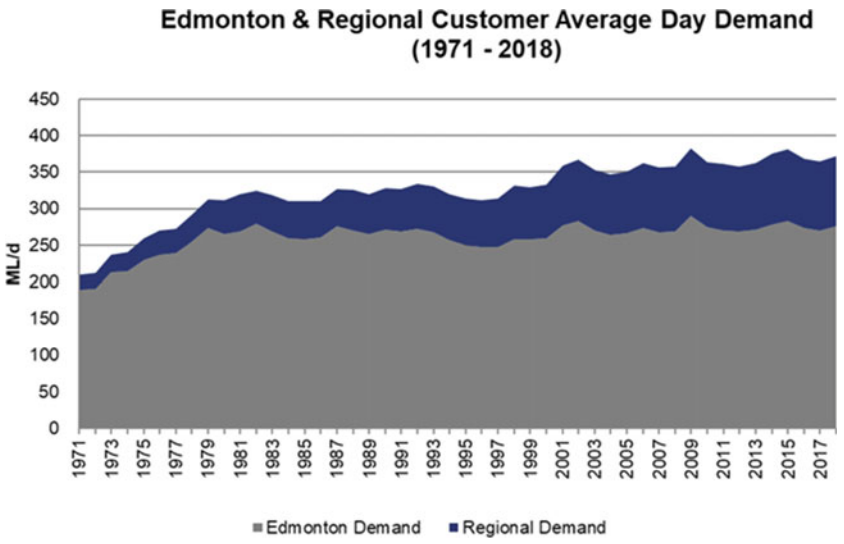

Fig. 2.17 Average daily water demand from 1971 to 2018 for the City of Edmonton and the larger metropolitan region. *Source* EPCOR Water Canada

Figure 2.18 clearly illustrates the decoupling of water demand from population growth. Since about 1980, per capita demand has declined at a significant rate while the population approximately doubled. Programmes and practices for the conservation and more efficient use of water have obviously been effective. Outdoor water use

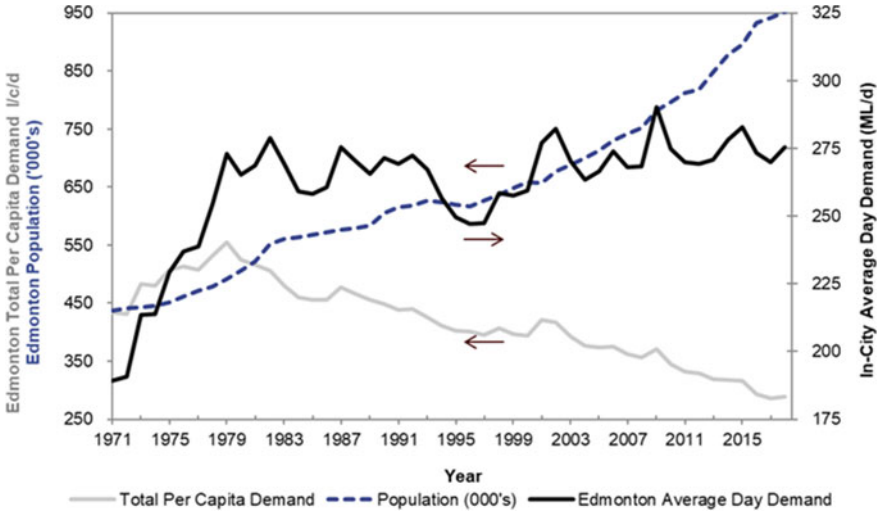

Fig. 2.18 Average daily demand, population and total per capita demand per year for the City of Edmonton from 1971 to 2018. *Source* EPCOR Water Canada

typically accounts for much of the water demand in North American cites. Although Edmonton has a relatively short summer compared to other cities, climate change projections of shorter winters and longer warmer summers could increase the demand for outdoor water use.

2.3.2 *Projected Water Demand*

Demand for water will grow in coming decades because Alberta's population is expected to reach 6.4 million by 2046, an increase of about 2.1 million people from 2017. It also is becoming more concentrated in urban centres; by 2046, almost 8 in 10 Albertans are expected to reside in the Edmonton–Calgary corridor (Treasury Board and Finance 2018). Based on population growth alone, increased demand for water is anticipated; however, water use and demand depend on other factors, including policies, population, infrastructure, technology, human behaviour and climate. While future water demand has been forecasted for Alberta River Basins, these studies considered different combinations of the determinants of demand, and some studies are outdated, for example, the forecasting of demand by 2015 (City of Calgary 2007).

AMEC Earth & Environmental (2007) completed an overview of current and future water use in Alberta for the Ministry of Environment. They examined licenced and actual water use to October 2006 for six sectors: municipal and residential, agricultural, commercial, petroleum, industrial and other. Forecasting was based on expected changes in population and economic activity. Thus, they were "business-as-usual" predictions since they did not account for improvements in water use efficiency. A 21% increase from current water use (2005) was the net result for the entire province; however, most of this increase was attributed to rising water demand in the irrigation and industrial (petroleum) sectors, and thus concentrated in the southern and more northerly river basins, respectively. For the NSRB, projections of the increase in water demand over 20 years (2005–2025) ranged from 15% for a low growth scenario to 118% for a high growth scenario. The increase in demand for a medium growth scenario was about 34%.

Accurate prediction of water usage is important for both short-term (operational) and long-term (planning) aspects of urban water management. Water demand forecasting models tend to overestimate long-term demands because they generally do not account for water conservation practices and reductions in per capita usage, such as the declining water consumption per customer over the past three decades at Edmonton (Fig. 2.18). As populations and economies grow, water demand does not necessarily increase at a proportional rate, given effective conservation and efficiency practices. A major "Residential End Uses of Water Study" (DeOreo et al. 2016) of North American water utilities found a 22% decrease in average annual indoor household water use from 1999–2016. Edmonton was one of three Canadian cities included in the study.

To improve the accuracy of demand forecasts for municipal water management, Liu and Davies (2019) developed a model for Edmonton and applied it to long-term

water demand forecasting using climate model projections of daily temperature and precipitation. Their model provides a projection of total demand based on inputs of daily and weekly water demand and meteorological variables. Their data-driven forecasting model is run in the framework of a system dynamics model that can be used to replicate physical structures and processes and explore the future demand for various water end uses under different scenarios related to policy, climate and population changes. The daily and weekly water demand models for Edmonton constructed by Liu and Davies (2019) reveal that maximum and average temperatures produce more accurate results than minimum temperature, probably because outdoor watering in summer relates more strongly to daytime average and high temperatures than to the daytime low. Furthermore, models using indices of the timing of water demand (e.g. "day-in-week" and "day-in-month") produced significantly better results than those without these indices that capture the periodicity of water demand. Outdoor water demand in summer is an important component of municipal water demand.

2.4 The Future Climate of the NSRB

Projections of the future climate of the NSRB have been previously derived from output from Global Climate Models at a relatively course scale (100 s km) with downscaling based on the statistical relationship between model and observed weather data (e.g. Jiang et al. 2017; Vaghefi et al. 2019). We have developed climate projections for the NSRB above Edmonton using high-resolution (25–50 km) data from Regional Climate Models (RCMs), which were applied to the dynamical downscaling of Earth System Models (ESMs). We accessed output for an ensemble of 10 RCMs from the data repository of the North American domain of the Coordinated Regional Climate Downscaling Experiment (NA-CORDEX). All RCMs were forced with RCP 8.5, a high emissions pathway. Monthly, seasonal and annual mean temperature (°C) and total precipitation (mm) were computed by averaging values for model grid points within the boundary of the NSRB. We determined changes in 30-year average temperature and precipitation for the near (2021–2050) and mid (2051–2080) future compared to the climate of the baseline period 1981–2010. Table 2.1 gives the multi-model mean changes. Mean temperature and total precipitation are projected to increase on seasonal and annual scales, with the greatest changes during the cool period (fall, winter). Mean summer temperature is expected to increase by 3.5 °C with almost no change in total precipitation.

Whereas Table 2.1 presents the mean multi-model climate changes, the scatterplot in Fig. 2.19 shows the range of mid-future (2051–2080) projections derived from the 10 RCMs. Increases in annual precipitation and temperature range from 2 to 18% and 2 to 4.5 °C, respectively. The largest temperature changes highlighted in Table 2.1 occur in winter. Figure 2.20 presents evidence of a dramatic decline in the frequency of extreme winter temperatures at Edmonton, as simulated by the Canadian Regional Climate Model version 5, with boundary conditions from the Community Earth System Model version 2 (CRCM5_cesm2). Since this is a model simulation,

Table 2.1 Multi-model mean changes in temperature and precipitation for near (2021–2050) and far (2051–2080) future compared to baseline (1981–2010)

Period	Climatic variable	2021–2050	2051–2080
Annual	Mean temperature (°C)	1.9	3.7
	Maximum temperature (°C)	1.7	3.4
	Minimum temperature (°C)	2.1	4.0
	Total precipitation (mm)	32.5	54.2
	Total precipitation (%)	6.9	11.5
Spring (MAM)	Mean temperature (°C)	1.8	3.0
	Maximum temperature (°C)	1.6	2.7
	Minimum temperature (°C)	2.1	3.3
	Total precipitation (mm)	9.5	26.9
	Total precipitation (%)	10.5	29.4
Summer (JJA)	Mean temperature (°C)	2.3	3.5
	Maximum temperature (°C)	**2.4**	3.6
	Minimum temperature (°C)	2.1	3.6
	Total precipitation (mm)	9.0	7.4
	Total precipitation (%)	3.9	3.3
Fall (SON)	Mean temperature (°C)	1.3	3.7
	Maximum temperature (°C)	1.1	3.5
	Minimum temperature (°C)	1.7	3.8
	Total precipitation (mm)	17.2	25.0

(continued)

Table 2.1 (continued)

Period	Climatic variable	2021–2050	2051–2080
	Total precipitation (%)	**21.2**	**30.9**
Winter (DJF)	Mean temperature (°C)	**2.2**	**4.9**
	Maximum temperature (°C)	1.9	**4.1**
	Minimum temperature (°C)	**2.5**	**5.5**
	Total precipitation (mm)	8.8	15.3
	Total precipitation (%)	13.9	24.0

The largest increases are highlighted with bold font

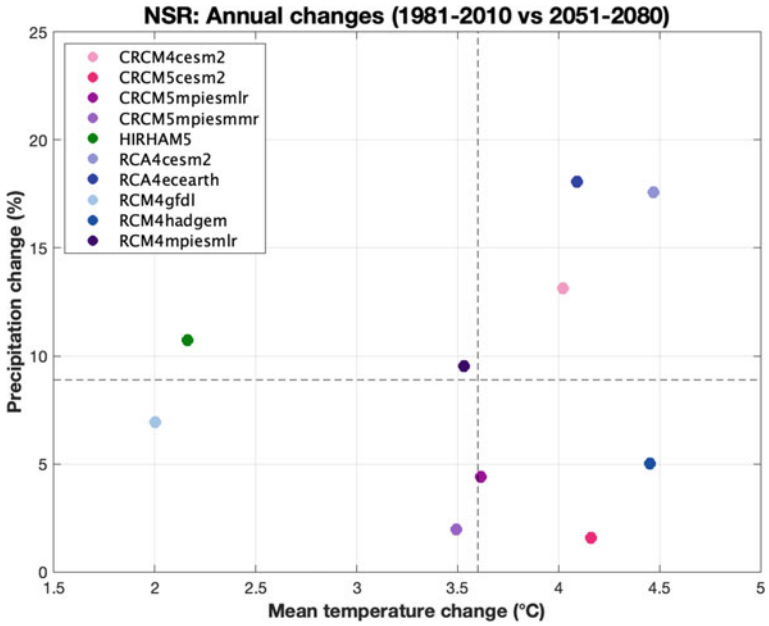

Fig. 2.19 Scatterplot of climate change projections derived from 10 RCMs

the sequence of extreme temperatures is arbitrary. A different RCM would produce a different sequence, although statistically (i.e. the range and trend) the results would be very similar.

Figures 2.21 and 2.22 are time series of total summer and spring precipitation, respectively, for the North Saskatchewan River Basin above Edmonton. For the

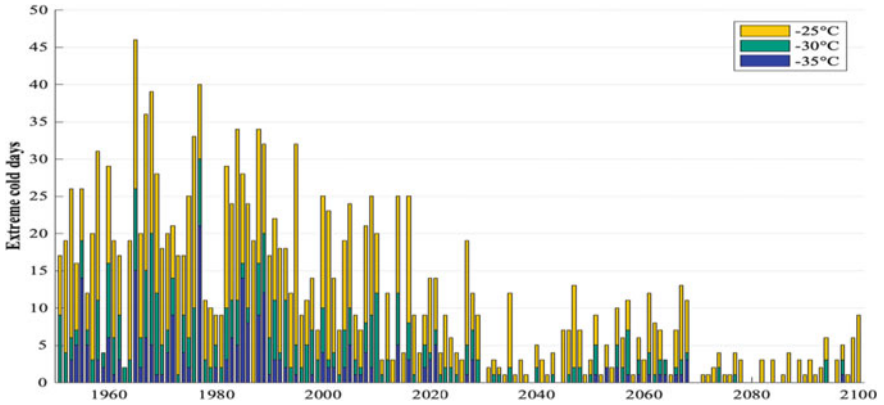

Fig. 2.20 Extreme minimum temperatures at Edmonton, 1951–2100, as simulated by CRCM5_cesm2 and RCP 8.5

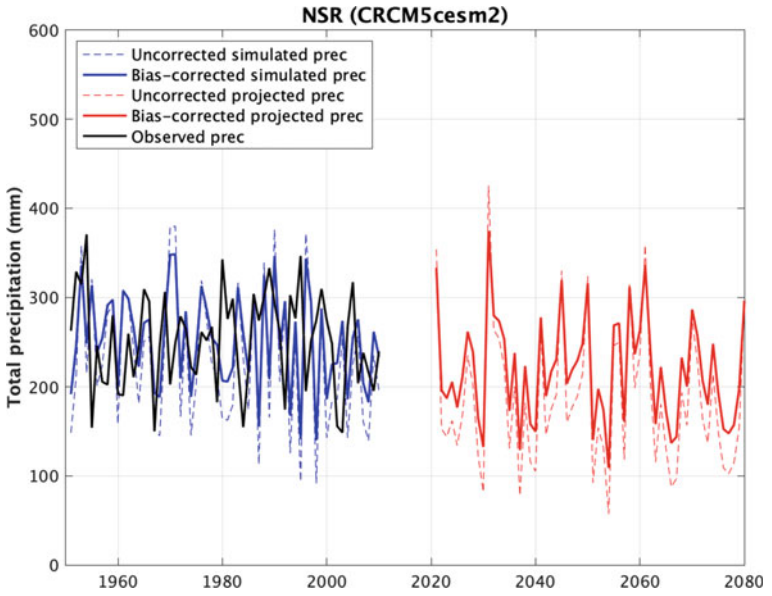

Fig. 2.21 Simulated and observed (1951–2015) total summer precipitation, North Saskatchewan River Basin above Edmonton. The bias corrected data is from CRCM5_cesm2

historical period (1951–2015), both simulated and observed data are shown. The historical and projected (2021–2080) model output is from CRCM5_cesm2 and was bias corrected. These plots illustrate a contrast between the negligible change in summer versus an upward trend in and spring. They also display the large inter-annual and decadal variability characteristic of the hydroclimate of the region.

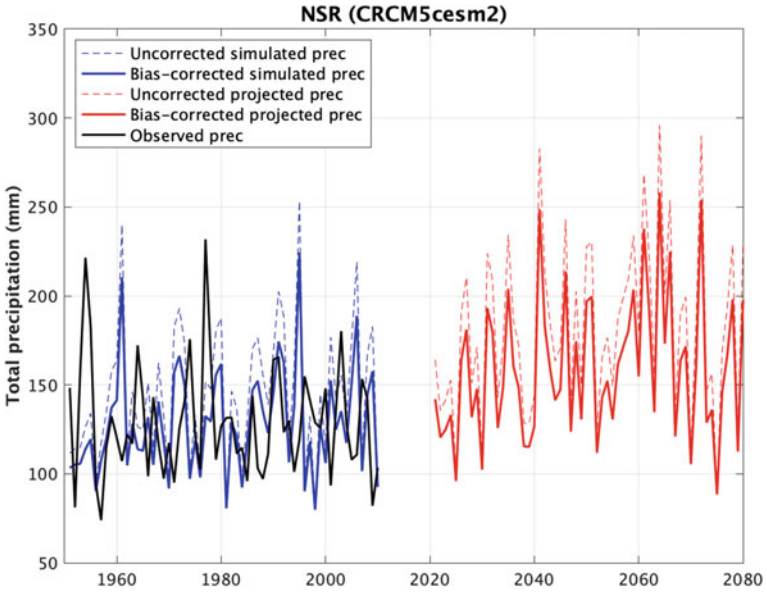

Fig. 2.22 Simulated and observed (1951–2015) total spring precipitation, North Saskatchewan River Basin above Edmonton. The bias corrected data is from CRCM5_cesm2

Figure 2.23 is a plot of the projected maximum daily precipitation changes at Edmonton from 1950 to 2100 as simulated by the CRCM5_cesm2 (RCP 8.5). According to the scatterplot in Fig. 2.16, this RCM/ESM experiment projects the least change in annual precipitation, plotting at about 2% on the vertical axis. Despite the negligible change in total annual precipitation, precipitation on one future day far exceeds prior extreme events. This time series also displays inter-annual and decadal variability; years with heavy precipitation events tend to cluster in wet decades and with dry decades in between.

2.5 Hydrological Response to Projected Climate Changes

Previous research on the impact of climate change on the North Saskatchewan River (NSR) (Golder 2008; Kienzle et al. 2012) found increased flow during winter and spring, earlier spring melt and decreased flow during the summer and fall. These shifts in the seasonal distribution of river flow are in response to projected climate changes: a warmer wetter winter and a warmer and possibility drier summer. Summer flows are impacted by reductions in the extent of glacier ice and summer snowpack at high elevations in the headwaters. These prior studies were based on the use of data from GCMs as inputs to hydrological models to project changes in average seasonal

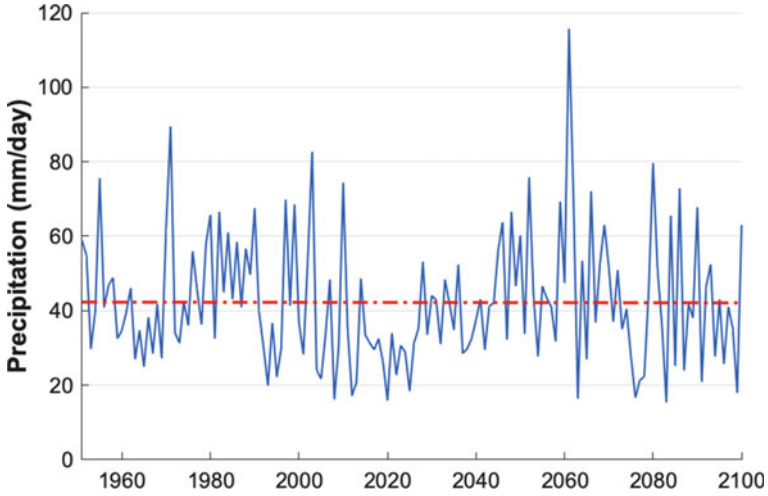

Fig. 2.23 Maximum daily precipitation at Edmonton, 1950–2100, as simulated by the CRCM5_cesm2 and RCP 8.5

flows. In contrast, our work is based on the use of high-resolution climate change projections from RCMs to drive runs of a calibrated distributed hydrological model.

2.5.1 Hydrological Modelling of the NSRB Above Edmonton

We simulated the hydrology of the NSRB above Edmonton using the Modélisation Environmentale–Surface et Hydrologie (MESH) grid-based modelling system (Fig. 2.24). MESH is a standalone land surface-hydrology model developed initially by Environment and Climate Change Canada (Pietroniro et al. 2007). It has been widely applied to various cold regions of Canada (Davison et al. 2006; Pietroniro et al. 2007). MESH has three components: (1) the Canadian Land Surface Scheme (CLASS) (Verseghy 1991; Verseghy et al. 1993) that computes the energy and water balances using physically based equations for soil, snow and vegetation canopy at a 30 min time step, (2) lateral movement of soil and surface water to the drainage system with either of the algorithms called WATROF (Soulis et al. 2000) or PDMROF (Mekonnen et al. 2014), and (3) hydrological routing using WATFLOOD (Kouwen et al. 1993) that collects overland flow and interflow from each grid cell at each time step and routes them through the drainage system. The river routing is based on a storage routing technique in which the channel roughness and storage characteristics control the inflows from the local grid and upstream river reach. The land model is run on each tile independently. The overall fluxes and prognostic variables for each grid cell are obtained by taking a weighted average of the results from tiles.

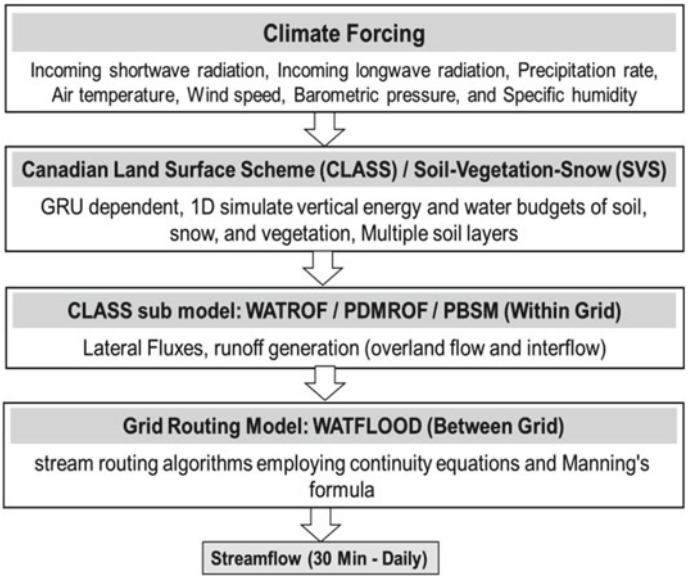

Fig. 2.24 MESH land-surface and hydrology modelling system schematic diagram

A 0.125° drainage database consisting of 278 grid cells was constructed using the Green Kenue tool (v3.4.3) as shown in Fig. 2.25. Topographic data was from the Canadian Digital Elevation Model (CDEM 2015) at a scale of 1:250,000. The shape files

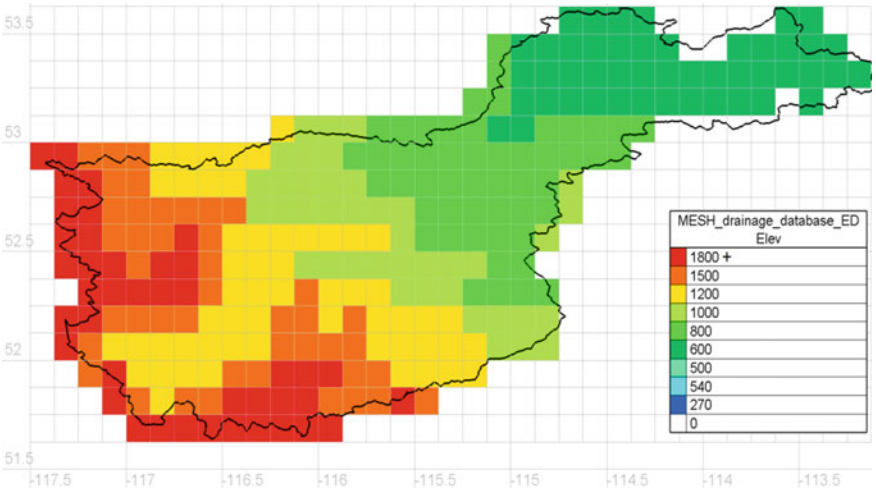

Fig. 2.25 Drainage database of NSR at Edmonton. Each grid represents one Grouped Response Unit (GRU) with soil, land use, drainage area, elevation, channel length and slope data

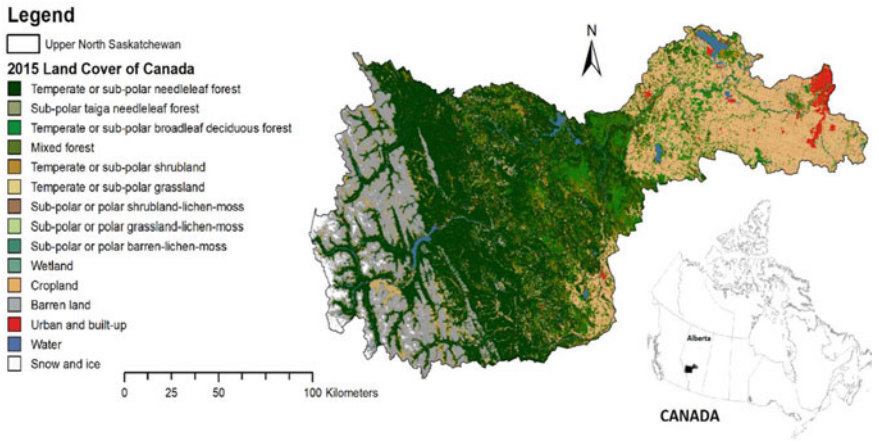

Fig. 2.26 Land-cover classification of Upper North Saskatchewan River Basin generated by the Canada Centre for Remote Sensing (CCRS)

of the catchment and rivers are available from the National Hydro Network—NHN—GeoBase Series (https://open.canada.ca/data/). The soil data was acquired from Agriculture and Agri-Food Canada. The 30-m land-cover data (Fig. 2.26, Pouliot el al. 2017) was obtained from the Canada Centre for Remote Sensing (CCRS). Twelve land-cover types were used to define Grouped Response Units (GRUs). For computational efficiency, a GRU-based approach combines areas of similar hydrological behaviour to address the complexity and heterogeneity of the drainage basin. Each model grid cell is represented by a limited number of distinct GRUs (tiles) weighted by their respective cell fractions. For large basins, this approach has been found more efficient with its operational simplicity while retaining the basic physics and behaviour of a distributed model (Pietroniro and Soulis 2003).

2.5.2 Calibration and Validation of the MESH Model

The MESH model was calibrated and validated using the bias-corrected historical gridded climate data WFDEI-GEM-CaPA (Asong et al. 2018). Future flows were simulated using bias-corrected data from 15 runs of the Canadian Regional Climate Model (CanRCM4) based on the RCP8.5 emission scenario (Asong el al. 2020; Scinocca et al. 2016). Running MESH requires three hourly climate forcing data for seven variables: shortwave radiation, longwave radiation, precipitation rate, air temperature, wind speed, barometric pressure and specific humidity.

Figure 2.27 is a plot of observed and simulated daily runoff of the NSR at Edmonton for the calibration (Feb 1995–Dec 2002) and validation (Jan 2003–Dec 2010) periods. Goodness of fit results for the calibration and validation are given in Table 2.2. The calibration NSE of 0.69 indicates good agreement between modelled

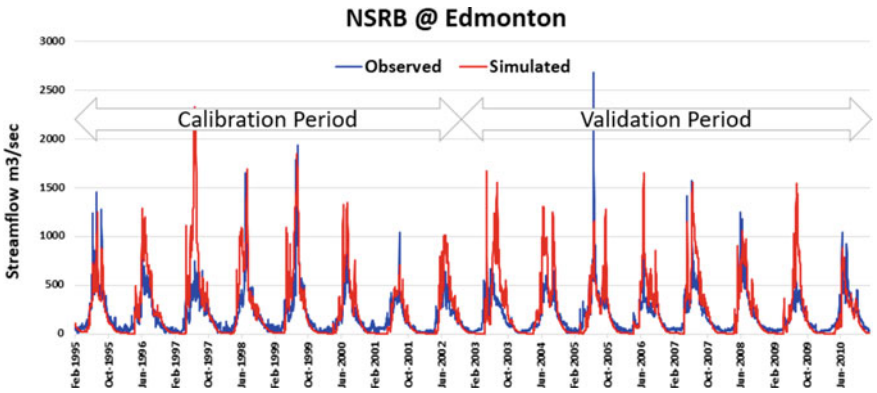

Fig. 2.27 Comparison of observed and simulated daily runoff of NSR at Edmonton for calibration (Feb 1995–Dec 2002) and validation period (Jan 2003–Dec 2010) using MESH hydrological model

and observed flows. The prediction of low flows (lnNSE) could be improved further to reduce bias. However, the overall performance of model dynamics and seasonal variability is well captured by the MESH model with a KGE value of 0.47 indicating a strong relationship between simulated and observed flows. MESH provides a close fit to the recorded flows for the calibration period, while for the independent validation period the performance is somewhat reduced, as expected in validation mode. The reduction is, however, limited, and the model is able to maintain a very good representation of the overall water balance and the inter-annual and seasonal variations. The NSE and KGE values cannot be directly compared and should not be treated as approximately equivalent (Knoben et al. 2019).

2.5.3 Streamflow Projections

The results of running the calibrated MESH model with 15 ensemble members of bias-corrected CanRCM4 (RCP 8.5) data from 1950 to 2100 are shown in Fig. 2.28. This ensemble of time series exhibits large variably around a trend of increasing flow. These results are for one ESM (CanESM2) and one RCM (CanRCM4). We have controlled for uncertainty with the use one GCM/RCM pair and one greenhouse gas emission scenario. Thus, differences among the streamflow projections reflect the internal variability of the hydroclimate in a warming climate. Figure 2.28 indicates that the future flow of the NSR will include the annual and decadal variability that is evident in our 800-year tree-ring reconstruction of the river flow. However, the range of annual flows will exceed those observed in the recent past. This very likely represents the amplification of the hydrological cycle in a warmer climate. Low flows, in particular, frequently reach those in the gauge record, even though a warming climate will be characterized by more precipitation and rising mean water levels.

Table 2.2 Goodness of fit results for the calibration and validation period of NSR at Edmonton streamflow station

	Calibration (Feb 1995–Dec 2002)			Validation (Jan 2003–Dec 2010)		
Goodness of fit statistic	Nash–Sutcliffe efficiency (NSE)	Log of Nash–Sutcliffe efficiency (lnNSE)	Kling–Gupta efficiency (KGE)	Nash–Sutcliffe efficiency (NSE)	Log of Nash–Sutcliffe efficiency (lnNSE)	Kling–Gupta efficiency (KGE)
	0.69	0.4	0.47	0.67	0.32	0.29

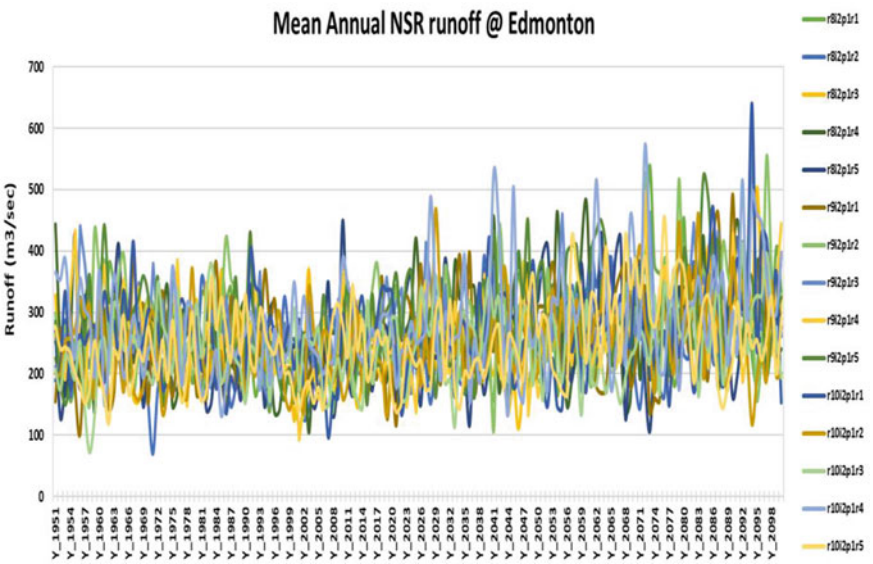

Fig. 2.28 Mean annual runoff of NSR at Edmonton using MESH and a 15-member ensemble of bias-corrected CanRCM4 data (RCP8.5)

Figure 2.29 is a plot of the annual water-year hydrograph for the baseline (1951–2010) and future periods (2041–2100). The daily flows were derived from the MESH model run with the 15-member ensemble of bias-corrected CanRCM4 data and the high emission scenario RCP 8.5. It clearly shows a shift in the hydrograph towards peak flows earlier in the year, with higher winter flows, early snowmelt and lower summer flows. There is a one-month shift towards earlier snowmelt and peak flow.

2.6 Discussion

Changes in the severity of extreme hydrological events, and in the seasonal distribution of water resources, will have major impacts on terrestrial and aquatic ecosystems and on the availability of municipal and industrial water supplies (Sturm et al. 2017; Fyfe et al. 2017). Both incremental long-term changes in water levels and extreme fluctuations around the changing baseline will have impacts requiring adaptation of water resource planning and policy. Water allocation and the design of storage and conveyance structures, such as reservoir and irrigation canals, are based mainly on average seasonal water levels, but otherwise water resources are managed to prevent the adverse impacts of flooding and drought. The operation, and possibly structural integrity, of infrastructure for drainage, water supply and treatment is vulnerable to climate change. Much of the risk is due to the expectation of more intense precipitation, prolonged low water levels and more extreme weather events.

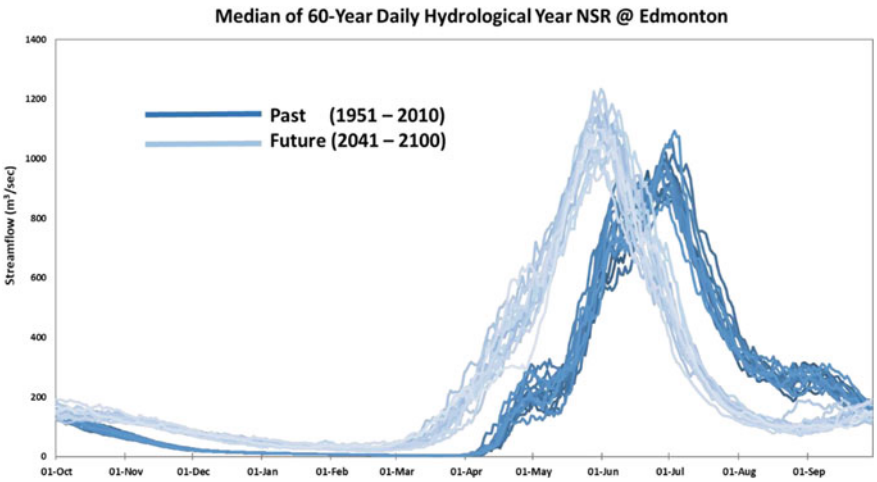

Fig. 2.29 Comparison of median 60-Year of daily NSR runoff at Edmonton for a baseline from (1951–2010) and future scenarios (2041–2100) derived from the MESH hydrological model run with the 15-member ensemble of bias-corrected CanRCM4 data and the high emission scenario RCP8.5

In this paper, we examined the implications of climate change for water security in western Canada, using the North Saskatchewan River Basin (NSRB) as a case study. We developed reconstructions of the pre-industrial streamflow and projections of future climate and hydrology. Most of the climate change in this region has been an increase in the lowest temperatures; minimum daily winter temperatures have increased by about 6 °C. There is no significant trend in the instrumental record of precipitation. Fluctuations in precipitation over the past 120 years are dominated by large differences between years and decades.

A decrease in the average flow of the North Saskatchewan River (NSR) at Edmonton since 1911 is consistent with a warming climate and the resulting loss of glacier ice and summer snowpack at high elevations in the headwaters of the river basin. However, the decline is relatively small compared to large natural inter-annual and decadal variability in flow. Natural cycles in water levels are very apparent in the paleohydrology of the NSR, an 815-year reconstruction of seasonal river flow from tree rings collected in the upper part of the river basin. The decadal cycle is particularly evident in the paleohydrology, with long periods of consistently low river levels and hydrological drought.

Future projections from RCMs suggest warmer and wetter conditions in winter and spring and, on average, drier conditions in mid to late summer. One of the most robust climate change projections is an increase in rainfall intensity. A warming climate will amplify both the wet and dry phases of the natural cycle in the regional hydroclimate. In response to the projected climate changes, the seasonal pattern of river flow will shift, with future river levels peaking about one month earlier. Cold

season (winter and early spring) flows will be significantly higher. River flows in June to August will be, on average, lower than in the past.

Our approach to research on water security examines the extent to which impacts of global climate change on water resources exceeds the natural variability in hydroclimate as captured by our tree-ring records. Proxy records of past climate and hydrology can be used to constrain future projections of regional hydroclimate (e.g. Ault et al. 2014; PAGES Hydro2k Consortium 2017; Schmidt et al. 2014; Smerdon et al. 2015). Historical model simulations and proxy records cannot be directly compared unless initial conditions are identical. Model simulation of the unforced (internal) variations, which the proxies depict, will differ among models. Therefore, the best approach to comparing paleo- and climate model data is based on their underlying statistical distributions and the full spectrum of variability. Despite uncorrelated temporal variability, the power spectra of the time series will reflect similar climate forcings, such as teleconnections between the regional climate and ocean–atmosphere oscillations. To illustrate these types of proxy-model comparisons, Fig. 2.30 is a plot of 200 years of tree-ring inferred annual normalized streamflow at Edmonton and output from the MESH hydrological model driven using precipitation and temperature from a pre-industrial control run of the CMIP6 model MRI ESM 2.0. The two curves exhibit similar inter-annual variability and range of streamflow. A wavelet transform of the winter and spring components of these time series (Fig. 2.31) reveals that they both have significant high-frequency variability corresponding to the influence of ENSO, although whereas this mode of variability spans for 2–8 years for the proxy streamflows, it is confined to a more narrow range (2–4 years) for the modelled river hydrology. Decadal scale variability is more prominent in the tree-ring record, suggesting that the climate model may not be fully simulating this significant mode of variability.

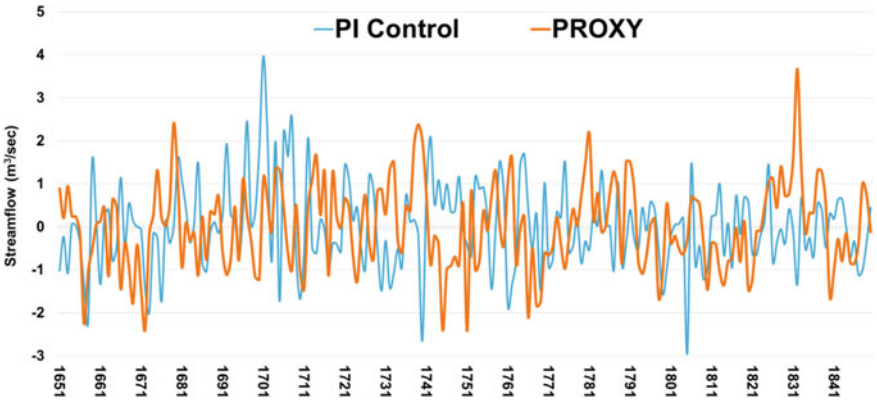

Fig. 2.30 200 years of tree-ring inferred annual normalized streamflow at Edmonton and output from the MESH hydrological model driven using precipitation and temperature from a pre-industrial control run of the CMIP6 model MRI ESM 2.0

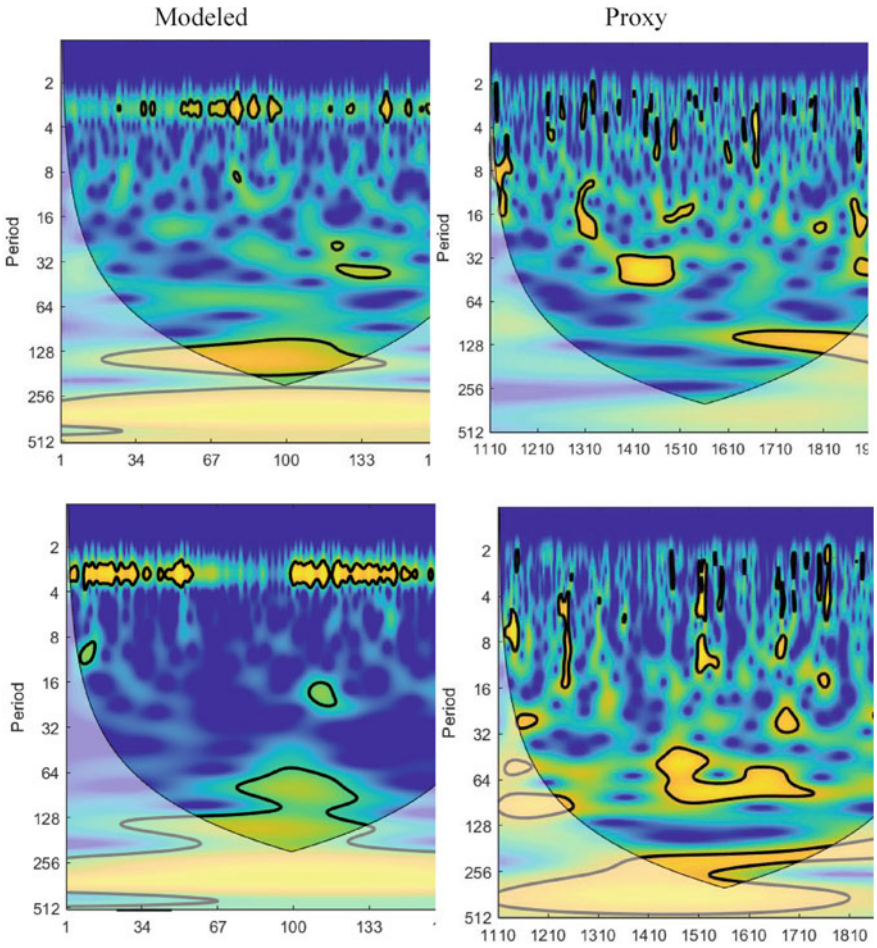

Fig. 2.31 Wavelet Transform of winter (top) and spring (bottom) modelled (left) and proxy (right) streamflow at Edmonton

As a warming climate amplifies the hydrological cycle, the range of river levels will expand, with larger departures from a shifting baseline of higher winter flows and lower summer flows. More precipitation falling as rain rather than snow, combined with earlier spring snow melt, will result in earlier peak streamflows, with subsequent reduced flows in summer, the season of highest water demand. Data from recent decades indicates that absolute water use and demand has increased but at a much lesser rate than the increasing population of the Edmonton region. As a result, there has been a decoupling of per capita water use from growth in the economy and population of the region.

Acknowledgements Funding for the research described in this paper was provided by EPCOR Utilities and the Natural Science and Engineering Council of Canada. The authors thank Mike Christensen for his comments and advice and Sheena Hatcher, Suzy Christoffel, Juan Mauricio Bedoya and Andrea Sanchez-Ponton for their assistance with field and laboratory research.

References

Abbott BW, Bishop K, Zarnetske JP, Minaudo C, Chapin FS, Krause S et al (2019) Human domination of the global water cycle absent from depictions and perceptions. Nat Geosci 12. https://doi.org/10.1038/s41561-019-0374-y

Adjusted and Homogenized Canadian Climate Data (AHCCD) (2017). Available online: https://ec.gc.ca/dccha-ahccd/default.asp?lang=En&n=B1F8423

AMEC Earth & Environmental (2007) Current and future water use in Alberta. Prepared for Alberta Environment, Edmonton, Alberta, 724 pp

Asong ZE, Wheater HS, Pomeroy JW, Pietroniro A, Elshamy ME, Princz D, Cannon A (2018) WFDEI-GEM-CaPA: A 38-year high-resolution meteorological forcing data set for land surface modeling in North America. Earth Syst Sci Data Discuss. https://doi.org/10.5194/essd-2018-128

Asong ZE, Elshamy ME, Princz D, Wheater HS, Pomeroy JW, Pietroniro A, Cannon A (2020) High-resolution meteorological forcing data for hydrological modelling and climate change impact analysis in the Mackenzie River Basin. Earth Syst Sci Data 12:629–645. https://doi.org/10.5194/essd-12-629-2020

Ault TR, Cole JE, Overpeck JT, Pederson GT, Meko DM (2014) Assessing the risk of persistent drought using climate model simulations and paleoclimate data. J Clim 27:7529–7549. https://doi.org/10.1175/jcli-d-12-00282.1

Barrow EB, Sauchyn DJ (2019) Uncertainty in climate projections and time of emergence of climate signals in western Canada. The Int J Climatol. https://doi.org/10.1002/joc.6079

Bawden AJ, Burn DH, Prowse TD (2015) Recent changes in patterns of western Canadian river flow and association with climatic drivers. Hydrol Res 46(4):551–565. https://doi.org/10.2166/nh.2014.032

Bonsal BR, Peters DL, Seglenieks F, Rivera A, Berg A (2019) Changes in freshwater availability across Canada. In: Bush E, Lemmen DS (eds) Chapter 6: Canada's changing climate report. Government of Canada, Ottawa, Ontario, pp 261–342

Burn DH, Aziz OIA, Pietroniro A (2004) A comparison of trends in hydrological variables for two watersheds in the Mackenzie River Basin. Can Water Res J 29(4):283–298. https://doi.org/10.4296/cwrj283

Canadian Digital Elevation Model (CDEM) (2015) computer file. Natural Resources Canada, Ottawa, ON

City of Calgary, Water Resources (2007) Water efficiency plan: 30-in-30, by 2033. Calgary, Alberta, p 80

Comeau LEL, Pietroniro AI, Demuth MN (2009) Glacier contribution to the North and South Saskatchewan Rivers. Hydrol Process 23:2640–2653. https://doi.org/10.1002/hyp.7409

Davison B, Pohl S, Domes P, Marsh P, Pietroniro A, MacKay M (2006) Characterizing snowmelt variability in a land-surface-hydrologic model. Atmos Ocean 44(3):271–287. https://doi.org/10.3137/ao.440305

DeOreo WB, Mayer P, Dziegielewski B, Kiefer J (2016) Residential end uses of water, version 2: executive report for more information about this project, please visit www.waterrf.org/4309. Prepared by: Water Research Foundation, 16 pp

Deser C, Phillips A, Bourdette V, Teng H (2012) Uncertainty in climate change projections: the role of internal variability. Clim Dyn 38:527–546. https://doi.org/10.1007/s00382-010-0977

Environment Canada (1995) The state of Canada's climate: monitoring variability and change. SOE Report 95-1. Atmospheric Environment Service, Environment Canada, Ottawa, Canada
EPCOR (2017) Source water protection plan. Edmonton's Drinking Water System, 138 pp
Fye F, Stahle D, Cook E, Cleaveland M (2006) NAO influence on sub-decadal moisture variability over central North America. Geophys Res Lett 33:L15707
Fyfe J, Derksen C, Mudryk L, Flato G, Santer B, Swart N, Molotch N, Zhang X, Wan H, Arora V, Scinocca J, Jiao Y (2017) Large near-term projected snowpack loss over the western United States. Nat Commun 8 https://doi.org/10.1038/NCOMMS14996
Gizaw MS, Gan TY (2015) Possible impact of climate change on future extreme precipitation of the oldman, bow and red deer river basins of Alberta. Int J Climatol 36(1):208–224
Golder Associates Ltd. (2008) Assessment of climate change effects on water yield from the North Saskatchewan River Basin
Grasby SE, Chen Z, Hamblin AP, Wozniak PRJ, Sweet AR (2009) Regional characterization of the Paskapoo bedrock acquifer system, southern Alberta. Can J Earth Sci 45(12):1501–1516. https://doi.org/10.1139/E08-069
Grinsted A, Moore JC, Jevrejeva S (2004) Application of the cross wavelet transform and wavelet coherence to geophysical time series. Nonlinear Process Geophys 11:561–566. https://doi.org/10.5194/npg-11-561-2004
Gurrapu S, St-Jacques J-M, Sauchyn DJ, Hodder KH (2016) The influence of the PDO and ENSO on the annual flood frequency of Southwestern Canadian Prairie Rivers. J Am Water Resour Assoc 52(5):1031–1045
Hawkins E, Sutton R (2009) The potential to narrow uncertainty in regional climate predictions. Bull Am Meteorol Soc 90(8):1095–1108. https://doi.org/10.1175/2009BAMS2607.1
Hayashi M, Farrow CR (2014) Watershed-scale response of groundwater recharge to inter-annual and inter-decadal variability in precipitation (Alberta, Canada). Hydrogeol J 22(8):1825–1839
Howard IM, Stahle DW, Feng S (2019) Separate tree-ring reconstructions of spring and summer moisture in the northern and southern Great Plains. Clim Dyn 52:5877–5897
Hughes AT, Smerdon BD, Alessi DS (2017) Hydraulic properties of the Paskapoo formation in west-central Alberta. Can J Earth Sci 54(8):883–892
IPCC (2014) Climate change 2014: synthesis report. Contribution of working groups I, II and III to the fifth assessment report of the intergovernmental panel on climate change. In: Pachauri, RK, Meyer LA (eds) Core writing team. IPCC, Geneva, Switzerland, 151 pp
Jiang R, Gan TY, Xie J, Wang N, Kuo CC (2017) Historical and potential changes of precipitation and temperature of Alberta subjected to climate change impact: 1900–2100. Theoret Appl Climatol 127(3–4):725–739
Jiménez Cisneros BE, Oki T, Arnell NW, Benito G, Cogley JG, Döll P et al (2014) Freshwater resources. In: Field CB, Barros VR, Dokken DJ, Mach KJ, Mastrandrea MD, Bilir TE et al (eds) Climate change 2014: impacts, adaptation, and vulnerability. Part A: global and sectoral aspects. Contribution of working group II to the fifth assessment report of the intergovernmental panel of climate change
Kerr SA, Andreichuk Y, Christoffel S, Sauchyn DJ (In review). Comparing paleo reconstructions of warm and cool season streamflow (1400–2018) for the North and South Saskatchewan River Sub-basins, Western Canada. Can Water Resour J
Kienzle SW, Nemeth MW, Byrne JM, MacDonald RJ (2012) Simulating the hydrological impacts of climate change in the upper North Saskatchewan River basin. J Hydrol 412–413:76–89
Knoben WJM, Freer JE, Woods RA (2019) Technical note: inherent benchmark or not? Comparing Nash-Sutcliffe and Kling-Gupta efficiency scores. Hydrol Earth Syst Sci 23:4323–4331. https://doi.org/10.5194/hess-23-4323-2019
Kouwen N, Soulis ED, Pietroniro A, Donald J, Harrington RA (1993) Grouped response units for distributed hydrologic modelling. J Water Resour Plan Manage 119(3):289–305
Liu H, Davies E (2019) Municipal water demand forecasting with ANN and SD models under climate change. In: Proceedings of the 8th international conference on water resources and environment research, ICWRER 2019, June 14th—18th, 2019, Hohai University, Nanjing, China.

MacDonald RJ, Byrne JM, Boon S, Kienzle SW (2012) Modelling the potential impacts of climate change on snowpack in the North Saskatchewan River Watershed. Water Resour Manage 26:3053–3076. https://doi.org/10.1007/s11269-012-0016-2

Marshall SJ, White EC, Demuth MN, Bolch T, Wheate R, Menounos B, Beedle MJ, Shea JM (2011) Glacier water resources on the eastern slopes of the Canadian Rocky mountains. Can Water Resour J 36(2):109–134. https://doi.org/10.4296/cwrj3602823

Marvel K, Cook BI, Bonfils C et al (2019) Twentieth-century hydroclimate changes consistent with human influence. Nature 569:59–65. https://doi.org/10.1038/s41586-019-1149-8

Meko DM, Woodhouse CA, Morino K (2012) Dendrochronology and Links to Streamflow. J Hydrol 412–413:200–209. https://doi.org/10.1016/j.jhydrol.2010.11.041

Mekonnen MA, Wheater HS, Ireson AM, Spence C, Davison B, Pietroniro A (2014) Towards an improved land surface scheme for prairie landscapes. J Hydrol 511:105–116. https://doi.org/10.1016/j.jhydrol.2014.01.020

Moore RD, Allen DM, Stahl K (2007) Climate change and low flows: influences of groundwater and glaciers. Final report prepared for Climate Change Action Fund, Natural Resources Canada, Vancouver, BC

Mudryk LR, Derksen C, Howell S, Laliberté F, Thackeray C, Sospedra-Alfonso R, Vionnet V, Kushner PJ, Brown R (2018) Canadian snow and sea ice: historical trends and projections. The Cryosphere 12:1157–1176. https://doi.org/10.5194/tc-12-1157-2018

North Saskatchewan Watershed Alliance (NSWA) (2012) Atlas of the North Saskatchewan River Watershed in Alberta. The North Saskatchewan Watershed Alliance Society, Edmonton, Alberta

North Saskatchewan Watershed Alliance (NSWA) (2014) Preliminary steps for the assessment of instream flow needs in the North Saskatchewan River Basin. Edmonton, Alberta

PAGES Hydro2k Consortium (2017) Comparing proxy and model estimates of hydroclimate variability and change over the Common Era. Clim Past 13:1851–1900. https://doi.org/10.5194/cp-13-1851-2017

Perez-Valdivia C, Sauchyn D (2012) Groundwater levels and teleconnection patterns in the Canadian Prairies. Water Resour Res 48(W07516):2012. https://doi.org/10.1029/2011WR010930

Pietroniro A, Soulis E (2003) A hydrology modelling framework for the Mackenzie GEWEX programme. Hydrol Process 17(3):673–676

Pietroniro A, Fortin V, Kouwen N, Neal C, Turcotte R, Davison B, Verseghy D, Soulis ED, Caldwell R, Evora N, Pellerin P (2007) Development of the MESH modelling system for hydrological ensemble forecasting of the Laurentian Great Lakes at the regional scale. Hydrol Earth Syst Sci 11:1279–1294. https://doi.org/10.5194/hess-11-1279-2007

Pomeroy J, Stewart RE, Whitfield PH (2005) The 2013 flood event in the Bow and Oldman River basins: causes, assessment, and damages. Can Water Resour J

Pouliot D, Latifovic R, Olthof I (2017) Development of a 30 m spatial resolution land cover of Canada: contribution to the harmonized North America Land Cover Dataset, 11–15 Dec, AGU Fall Meeting 2017

Rood SB, Samuelson GM, Weber JK, Wywrot KA (2005) Twentieth-century decline in streamflows from the hydrographic apex of North America. J Hydrol 306(1–4):215–233. https://doi.org/10.1016/j.jhydrol.2004.09.010

Sauchyn D, Ilich N (2017) Nine hundred years of weekly streamflows: stochastic downscaling of ensemble tree-ring reconstructions. Water Resour Res 53:9266–9283. https://doi.org/10.1002/2017WR021585

Sauchyn D, Vanstone J, Perez-Valdivia C (2011) Modes and forcing of hydroclimatic variability in the Upper North Saskatchewan River Basin since 1063. Can Water Resour J 36(3):205–217

Sauchyn DJ, Vanstone J, St. Jacques JM, Sauchyn R (2015) Dendrohydrology in Canada's western interior and applications to water resource management. J Hydrol 529:548–558

Schmidt GA et al (2014) Using palaeo-climate comparisons to constrain future projections in CMIP5. Clim Past 10:221–250. https://doi.org/10.5194/cp-10-221-2014

Scinocca JF, Kharin VV, Jiao Y, Qian MW, Lazare M, Solheim L, Dugas B (2016) Coordinated global and regional climate modelling. J Clim 29:17–35. https://doi.org/10.1175/JCLI-D-15-0161.1

Smerdon JE, Cook BI, Cook ER, Seager R (2015) Bridging past and future climate across paleoclimatic reconstructions, observations, and models: a hydroclimate case study. J Clim 28:3212–3231. https://doi.org/10.1175/jcli-d-14-00417.1

Soulis ED, Snelgrove KR, Kouwen N, Seglenieks F, Verseghy DL (2000) Towards closing the vertical water balance in Canadian atmospheric models: coupling of the land surface scheme CLASS with the distributed hydrological model watflood. Atmos Ocean 38(1):251–269. https://doi.org/10.1080/07055900.2000.9649648

St. Jacques J-M, Sauchyn DJ, Zhao Y (2010) Northern Rocky Mountain streamflow records: global warming trends, human impacts or natural variability? Geophys Res Lett 37(6)

St. Jacques JM, Huang YA, Zhao Y, Lapp SL, Sauchyn DJ (2014) Detection and attribution of variability and trends in streamflow records from the Canadian Prairie Provinces. Canad Water Resour J 39(3):270–284. https://doi.org/10.1080/07011784.2014.942575

Stahle DW, Cook ER, Burnette DJ, Torbenson MCA, Howard IM, Griffin D, Villanueva JV, Cook BI, Williams PA, Watson E, Sauchyn DJ, Pederson N, Woodhouse CA, Pederson GT, Meko DM, Coulthard B, Crawford CJ (2020) Dynamics, variability, and change in seasonal precipitation reconstructions for North America. J Clim 33:3173–3195

Sturm M, Goldstein M, Parr C (2017) Water and life from snow: a trillion-dollar science question. Water Resour Res 53:3534–3544. https://doi.org/10.1002/2017WR020840

Szeto K, Zhang X, White ER, Brimelow J (2016) The 2015 extreme drought in Western Canada. Explaining extreme events of 2015 from a climate perspective. In: Herring S et al (eds) Chapter 9, Special Supplement to the Bulletin of the American Meteorological Society, vol 97, no 12

Tam BY, Szeto K, Bonsal B, Flato G, Cannon AJ, Rong R (2018) CMIP5 drought projections in Canada based on the standardized precipitation evapotranspiration index. Can Water Resour J/Revue Canadienne Des Ressources Hydriques. https://doi.org/10.1080/07011784.2018.1537812

Tennant C, Menounos B (2013) Glacier change of the Columbia Icefield, Canadian Rocky Mountains, 1919–2009. J Glaciol 59(216):671–686. https://doi.org/10.3189/2013JoG12J135

Teufel B, Diro GT, Whan KM, Jeong DI, Ganji A, Huzly O, Winger K, Gyakum JR, de Elia R, Zwiers FW, Sushama L (2017) Investigation of the 2013 Alberta flood from weather and climate Perspectives. Clim Dyn 48:2881

Thompson J (2016) An update on water allocation and use in the North Saskatchewan River Basin in Alberta. Available at: https://www.saskriverbasin.ca/images/files/Water%20Use%20Update-John%20Thompson.pdf

Treasury Board and Finance (2018) Office of Statistics and Information – Demography, Population Project, Alberta and Census Divisions 2018–2046, July 3

Vaghefi SA, Sauchyn DJ, Andreichuk Y, Iravani M, Goss GG, Faramarzi M (2019) Regionalization and parameterization of a hydrologic model significantly affect the cascade of uncertainty in climate-impact projections. Clim Dyn 1–26. https://doi.org/10.1007/s00382-019-04664-w

Verseghy D (1991) Class-a Canadian land surface scheme for GCMS. I. Soil model. Int J Climatol 11(2):111–133. https://doi.org/10.1002/joc.3370110202

Verseghy D, McFarlane NA, Lazare M (1993) CLASS—a Canadian land surface scheme for GCMs, II. Vegetation model and coupled runs. Int J Climatol 13(4):347–370. https://doi.org/10.1002/joc.3370130402

Vincent LA, Wang XL, Milewska EJ, Wan H, Yang F, Swail V (2012) A second generation of homogenized Canadian monthly surface air temperature for climate trend analysis. J Geophys Res 117:D18110. https://doi.org/10.1029/2012JD017859

Worley Parsons (2009) North Saskatchewan River Basin overview of groundwater conditions, issues, and challenges.

Zhang X, Flato G, Kirchmeier-Young M, Vincent L, Wan H, Wang X, Rong R, Fyfe J, Li G, Kharin VV (2019) Changes in temperature and precipitation across Canada. In: Bush E, Lemmen DS (eds), Chapter 4, Canada's changing climate report. Government of Canada, Ottawa, Ontario

Chapter 3
Forcing of Global Hydrological Changes in the Twentieth and Twenty-First Centuries

V. Ramaswamy, Y. Ming, and M. D. Schwarzkopf

3.1 Introduction

Climate over the twentieth century has been forced by natural (solar irradiance changes, aerosols from major volcanic eruptions) and anthropogenic (well-mixed and short-lived greenhouse gases, short-lived aerosols, land-use change) factors (Ramanathan et al. 2001; Forster et al. 2007; Myhre et al. 2013; Ramaswamy et al. 2019). The forcings have effected changes in the coupled climate system comprising the atmosphere, oceans, land and ice, with clear evidence of an anthropogenic fingerprint on changes in several climate variables (IPCC 2007, 2013). In this study, we discuss the anthropogenic aerosol forcing and its impacts upon the climate system and contrast the temperature and precipitation changes with that due to the well-mixed (equivalently, long-lived) greenhouse gases.

We employ the NOAA/OAR/GFDL 3rd generation Climate Model ("CM3") for the investigation. We discuss how the aerosols have perturbed the radiative energy balance of the climate system over the twentieth and twenty-first centuries, and how the system has responded to the radiative forcings. The thermodynamic and dynamic responses induce changes in the surface heat and moisture balance, in turn affecting the hydrologic cycle of precipitation and evaporation.

The CM3 model is based on the finite volume cubed sphere atmospheric dynamical core, with ocean, land, sea-ice components forming the coupled climate system (Fig. 3.1). See Donner et al. (2011) and Griffies et al. (2011) for further descriptions of the atmosphere and coupled climate model, respectively. The forcings considered in the model include that due to the well-mixed greenhouse gases (WMGG: CO_2, CH_4, N_2O and CFCs), stratospheric and tropospheric ozone (O_3), land-use changes, volcanic aerosols and solar irradiance changes. The emissions and forcings over

V. Ramaswamy (✉) · Y. Ming · M. D. Schwarzkopf
NOAA/Geophysical Fluid Dynamics Laboratory, Princeton, NJ, USA
e-mail: V.Ramaswamy@noaa.gov

© The Author(s), under exclusive license to Springer Nature Singapore Pte Ltd. 2021

A. Pandey et al. (eds.), *Hydrological Aspects of Climate Change*,
Springer Transactions in Civil and Environmental Engineering,
https://doi.org/10.1007/978-981-16-0394-5_3

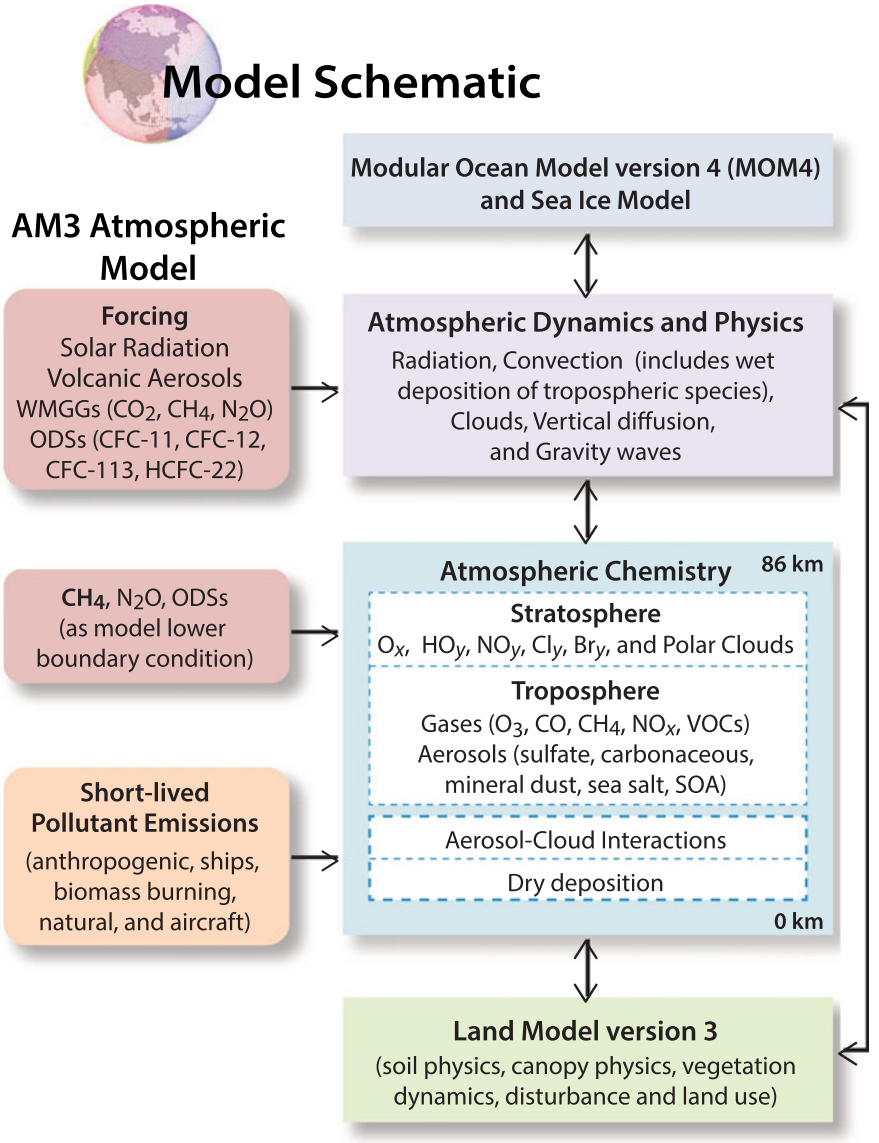

Fig. 3.1 Schematic of NOAA/GFDL 3rd-generation coupled climate model "CM3", with Atmospheric Model (AM3), Ocean Model (MOM4 and sea-ice) and Land Model version 3. The other modules shown are: Atmospheric Dynamics and Physics, and Atmospheric Chemistry. The forcings driving the model's climate from pre-industrial to present are indicated and include natural and human-influenced factors (long-lived or equivalently well-mixed, and short-lived species). See Donner et al. (2011), Griffies et al. (2011), Levy et al. (2013), and Naik et al. (2013)

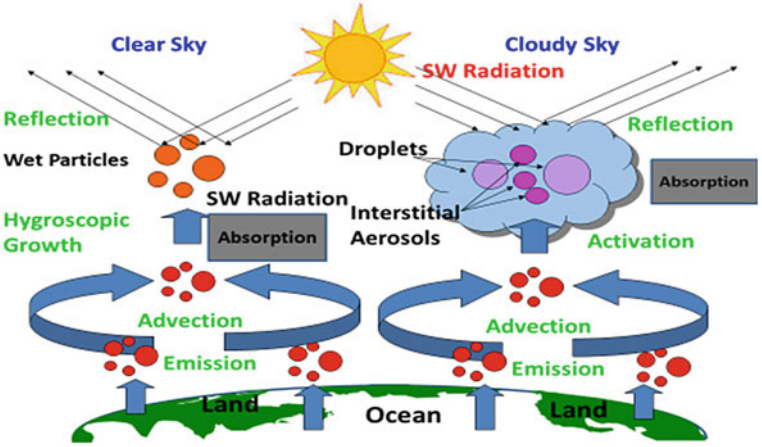

Fig. 3.2 Schematic of the aerosol-climate interactions represented in the climate model. The aerosols undergo micro-physical changes including hygroscopic growth and incorporations in clouds that can alter cloud properties. The aerosol cycle includes a consistency with the meteorology as simulated by the model, e.g. advection from source regions

the twentieth and twenty-first centuries are described in Bollasina et al. (2011) and Levy et al. (2013). The aerosol forcing (see Fig. 3.2) consists of the "direct" aerosol effect of scattering and absorption of radiation and the interactions of aerosols with clouds, which enhance the lifetime and albedo of clouds leading to the "indirect" effect (Forster et al. 2007). Aerosol and cloud water transport is interactive and therefore self-consistent with the model's meteorology (Ming et al. 2007). This allows a self-determination within the model itself of the feedbacks between the aerosol effects on radiation and circulation and in turn the effects of circulation on aerosol concentrations in the atmosphere.

3.2 Aerosol Radiative Forcing

The main focus is the aerosol-climate interactions depicted schematically in Fig. 3.2. Aerosols considered in the model are sulphate, black carbon (BC), organic carbon (OC), sea-salt, dust and secondary organics (see also Fig. 3.1). Sulphate and organic aerosols arise from both natural and anthropogenic emissions, while BC is a product of human influences. Short-lived gases playing a role in tropospheric chemistry include NO_x, CO and volatile organic carbons (VOCs). The prescription of the time-dependent anthropogenic emissions is described in Levy et al. (2013) and Naik et al. (2013). Sulphate and sea-salt are assumed to be hygroscopic; other aerosol species are not. BC and sulphate are assumed to exist as an internal mixture, and the resultant mixture is, like pure sulfate, considered to be hygroscopic. Aerosol–cloud interactions involve sulphate, BC and OC. Anthropogenic aerosols' interaction

with radiation is primarily in the shortwave spectrum. They reduce the net radiation entering the climate system at the top-of-the-atmosphere (TOA) and that reaching the surface (Fig. 3.2). Anthropogenic greenhouse gases, in contrast, reduce the infrared radiation escaping to space, with the climate system trapping more energy.

Forster et al. (2007) illustrated the significance of the anthropogenic aerosols in the net radiative forcing between present-day (2000) and pre-industrial times (1860) at the top-of-the-atmosphere (TOA) and surface. Noteworthy is the large positive anthropogenic contribution occurring at TOA nearly everywhere around the globe due to the positive greenhouse gas forcing. However, over regions of the Northern Hemisphere where the aerosol emissions are large, e.g. Asia, their strong scattering of insolation renders the net anthropogenic TOA forcing negative. In contrast to the TOA forcing, the Northern Hemisphere anthropogenic surface forcing has a large negative value particularly over continents due to the aerosol reduction of shortwave radiation; the WMGGs on the other hand have a positive forcing at the surface, but this is less in magnitude than aerosol effects.

The aerosol forcing since preindustrial times includes absorption and scattering effects, the latter forming a substantial component due to the aerosol interactions with clouds which enhances their albedo. Figure 3.3 illustrates the pre-industrial to present-day aerosol TOA forcing in the CM3 model which accounts for the direct and indirect aerosol effects (Figs. 3.1 and 3.2). The net aerosol effective radiative forcing (ERF; see Myhre et al. 2013, Ramaswamy et al. 2019) is -1.8 W/m^2. The reduction in the radiative flux at the surface is greater in magnitude (-3.6 W/m^2). Effects are most pronounced over continental Northern Hemisphere. This highlights one of the most consequential aspects, viz. the difference in forcing created by the aerosols between TOA and surface, with atmospheric aerosol-related absorption accounting for the difference. It should be noted that the forcing by anthropogenic aerosols has uncertainties owing to gaps in the knowledge about aerosol–cloud interactions (Seinfeld et al. 2016). The estimate from the model version employed here of the "indirect" effect lies at the upper tier of values assessed (Myhre et al. 2013; Smith et al. 2020).

3.3 Twentieth Century Climate Response to Forcings

We conduct model simulations to investigate the response of the climate system in the twentieth century under the action of all the natural and anthropogenic forcings depicted in Fig. 3.1 (labelled in this paper as AllForc or AllForcing). The AllForc simulations are performed with five ensemble members, with each member being initialized from a different climate state in the year 1860 representing pre-industrial time. The period 1995-2000 is assumed to represent "present-day" in the simulations. We also consider how the twentieth century would have responded under the action of a subset of forcings, in effect asking the question—what if the climate system had been forced only by specific forcings or forcing combinations? This enables clarification of the roles of the different forcing agents. The subsets considered in the present

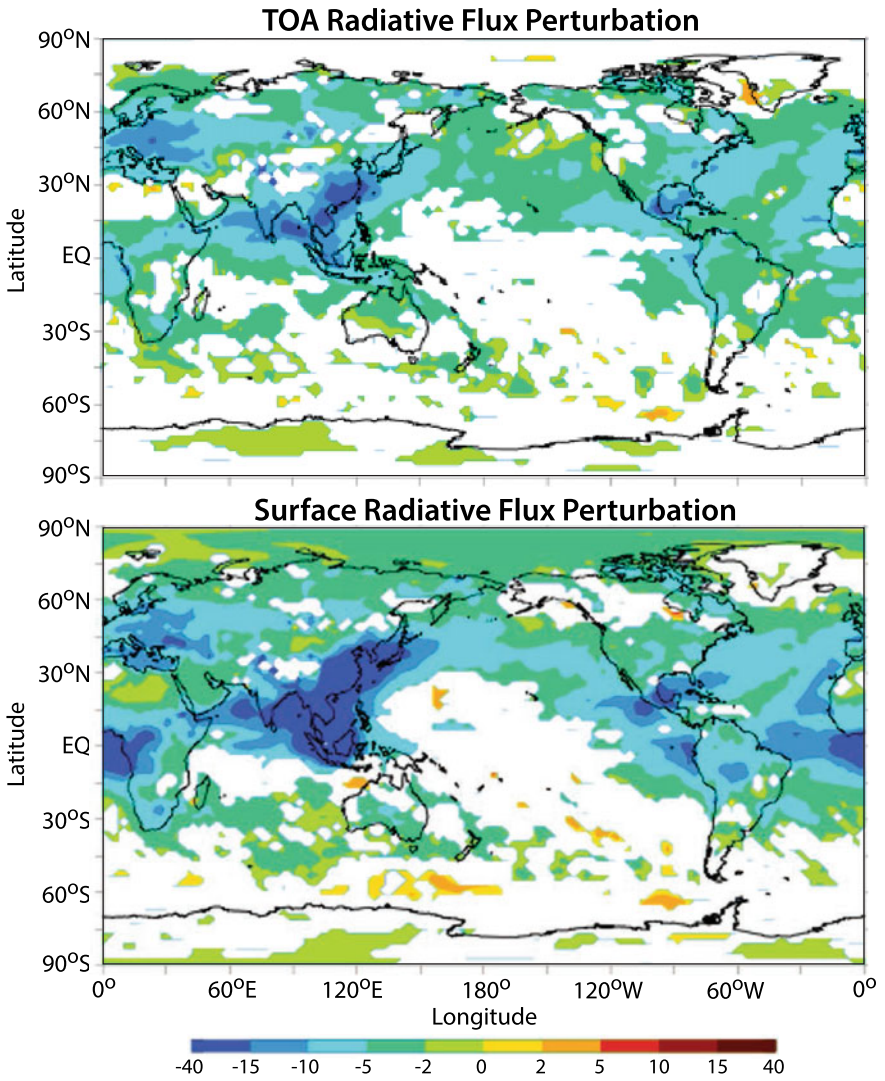

Fig. 3.3 Annual mean all-sky anthropogenic aerosol-induced effective radiative forcing (for ERF definition, see Myhre et al. 2013) between present-day and pre-industrial time (1860) at the top-of-the-atmosphere (TOA) and surface (W m^{-2})

study are anthropogenic (Anthro/p viz., WMMG, ozone and tropospheric aerosols) only; WMGG-only, or WMGG plus ozone (WMGGO3) with O_3 effects considerably smaller than WMGG (factor of 8 less); tropospheric aerosol only (Aerosol), with a subset being aerosol indirect effect only (Aerosol Ind); and natural (Natural: solar irradiance changes and stratospheric aerosols from volcanic eruptions) forcing. The forcing subset simulations are performed with three ensemble members.

(a) **Surface temperature**

Figure 3.4 illustrates the effect on the global-mean surface temperature change over approximately the last fifty years of the twentieth century. The AllForc result compares reasonably well against the observed temperature change ("CRU"). The anthropogenic forcing contributes to the AllForc, while the effect of natural forcing is negligible. The anthropogenic result includes contributions of opposite signs from WMGGO3 (essentially WMGG) and aerosols (Mitchell et al. 1995). While WMGGO3 i.e. anthropogenic greenhouse gases constitute the most dominant forcing agent, the anthropogenic aerosols offset about a third of the magnitude of the greenhouse gas effect. The aerosol indirect (aerosol–cloud interaction) effect has a major bearing on the total aerosol effect. There is some scatter among the different ensemble members, underscoring the importance of the initial climate state in governing the precise evolution of the climate response under the action of the different forcings; however, the reduction of the WMGGO3 effect by anthropogenic aerosols is markedly evident.

(b) **Precipitation**

Figure 3.5 illustrates the effect due to the forcings on the change in the annual mean precipitation between 1990–2000 and 1901–1910. As will be evident later (Fig. 3.8), there is little variation between 1900 and approximately 1950 such that the principal change occurs between approximately 1950 to 2000. Precipitation is a noisier

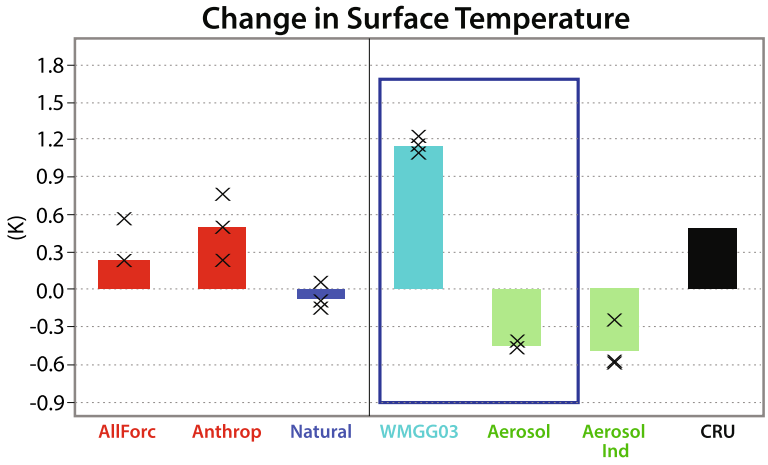

Fig. 3.4 Global-and-annual-mean surface temperature change (K) in response to radiative forcings, computed for the period 1996–2000 minus 1951–1955. Shown are the responses to all the known natural and anthropogenic forcings (AllForc), and for different subsets of forcings, respectively, anthropogenic forcing only (Anthrop), natural forcing only (Natural), well-mixed greenhouse gases and ozone only (WMGGO3), tropospheric aerosol only (Aerosol, comprising "direct" and "indirect" effects) and aerosol "indirect" effect only (Aerosol Ind). Also shown is the estimate of the observed temperature change (CRU) over the period. The crosses denote the results obtained for the individual ensemble members, while the coloured bars represent the ensemble mean

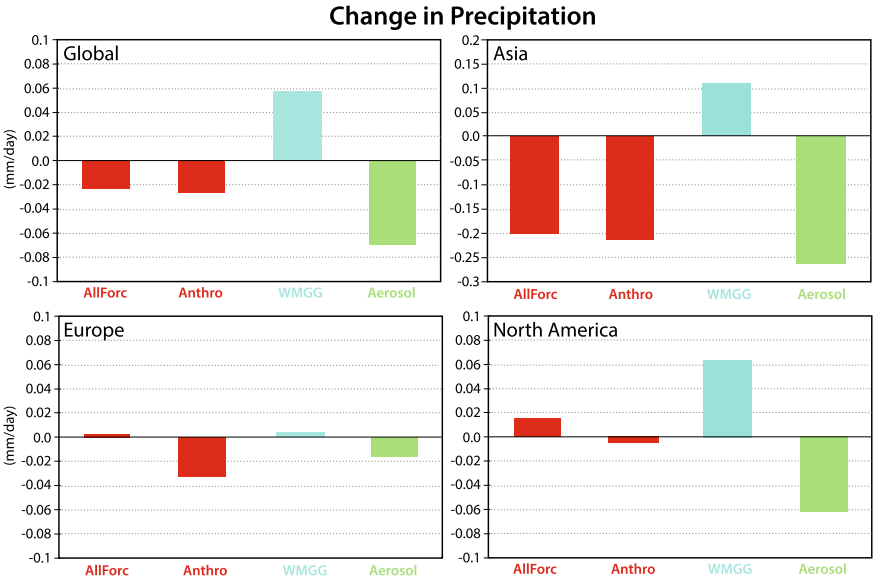

Fig. 3.5 Annual mean precipitation (mm/day) change (1991–2000 minus 1901–1910) in response to forcings over Global (top left), Asia (top right), Europe (bottom left) and North America (bottom right). Simulation ensemble mean values shown: all natural and anthropogenic forcings (AllForc), anthropogenic only (Anthro), well-mixed greenhouse gases only (WMGG) and tropospheric aerosol only (Aerosol)

field than temperature in both observations and simulations. While there is substantial scatter among the different ensemble members raising the issue of statistical significance, the aerosol effect compared against WMGG shows a significant, and almost complete, offset. This offset is much more striking than that arising for surface temperature change (Fig. 3.4). This is manifested in Fig. 3.5 over all regions shown: Global, Asia, Europe and N. America.

The anthropogenic signal represents the net resulting from the opposing tendencies due to greenhouse gases and aerosols. For Global and Asia, the change due to anthropogenic forcing is almost the same as the AllForc. In each region, except for Europe, the climate response to WMGG-only change is one of clearly causing an increase in precipitation. This is consistent with well-known theoretical principles and earlier modelling works (e.g. Manabe and Stouffer 1980; Ramaswamy and Chen 1997; Ming and Ramaswamy 2009). For Global, Asia and N. America, the aerosol effect is strong enough to negate the WMGG effects, while in Asia, the aerosol magnitude overwhelms WMGG. In the case of Global and Asia, the precipitation is reduced in AllForc due to a dominant anthropogenic aerosol effect, skewed towards an aerosol control of the trend. These results are consistent with Ramanathan et al. (2001) and Chung and Ramanathan (2006).

The reduction in precipitation arising due to the aerosol effect has other important connotations, summarized briefly below. As shown in Ramaswamy and Chen

(1997), Ming and Ramaswamy (2009), and Ocko et al. (2014), aerosol presence causes an asymmetric forcing pattern between the Northern and Southern Hemisphere (Fig. 3.3). The aerosol reduction of forcing in the Northern Hemisphere induces a change in the meridional (Hadley) circulation that is absent for the WMGG perturbation. The change in circulation causes the Inter-Tropical Convergence Zone (ITCZ) to shift southward, thus affecting precipitation patterns in the tropical regions (Chung and Ramanathan 2006; Ming and Ramaswamy 2011), with reduction of precipitation north of the equator in the tropics and increase in the southern equatorial region (Ramaswamy and Chen 1997; Ming and Ramaswamy 2009; Ocko et al. 2014). This is to be contrasted to the effects due to the WMGG which tend to weaken the Walker (tropical east–west) circulation. Bollasina et al. (2011) demonstrated that anthropogenic aerosols cause a decrease of monsoon precipitation in the north-central India over the last half of the twentieth century, an explanatory factor consistent with observation of decreased rainfall trend. In fact, CM3 simulations show that the observed decrease of the monsoon over north-central India over the late twentieth century can be explained only by invoking aerosol forcing; WMGG-only forcing cannot explain it. A large part of this monsoonal effect is likely due to the aerosols in the Indian region but remote aerosol effects could also be a contributing factor (Bollasina et al. 2014). Randles and Ramaswamy (2008) and Ocko et al. (2014) demonstrate how scattering and absorbing aerosols can play important and distinctive roles on changes in the meridional circulation, ITCZ location, precipitation and poleward heat transport.

The precipitation reduction in the Northern Hemisphere over the last 30 years of the twentieth century has been shown to be well correlated with aerosols, particularly anthropogenic sulphur emissions (Polson et al. 2014). IPCC (2007, 2013) have further shown the general reduction of precipitation in the observations over the latter part of the twentieth century. A decrease in precipitation is also evident over land in observations (IPCC 2007) and over tropical land areas over the period 1960s to 1990s (Chung and Ramanathan 2006; Zhang et al. 2007; Bollasina et al. 2011). We conclude that the model simulation of aerosol-induced precipitation decrease (Fig. 3.5) has a fair consistency with analyses of the observed trends.

(c) Surface heat flux balance

Figure 3.6 illustrates the balance of global-and-annual mean surface heat fluxes in response to All Forc, anthropogenic, WMGG and aerosol forcings over the same time period as for precipitation. The solar and longwave components of the radiation field are considered along with sensible and latent heat flux exchanges. Latent heat flux is more relevant for this analysis than sensible heat. Consider the WMGG first (bottom left). The greenhouse gas increase and the atmospheric temperature and water vapour increase due to feedbacks (Ramanathan 1981) enhance the net longwave at the surface, while the shortwave change is negligible. To balance this effect, there is increased evaporation and a loss of latent heat from the surface which the atmosphere gains upon condensation, with consequent increase in precipitation (Fig. 3.5). The increased vigour of the hydrologic cycle (precipitation) under WMGG increase is well known (Manabe and Stouffer 1980; IPCC 2001, 2007, 2013).

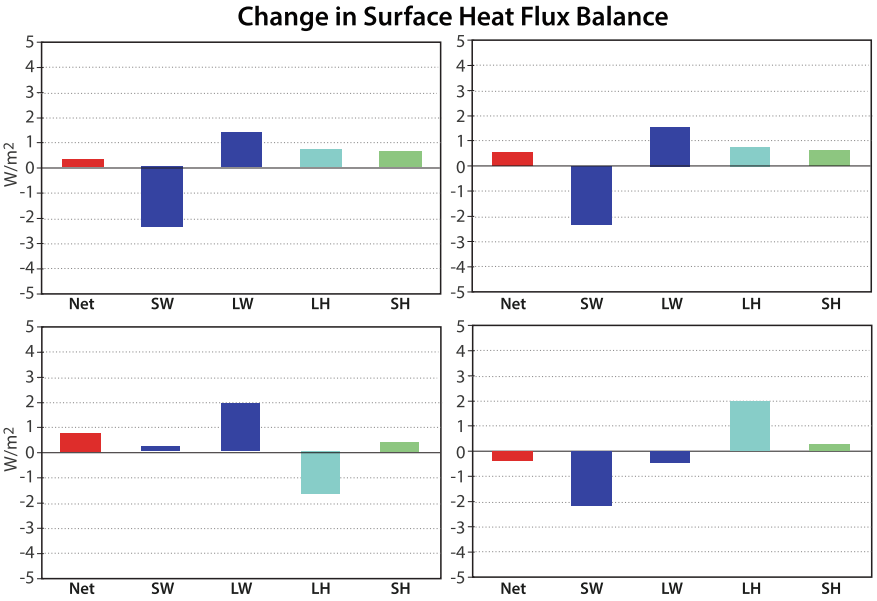

Fig. 3.6 Global-and-annual-mean heat balance at the surface for the climate response to forcings (1991–2000 minus 1901–1910) with ensemble mean values shown. AllForc (all natural + anthropogenic forcings) (top left), anthropogenic only (top right), well-mixed greenhouse gases only (bottom left) and aerosols only (bottom right). Components of the heat balance are shortwave (SW), longwave (LW), latent heat (LH), sensible heat (SH) and residual (Net). Positive values denote heat gain by the surface

For the aerosol case, there is a decrease of solar flux at the surface (Persad et al. 2014) which is not present for WMGG. The longwave radiative component is also a heat loss at the surface due to cooling of the atmosphere in the lower layers but is less than the shortwave effect. The surface has to balance by reducing evaporation. Consequently, there is a lessening of the latent heat flux loss, i.e. a heat gain by the surface unlike the WMGG case. The anthropogenic and AllForc cases are almost similar owing to negligible influence of natural forcing. Note that the aerosol effect through the shortwave reduction and the WMGG effect through the longwave increase are both manifested in the AllForc case. The aerosol influence on the latent heat though outweighs that due to WMGG. As stated earlier, it must be noted that the aerosol forcing in this study is likely near the upper limit of the assessed estimated range due to an overestimate in the representation of the aerosol-cloud interactions. Nevertheless, the strong effect of aerosols relative to WMGG in affecting the surface heat balance and skewing precipitation towards the aerosol-dominated solution is a distinct feature of the surface-atmosphere physical processes. (Preliminary analysis of results from the next-generation GFDL model, CM4, which has a somewhat lesser aerosol forcing than in CM3, also indicates a near compensation of the WMGG-only response).

Figure 3.7 emphasizes the global-and-annual-mean nature of the contrast in latent heat flux changes between the anthropogenic WMGG and aerosols. Over most of the globe, with exceptions in mid-to-high southern latitudes, WMGG tends to increase

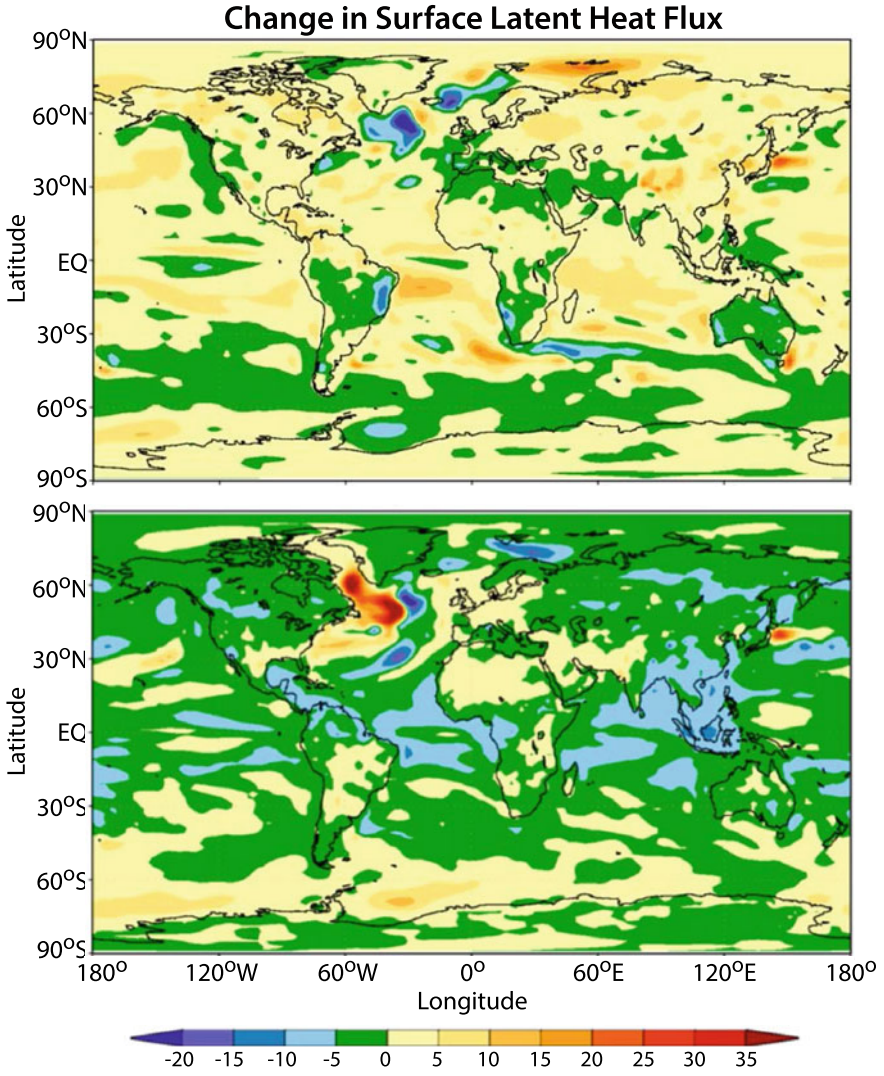

Fig. 3.7 Latitude–longitude change in the annual mean latent heat flux at the surface (in W m^{-2}) (1996–2000 minus 1951–1955) with ensemble-mean values shown. Top panel: Well-mixed greenhouse gas forcing only. Bottom panel: Anthropogenic aerosol forcing only. Positive sign denotes more latent heat release by the surface due to evaporation in response to the forcing, while negative sign indicates less latent heat released by the surface

the evaporation from the surface. In contrast, anthropogenic aerosols reduce evaporation consistent with Fig. 3.6, being dominant in almost the entire Northern Hemisphere where most of the anthropogenic emissions and therefore the aerosol concentrations occur, but with the effect spread away from source regions as well (Paynter and Frohlicher 2015).

Other model results, for example, performed for the World Climate Research Program's Coupled Model Intercomparison Project 5 (CMIP5), illustrate (not shown here) reasonably similar results as shown in Fig. 3.5 for the effects of anthropogenic forcing in the latter half of the twentieth century viz. a reduction in the global-mean precipitation. Further, several of these models also show a concomitant decrease of the shortwave flux at the surface over this period. Whereas, for the WMGG-only simulations, they indicate an increase in the longwave component at the surface; however, the models' aerosol shortwave reduction effect outweighs the WMGG effect. The CMIP5 model results corroborate the present model simulations (Figs. 3.5 and 3.6). There is thus a reasonable qualitative consistency across models in the fundamental physics from forcing to processes to precipitation change despite inter-model quantitative differences. While the aerosol forcing and effects are more uncertain than WMGG (IPCC 2007, 2013; Seinfeld et al. 2016), there is a high plausibility of the physical linkage between forcings and the change in the surface radiative, sensible and latent heat fluxes and in turn the resultant effects on evaporation and precipitation.

3.4 Twenty-First Century Climate Response to Forcings

Similar to the investigation above for the twentieth century, we perform additional simulations from present-day (2000) to 2100 under the actions of emissions scenarios and examine the entire time series from pre-industrial (1860) to 2100. Figure 3.8 illustrates the simulated precipitation change in the global-and-annual-mean relative to the "control" value in the year 1860. From 1860 to year 1900, both greenhouse gases (WMGG) and anthropogenic aerosols effects are small (time period "1"). The aerosol effect becomes increasingly comparable in magnitude to the greenhouse gases' (WMGG) effect from ~1900 onwards and indicates a significant offset by approximately present-day (~1990s; time period "2"). The AllForcings result is skewed towards the aerosol result as a result of the reduction in the vigour of the hydrologic cycle (through reduced solar heating at surface, decrease in evaporation and precipitation), outcompeting the increase for WMGG-only (consistent with Figs. 3.5, 3.6 and 3.7).

Beginning in ~2000 and continuing into the twenty-first century, the emissions scenarios call for a projected decrease in anthropogenic aerosol emissions and a continued increase in WMGG emissions (IPCC 2007, 2013; Levy et al. 2013). The result for AllForcings is shown from year 2000 to 2100 as an ensemble encompassing simulations performed for different projected scenarios (IPCC 2013). The results for all the scenarios are illustrated as a band stretching from 2000 to 2100. The aerosol influence on precipitation is reduced in the future, and the AllForcings

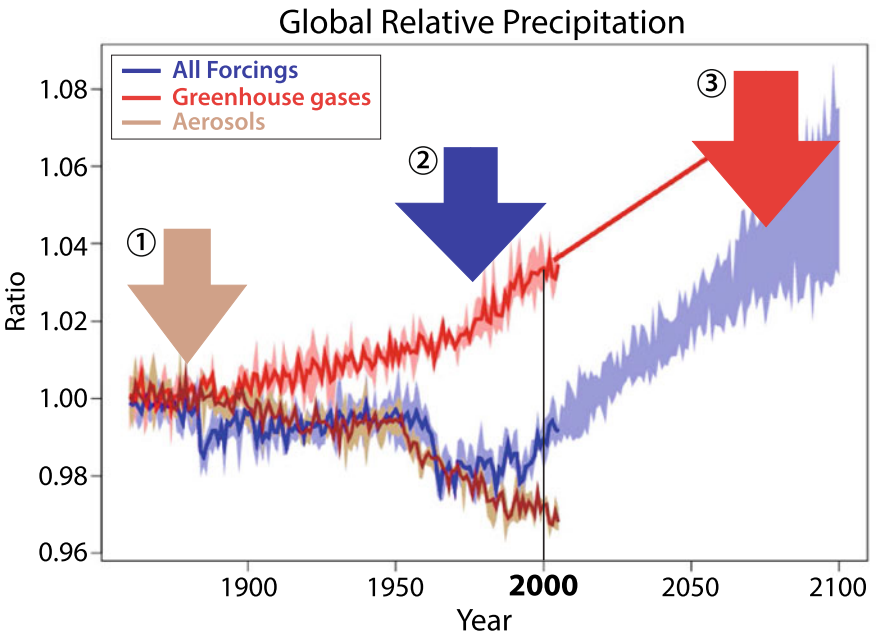

Fig. 3.8 Ratio of the global-and-annual-mean precipitation evolution over time relative to the "pre-industrial" (1860) control. Past to year 2000 results are from a five-member ensemble for historical (AllForcings), a three-member historical ensemble with anthropogenic greenhouse gases forcing only, and a three-member historical ensemble with anthropogenic aerosol forcing only. The envelope around the bold-faced lines indicates the ensemble model deviations. For future projections (beyond year 2000), the AllForcing results for a three-member ensemble for RCP4.5 and a one-member simulation each for RCP2.6, RCP6 and RCP8.5 emissions scenarios (IPCC 2013) are shown, with the blue shading encompassing the range of the results. In terms of influence likely to have been exerted by the anthropogenic forcings over the different periods, three broadly distinct time periods as labeled 1, 2, 3 are suggested for comparing the impacts due to greenhouse gases and aerosols between preindustrial and 2100

result skews increasingly towards a WMGG-like result as the twenty-first century progresses beyond 2050 (time period "3"), unlike the aerosol-dominant period of ~1980s and 1990s. This suggests an increase in precipitation that is higher in 2100 than in the past, with a much increased vigour of the global hydrologic cycle now due to the dominance of the WMGG forcing. While the uncertainty of the aerosol decrease, climate sensitivity and internal variability affects the precise estimate of the changes (IPCC 2013), the tendency for precipitation to increase relative to the present, and become more so than in 1860, represents the understanding based on current knowledge of the physical processes.

In response to continued WMGG increase and aerosol decrease, a reversal from the results shown in Fig. 3.5 (for pre-industrial to 2000) is to be expected in going from 2000 to 2100. While Fig. 3.8 is for the global mean, the pattern in trend holds for most of the Northern Hemisphere continents especially Asia. In fact, simulations

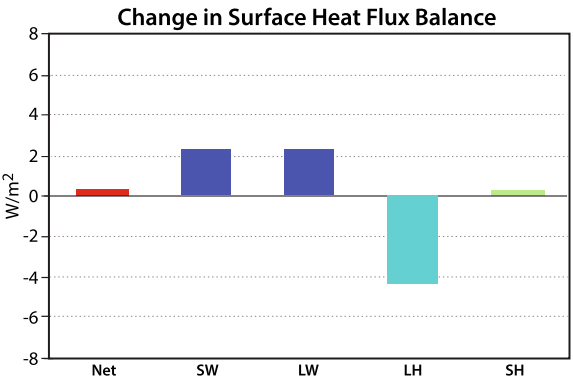

Fig. 3.9 As in Fig. 3.6, top panel, but for the change in the surface heat balance due to the climate change simulated for year 2100 minus 2000 under the RCP4.5 emissions scenario

indicate that Asia region would see a significant reversal in the twenty-first century, with the contribution in East Asia due to the decrease in aerosols by itself causing an increase of ~25% in precipitation by 2100 relative to 2000 (Levy et al. 2013).

As is to be expected from the discussions related to Figs. 3.5, 3.6 and 3.7, the surface heat balance from 2000 to 2100 (Fig. 3.9) also follows an expected reversal. With the decrease in aerosols, the 2000–2100 surface heat balance shows an increase in the shortwave radiative flux at the surface. The longwave is also an increase because of the continued WMGG increase. Thus, the two radiative components now act in concert, not offsetting each other from 2000 to 2100. The surface latent heat change is hence more strongly negative than for 1860–2000 (Fig. 3.6), with greater evaporation and loss of heat from the surface than in 2100. This reinforces the argument for the increased vigour of the hydrologic cycle and consequently increased precipitation in 2100 compared to present-day.

3.5 Summary and Conclusions

While anthropogenic greenhouse gas emissions have been the principal radiative drivers of climate change over the twentieth century, aerosol emissions resulting in sulphate, black carbon and organic carbon aerosols have counteracted to some degree the radiative forcing due to the greenhouse gases. Climate model simulations indicate that the net aerosol effect, including their scattering and absorbing effects and their interactions with clouds, has offset partially the effect of greenhouse gases on surface temperature. More strongly, however, has been the effect of aerosols on precipitation. In contrast to the greenhouse gas effects on increasing the vigour of the hydrologic cycle and increasing global precipitation, aerosols in the net decrease precipitation. The mechanistic aspects are traced through the effect of aerosol forcing on the surface heat balance where their shortwave flux reduction at the TOA and surface results in lessening evaporation and therefore precipitation. This effect is in contrast to that for

greenhouse gases where there tends to be an increase in latent heat loss from surface via evaporation with an accompanying increase of precipitation.

The aerosol influences extend further in terms of contrast with greenhouse gases. Aerosol forcing is hemispherically asymmetric which also makes the net (WMGG plus aerosol) anthropogenic forcing less positive in the Northern than in the Southern Hemisphere. This induces a change in the meridional (Hadley) circulation causing a precipitation anomaly of opposite sign across the equatorial region (Bollasina et al. 2011). This does not occur for the WMGG-only case as their forcing is symmetric across the hemispheres (Ramaswamy and Chen 1997; Ming and Ramaswamy 2009, 2011). The aerosol magnitude is comparable to or even has the possibility of outweighing completely the greenhouse gas effects on precipitation. The North–South asymmetry in the case of aerosol concentrations also affects the poleward heat transport differently than for greenhouse gases (Ocko et al. 2014). Anthropogenic aerosol effects have also caused a reduction of the monsoonal (June–September) precipitation in north-central India over the last half of the twentieth century (Bollasina et al. 2011). Aerosol effects in fact need to be invoked to explain the precipitation reduction anomalies, while greenhouse gases alone cannot explain the late twentieth century observations. An offshoot of this is the point that anthropogenic aerosols especially over Asia could have masked any potential of finding signals in precipitation attributable to global warming over the latter half of the twentieth century.

In the twenty-first century, the emissions scenarios project a continued human-influenced increase in greenhouse gas emissions and a decrease in aerosol precursor emissions owing to various concerns including air quality and health (IPCC 2007; Ramaswamy 2009). While the processes related to greenhouse gas influences in the twentieth century will continue into the twenty-first century, for the aerosol case there will be a reversal due to their reduction. Thus, whatever their influence in the twentieth century, there can be expected to be a reversal of the physics, e.g. lesser hemispheric asymmetry in radiative forcing in the twenty-first century and relative strengthening of the South Asian monsoon system. This leads to the expectation that, with now less surface shortwave reduction by aerosols, the tendency would be for less reduction in evaporation. For the change from year 2000 through the end of the twenty-first century, the scenario of emissions leads us to postulate that aerosol and greenhouse gas scenarios will act in concert to increase precipitation. The changes in global precipitation, from preindustrial to present, and from present to 2100 is on the order of 5%. Because the radiative forcing influences the South Asian monsoon low-pressure systems, the reversal caused in the aerosol forcing becomes consequential for the occurrence of the monsoon depressions (Dong et al. 2020).

The change in meridional circulation induced by aerosols in the latter part of twentieth century (e.g. poleward heat transport anomalies) can be expected to diminish in the twenty-first century, and the climatic consequences such as the ITCZ southward shift reversed, as the aerosol emissions decrease. A caveat in the estimates of the climate effects for the twentieth and twenty-first centuries is the uncertainty concerning aerosols, extending from emissions of the different aerosol species, concentrations in the atmosphere, interaction with clouds, space-time forcing and

the climate sensitivity. Nevertheless, the fundamental awareness of the physical processes concerning aerosol-climate interactions is growing, with further advances in knowledge to be expected that bolster the science via improved theory, observations and mathematical modelling.

References

Bollasina MA, Ming Y, Ramaswamy V (2011) Anthropogenic aerosols and the weakening of the South Asian summer monsoon. Science 334:502–505. https://doi.org/10.1126/science.1204994

Bollasina MA et al (2014) Contribution of local and remote anthropogenic aerosols to the 20th century weakening of the South Asian monsoon. Geophys Res Lett 41(2). https://doi.org/10.1002/2013GL058183

Chung CE, Ramanathan V (2006) Weakening of North Indian SST gradients and the monsoon rainfall in India and the Sahel. J Clim 19:2036–2045. https://doi.org/10.1175/JCLI3820.1

Dong W, Ming Y, Ramaswamy V (2020) Projected changes in South Asian monsoon low-pressure systems. J Clim 33(17). https://doi.org/10.1175/JCLI-D-20-0168.17275-7287

Donner LJ et al (2011) The dynamical core, physical parameterizations, and basic simulation characteristics of the atmospheric component AM3 of the GFDL Global Coupled Model CM3. J Clim 24(13). https://doi.org/10.1175/2011JCLI3955.1

Forster P et al (2007) Changes in atmospheric constituents and in radiative forcing. In: Solomon S et al (eds) Climate change 2007: the physical science basis. Cambridge University Press, pp 129–234

Griffies SM et al (2011) The GFDL CM3 coupled climate model: characteristics of the ocean and sea ice simulations. J Clim 24(13). https://doi.org/10.1175/2011JCLI3964.1

IPCC (2001) Climate change 2001: the scientific basis. In: Houghton JT et al (eds). Cambridge University Press, 881 pp

IPCC (2007) Climate change 2007: the physical science basis. In: Solomon S et al (eds). Cambridge University Press, 996 pp

IPCC (2013) Climate change 2013: the physical science basis. In: Stocker TF et al (eds). Cambridge University Press, 1535 pp

Levy II H et al (2013) The roles of aerosol direct and indirect effects in past and future climate change. J Geophys Res Atmos 118. https://doi.org/10.1002/jgrd.50192

Manabe S, Stouffer RJ (1980) Sensitivity of a global climate model to an increase of CO_2 concentration in the atmosphere. J Geophys Res 85(C10):5529–5554

Ming Y, Ramaswamy V (2009) Nonlinear climate and hydrological responses to aerosol effects. J Clim 22:1329–1339. https://doi.org/10.1175/2008JCLI2362.1

Ming Y, Ramaswamy V (2011) A model investigation of aerosol-induced changes in tropical circulation. J Clim 24:5125–5133. https://doi.org/10.1175/2011JCLI4108.1

Ming Y et al (2007) Modeling the interactions between aerosols and liquid water clouds with a self-consistent cloud scheme in a general circulation model. J Atmos Sci 64(4). https://doi.org/10.1175/JAS3874.1

Mitchell JF, Johns TC, Gregory JM, Tett SFB (1995) Climate response to increasing levels of greenhouse gases and sulfate aerosols. Nature 376:501–504. https://doi.org/10.1038/376501a0

Myhre G et al (2013) Anthropogenic and natural radiative forcing. In: Stocker TF et al (eds) Climate change 2013: the physical science basis. Cambridge University Press, pp 659–740

Naik V et al (2013) Impact of preindustrial to present day changes in short-lived pollutant emissions on atmospheric composition and climate forcing. J Geophys Res Atmos 118. https://doi.org/10.1002/jgrd.50608

Ocko IB, Ramaswamy V, Ming Y (2014) Contrasting climate responses to the scattering and absorbing features of anthropogenic aerosol forcings. J Clim 27:5329–5345. https://doi.org/10.1175/JCLI-D-13-00401.1

Paynter D, Frolicher TL (2015) Sensitivity of radiative forcing, ocean heat uptake, and climate feedback to changes in anthropogenic greenhouse gases and aerosols. J Geophys Res. https://doi.org/10.1002/2015JD023364.

Persad G, Ming Y, Ramaswamy V (2014) The role of aerosol absorption in driving clear-sky solar dimming over East Asia. J Geophys Res Atmos 119(17). https://doi.org/10.1002/2014JD021577

Polson D, Bollasina M, Hegerl GC, Wilcox LJ (2014) Decreased monsoon precipitation in the Northern Hemisphere due to anthropogenic aerosols. Geophys Res Lett 41:6023–6029. https://doi.org/10.1002/2014GL060811

Ramanathan V (1981) The role of ocean-atmosphere interactions in the CO_2 climate problems. J Atmos Sci 38:918–930. https://doi.org/10.1175/1520-0469(1981)038%3c0918:TROOAI%3e2.0.CO;2

Ramanathan V, Crutzen PJ, Kiehl JT, Rosenfeld D (2001) Aerosols, climate, and the hydrological cycle. Science 294:2119–2124. https://doi.org/10.1126/science.1064034

Ramaswamy V (2009) Anthropogenic climate change in Asia: key challenges. EOS 90(49):469–471

Ramaswamy V, Chen C-T (1997) Linear additivity of climate response for combined albedo and greenhouse perturbations. Geophys Res Lett 24(5):567–570

Ramaswamy V et al (2001) Radiative forcing of climate change. In: Houghton JT et al (eds) Climate change 2001: the scientific basis. Cambridge University Press, pp 349–416

Ramaswamy V et al (2019) Radiative forcing of climate: the historical evolution of the radiative forcing concept, the forcing agents and their quantification, and applications. In: A century of progress in atmospheric and related sciences: celebrating the American Meteorological Society centennial. Meteorological monographs, vol 59. American Meteorological Society, Boston. https://doi.org/10.1175/AMSMONOGRAPHS-D-19-0001.114.1-14.100

Randles CA, Ramaswamy V (2008) Absorbing aerosols over Asia: a geophysical fluid dynamics laboratory general circulation model sensitivity study of model response to aerosol optical depth and aerosol absorption. J Geophys Res 113:D21203. https://doi.org/10.1029/2008JD010140

Seinfeld JH et al (2016) Improving our fundamental understanding of the role of aerosol–cloud interactions in the climate system. Proc Natl Acad Sci 113(21). https://doi.org/10.1073/pnas.1514043113

Smith CJ et al (2020) Effective radiative forcing and adjustments in CMIP6 models. Atmos Chem Phys 20:9591–9618. https://doi.org/10.5194/acp-20-9591-2020

Zhang X, Zwiers F, Hegerl G et al (2007) Detection of human influence on twentieth-century precipitation trends. Nature 448:461–465

Chapter 4
Indian Summer Monsoon System: A Holistic Approach for Advancing Monsoon Understanding in a Warming World

Raghu Murtugudde

4.1 Introduction

This chapter is focused on the Indian Summer Monsoon (ISM) response to global warming. A holistic monsoon framework is suggested as necessary for a complete understanding of the ISM response to global warming. ISM is a multi-scale system with many components. The global dynamic context for this system is needed to deliver reliable projections of ISM for the future. This is critical especially since the state of the art coupled climate models and earth system models of the IPCC class largely fail to reproduce the observed trend in ISM. Future projections are also found to be dynamically inconsistent. A similar doubt on the reliability of future projections of the East African Summer Monsoon (EASM) is also raised. Considering the intimate interactions between the ISM and EASM, one must wonder about the global dynamic projections within which these monsoons reside.

Some of the chronic biases in the IPCC class models persist—the cold tongue bias in the eastern tropical Pacific, the double ITCZ in the Pacific, the reversed SST gradient in the equatorial Atlantic and the reversed thermocline gradient in the tropical Indian Ocean are the most glaring biases. These biases have tended to be diagnosed separately, and a multitude of potential explanations have been offered. But solutions have evaded the modellers. It is unclear if a different approach that focuses on the interlinked-processes rather than technical details in terms of local feedbacks will help. For example, can the monsoon-ENSO-ITCZ system be considered as a dominant heat source that control the pantropical interactions lead to a different framework for understanding model process deficiencies and the relation between

R. Murtugudde (✉)
Department of Atmospheric and Oceanic Science, Earth System Science Interdisciplinary Centre, University of Maryland, College Park, MD, USA
e-mail: mahatma@umd.edu

Indian Institute of Technology Bombay, Mumbai, India

© The Author(s), under exclusive license to Springer Nature Singapore Pte Ltd. 2021

A. Pandey et al. (eds.), *Hydrological Aspects of Climate Change*,
Springer Transactions in Civil and Environmental Engineering,
https://doi.org/10.1007/978-981-16-0394-5_4

each of these biases? A good start for any holistic framework may be to consider the ISM itself in a better framework. This is the main goal of this chapter.

India's water resources are inextricably tied to the ISM and its vagaries. Many studies now exist that diagnose the groundwater recharge in the context of groundwater mining for agriculture and other uses. Agriculture remains the most dominant consumer of freshwater. ISM trends and increasing extremes, and crop choices play into compounding groundwater depletion. Any future strategies for managing water resources in India thus require reliable future projections of ISM.

Future projections cannot be trusted unless the models can reproduce the recent trends in the mean, spatial variability and extremes. Much attention is being paid to advancing process and predictive understanding of ISM from short (days 1–3), medium (days 3–10) and extended (weeks 2–4) range to seasonal and longer timescales. India has produced its first ESM and future projections under the CMIP6 protocol which bring it to the world stage on the upcoming IPCC AR6.

A holistic framework for ISM then must consider all its components. Among the components of the ISM, the seasonal mean rainfall is of the biggest concern. The length of the rainy season (LRS) is determined by the onset and withdrawal, but rainfall within the season tends to be distributed in wet and dry spells known as the active and break periods. These active and break events are closely related to the Monsoon Intraseasonal Oscillations (MISOs) which are northward propagating systems emanating from the tropics. The ISM system (ISMS) is thus made up of the seasonal total rainfall, onset, active and break events, Monsoon Intraseasonal Oscillations (MISOs) and withdrawal. The large-scale dynamic context in which the ISMS resides must be an integral part of any analysis to advance the understanding of ISM and its response to global warming.

Monsoon low-pressure systems and depressions or lows are also an integral component of the ISMS. However, these are a synoptic scale phenomenon and the fundamental understanding of the generation and propagation of these lows and depressions are still not complete. The models are also not reliable enough for advancing the processes understanding of these synoptic disturbances let alone explore their response to global warming. There is also a debate about whether there is indeed a trend in the number of depressions in the available data. These low-pressure systems have a strong synergy with active/break events and we expect that any advances in active/break mechanisms will likely advance the understanding of these low-pressure systems as well.

Numerous studies exist on the individual components of the ISMS diagnosing their variability at various timescales and their responses to global warming. Any progress on further understanding will likely depend on considering all components of the ISMS together to elicit any relations that exist between the components that add up to the ISM and its response to global warming. The most frequently reported ISMS response to warming has been the increase in monsoon extremes. It is also evident now that the extremes are becoming more widespread as well. Some studies are beginning emerge to explain the mechanisms that drive widespread extremes. To advance that knowledge further to improve the predictions of extremes is a challenge that awaits us now.

However, no attempts have been made, the best of our knowledge, to establish a relation between the response of the onset, withdrawal and the extremes together in the large-scale dynamic context. Since the LRS is determined by the onset and withdrawal, it is critical to understand if and how the LRS and the trend in mean rainfall may combine to deliver the extremes.

It appears that the ISMS response to natural variability at all timescales and to global warming tends to project onto the duration, frequency and intensity of active and break periods. Global warming also appears to have slowed down the northward propagation speed of MISOs. And yet, no credible studies exist to tie these seemingly disparate responses of the components of ISMS together or even to conjecture the potential dependence of the components on each other. The impact of global warming on the dynamic and thermodynamic responses on the ISMS is quite incomplete in that sense.

To re-emphasize, only a holistic systemic view of ISM may lead to a real understanding of its response to global warming. A holistic view of ISMS would then require that we place ISMS in the context of global circulation and consider the trend in each feature, i.e. the seasonal mean, the onset, active/break events, MISOs, extremes and the withdrawal. This framework may also allow us to better identify the processes that are yet to be fully understood. Fortunately, it appears to first order that all changes in ISMS in a warming world are indeed manifested in these features. Hence, a synthesis of the studies focusing on the components of ISMS may be a good start for identifying knowledge gaps in the ISMS response to global warming.

One additional global context needed for the ISMS is the relation between the ISM and the pantropical rain-band, viz. the Inter-Tropical Convergence Zone or the ITCZ. It has been argued that ISM itself is part of the ITCZ; a Tropical Convergence Zone or a TCZ. It is however unclear if the unique features specific to ISM such as the dramatic onset and the not-so-dramatic withdrawal with the dominant intraseasonal timescales of the MISOs and the active/break periods can be explained by the same physics as the ITCZ. Especially considering the marine ITCZ which persists over the southern tropical Indian Ocean even during the ISM.

It is also unclear how the topographic bucket created by the African highlands, the Himalayan and the Burmese mountains influences the nature of the TCZ as such. For example, the mean rainfall during ISM is characterized by the orographic rainfall over the West Coast of India, the Himalayan Foothills and the eastern edge of the Bay of Bengal. This rainfall distribution is quite unlike the distinct rain-band seen as the ITCZ across entire tropics (see Fig. 4.1). Besides, the zonal mean meridional location of the ITCZ is related to the southward cross-equatorial energy transport by the atmosphere. This is a response to compensate for the northward transport by the ocean which is mechanically forced from the cooler Southern Hemisphere to the warmer Northern Hemisphere. It is unclear if the ISM as a TCZ is a part of this energy transport. Regional energy budgets and their impacts on zonal shifts in rainfall have been proposed, and they may be needed for understanding the ISMS relation with the ITCZ. This is discussed further in a following section.

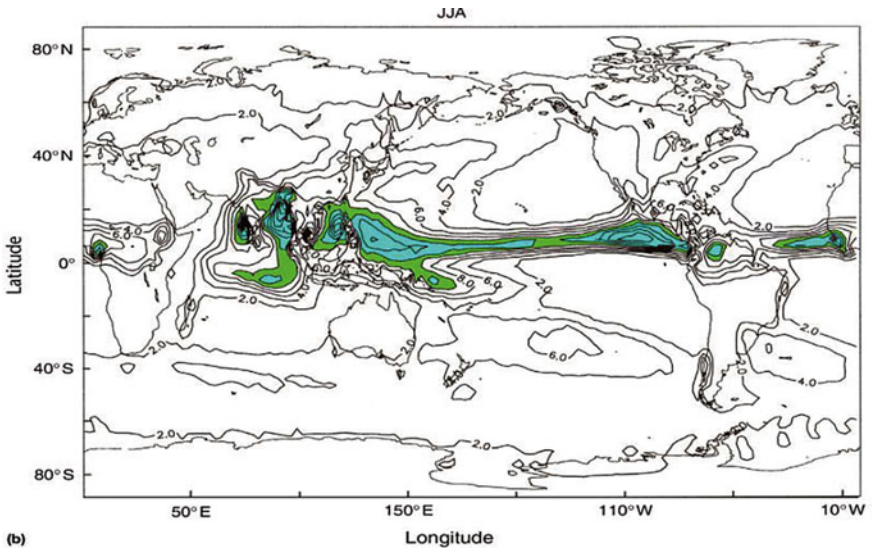

Fig. 4.1 Mean rainfall for June–July–August shows that the Indian Ocean sector is dominated an oceanic ITCZ and maximum rainfall along the Western Ghats, Himalayan foothills and the Bay of Bengal. The global ITCZ in the Northern Hemisphere nearly disappears off the Somali coast and to the east of the Burmese mountains. The critical question is whether the ISMS is governed by similar dynamics as the ITCZ and if so, can the ISMS response to global warming be understood with similar mechanisms. Figure reproduced from the Encyclopaedia of Atmospheric Sciences, Second Edition, 2014

The reader will note our frugality in terms of citations. Following the tradition of a book chapter, we minimize extensive citations which can reduce readability. We offer a brief summary of what has been reported thus far on the response of ISMS components to global warming. We focus on the processes without necessarily separating them into atmospheric and oceanic components since all the processes of ISMS are coupled processes to some degree or the other. There are gaps in the understanding of atmospheric and oceanic processes in each component of ISMS, and the coupling strength may be seasonally varying as well. Such details of coupling are beyond the scope of this brief exposé.

For each component, we raise what we deem are important open questions for advancing the understanding of ISMS in a warming world. The dynamic/thermodynamic processes behind the spatio-temporal distribution of ISM are not studied extensively beyond the orographic processes. We thus focus on ISM as the rainfall averaged over India for simplification.

4.1.1 ISMS Components and Global Warming: Gaps in Knowledge

Some components of the ISMS have already responded to global warming. The seasonal total ISM has reduced by up to 10% over the past century (Roxy et al. 2015). The ISM onset is reported to have shifted to a delay after the mid-1970s when a well-known climate regime shift was reported. Compared to the long-term mean onset date of June 01, the onset tended to occur a few days earlier prior to this regime shift, while it has been occurring later by a few days since the mid-1970s regime shift (Sahana et al. 2015). The average withdrawal date has been occurring earlier than the long-term mean date since the same regime shift compared to the years before (Sabeerali et al. 2012). The propagation speed of MISOs has slowed down across the regime shift (Sabeerali 2014). Monsoon extremes and the spatial variability are both reported to have increased (Goswami et al 2006; Ghosh et al. 2012), while the extremes have also been shown to have become widespread (Roxy et al. 2016). Singh et al. (2014) found that the frequency of the break periods has increased since the 1950s, while their intensity has weakened, but the intensity of the wet periods has increased. However, a study by Karmakar et al. (2015) found that the low-frequency (20–60 days) MISOs have decreased in strength over the past 6 decades but the synoptic scale or the 3–9 day variability has increased. They also find that the extreme rain events in the active phase have decreased, but they have increased in the break periods.

The active/break timescales are the intrinsic scale selection to filter all timescales by the ISMS. This potential interplay between the synoptic (less than 10 days) and extended range or sub-seasonal-to-seasonal (S2S) timescales implies that all natural and forced variabilities of ISMS may be cast as a fundamental process of generating of S2S regimes. In other words, all ISMS variabilities may be better understood as the probability density function of the S2S timescale ISMS. This concept needs further development to integrate the various gaps being identified here in the ISMS components.

With this brief background, we consider each component of the ISMS to identify our own favourite missing links in the understanding of ISMS response to global warming. Such an exercise can hardly be comprehensive. We only intend this to be an exercise in advancing the concept of the ISM as a system.

4.1.1.1 ISMS and ITCZ Responses to Global Warming

The ideas of energy constraints for explaining the zonal mean meridional location of the ITCZ and its width are fairly recent (Kang et al. 2008; Schneider et al. 2014; Byrne and Schneider 2016). The idea has been extended to regional energy fluxes in the zonal and meridional direction to explain zonal shifts of rainfall over the continents (Boos and Korty 2016). Gadgil (2018) presents some arguments for the ISM being just the northward migration of the ITCZ (see Fig. 4.2). Considering Fig. 4.1 and the

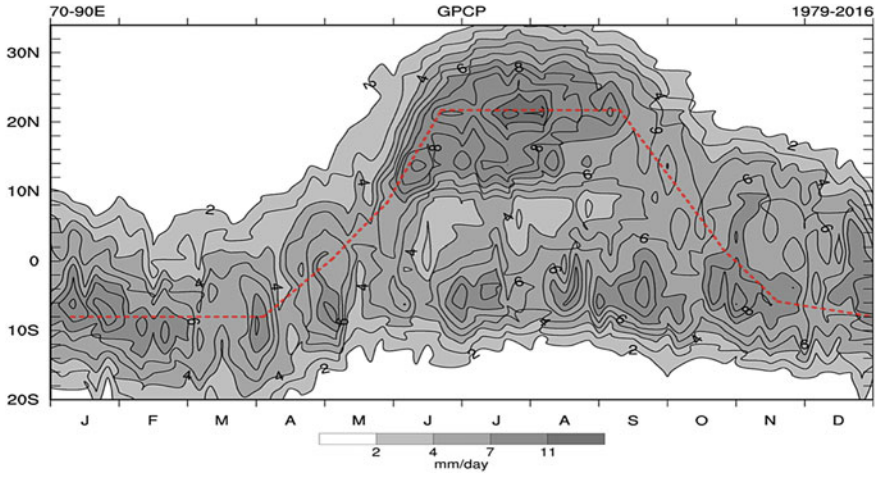

Fig. 4.2 Seasonal cycle of pentad rainfall zonally averaged over 70–90 °E. The equatorial crossing of the ITCZ with the sun begins during March, but the marine ITCZ is retained by the warm Indian Ocean, and a monsoon trough is established over the Indian subcontinent. The key open question is whether the ISM is governed by the ITCZ dynamics and whether the ISM response to global warming can be understood with the ITCZ framework. Figure reproduced from Gadgil (2018)

pre-monsoon movement of the sea level pressure trough marching northwestward from the western Pacific, it is evident that the ISM is more than just the northward migration of the ITCZ.

Gadgil (2018) argues that the ISM is not a land–sea breeze. This argument however may be incomplete since the seasonal variability of the Indian Ocean SSTs and the reversal of the monsoonal circulation do occur in the presence of the land–sea contrast. It is evident that once the ISM settles in on the Indian subcontinent, the monsoonal heating begins to draw in the cross-equatorial southwesterly winds and the moisture flux to support the massive rainfall during the ISM. It is unclear if the land–sea breeze versus the ITCZ argument would exist if the Indian Ocean was much cooler and whether the Indian Ocean would be much cooler if the Indian landmass was much further north.

Without digressing too far into this debate about whether the ISM is a land–sea breeze or the ITCZ, one can identify the gaps in understanding of the ISMS. As Fig. 4.2 shows, the equatorial crossing of the ITCZ begins to occur in March with the sun's crossing into the Northern Hemisphere. The ITCZ fails to cross the equator completely since the warm Indian Ocean retains the marine ITCZ as the continental monsoon trough gets set up over northern India. The ITCZ crossing and splitting occurs over the eastern Indian Ocean (see Fig. 4.3) with the western Indian Ocean being dominated by the strong seasonally persistent southwesterlies and also creates much colder SSTs because of Somali upwelling.

A critical gap in the understanding is whether there is any relation between the equatorial crossing of the ITCZ and the monsoon onset. And how the regional ITCZ

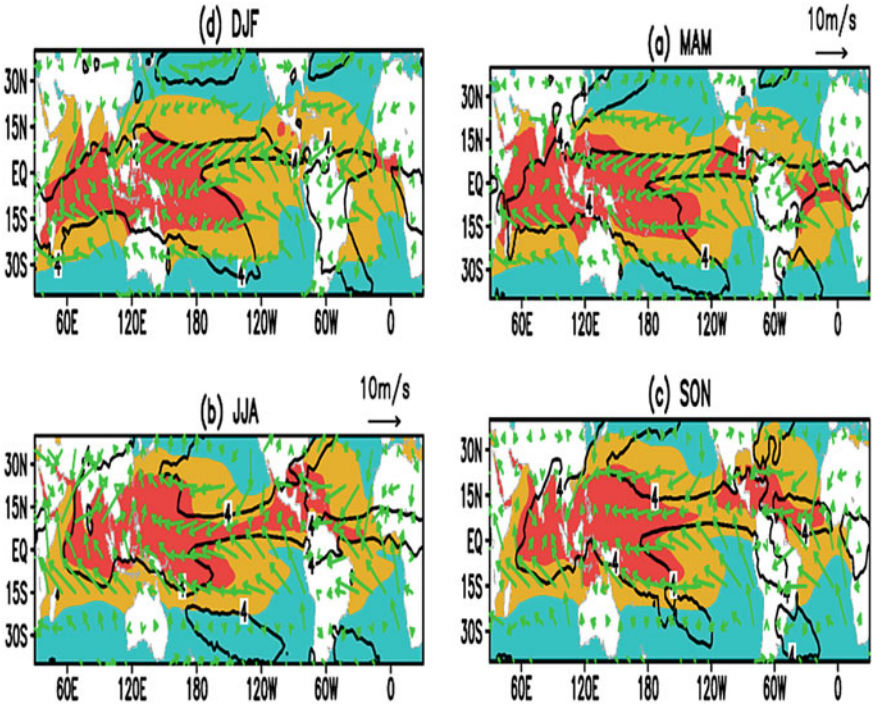

Fig. 4.3 Seasonal mean SSTs (colours), rainfall (10 mm/day contour) and winds (vectors) shown schematically to illustrate the Indian Summer Monsoon System (ISMS) in the global context. The intimate relation of ISMS with the global ITCZ and its seasonal progression are evident as well as the relatively dominant role of the eastern Indian Ocean. The processes of ITCZ equatorial crossing in the central-eastern tropical Indian Ocean and the likely relation of ISMS with the meridional migration of the Indo-Pacific warm pool remain a critical knowledge gap

dynamics over the Indian Ocean sector are related to the northwestward migration of the low-pressure trough and its variability at low-frequencies or in relation to the tropical climate modes such as ENSO, IOD and the Atlantic Zonal Mode (AZM). This is especially critical since the ocean warming over the Indo-Pacific warm pool region appears to be larger than elsewhere in the tropics. The Indo-Pacific warm pool is also reported to be expanding at a rapid rate with quantifiable impacts on the MJO lifecycle (Roxy et al. 2019). That raises questions about potential changes in the relation between the MJOs and MISOs which discussed further below.

The ITCZ is observed to have narrowed without drifting from its mean position in the recent decades (Byrne et al. 2018). It is unclear what this would imply for the ISM if ISM is also governed by the ITCZ dynamics. Zonal and meridional energy fluxes and any shifts in ISM may also become critical. While the land versus ocean warming and the impact of aerosols and solar dimming on land warming have been invoked to explain the decrease in mean rainfall (Roxy et al. 2015), an alternative explanation has related the ISM decrease to a westward shift caused by the ocean

warming (Annamalai et al. 2013). There is clearly a gap in the understanding of the ISMS in the ITCZ framework encompassing all components of the ISMS.

A more challenging aspect of the ISMS-ITCZ relation would be any indirect effects of the natural modes of variability on the ITCZ-ISMS complex. For example, the ISM is clearly affected by the El Niño Southern Oscillation (ENSO), but only 50% of ISM droughts are explained by ENSO. It is now clear that the Atlantic Niño or the AZM also has a significant impact on the ISM. While the relation between the Indian Ocean Dipole/Zonal Mode and the ISM remains somewhat speculative, it is undeniable that all these tropical modes interact with the ITCZ and thus the ISMS. The response of these modes of variability to global warming is not fully understood, but any changes in their frequency, magnitude or duration are bound to impact the ITCZ-ISMS complex.

An additional factor that may be of significance for the ITCZ-ISMS system is related to the pre-monsoon equatorial crossing of the ITCZ. Not much attention has been paid to the SST trends over the Indian Ocean during the pre-monsoon season. Trends in pre-monsoon shower activity are reported to have decreased during March in recent decades, but an increase during April–May is noted. However, no clear separation between multi-decadal variability and these trends has been made. It is also unclear if the pre-monsoon land–ocean conditions affect only the beginning of the season or the entire season. Modelling studies indicate that the pre-monsoon impacts may only be important for the early phase. A special focus may be needed to close the gaps in the understanding of the ITCZ-ISMS response to pre-monsoon warming.

In summary, one must emphasize that the response of ISMS to global warming should not be separated from that of the ITCZ since the two are most likely intimately tied together. They are likely components of a global system, especially if ISMS is indeed governed by ITCZ dynamics.

4.1.1.2 Response of the ISM Onset to Global Warming

Monsoon onset is likely the most dramatic and anticipated feature of the ISMS and yet there is no consensus about whether it is a significant indicator of ISMS variability or change. In other words, there is no robust relation between the onset date and the seasonal mean rainfall. However, it is eagerly awaited by the farmers and is also associated with significant dynamical changes in the strength and the height of the low-level jet or the Find later jet that begins to pipe in the massive moisture flux needed to fuel the ISM.

As noted above, Sahana et al. (2015) reported a shift in the ISM onset to a later than the long-term mean date since the mid-1970s. A delay in the development of the easterly vertical shear and thus the northward propagating systems were conjectured to have caused this delay. The relation between early northward propagating activities and the monsoon onset (Zhou and Murtugudde 2014) would support this hypothesis. The missing knowledge here may be the very mechanism that drives the northward propagations. MISOs are now argued to be driven by the meridional gradient of the

zonal winds over the northern Indian Ocean and the barotropic instability associated with this horizontal shear (Zhou et al. 2017). This horizontal shear and the barotropic instability are a result of coupled ocean–atmosphere process called the Central Indian Ocean mode. This is in sharp contrast to the earlier mechanism that relied on the vertical shear (Jiang et al. 2004).

The relation between the delayed onset and early MISO activities will be valid no matter what the actual mechanism of MISO is. However, the dynamic and thermodynamic response of the ISMS to global warming will determine the changes in vertical versus horizontal shear. That will also determine the oceanic versus continental precipitation changes. These changes in turn must be placed in the context of the ITCZ and its equatorial crossing and how they respond to global warming. Considering that the ITCZ transition occurs in the eastern Indian Ocean, the response of the Indo-Pacific Walker circulation to global warming is also relevant for the ISM onset and the ISMS as a whole.

Another player to be understood better is the role of global SSTs on the onset. Preenu et al. (2017) depict the Indo-Pacific SST anomaly patterns associated with the early and late onsets of ISM. While these patterns have some commonalities with ENSO, it is unclear how the Indo-Pacific warming is impacting the ISM onset variability and trend. It is also unclear how the Atlantic SSTs are impacting the onset which were not considered by Preenu et al. (2017).

4.1.1.3 MISOs in a Warming World

Sabeerali et al. (2014) diagnosed reanalysis products and satellite data to show that MISOs have slowed down in the recent warming period to a nearly standing mode. Warmer Indian Ocean is found to have increased the moisture convergence which in the context of the large-scale circulation leads to a slowdown of the northward propagation. But the variance in the intraseasonal ISM precipitation has increased over the same period. This is consistent with the responses in active and break periods to warming (Singh et al. 2014).

Details of the mechanism for the reduced northward propagation speeds are not fully understood. Considering a global slowdown of cyclones, it may be worth testing the hypothesis that warmer oceans drag down all cyclonic features. The upper ocean heat content may be a suspect especially considering that the MJOs have also responded with similar changes in their residence time over the Indian Ocean and the western Pacific (Roxy et al. 2019). Basic understanding of the air–sea interactions during MJOs and MISOs is still inadequate especially in terms of the scales of the SST anomalies associated with atmospheric processes. The response of these air–sea coupling processes to changes in the wavenumber and frequency of the ocean and the atmosphere may be critical for how MISO and MJO are responding to global warming.

Many other details may be critical as well such as soil moisture, terrestrial vegetation and large-scale steering winds. It is also unclear how the warmer Bay of Bengal may respond to further warming compared to the cooler Arabian Sea and how these

may impact the MISOs and the transition from the MJO season to the MISO season. The variance of intraseasonal ISM appears to be dependent on these regional ocean contrasts (Xi et al. 2015). It is unclear if the relatively different warming rates of the Arabian Sea and the Bay of Bengal and the rest of the Indian Ocean are influencing the MISO response in terms of a shift in frequencies from a decrease in lower frequencies (20–60 days) to an increase at synoptic scales (less than 10 days; Karmakar et al. 2015).

A caveat needed here is that the basic mechanistic understanding of MISOs and MJOs being seriously deficient makes it nearly impossible to be completely confident about the missing knowledge on their response to global warming. This is especially made more difficult by the general inability of the models to accurately simulate these modes of intraseasonal variability in free simulations (natural variability) and historic reconstructions (typically twentieth century simulations with natural and anthropogenic forcings). Despite these limitations, many studies explore MISO/MJO responses to global warming. But such projections must be viewed with caution.

4.1.1.4 Active and Break Event Responses to Global Warming

It should be evident that if MISO/MJO mechanisms are not fully understood, then the processes governing the active and break periods would also be incomplete. In general, MISOs are more dominant over the oceans with some differences in them over the Arabian Sea and the Bay of Bengal and may contribute together to the active/break events of the subcontinent (Roxy and Tanimoto 2007) with different propagating speeds over the two seas (Karmakar and Misra 2020).

There has been no consistency check between MISOs and the local Hadley cell explanation involving alternating subsidence/ascent over the equatorial Indian Ocean and the core monsoon zone. In other words, does the MISO propagation project onto the local Hadley cell or does the local Hadley cell generate and modulate MISOs as a horizontal eddy transport mechanism? The MISO response to global warming may depend on such details.

ENSO timescale ISM variability seems to suggest that deficit monsoon years tend to be dominated by break periods at 30–60 day timescales, and wet monsoon years appear to have more 10–20 day active periods. It is evident that the lower-frequency MISOs propagate northeastward, whereas the higher-frequency ones propagate northwestward. Considering the different SST trends in the regions where these originate, it is unclear if the two frequencies are responding differently. The processes of rainfall at intraseasonal timescales are controlled by the ocean off the west coast of India, whereas the atmospheric instabilities deliver rainfall over the Bay of Bengal (Xi et al. 2015). Differential warming of the two seas also must be understood in this context and whether such details contribute to the responses of the active/break events to global warming.

Moisture source calculations indicate that the oceanic sources contribute significantly to the 30–60 day mode, while the terrestrial sources are a bigger contributor to the 10–20 day mode. Impacts of land and ocean warming as well as irrigation

water and vegetation changes must then impact the ISMS response via these moisture source mechanisms and related feedbacks. Moisture source responses must be considered as a part of the dynamic and thermodynamic components of the ISMS response to global warming.

The other unclosed loop is the relation between the large-scale structures associated with the active/break periods and their interaction with the local Hadley cell. There are low-level circulation anomalies stretching from northwest of India down to the tropical western Pacific during the active/break events. The strength of this circulation varies coherently with the active/break rainfall variability. An east–west pattern of out-of-phase rainfall between India and East Asia also occurs during active/break periods.

An asymmetry in the more rapid transition from an active to a break period compared to a slower transition from a break to an active period is noted in observations. Considering the role of the purported increase in the synoptic scale intraseasonal variability in the recent decades (Karmakar et al. 2015), there needs to a clearer understanding of the ISMS response to global warming in terms of the land – ocean warming and their impacts on the large-scale circulation patterns of relevance to these different timescales.

Since the active/break processes are a see-saw of convection over the tropics and the Indian subcontinent, one would expect that the convective phase of the MJOs in the tropics may play a role in this see-saw as well. Such a relation is indeed seen where the active phase of MJO over the Indian sector induces a break period over the ISM region. We circle back to the finding that MJOs respond to global warming, specially the expansion of the Indo-Pacific warm pool, by reducing their residence over the Indian sector and increasing it over the Maritime Continent (Roxy et al. 2019). The relation between this MJO response and the ISMS response must now be reconciled. Note that the MJO season typically spans the October-April period and thus the definition of MJOs during ISM needs to be considered carefully, especially in terms of the eastward vs. northward propagation of intraseasonal oscillations during boreal summer. This may be related to the zonal modes in each of the tropical oceans.

A holistic view of the active/break events, MISOs, MJOs and the ITCZ would require that we consider the northwest–southeast circulation pattern, the local Hadley cell, the persistent generation of propagating convective events over the western Indian Ocean, the eastward propagating MJOs and the northward steering of the MISOs, together. Which means the ISMS domain is much larger than just the Indian subcontinent. This is especially so when the lower-frequency influences from the higher latitude ocean and land processes (North Atlantic and Pacific, Southern Ocean, Eurasian snow) are also brought into the picture. To the extent that all these influences project onto the active/break processes as an integral and intrinsic timescale of the ISMS, a prioritized bridging of knowledge gaps from the bottom-up, i.e. the intraseasonal timescale ISMS processes up to lower frequencies may be a smoother path to a complete ISMS understanding.

4.1.1.5 ISM Withdrawal

ISM withdrawal is not as dramatic as the onset, but it is much more variable than the onset. The withdrawal also tends to contribute disproportionately the inter-annual variability of the ISM. Moisture source studies have pointed out that the contribution of recycled precipitation in the form evapotranspiration is critical for the amount of rain during the withdrawal as well as for the timing of the withdrawal.

Large-scale dynamics observed to impact the onset and the ISM are also important during the withdrawal. The regime shift of 1976 is seen as a shift in the withdrawal as well. The impact of the Arabian Sea and the eastern tropical Pacific (ENSO) impacts tended to lead to a withdrawal that occurred a few days after the long-term mean withdrawal date of October 03 prior to the regime shift. The impact of the Arabian Sea has been found to be absent after the regime shift with a much reduced impact of the eastern Pacific SSTs leading to a withdrawal that is a few days earlier than the mean data of October 03. The eastern Indian Ocean has been a more dominant player in the post-1976 period. A vast literature exists on the changes in ENSO evolution and patterns and the decadal variability of IOD which would seem consistent with these changes in withdrawal as well.

The role of the Atlantic Niño has not been considered during the withdrawal phase. It is also unclear how the eastern Indian Ocean induces withdrawal variability or shift. Remembering that the eastern Indian Ocean is also the theatre of action for the cross-equatorial ITCZ transition prior to the monsoon as well as the withdrawal phase (see Fig. 4.3), one must conjecture that the global ITCZ dynamics may also be a player in the withdrawal variability. It is fair to say that there has generally been less attention paid to the withdrawal phase of the ISMS as compared to the other components.

4.1.1.6 ISMS and the ISM Extremes

Some of the observations of ISM indicate that the downward trend of the last several decades may be reversing in the last decade or so. The IMD dataset however shows that the trend has flattened but no recovery of the monsoon is evident. Just as the causes for the downward trend have ranged from aerosols to irrigation to land-use change and land warming or a lack thereof, the recovery has also led to invoking several of these mechanisms. The zonally asymmetric Indian Ocean warming and its feedbacks to the Pacific response to global warming are also important as stated earlier, especially in the context of the ISMS-ITCZ interactions under global warming.

Despite these potentially non-stationary trends in the ISM, extreme rainfall events have been reported to be generally increasing and becoming more widespread. A recent review by Singh et al. (2019) summarizes the state of the knowledge on extremes in the context of historical changes and anthropogenic forcing. The main caveat is that the definition of "extreme" may affect the conclusion. The review notes the role of the interaction of intraseasonal variability with various other

timescales to produce the extremes and that the relative role of the Arabian Sea and the Bay of Bengal are not fully understood in determining the spatial scale of the extremes. Essentially, the moisture fluxes and advection processes (large-scale winds vs. synoptic low-pressure systems) from the two seas must be understood in the context of the changes in the other related components of the ISMS such as the propagation speeds of MISOs, Indian Ocean warming and the observed changes in the frequency and duration of active and break periods. Impact of land-use land change on extremes also remains a serious gap in process understanding.

Spatial variability if ISM has been decreasing while the spatial variability of the extremes has been increasing (Ghosh et al. 2016). But the role of land warming and humidity increases on rainfall extremes are not fully understood, especially in terms of the spatial variability of the extremes. These tend to leak into uncertainties in attribution of extremes themselves to anthropogenic forcings such as land-use change and aerosols. The differences between different datasets, especially at regional scales only add to difficulties in attribution of natural versus anthropogenic drivers of precipitation extremes. Lack of fidelity at regional scales in models and the ubiquitous dry ISM bias are just some of the model biases which will be major challenges for advancing the understanding of extremes.

In summary, processes that govern the spatial-temporal variability and trend of extremes appear to be intimately tied to several other component of the ISMS including the land–ocean–atmosphere feedbacks. Any process understanding of extremes then must occur within the ISMS-ITCZ complex and its response to climate modes and anthropogenic forcings.

4.2 Summary

A succinct summary on the concept of ISMS may be best elicited with the structure of the seasonal rainfall distribution across the tropics along with the SSTs and surface winds. Figure 4.3 shows the outline of the 10 mm/day rainfall contour for DJF, MAM, JJA and SON.

The 10 mm/day rainfall contour is chosen as a proxy for the ITCZ and its relation to the meridional migration of the Indo-Pacific warm pool. The southeastward extension of the SPCZ is argued to be related to the zonal asymmetry of the SSTs in a mean sense, while its inter-annual and longer timescale variabilities are related to the climate modes such as ENSO and IPO which modulate the SST distribution. It is curious that ITCZ in the Indian Ocean bears some resemblance to the SPCZ but its relation to SSTs is not yet explored.

The northward migration of the ITCZ over the Indian Ocean in spring months is seen as a central Indian and northwestern tropical Pacific phenomenon. The Indian Ocean influences on the Pacific at ENSO, and longer timescales occur through this channel via Kelvin waves and perturbations of the Philippine anticyclone. ISMS must thus be considered in the global framework of ITCZ and warm pool migrations

with additional attention to the missing processes via which the Atlantic influences the ISMS.

The ISM withdrawal phase also occurs towards the southeast into the western tropical Pacific and with the southward migration of the Indo-Pacific warm pool. All components of the ISMS must thus be placed in the framework of this SST-ITCZ response to the seasonal cycle of radiative forcing and the scale selections involved in determining the onset, active/break periods, extremes and the withdrawal.

We have clearly ignored the spatial distribution of rainfall over the Indian subcontinent since fundamental processes that determine this distribution are not well understood. Needless to say that this may become the Achilles Heel for a complete process and predictive understanding of ISMS.

We want to re-emphasize that both the ITCZ and ISMS are fully coupled phenomena and there are intricate atmosphere, land and ocean processes as well as coupled feedbacks at play at all timescales. Observational needs will also benefit from focusing on this ITCZ-ISMS complex as a whole. The same goes for the modelling since the approach of diagnosing model biases in each basin—cold tongue and double ITCZ biases in the Pacific, reversed thermocline gradient in the tropical Indian Ocean and the reversed SST gradient in tropical Atlantic Ocean are likely related the pantropical ITCZ processes and related feedbacks with the heat source of the ISMS.

For example, when a model captures the mean seasonal cycle of the ISM but does not accurately represent MISOs or MJOs, are different errors cancelling each other out or are there processes in nature which can indeed produce the seasonal ISM without these intraseasonal modes? Such questions are hard tease apart in the observations alone. Coupled reanalyses and reliable models which can capture all the important timescales of the ITCZ-ISMS complex are needed for making a significant dent in bridging the knowledge gaps identified here.

Acknowledgements We gratefully acknowledge the Visiting Professor position at the Indian Institute of Technology—Bombay which offered complete freedom to work on this project. We are indebted to Dr. Jieshun Zhou of NOAA, USA, for assistance in preparing Fig 4.3.

References

Annamalai H, Hafner J, Sooraj KP, Pillai P (2013) Global warming shifts the monsoon circulation, drying South Asia. J Clim 26. https://doi.org/10.1175/JCLI-D-12-00208.1

Boos W, Korty R (2016) Regional energy budget control of the intertropical convergence zone and application to mid-Holocene rainfall. Nat Geosci 9:892–897. https://doi.org/10.1038/ngeo2833

Byrne MP, Schneider T (2016) Narrowing of the ITCZ in a warming climate: physical mechanisms. Geophys Res Lett. https://doi.org/10.1002/2016GL070396

Byrne MP, Pendergrass AG, Rapp AD, Wodzicki KR (2018) Response of the intertropical convergence zone to climate change: location, width, and strength. Curr Clim Change Rep 4:355–370. https://doi.org/10.1007/s40641-018-0110-5

Gadgil S (2018) The monsoon system: land–sea breeze or the ITCZ? J Earth Syst Sci 127. https://doi.org/10.1007/s12040-017-0916-x

Ghosh S, Das D, Kao SC, Ganguly AR (2012) Lack of uniform trends but increasing spatial variability in observed Indian rainfall extremes. Nat Clim Change 2:86–91. https://doi.org/10.1038/nclimate1327

Ghosh S, Vittal H, Sharma T, Karmakar S, Kasiviswanathan KS, Dhanesh Y, Sudhee KP, Gunthe SS (2016) Indian summer monsoon rainfall: implications of contrasting trends in the spatial variability of means and extremes. PLoS ONE 11(7):e0158670. https://doi.org/10.1371/journal.pone.0158670

Goswami BN, Venugopal V, Sengupta D, Madhusoodanan MS, Xavier P (2006) Increasing trend of extreme rain events over India in a warming environment. Science 314:1442–1445. https://doi.org/10.1126/science.1132027

Jiang XN, Li T, Wang B (2004) Structures and mechanisms of the northward propagating boreal summer intra-seasonal oscillation. J Clim 17:1022–1039. https://doi.org/10.1175/1520-0442(2004)017,1022:SAMOTN.2.0.CO;2

Kang SM, Held IM, Frierson DMW, Zhao M (2008) The response of the ITCZ to extratropical thermal forcing: idealized slab-ocean experiments with a GCM. J Clim 21:3521–3532. https://doi.org/10.1175/2007JCLI2146.1

Karmakar N, Misra V (2020) Differences in northward propagation of convection over the Arabian Sea and Bay of Bengal during boreal summer. Geophys Res Lett 125. https://doi.org/10.1029/2019JD031648

Karmakar N, Chakraborty A, Nanjundiah RS (2015) Decreasing intensity of monsoon low-frequency intraseasonal variability over India. Environ Res Lett 10. https://doi.org/10.1088/1748-9326/10/5/054018

Preenu PN, Joseph PV, Dineshkumar PK (2017) Variability of the date of monsoon onset over Kerala (India) of the period 1870–2014 and its relation to sea surface temperature. J Earth Syst Sci 126. https://doi.org/10.1007/s12040-017-0852-9

Roxy MK, Tanimoto Y (2007) Role of SST over the Indian Ocean in influencing the intraseasonal variability of the Indian summer monsoon. J Meteorol Soc Jpn 85:349–358

Roxy M, Kapoor KR, Terray P, Murtugudde R, Ashok K, Goswami BN (2015) Drying of Indian subcontinent by rapid Indian Ocean warming and a weakening land-sea thermal gradient. Nat Commun 6, Article # 7423. https://doi.org/10.1038/ncomms8423

Roxy MK, Athulya R, Mujumdar M, Murtugudde R, Ghosh S, Pathak A, Terray P, Krishnan R, Rajeevan M (2016) A four-fold increase in widespread extreme rain events over central India. Nat Commun. https://doi.org/10.1038/s41467-017-00744-9

Roxy MK, Dasgupta P, McPhaden MJ, Suematsu T, Zhang C, Kim D (2019) Twofold expansion of the Indo-Pacific warm pool warps the MJO lifecycle. Nature 575:647–651. https://doi.org/10.1038/s41586-019-1764-4

Sabeerali CT, Rao SA, Ajayamohan RS, Murtugudde R (2012) On the relationship between Indian summer monsoon withdrawal and Indo-Pacific sea surface temperature anomalies before and after 1976/77 climate shift. Clim Dyn 39:841–859. https://doi.org/10.1007/s00382-011-1269-9

Sabeerali CT, Rao SA, George G, Rao DN, Mahapatra S, Kulkarni A, Murtugude R (2014) Modulation of monsoon intra-seasonal oscillations in the recent warming period. J Geophys Res 119:5185–5203. https://doi.org/10.1002/2013JD021261

Sahana AS, Ghosh S, Ganguly A, Murtugudde R (2015) Shift in Indian summer monsoon onset during 1976/1977. Environ Res Lett 10. https://doi.org/10.1088/1748-9326/10/5/054006

Schneider T, Bischoff T, Haug G (2014) Migrations and dynamics of the intertropical convergence zone. Nature 513:45–53. https://doi.org/10.1038/nature13636

Singh D, Tsiang M, Rajaratnam B, Diffenbaugh NS (2014) Observed changes in extreme wet and dry spells during the South Asian summer monsoon season. Nat Clim Change 4:456–461. https://doi.org/10.1038/nclimate2208

Singh D, Ghosh S, Roxy MK, McDermid S (2019) Indian summer monsoon: extreme events, historical changes, and role of anthropogenic forcings. WIREs Clim Change 10. https://doi.org/10.1002/wcc.571

Xi J, Zhou L, Murtugudde R, Jiang L (2015) Impacts of intraseasonal SST anomalies on precipitation during Indian summer monsoon. J Clim 28:4561–4575. https://doi.org/10.1175/JCLI-D-14-00096.1

Zhou L, Murtugudde R (2014) Impact of northward propagating intraseasonal variability on the onset of Indian summer monsoon. J Clim 27:126–139. https://doi.org/10.1175/JCLI-D-13-00214.1

Zhou L, Murtugudde R, Chen D, Tang Y (2017) A central Indian Ocean mode and heavy precipitation during Indian summer monsoon. J Clim. https://doi.org/10.1175/JCLI-D-16-0347.1

Chapter 5
Observed Climate Change Over India and Its Impact on Hydrological Sectors

Pulak Guhathakurta and Nilesh Wagh

5.1 Introduction

The climate of India is largely dominated by the southwest monsoon and the associated circulation features. Most of the annual rainfall over India is received during the four months of southwest monsoon season (June to September). Nearly 70–80% of annual rainfall of the country is being received during the southwest monsoon season. However, there is a large spatial variability in the rainfall distribution. Among the climate variables, precipitation is the most important process for the water sector. It is a variable that drives the key natural resource process in a river basin. Therefore, it is most widely analysed in climate change impact studies. Temperature the most important climate parameter that is directly linked with the climate change can influence the rainfall pattern as well as hydrological disasters like drought and flood. Run-off from a river basin is the integrated outcome of climatic inputs and basin topography, land use/cover and water management infrastructure. Therefore, a change in the precipitation and other relevant climatic variables, land use/land cover and water utilization leads to a change in water yield from a catchment and its temporal distribution. Global warming is unequivocal and already studies (Guhathakurta et al. 2011, 2015) reported an increase in the magnitude and frequency of extreme precipitation events over Indian region. Temperature plays crucial role in defining the water stress regions and thus has significant impact on the onset and persistence of drought simultaneously with lack of precipitation. Guhathakurta et al. (2017) using more than 100 years of district rainfall data have identified the districts with significant drought incidences.

There are many studies either using station data or gridded data identifying the changes in mean rainfall pattern and its variability of spatial scales like states,

P. Guhathakurta (✉) · N. Wagh
India Meteorological Department, Ministry of Earth Sciences, Pune, Maharashtra 411005, India

© The Author(s), under exclusive license to Springer Nature Singapore Pte Ltd. 2021

A. Pandey et al. (eds.), *Hydrological Aspects of Climate Change*,
Springer Transactions in Civil and Environmental Engineering,
https://doi.org/10.1007/978-981-16-0394-5_5

districts, etc. However, for assessing impact on water resources as well as agriculture, there is need to have assessment of climate change impact in river basin scales. In this study, we have analysed both temperature and rainfall patterns and variability of 101 river sub-basins and 25 major river basins of India. Spatial trend analysis of mean temperature, day temperature (maximum temperature) and night temperature (minimum temperature) resulted to separate the river basins which are most vulnerable to climate change impact and thus will help to better adaptation strategies by the planners. The mean rainfall and variability of river basins and a detailed analysis of changing monsoon rainfall pattern based on the long period data series constructed from the high resolution gridded data are the final outcome of the climate change impact on hydrological sectors.

Jain et al (2017) using IMD gridded data for the period 1951–2011 has done trend analysis of annual rainfall of seven river basins of India but could not find any significant trend. However, Bisht et al. (2018) using the data for the period 1901–2015 have done spatio-temporal trends of rainfall across Indian river basins and got significant decreasing trends in monsoon rainfall in Ganga and other basins. In our present paper, we have used data up to 2019 and analysed (i) all India mean temperature, maximum temperature and minimum temperature trends, (ii) Spatial temperature trend patterns for 101 river basins of India, (iii) mean and variability of rainfall pattern for 25 major river basins and their trends.

5.2 Data and Methodology

Two types of datasets were mainly utilized for analysis in this study, temperature and rainfall. For temperature, we have used 0.5×0.5 deg daily gridded data for the period 1951–2019, while for rainfall, we have used 0.25×0.25 deg daily gridded data for the period 1901–2019 from India Meteorological Department, Pune. All India monthly, seasonal and annual maximum, minimum and mean temperature series for the period 1901–2019 available at India Meteorological Department, Pune, is used to study the changes in the all India scale. Monthly and weekly time series of rainfall and temperature long period data series of all the 25 major basins and 101 sub-basins are constructed using GIS tool and basin shapefiles. These time series are analysed for trend and variability in different temporal scales.

5.3 Results and Discussions

5.3.1 All India Mean Temperature Trend

Mean temperature anomalies for all India are prepared, and mean temperature anomaly trends during winter, pre-monsoon, SW monsoon, post-monsoon and annual seasons are analysed.

5.3.1.1 Annual Mean Temperature Anomalies

Figure 5.1 shows the annual mean temperature anomaly time series over India for the period 1901–2019. Also, 9 point binomial filter and the trend line of annual temperature anomaly are shown in the figure. It can be seen that the all India mean temperature anomaly was positive for the all 22 years since 1998 and year 2016 being the warmest with anomaly of +0.71 °C. It is also noticeable that anomalies prior to 1998 were mostly negative with highest negative anomaly of −0.96 °C observed in the year 1917. There is overall increase of all India annual mean temperature of + 0.61 °C/100 years during the period which is significant at 99% level.

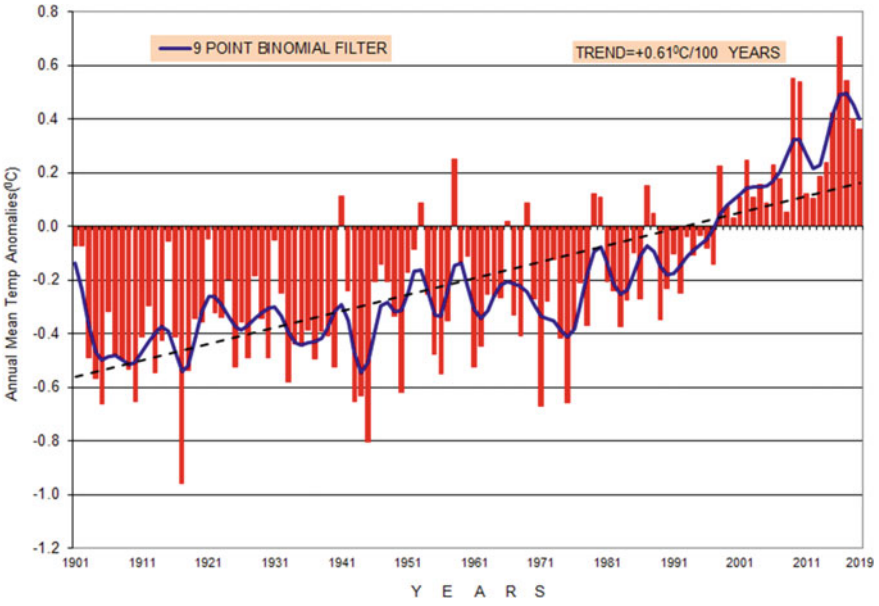

Fig. 5.1 All India annual mean temperature anomalies

5.3.1.2 Winter Mean Temperature Anomalies

Figure 5.2 shows the time series of mean temperature anomaly for winter months (January and February). The trend analysis for mean temperature for winter shows a significant increase at +0.68 °C/100 years. The figure also shows that the 2016 was the warmest winter with the anomaly of +1.15 °C while the year 1905 was the coolest with highest negative anomaly of −2.3 °C. Winter temperature anomaly was positive for all the last 5 years since 2015.

5.3.1.3 Pre-monsoon Mean Temperature Anomalies

Figure 5.3 shows the time series of mean temperature anomaly for the pre-monsoon season (March April and May). It can be seen that there is a significant increase of all India mean temperature during pre-monsoon season at +0.58 °C/100 years. It can also be noticed that 2010 was the warmest summer with the anomaly of +1.28 °C while 1917 was coolest with mean temperature anomaly of −1.45 °C. Also since the year 1998, mean temperature anomaly was positive for past 21 years.

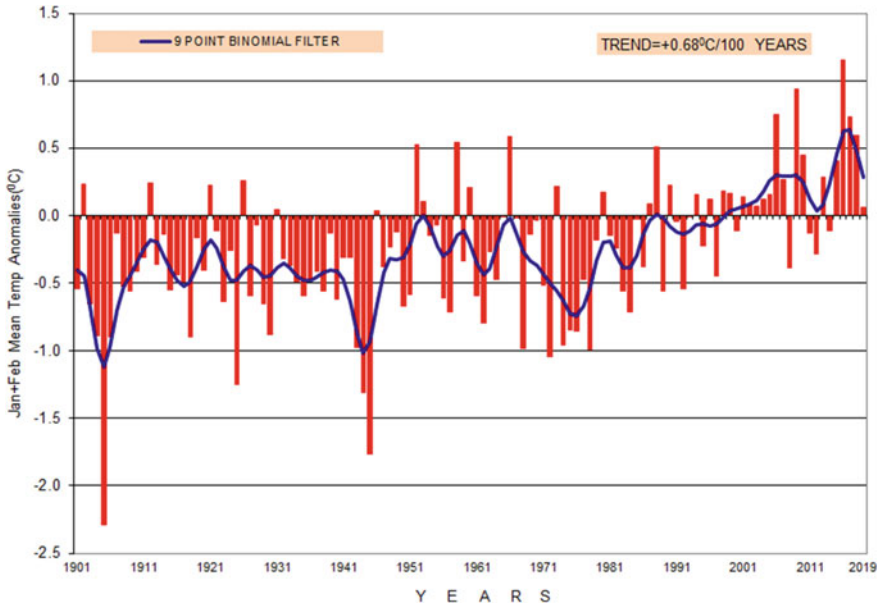

Fig. 5.2 All India winter mean temperature anomalies

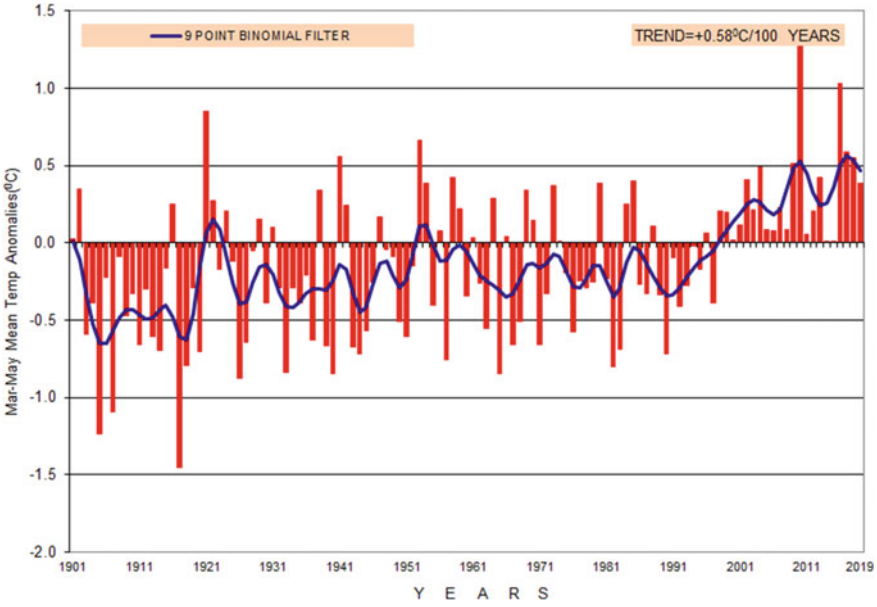

Fig. 5.3 All India pre-monsoon mean temperature anomalies

5.3.1.4 Southwest Monsoon Mean Temperature Anomalies

Figure 5.4 shows the time series for mean temperature anomaly for the southwest monsoon season (June, July, August and September). From the figure, it can be seen that there is a significant increase of all India mean temperature during southwest monsoon season at +0.41 °C/100 years. It can also be noticed that southwest monsoon season of 2019 was the warmest among past 119 years with the anomaly of +0.58 °C.

5.3.1.5 Post-monsoon Mean Temperature Anomalies

Figure 5.5 shows the time series for mean temperature anomaly for post-monsoon season (October, November and December). There was a significant increase in all India mean temperature during post-monsoon season at +0.88 °C/100 years, which is highest among of all seasons. The anomaly was highest in the year 2015(0.84 °C) for the last 119 year.

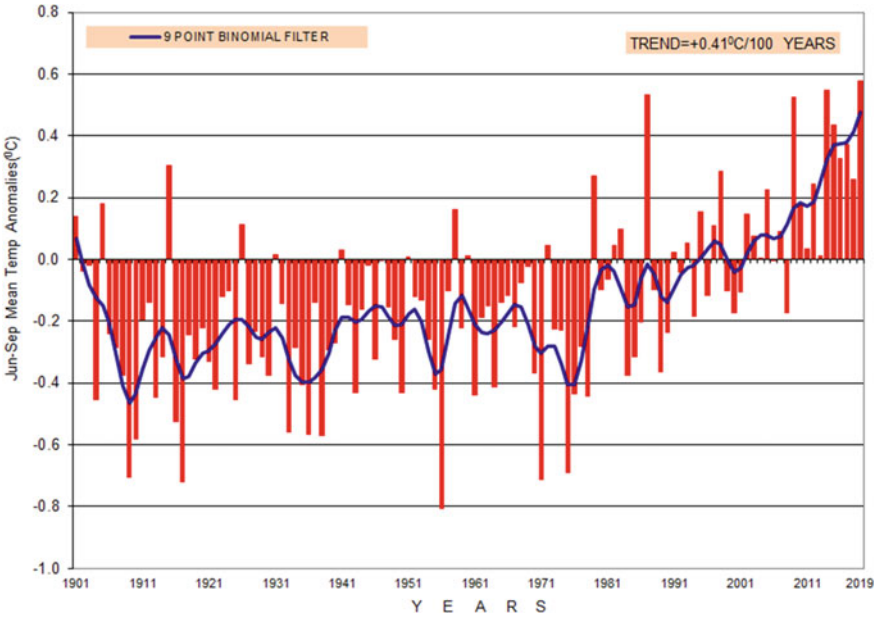

Fig. 5.4 All India Southwest monsoon mean temperature anomalies

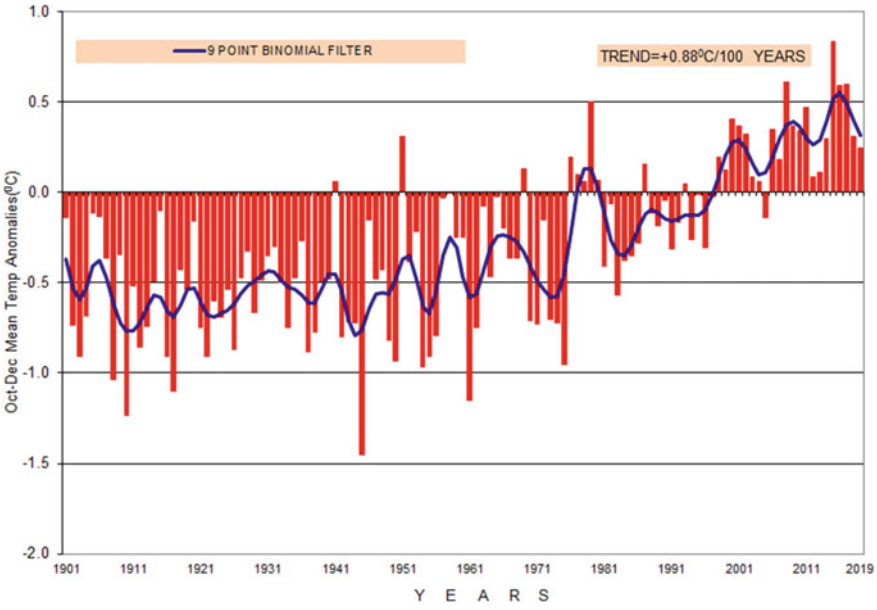

Fig. 5.5 All India post-monsoon mean temperature anomalies

5.3.2 All India Maximum Temperature Trend

Maximum temperature anomalies for all India are prepared, and trend analysis is used to analyse maximum temperature anomaly trends during winter, pre-monsoon, SW monsoon, post-monsoon and annual seasons.

5.3.2.1 Annual Maximum Temperature Anomalies

Figure 5.6 shows the annual maximum temperature anomaly time series over India for each year since 1901. The dark blue line on chart represents 9 point binomial filter, whereas the dashed blue line represents the trend line of annual temperature anomaly. It can be seen that the all India maximum temperature anomaly was positive for the all 21 years since 1999 and it was the year when the significant increase started. Also, in the year 2016, maximum temperature was highest with anomaly of +0.85 °C. It is also noticeable that anomalies prior to 1999 were mostly negative. There is overall increase in all India annual maximum temperature of +1.0 °C/100 years which is significant at 99% level.

5.3.2.2 Winter Maximum Temperature Anomalies

Figure 5.7 shows the time series of maximum temperature anomaly for winter months (January and February). The trend analysis for maximum temperature during winter

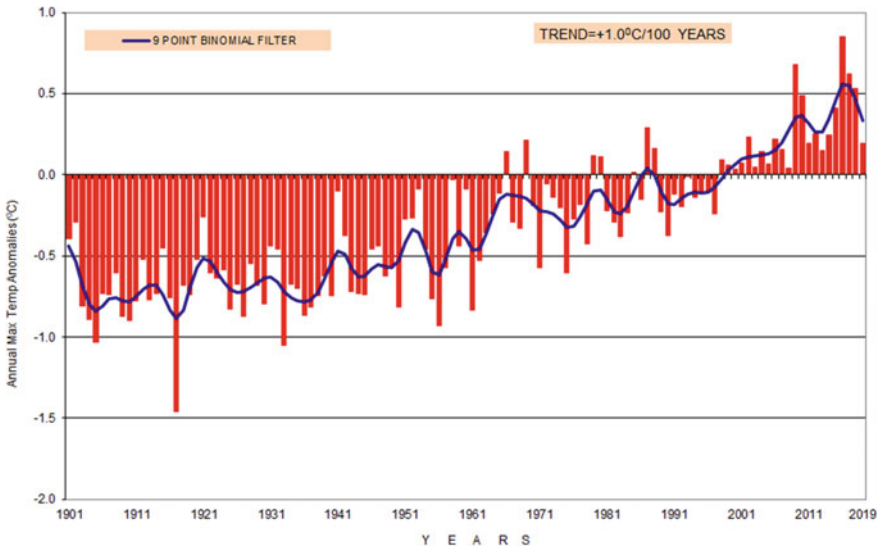

Fig. 5.6 All India annual maximum temperature anomalies

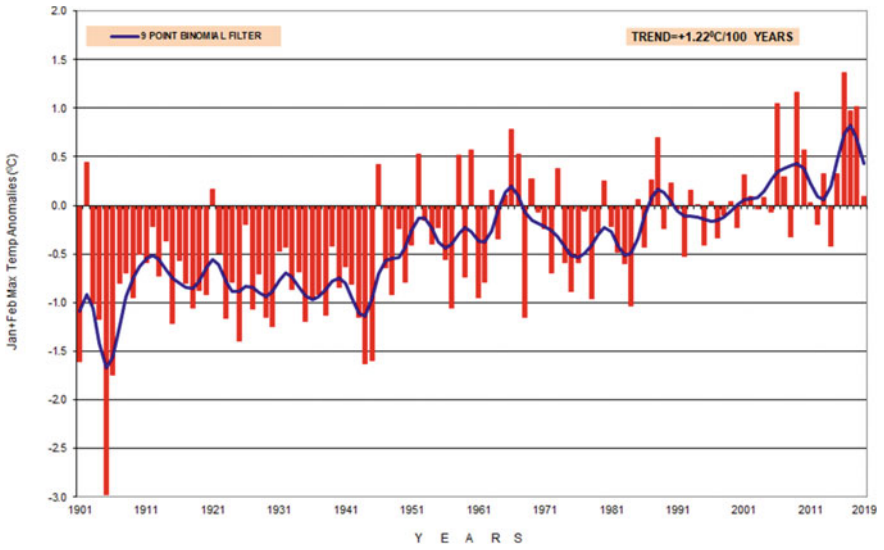

Fig. 5.7 All India winter maximum temperature anomalies

shows that there is a significant increase of all India maximum temperature at + 1.22 °C/100 years. It can be seen that the day temperature was warmer for the successive five years since 2015. The figure also shows that all the four years when maximum temperature anomaly was more than +1.0 °C were on 2006, 2009, 2016 and 2018.

5.3.2.3 Pre-monsoon Maximum Temperature Anomalies

Figure 5.8 shows the time series of maximum temperature anomaly for the pre-monsoon season (March, April and May). The trend analysis for maximum temperature during pre-monsoon season shows that there is a significant increase of all India maximum temperature at +0.95 °C/100 years. It can be seen that the day temperature was warmer for the successive four years since 2016. The figure also shows that two years when maximum temperature anomaly was more than +1.0 °C were on 2010 and 2016.

5.3.2.4 Southwest Monsoon Maximum Temperature Anomalies

Figure 5.9 shows the time series for maximum temperature anomaly for the southwest monsoon season (June, July, August and September). The trend analysis for maximum temperature during southwest monsoon season shows that there is a significant increase of all India maximum temperature at +0.76 °C/100 years. It can be

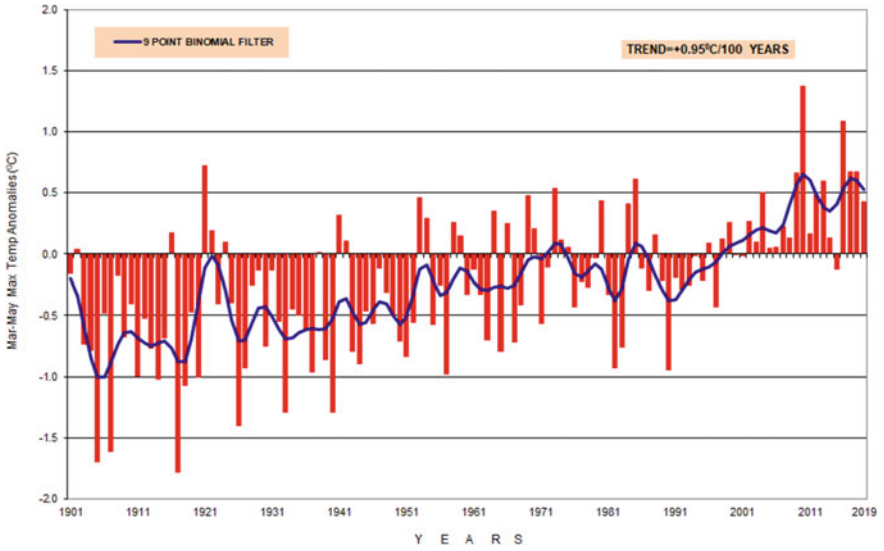

Fig. 5.8 All India pre-monsoon maximum temperature anomalies

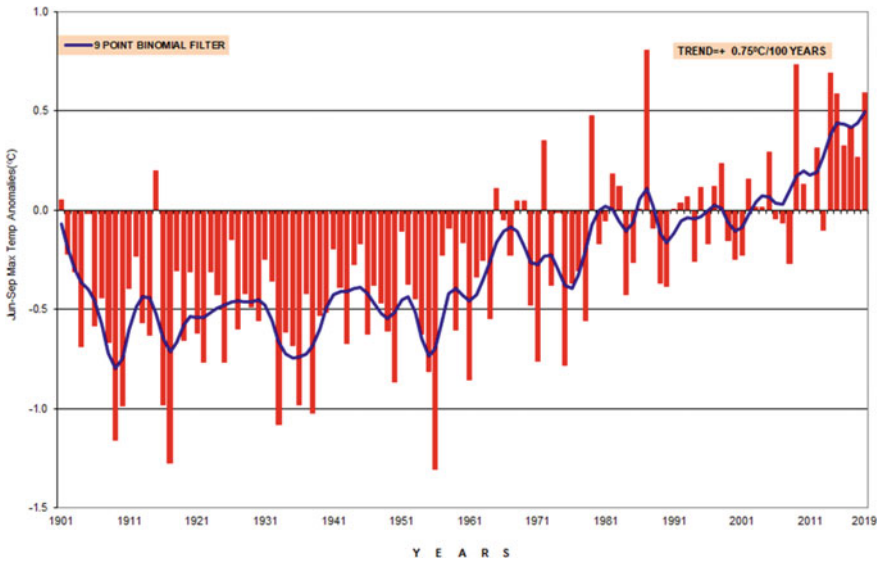

Fig. 5.9 All India Southwest monsoon maximum temperature anomalies

seen that the day temperature was warmer for the successive six years since 2014. The figure also shows that all the five years when maximum temperature anomaly was more than +0.5 °C were on 1987, 2009, 2014, 2015 and 2019.

5.3.2.5 Post-monsoon Maximum Temperature Anomalies

Figure 5.10 shows the time series for maximum temperature anomaly for post-monsoon season (October, November and December). The trend analysis for maximum temperature during post-monsoon season shows that there is a significant increase of all India maximum temperature at +1.24 °C/100 years, which is highest among of all seasons. All the six years when maximum temperature anomaly was more than +0.5 °C were on 2000, 2008, 2011, 2016, 2017 and 2018.

5.3.3 All India Minimum Temperature Trend

Minimum temperature anomalies for all India are prepared, and trend analysis is used to analyse minimum temperature anomaly trends during winter, pre-monsoon, SW monsoon, post-monsoon and annual seasons.

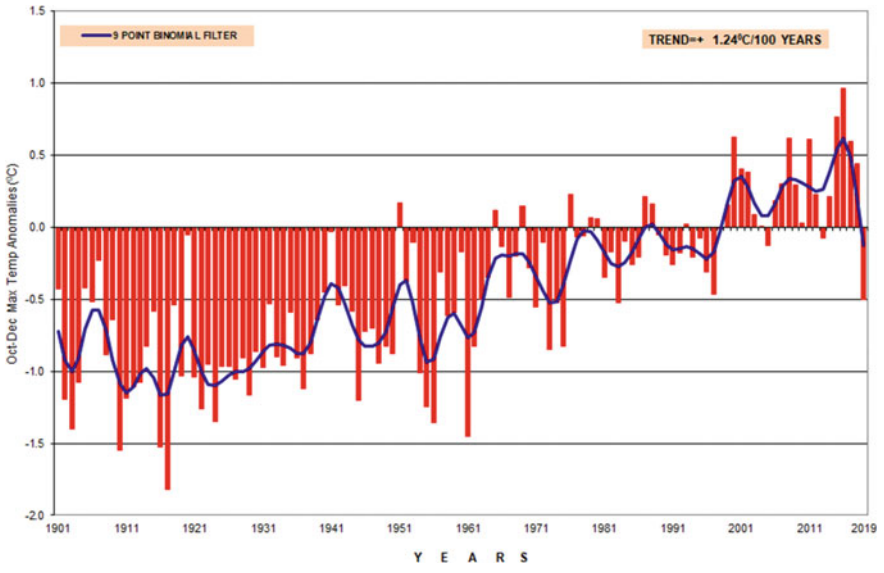

Fig. 5.10 All India post-monsoon maximum temperature anomalies

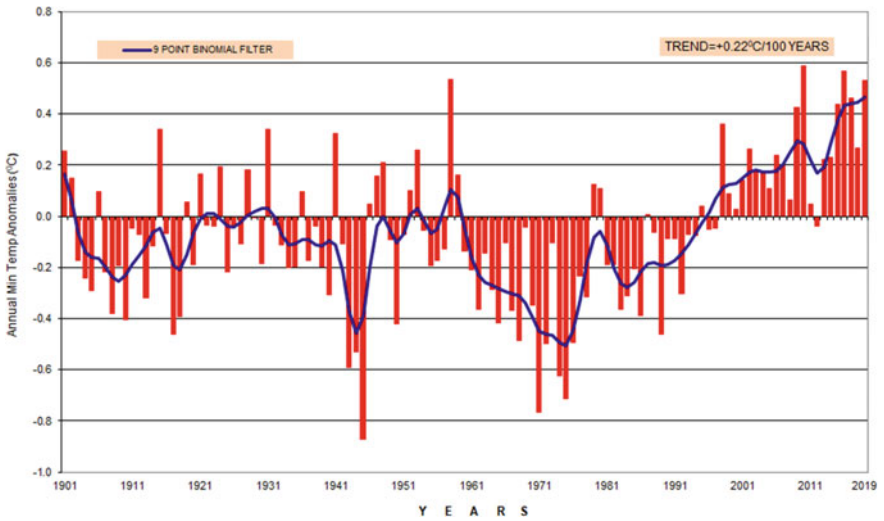

Fig. 5.11 All India annual minimum temperature anomalies

5.3.3.1 Annual Minimum Temperature Anomalies

Figure 5.11 shows the annual minimum temperature anomaly time series over India for each year since 1901. The dark blue line on chart represents 9 point binomial filter, whereas the dashed blue line represents the trend line of annual temperature anomaly. All India minimum temperature anomaly was positive for all the 22 years since 1998. Also, in the year 2010, minimum temperature was highest with anomaly of +0.59 °C. In last 119 years, there is overall increase in all India annual minimum temperature at the rate of +0.22 °C/100 years.

5.3.3.2 Winter Minimum Temperature Anomalies

Figure 5.12 shows the time series of minimum temperature anomaly for winter season (January and February). The trend analysis for minimum temperature during winter shows that there is a slight increase of all India minimum temperature at $+0.14^0$ C/100 years.

5.3.3.3 Pre-monsoon Minimum Temperature Anomalies

Figure 5.13 shows the time series of minimum temperature anomaly for the pre-monsoon season (March, April and May). The trend analysis for minimum temperature during pre-monsoon season shows that there is a slight increase of all India minimum temperature at +0.20 °C/100 years.

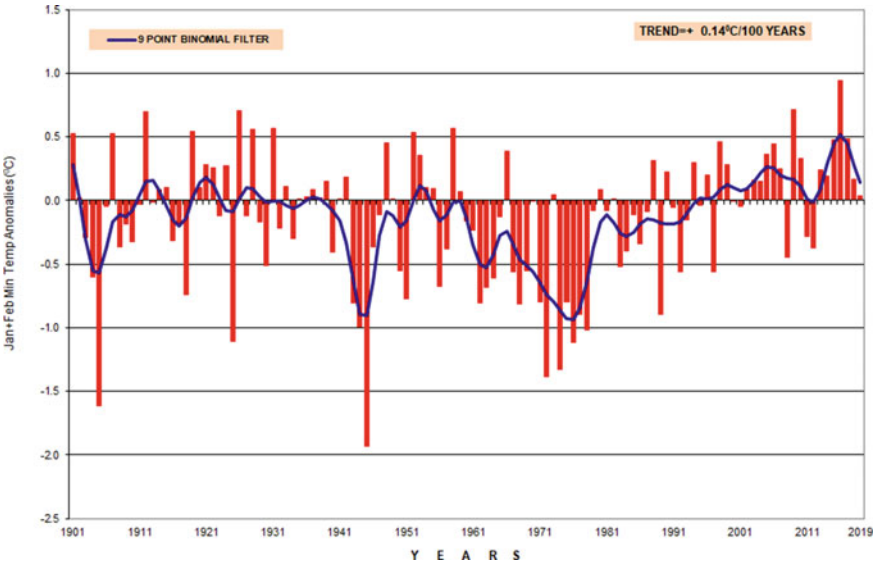

Fig. 5.12 All India winter minimum temperature anomalies

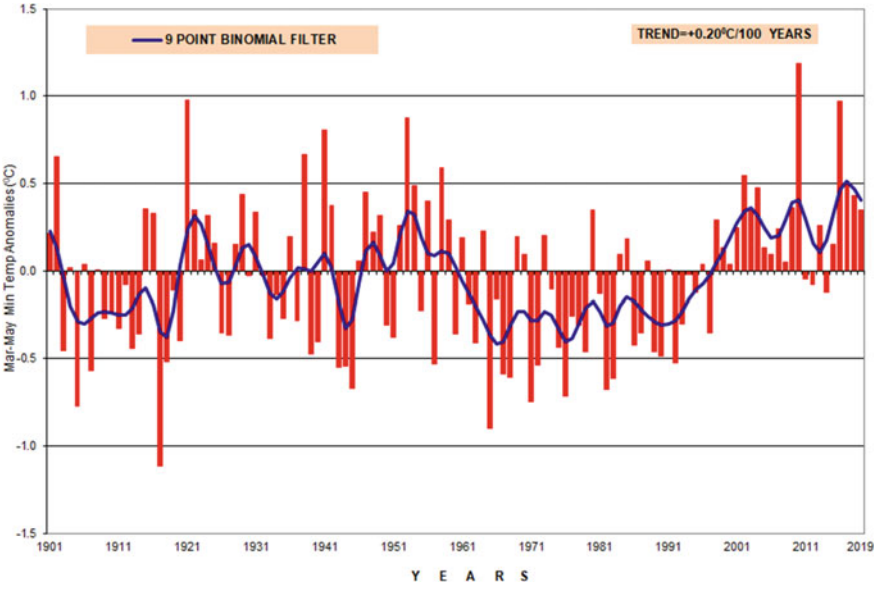

Fig. 5.13 All India pre-monsoon minimum temperature anomalies

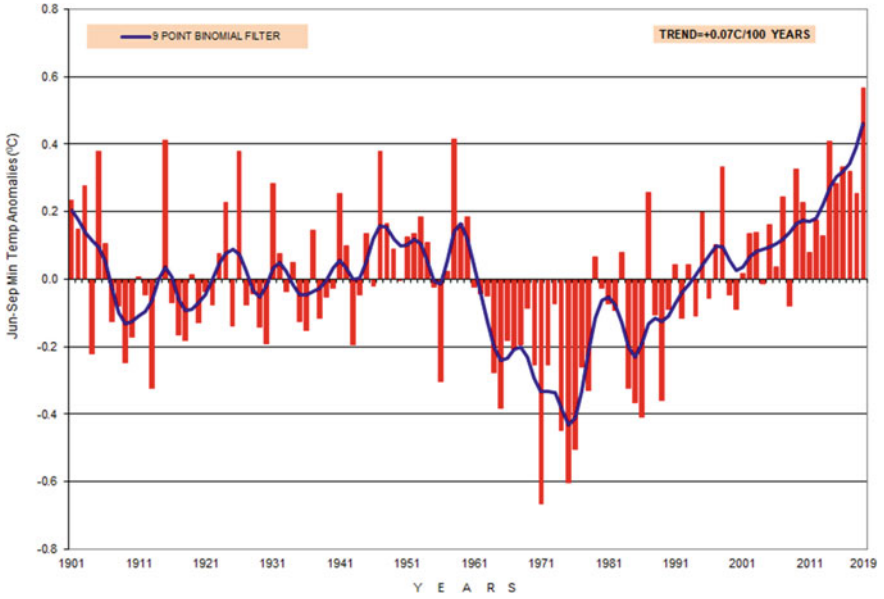

Fig. 5.14 All India Southwest monsoon minimum temperature anomalies

5.3.3.4 Southwest Monsoon Minimum Temperature Anomalies

Figure 5.14 shows the time series for minimum temperature anomaly for the southwest monsoon season (June, July, August and September). The trend analysis for minimum temperature during southwest monsoon season shows that there is almost no increase of all India minimum temperature at +0.07 °C/100 years.

5.3.3.5 Post-monsoon Minimum Temperature Anomalies

Figure 5.15 shows the time series for minimum temperature anomaly for post-monsoon season (October, November and December). The trend analysis for minimum temperature during post-monsoon season shows that there is a significant increase of all India minimum temperature at +0.59 °C/100 years.

Increase of minimum temperature was significant in pre- and post-monsoon seasons only.

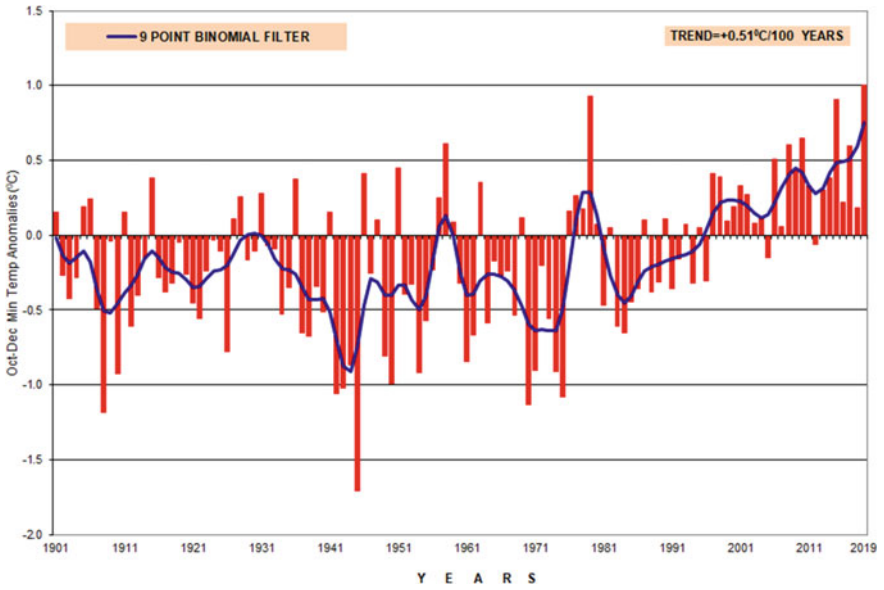

Fig. 5.15 All India post-monsoon minimum temperature anomalies

5.3.4 Spatial Pattern of Temperature Trend

Spatial analysis of temperature trend is analysed using IMD's gridded temperature data for the period 1951–2019. Trend analysis is done on the temperature time series constructed for 101 river sub-basins of India in order to assess hydrological impact on each of river sub-basin.

5.3.4.1 Annual Mean Temperature Trend

Figure 5.16 shows the annual mean temperature trend map for river sub-basins over India. It can be seen that during past 69 years annual mean temperature has been increased significantly for all the sub-basins of southern, western, central and north-eastern parts of the country excluding some eastern and northern parts. Significant decrease in mean temperature has been seen in eight sub-basins of extreme northern parts of the country. Maximum increase of 1.93 °C/decade has been noticed over the sub-basins Barmer and Churu with increase of 1.9 °C/decade of Indus basin followed by Periyar and others under the West flowing rivers South of Tapi Basin by increase of 1.78 °C/decade. Maximum decrease of −4.21 °C/decade has been noticed over Sulmar sub-basin under river basin Area of North Ladakha not draining into Indus in the extreme northern parts of India.

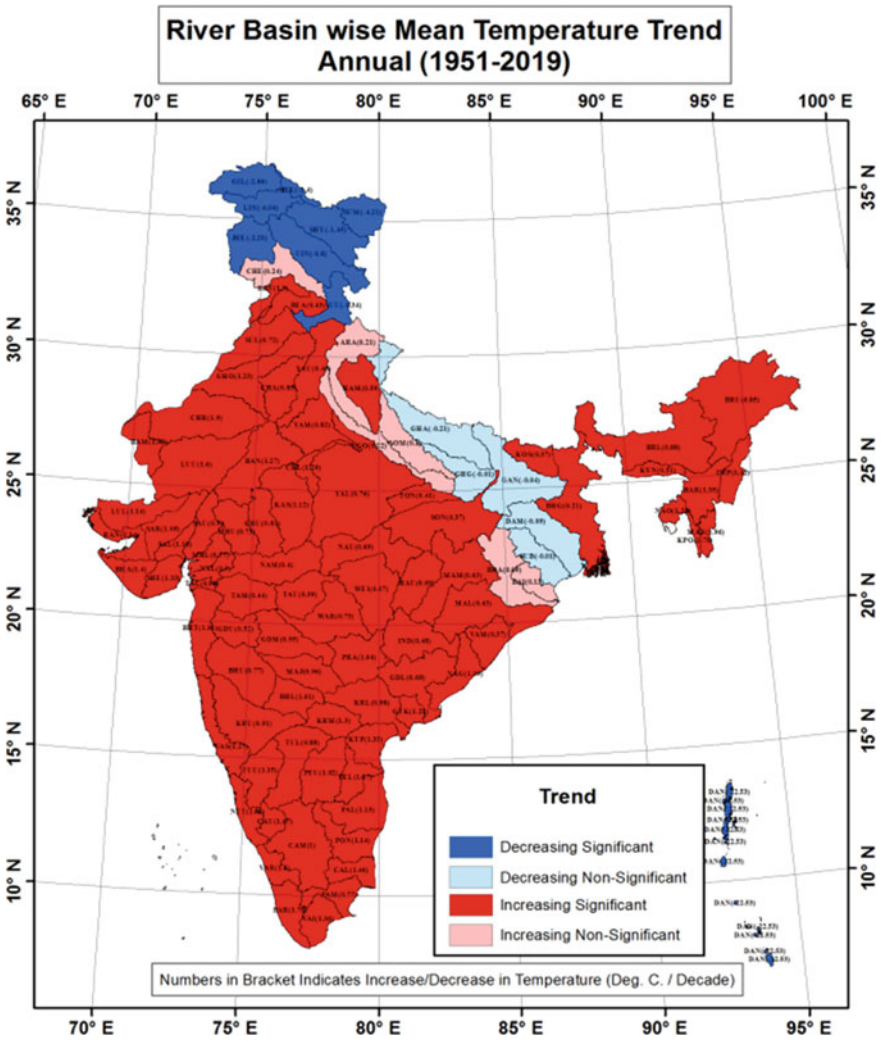

Fig. 5.16 Annual mean temperature anomaly trend

5.3.4.2 Annual Maximum Temperature Trend

Figure 5.17 shows the annual maximum temperature trend map for river sub-basins over India. Except eastern and northern parts, all the sub-basins reported significant increasing trends in annual maximum temperature. Increase of day temperature is high and around 2 °C/decade or more over almost all the river sub-basins of southern peninsular India. For the remaining sub-basins where significant increase has been noticed, it is around 1 °C/decade or more. Significant decreasing trend has

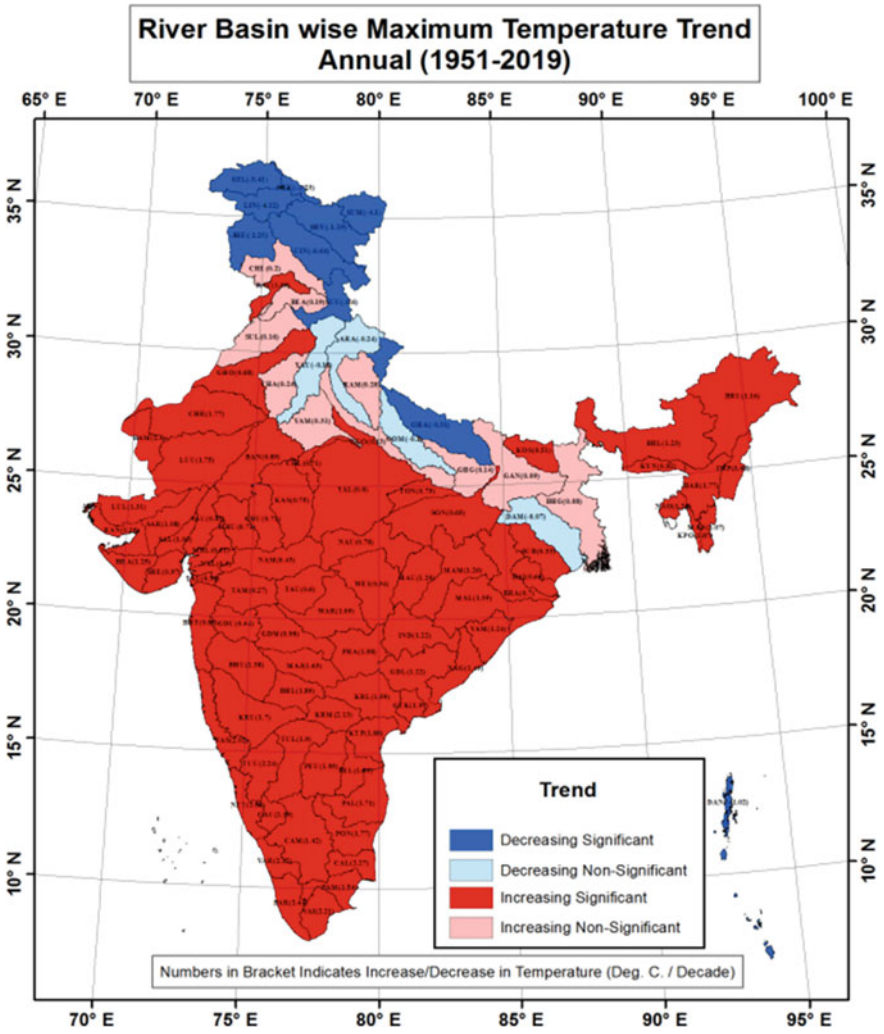

Fig. 5.17 Annual maximum temperature anomaly trend

been noticed over ten river sub-basins in extreme northern parts of India. Maximum decreasing trend (−6.2 °C/decade) is seen over Lower Indus sub-basin.

5.3.4.3 Annual Minimum Temperature Trend

Figure 5.18 shows the annual minimum temperature trend map for river sub-basins over India. Minimum temperature has been decreased over seven sub-basins of extreme northern parts of India and also six sub-basins viz. Indravati, Mahanadi

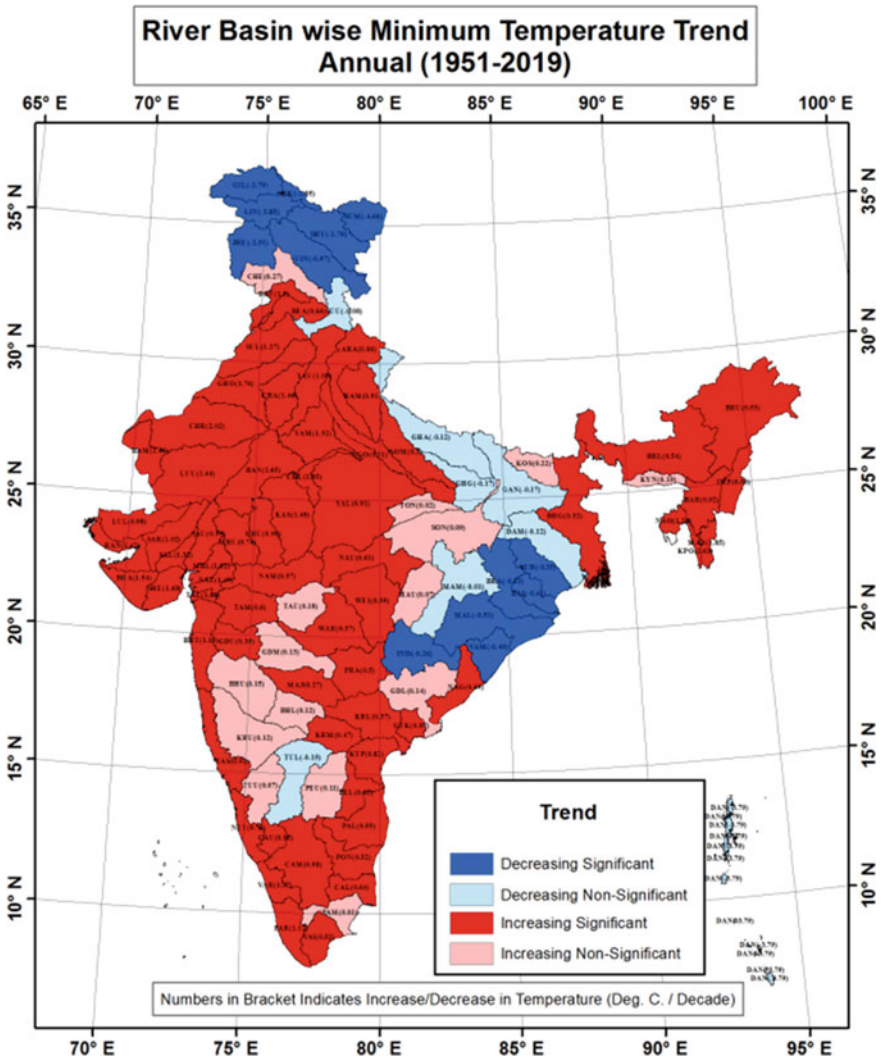

Fig. 5.18 Annual minimum temperature anomaly trend

Lower, Vamsadhara and other, Baitarni, Brahmani and Subernarekha sub-basins over Orissa and adjoining areas. Maximum decreasing trend (−5.85 °C/decade) is seen over Lower Indus sub-basin. Significant increase in night temperature has been noticed in the western parts, central parts, southern parts and also northeastern parts including Bhagirathi sub-basin. Maximum increase has been seen over Churu sub-basin 2 °C/decade.

5.3.5 *Rainfall Patterns Over Major River Basins*

Spatial analysis of average rainfall (1901–2019) over major river basins of India is analysed using GIS. The average rainfall is computed for monsoon months, both cumulative rainfall of the southwest monsoon season and for individual months (Figs. 5.19 and 5.20). These maps show the rainfall spatial patterns over major river basins. Table 5.1 shows the average rainfall statistics for the major river basins which received highest and lowest during monsoon season.

The average rainfall received by these major river basins during June is in the range of 20–600 mm. Basins in northwestern and southern peninsular India receive relatively low average rainfall below 100 mm, whereas most basins in northern and central India receive moderate average rainfall below 200 mm. River basins in Western Ghat and northeast India receive higher average rainfall around 400–600 mm. River basins with lowest average rainfall are Area of Inland drainage in Rajasthan, East flowing rivers between Pennar and Kanyakumari and Area of North Ladakh not draining into Indus Basin. The river basins which receive highest average rainfall during June are Barak and Others, West flowing rivers from Tapi to Tadri and West flowing rivers from Tadri to Kanyakumari.

The average rainfall received by these major river basins during July is in the range of 30–800 mm. Basins in northwestern and southern peninsular India receive relatively low average rainfall below 200 mm, whereas most basins in northern and central India receive relatively moderate average rainfall around 200–400 mm. River basins in northeast India receive relatively high average rainfall around 400–600 mm, whereas river basins in Western Ghat region of India receive highest average rainfall around 600–1000 mm. Table 5.1 shows that river basins with lowest average rainfall are East flowing rivers between Pennar and Kanyakumari and Area of North Ladakh not draining into Indus Basin. Table 5.1 also shows that the river basins which receive highest average rainfall during July are Barak and Others, West flowing rivers from Tapi to Tadri, Brahmaputra and West flowing rivers from Tadri to Kanyakumari.

The average rainfall received by the major river basins during August is in the range of 40–700 mm. Basins in northwestern and southern peninsular India receive relatively low average rainfall below 200 mm, whereas most basins in northern, central and northeast India receive relatively moderate average rainfall around 200–400 mm. River basins in Western Ghat region of India receive highest average rainfall around 400–700 mm. Table 5.1 shows that river basins with lowest average rainfall are Pennar and Area of North Ladakh not draining into Indus Basin. Table 5.1 also shows that the river basins which receive highest average rainfall during August are Barak and Others, West flowing rivers from Tapi to Tadri and West flowing rivers from Tadri to Kanyakumari.

The average rainfall received by the major river basins during September is in the range of 30–350 mm. Basins in northwestern and southern peninsular India receive relatively low average rainfall below 150 mm, whereas most basins in northern and central India receive relatively moderate average rainfall around 150–250 mm. River basins in Western Ghat and northeast India receive highest average rainfall around

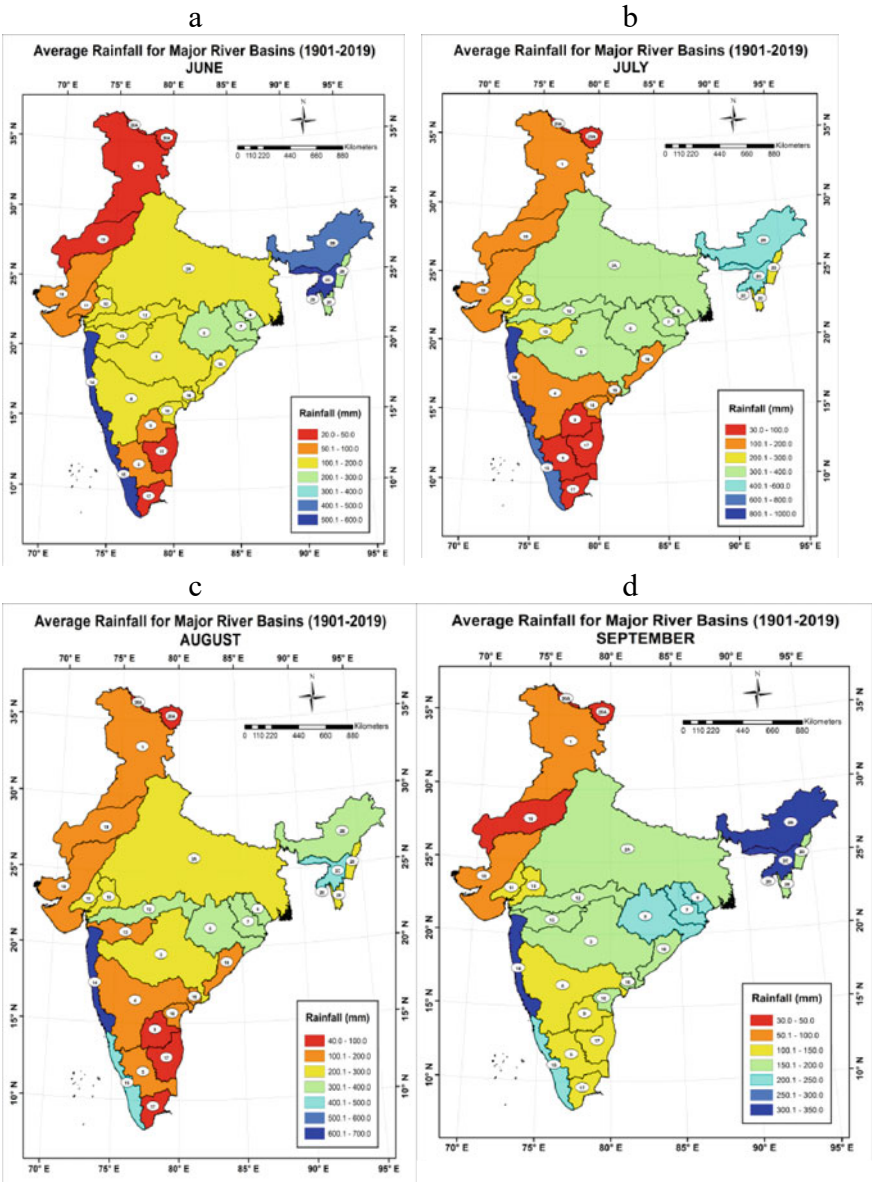

Fig. 5.19 Average Rainfall over Major River Basins of India for **a** June **b** July **c** August and **d** September

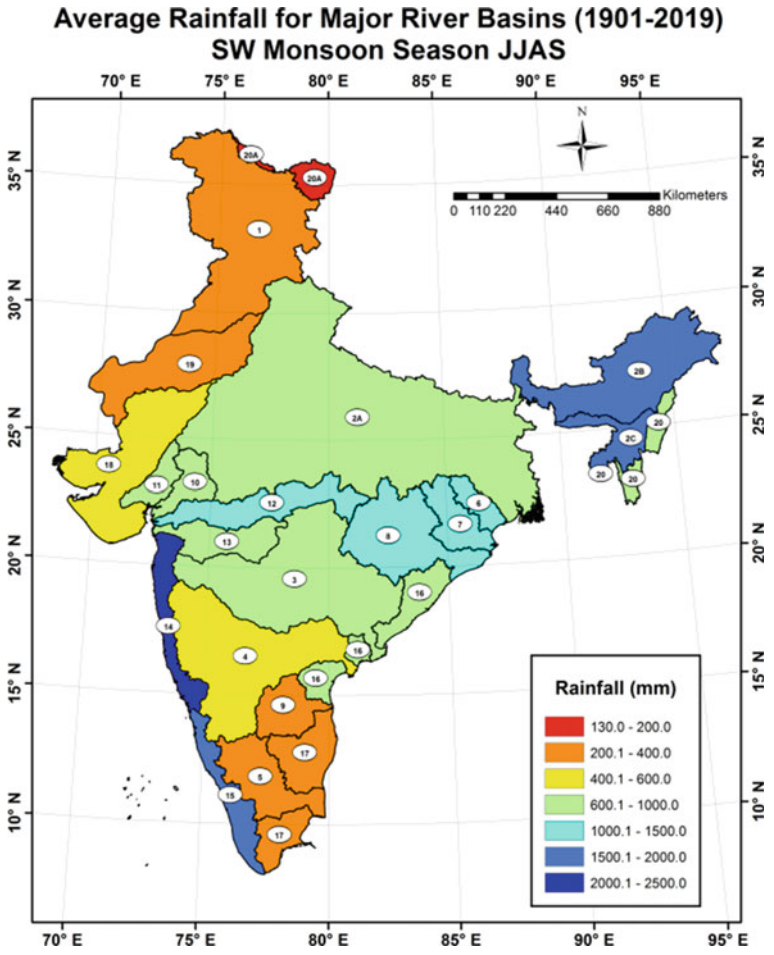

Fig. 5.20 Average Rainfall over major river basins for Southwest Monsoon season

250–350 mm. Table 5.1 shows that river basins with lowest average rainfall are Area of Inland drainage in Rajasthan and Area of North Ladakh not draining into Indus Basin. Table 5.1 also shows that the river basins which receive highest average rainfall during September are Barak and Others and West flowing rivers from Tapi to Tadri.

The average rainfall received by the major river basins during monsoon season is in the range of 130–2500 mm. Basins in northwestern and southern peninsular India receive relatively low average rainfall below 600 mm, whereas most basins in northern and central India receive relatively moderate average rainfall around 600–1500 mm. River basins in Western Ghat and northeast India receive higher average rainfall around 1500–2500 mm. Table 5.1 shows that river basins with lowest average rainfall are Area of Inland drainage in Rajasthan, East flowing rivers between Pennar and Kanyakumari and Area of North Ladakh not draining into Indus Basin. Table 5.1

Table 5.1 Average rainfall statistics for major river basins of India

Basin	Average rainfall				
	June	July	August	September	JJAS
Ganga	131.5	305.5	295.1	180.7	912.8
Brahmani and Baitarni	216.6	355.6	353.0	242.7	1167.9
Area of Inland drainage in Rajasthan	**36.0**	106.8	104.0	**49.5**	**296.3**
Barak and Others	**506.3**	**491.6**	**420.2**	**310.3**	**1728.4**
Indus (Up to border)	49.6	127.8	125.9	70.1	374.0
West flowing rivers of Kutch and Saurashtra including Luni	61.5	184.3	139.4	74.0	459.2
Krishna	107.7	158.8	136.3	148.9	551.7
West flowing rivers from Tapi to Tadri	**511.6**	**978.0**	**647.6**	**309.3**	**2446.5**
Brahmaputra	453.7	**499.1**	399.9	317.3	**1669.2**
Cauvery	69.8	95.6	104.2	121.3	391.8
Godavari	168.8	303.7	277.3	195.3	945.1
East flowing rivers between Mahanadi and Pennar	122.1	175.7	182.2	184.1	664.0
Minor rivers draining into Myanmar and Bangladesh	270.5	276.8	246.5	177.4	969.9
Mahanadi	200.0	379.9	374.7	225.2	1179.9
Mahi	106.2	295.5	267.9	149.4	819.0
Narmada	144.6	355.9	329.8	192.7	1023.0
West flowing rivers from Tadri to Kanyakumari	**555.1**	**724.6**	**470.8**	233.6	**1984.1**
East flowing rivers between Pennar and Kanyakumari	**45.8**	**68.5**	97.9	114.0	**326.2**
Pennar	58.7	85.2	**94.1**	127.8	365.7
Sabarmati	89.3	282.8	222.6	119.5	714.2
Area of North Ladakh not draining into Indus Basin	**20.7**	**38.1**	**41.6**	**33.1**	**132.3**
Subernarekha	227.7	320.8	324.5	246.9	1120.0
Tapi	138.6	244.5	198.4	150.7	732.2

also shows that the river basins which receive highest average rainfall during JJAS are Barak and Others, West flowing rivers from Tapi to Tadri, Brahmaputra and West flowing rivers from Tadri to Kanyakumari.

5.3.6 Rainfall Variability Over Major River Basins

Spatial analysis of rainfall's coefficient of variation over major river basins of India is analysed using GIS. The coefficient of variation is computed using monthly rainfall series since 1901 to 2019 for major river basins of India. Maps are prepared for monsoon months, both cumulative and for individual months. These maps show the spatial rainfall variability over major river basins for different months during monsoon season (Fig. 5.21 and 5.22). Table 5.2 shows the rainfall coefficient of variation statistics for each river basin.

The coefficient of variation of rainfall for these major river basins during June is in the range of 20–110%. Basins in extreme western and extreme north India show very high variability, whereas most basins in northern and southern India show moderate rainfall variability around 40–60%. Basins in Western Ghat, central and northeast India show low rainfall variability around 20–40%. Table 5.2 shows that river basins with highest rainfall variability are Area of North Ladakh not draining into Indus Basin, West flowing rivers of Kutch and Saurashtra including Luni and Sabarmati. Table 5.2 also shows that river basin with lowest rainfall variability is Brahmaputra.

The coefficient of variation of rainfall for these major river basins during July is in the range of 15–130%. Basins in extreme western and extreme north India show very high variability, whereas most basins in northern and southern India show moderate rainfall variability around 30–50%. Basins in Western Ghat, central and northeast India show low rainfall variability around 15–30%. Table 5.2 shows that river basins with highest rainfall variability are Area of North Ladakh not draining into Indus Basin. Table 5.2 also shows that river basin with lowest rainfall variability is Ganga, Brahmaputra, Mahanadi and East flowing rivers between Mahanadi and Pennar.

The coefficient of variation of rainfall for these major river basins during August is in the range of 15–150%. Basins in extreme western and extreme north India show very high variability, whereas most basins in Western Ghat, northern and southern India show moderate rainfall variability around 30–50%. Basins in central and northeast India show low rainfall variability around 15–30%. Table 5.2 shows that river basins with highest rainfall variability are Area of North Ladakh not draining into Indus Basin. Table 5.2 also shows that river basin with lowest rainfall variability is Ganga, Brahmani and Baitarni and Mahanadi.

The coefficient of variation of rainfall for these major river basins during September is in the range of 25–160%. Basins in extreme western and north India show very high variability, whereas few basins in Western Ghat and western India show moderate rainfall variability around 40–60%. Basins in central, southern and northeast India mostly show low rainfall variability around 25–40%. Table 5.2 shows that river basins with highest rainfall variability are Indus (up to border), Mahi, Sabarmati, West flowing rivers of Kutch and Saurashtra including Luni, Area of Inland drainage in Rajasthan and Area of North Ladakh not draining into Indus Basin. Table 5.2 also shows that river basin with lowest rainfall variability is Brahmaputra.

The coefficient of variation of rainfall for these major river basins during south monsoon season is in the range of 15–115%. Basins in extreme north India show

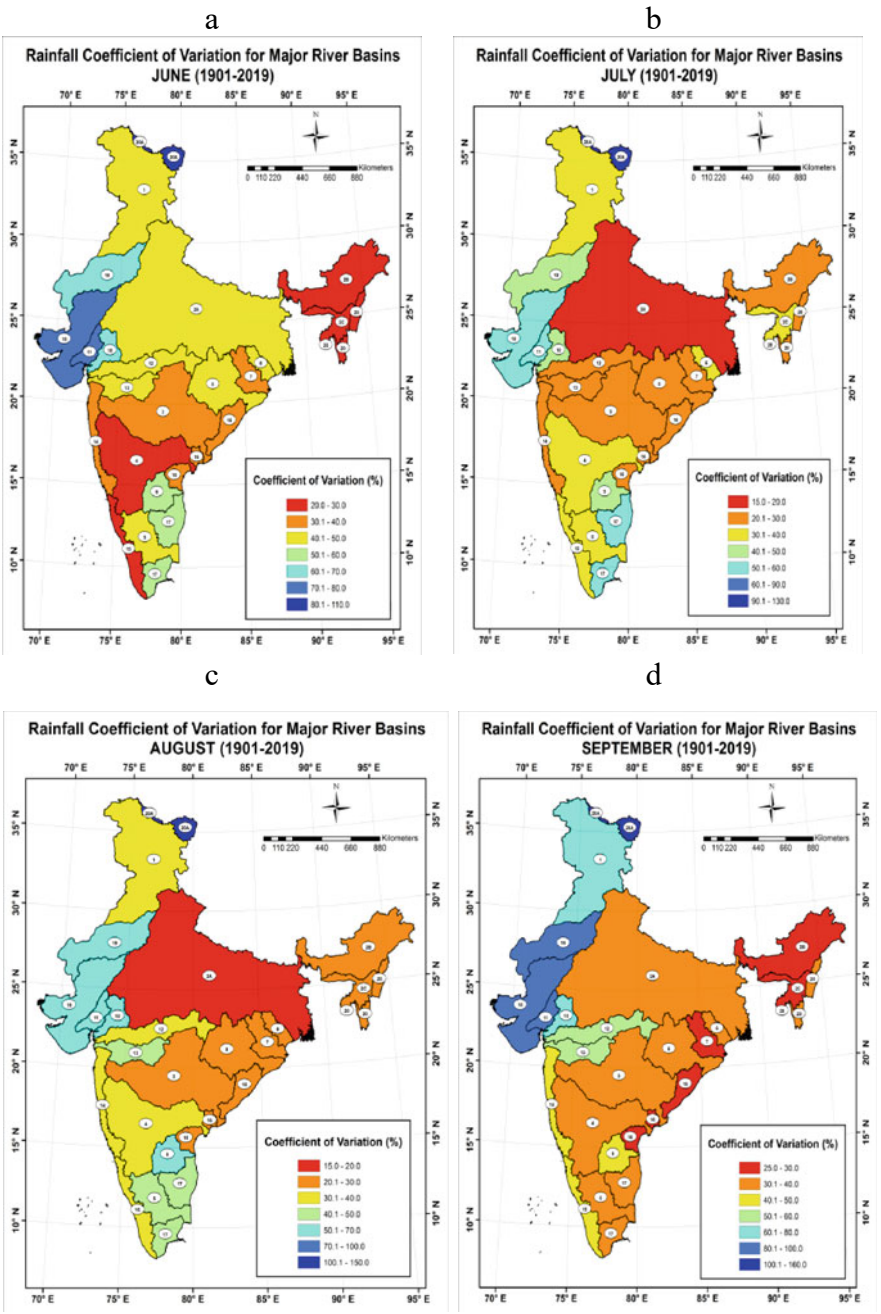

Fig. 5.21 Rainfall coefficient of variation over major river basins of India for **a** June **b** July **c** August and **d** September

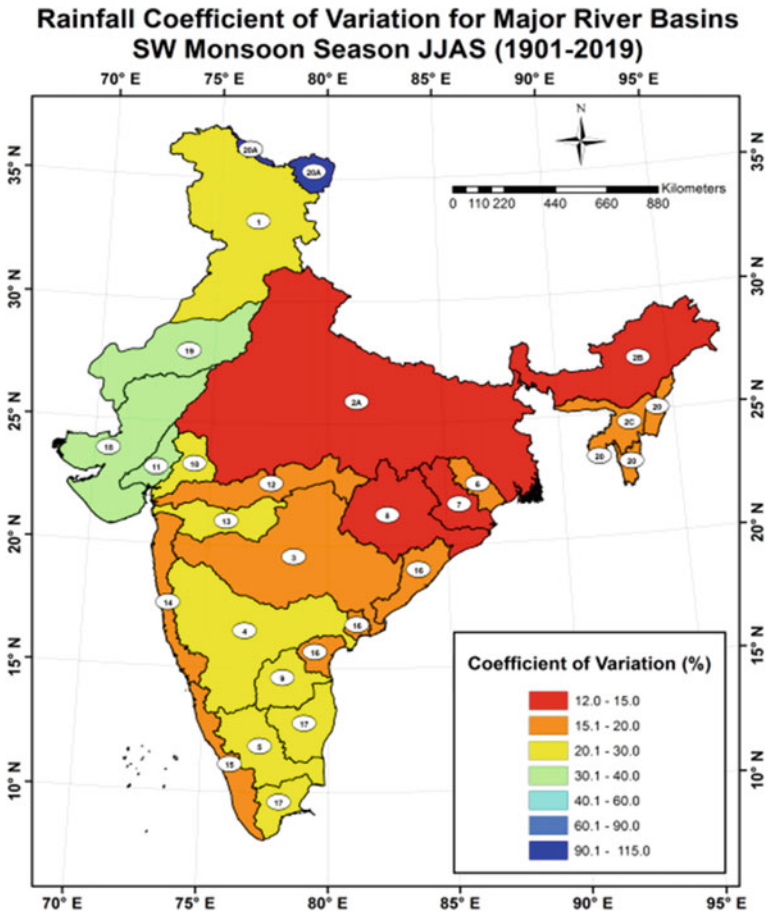

Fig. 5.22 Rainfall coefficient of variation over major river basins for southwest monsoon

very high variability, whereas basins in extreme western, north and southern India show moderate rainfall variability around 20–40%. Basins in Western Ghat, central and northeast India mostly show low rainfall variability around 12–20%. Table 5.2 shows that river basins with highest rainfall variability are Area of North Ladakh not draining into Indus Basin. Table 5.2 also shows that river basin with lowest rainfall variability is Ganga, Brahmaputra, Brahmani and Baitarni and Mahanadi.

5.3.7 Rainfall Trends Over Major River Basins

Spatial analysis of rainfall trend over major river basins of India is analysed using GIS. The rainfall trend is computed using monthly rainfall series since 1901 to 2019

Table 5.2 Rainfall coefficient of variation for major river basins of India

Basin	Rainfall coefficient of variation (%)				
	June	July	August	September	JJAS
Indus (Up to border)	48.63	34.08	33.33	**72.82**	27.91
Ganga	40.89	**19.81**	**17.34**	31.98	**12.52**
Brahmaputra	**22.80**	**21.54**	26.62	**26.47**	**14.64**
Barak and Others	26.58	30.81	25.57	29.12	**19.92**
Godavari	35.47	23.93	25.05	34.72	**15.34**
Krishna	29.22	33.83	35.47	37.39	**21.43**
Cauvery	40.28	37.94	43.93	38.70	**22.97**
Subernarekha	41.94	30.43	28.20	32.32	**16.32**
Brahmani and Baitarni	39.49	29.12	**24.73**	29.46	**14.25**
Mahanadi	45.85	**24.26**	**22.69**	33.57	**14.52**
Pennar	56.76	49.12	58.29	42.74	27.90
Mahi	63.16	40.66	53.07	**77.80**	29.36
Sabarmati	**73.82**	51.46	59.74	**86.67**	33.75
Narmada	48.32	28.07	30.52	53.43	**18.36**
Tapi	42.13	29.78	40.15	52.39	**21.04**
West flowing rivers from Tapi to Tadri	31.75	25.97	33.08	45.44	**16.85**
West flowing rivers from Tadri to Kanyakumari	28.26	31.40	35.79	44.72	**19.03**
East flowing rivers between Mahanadi and Pennar	36.13	**24.78**	26.94	29.39	**15.59**
East flowing rivers between Pennar and Kanyakumari	56.88	51.97	42.92	32.61	25.44
West flowing rivers of Kutch and Saurashtra including Luni	**74.43**	52.30	65.49	**90.51**	36.95
Area of Inland drainage in Rajasthan	69.87	45.93	52.02	**84.12**	32.69
Minor rivers draining into Myanmar and Bangladesh	29.69	25.51	26.56	30.52	**19.94**
Area of North Ladakha not draining into Indus Basin	**106.78**	**125.16**	**143.86**	**151.17**	**110.39**

Bold figures are having high variabilities and low variabilities

for major river basins of India. Figures 5.23 and 5.24 shows the trends in rainfall over major river basins for the monsoon months as well as for the southwest monsoon season.

During month of June, basins in northwestern, western and southern India show significant increasing trend. Basins in central India show non-significant decreasing trend, whereas few basins in west peninsular, east central and northeast India show significant decreasing trend. River basins with significant decreasing trend are Mahanadi, Brahmaputra and West flowing rivers from Tadri to Kanyakumari.

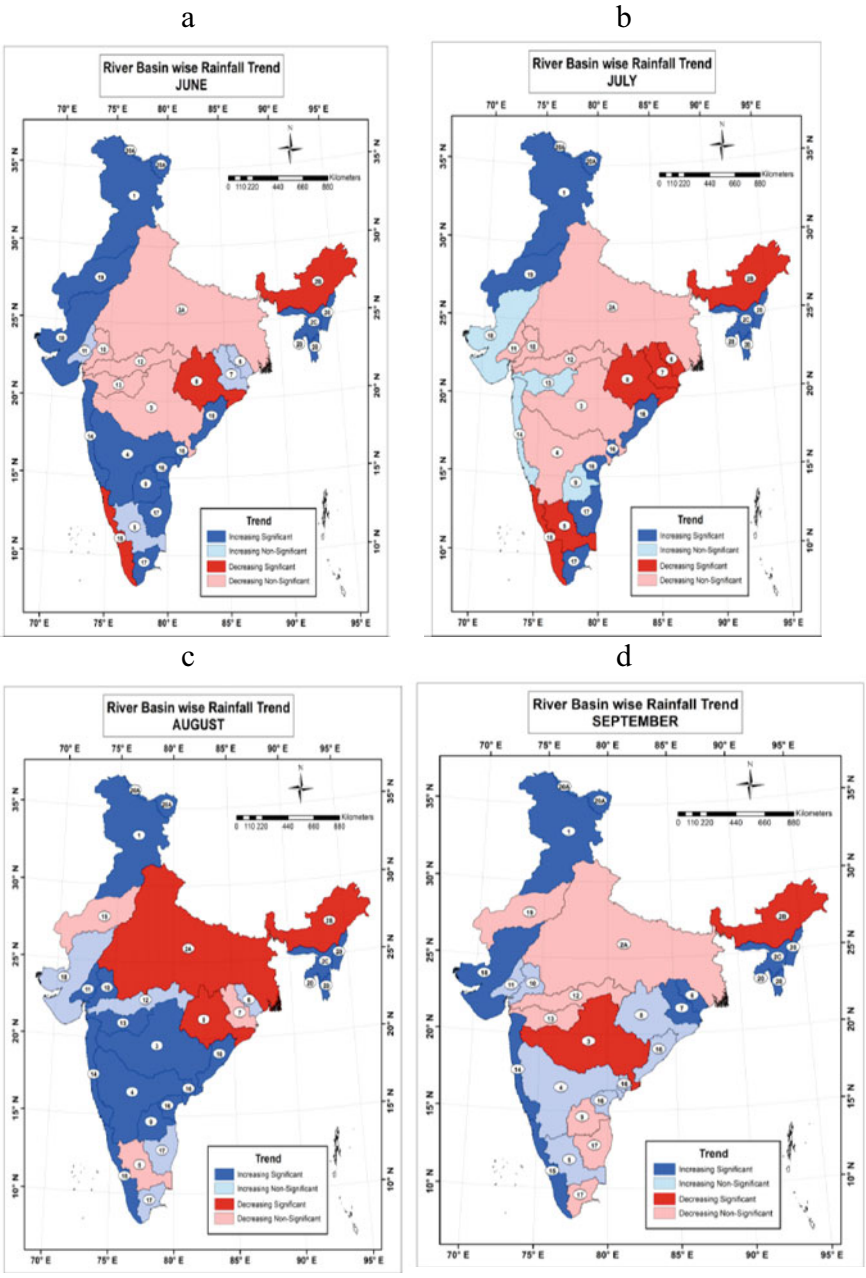

Fig. 5.23 Rainfall trend over Major river basins of India for **a** June **b** July **c** August and **d** September

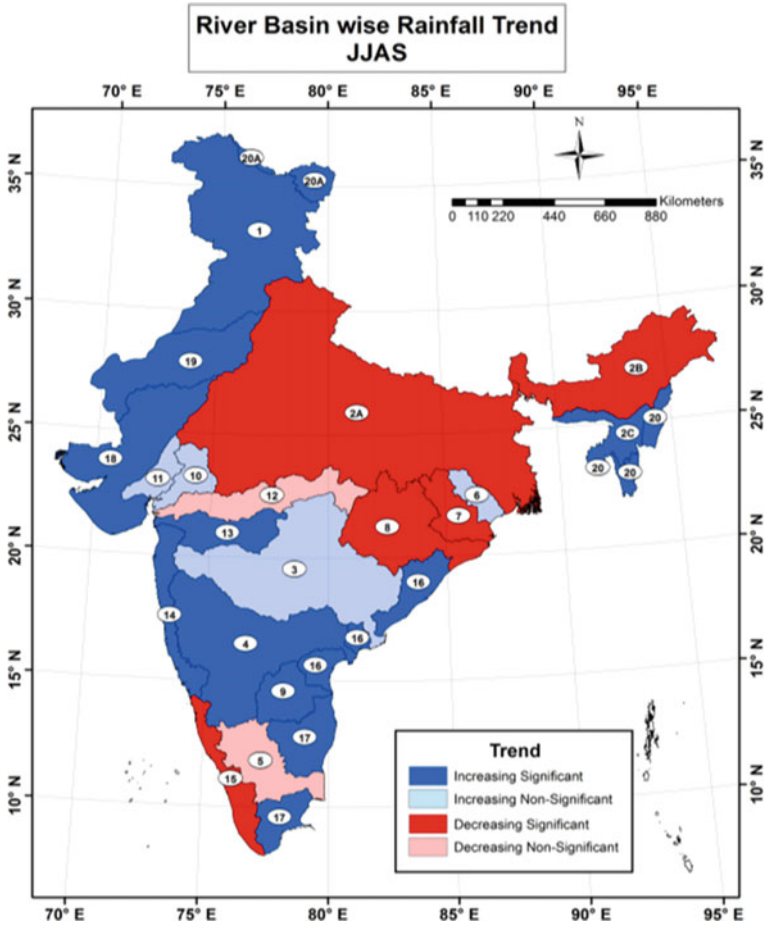

Fig. 5.24 Rainfall trend over major river basin for southwest monsoon

During month of July, basins in north and southeastern peninsular India show significant increasing trend, whereas basins in western India show non-significant increasing trend. Basins in central India mostly show non-significant decreasing trend, whereas few basins in west peninsular, east central and northeast India show significant decreasing trend. Figure 5.23b also shows that river basins with significant decreasing trend are Cauvery, Mahanadi, Subernarekha, Brahmaputra and West flowing rivers from Tadri to Kanyakumari.

During month of August, basins in north, western, central and south peninsular India show significant increasing trend. Basins in north central and northeast India show significant decreasing trend. River basins with significant decreasing trend are Ganga, Mahanadi and Brahmaputra.

In September, basins in north and extreme western India show significant increasing trend, whereas basins in south central and east central India show non-significant increasing trend. Basins in central and east peninsular India mostly show non-significant decreasing trend, whereas few basins in central and northeast India show significant decreasing trend. River basins with significant decreasing trend are Godavari and Brahmaputra.

5.3.7.1 Rainfall Trend During Southwest Monsoon Over River Basins

Figure 5.24 shows the map for rainfall trend over major river basins during southwest monsoon season (JJAS). Basins in northern and western India and peninsular India show significant increasing trend, whereas basins in central India show non-significant increasing trend. Basins in extreme west peninsular, north central and northeast India show significant decreasing trend. River basins with significant decreasing trend during southwest monsoon season are Ganga, Mahanadi, Brahmani and Baitarni, Brahmaputra and West flowing rivers from Tadri to Kanyakumari. River basins with significant increasing trends in during southwest monsoon season are West flowing rivers South of Tapi Basin, West flowing rivers of Kutch and Saurashtra including Luni Basin, Tapi Basin, Pennar Basin, Krishna Basin, Barak and other Basins, East flowing rivers between Mahanadi and Godavari Basin, East flowing rivers South of Cauvery Basin.

5.4 Conclusion

Climate change has major impact on temperature and rainfall patterns of India. We have examined both for all India. Temperature and rainfall are the two important climate parameters which have significant influence on various sectors of the society as well as health. Also for hydrological analysis, drought and water management, it is needed to analyse both these parameters together.

This study examined the temperature trends over India during various seasons, also spatial analysis of temperature trends over 101 river sub-basins of India. A comprehensive analysis of rainfall over major river basins has shown the rainfall patterns and trends during different months of monsoon.

Temperature trend analysis showed that all India annual mean temperature has increased +0.61 °C/100 years. Annual maximum temperature has increased at the rate of +1.0 °C/100 years (winter 1.22 °C/100 years, summer 0.95 °C/100 years, monsoon 0.75 °C/100 years and post-monsoon 1.24 °C/100 years). In last 119 years, minimum temperature increased at the rate of 0.22 °C/100 years. All India Mean Temp Anomaly was +ve for all the 22 years since 1998. Year 2016 being the warmest with anomaly of +0.71 °C. Global-mean temperature anomaly was +ve for all the recent 44 years since 1977. Year 2016 being the warmest with anomaly of +0.99 °C.

Year 2016 was the warmest winter in India with anomaly of 1.15 °C, while Year 2010 was the warmest summer in India with anomaly of 1.28 °C.

Spatial analysis of annual maximum temperature, minimum temperature as well as mean temperature trends has been done for the period 1951–2019. Annual mean temperature has been increased significantly for all the sub-basins of southern, western, central and northeastern parts of the country excluding some eastern and northern parts. Significant decrease in mean temperature has been seen in eight sub-basins of extreme northern parts of the country. Significant increasing trends in annual maximum temperature have been noticed in all the sub-basins except eastern and northern parts. Increase of day temperature is high and around 2 °C/decade or more over almost all the river sub-basins of southern peninsular India. Significant decreasing trend in maximum temperature has been noticed over ten river sub-basins in extreme northern parts of India. Maximum decreasing trend (−6.2 °C/decade) is seen over Lower Indus sub-basin. Significant increase in night temperature has been noticed in the western parts, central parts, southern parts and also northeastern parts including Bhagirathi sub-basin. Maximum increase has been seen over Churu sub-basin (2 °C/decade).

Rainfall pattern over river basin showed that there is significant decrease of rainfall in Brahmaputra basin for all the monsoon months, Mahanadi basin for June, July and August rainfall, Ganga basin in August rainfall, Cauvery Basin in July rainfall, Godavari basin in September rainfall and West flowing river basin from Tadri to Kanyakumari in June and July rainfall. August rainfall is having contrasting feature with southern parts having decreasing trend and central, eastern and northeastern parts decreasing trend. Significant decreasing trends are seen in SW monsoon rainfall for Ganga, Brahmaputra, Mahanadi and Brahmani and Baitarni Basins and West flowing river basin from Tadri to Kanyakumari. Significant increasing trends are seen in SW monsoon rainfall for West flowing rivers South of Tapi Basin, West flowing rivers of Kutch and Saurashtra including Luni Basin, Tapi Basin, Pennar Basin, Krishna Basin, Barak and other Basins, East flowing rivers between Mahanadi and Godavari Basin, East flowing rivers South of Cauvery Basin. Recent changes (1989–2018) are more alarming as there are very few sub-basins where significant increasing trends are noticed but most of the sub-basins of Ganga and Brahmaputra basins are showing decreasing trends in the recent 30 years also.

Acknowledgements Authors are thankful to India Meteorological Department for providing resources and research platform for carrying out this work.

References

Bisht DS, Chatterjee C, Raghuwanshi NS, Sridhar V (2018) Spatio-temporal trends of rainfall across Indian river basins. Theor Appl Climatol 132:419–436. https://doi.org/10.1007/s00704-017-2095-8

Guhathakurta P, Sreejith OP, Menon PA (2011) Impact of climate changes on extreme rainfall events and flood risk in India". J Earth Syst Sci 120(3):359–373

Guhathakurta P, Rajeevan M, Sikka DR, Tyagi A (2015) Observed changes in southwest monsoon rainfall over India during 1901–2011. Int J Climatol 35:1881–1898

Guhathakurta P, Menon P, Inkane PA, Krishnan U, Sable ST (2017) Trends and variability of meteorological drought over the districts of India using standardized precipitation index. J Earth Syst Sci 126(8):126, 120

Jain SK, Nayak PC, Singh Y, Chandniha SK (2017) Trends in rainfall and peak flows for some river basins in India. Curr Sci 112(8):1712–1726

Chapter 6
Importance of Data in Mitigating Climate Change

Ashwin B. Pandya and Prachi Sharma

6.1 Introduction: Climate Change and Water Security

The critical importance of water is apparent in all walks of life, from fulfilling our basic domestic requirements of food and water to agricultural needs as well as industrial production of various goods and other ancillary services. Everybody is a stakeholder when it comes to water resources. However, the changing climate in recent years is bringing a transformation in the hydrological regime. The impacts of climate change are visible mostly through the medium of water such as changes in the hydrological cycle, frequent and extreme floods and droughts, increased snowmelt, rising of sea levels and so forth. Other impacts of climate change on hydrology are apparent via changes in atmospheric circulation patterns, altered base flows, higher sediment flow, changes in ecosystems (aquatic and terrestrial) as well as changes in the biological and physical properties of soil (Muir et al. 2018).

At the same time, the demand for water resources is increasing whereas the supplies are decreasing (The Financial Express 2019). In quantitative terms, matching the demands and supplies of the whole spectrum of stakeholders with equity would achieve the goal of water security. Water security is broadly defined as "*the capacity of a population to safeguard sustainable access to adequate quantities of acceptable quality water for sustaining livelihoods, human well-being, and socio-economic development, for ensuring protection against water-borne pollution and water-related disasters, and for preserving ecosystems in a climate of peace and political stability*" (UN-Water 2013). Additionally, 7 out of 17 goals of Sustainable Development Goals (SDGs) are directly influenced by water management in agriculture, goal 1 (end poverty), goals 2 (zero hunger), goal 3 (good health and well-being), goal 6 (clean water and sanitation), goal 8 (decent work and economic growth), goal 13 (climate action) and goal 17 (partnerships to achieve the goal). Thus, achieving

A. B. Pandya (✉) · P. Sharma
International Commission on Irrigation and Drainage, New Delhi, India

© The Author(s), under exclusive license to Springer Nature Singapore Pte Ltd. 2021

A. Pandey et al. (eds.), *Hydrological Aspects of Climate Change*,
Springer Transactions in Civil and Environmental Engineering,
https://doi.org/10.1007/978-981-16-0394-5_6

water security becomes critical not just because of climate change but from different perspectives of ecosystem, environment, social, culture and economy.

Also, several studies have indicated that water management, food production and energy supply cannot be studied in isolation, rather they are co-related and their management should be planned considering the nexus approach for water-food-energy (Water, Food and Energy UN-Water 2020). While water is directly available in nature, food and energy are derived from water as one of the key initial ingredients. Thus, in a way, food and energy security are directly dependent on water security. However, it is abundantly evident that climate change is threatening the water security and by extension, hampering the sustainability of food systems and energy supplies as well.

This chapter describes the essential role that data plays in day-to-day planning at micro level as well as shaping policy-decisions at macro level which ultimately would help in mitigating the impacts of climate change and global warming, especially with reference to India.

6.2 Water Resources in India

With a geographical area of 329 Million ha, which is 2.4% of world's area, India houses nearly 17.2% of the world's population (CWC 2020). An overview of the major hydrological parameters for India is given in Table 6.1. Moreover, with diverse agroecological zones with varying rainfall patterns throughout the year, the water sector is under stress in many regions, especially during non-monsoon season. Some of the major challenges that the water sector in India is facing is the high spatial and temporal variability in water availability across the country. Being a developing country with one of the largest populations and diverse economy, there is an ever-rising demand of water for various purposes. The increasing water pollution has degraded the water quality in natural streams and aquifers. Over utilisation of the current water resources has posed a serious threat on the sustainability of water resources in the country, particularly the groundwater resources.

Table 6.1 Overview of water resources in India

S. No.	Parameter	Volume
1	Average annual precipitation	4000 BCM
2	Average precipitation during monsoon	3000 BCM
3	Natural runoff	1986.5 BCM
4	Utilizable surface water resources	690 BCM
5	Total utilizable ground water resources	433 BCM
6	Total annual utilizable water resources	1123 BCM
7	Per capita water availability	1720.29 cum

Source Central Water Commission, India

Table 6.2 Database scenario in India major institutions responsible for data

S. No.	Indian agency	Data/Information
1	India Meteorological Department (IMD)	Meteorological data
2	Central Water Commission (CWC)	River flow and quality information from key gauging stations
3	Central Ground Water Board (CGWB)	Groundwater data
4	National Remote Sensing Centre (NRSC)	Water resources, land use and agricultural data
5	National Water Informatics Centre (NWIC)	Comprehensive national water resources data
6	State Water Resources Departments	Surface and groundwater information for intra-state sources
7	Agriculture Department of State	Agricultural data
8	Bureau of Economics and Statistics	Economic aspects of water productivity
9	Specialized Institutes e.g. Wild Life Institute of India	Environmental data
10	Specialized Institutes e.g. Tata Institute of Social Sciences	Social data

Moreover, there are increasing complexities in water management across boundaries as for the operations, planning, management and monitoring of the water sector projects, several institutions are responsible at the federal, state and municipal levels. Also, water is a state subject in India, water sharing needs to be coordinated among states as well as neighbouring countries. Some of the important Indian institutions, which provide hydrological data, are given in Table 6.2.

6.3 Usage of Data-Based Tools for Assessment of Climate Impacts on Water Security

6.3.1 Role of Data in Water Development, Management and Ensuring Security

The management decisions for water resources at all levels are not taken randomly, instead they rely on good quality data to form a scientifically supported cohesive argument for large scale implementation. By providing a better quantitative understanding of the water cycle, data complements the objective and unbiased information, helps to derive knowledge about water resources for sound planning, management, informed decision-making and ensuring good governance of water resources to cater to the interests of all stakeholders involved. Data helps in understanding the resources availability and assessment of topography (surface/groundwater) of the region. It helps in

optimizing water use through understanding current usage patterns and implementing measures to achieve required efficiency.

In India, the primary source of water is precipitation during monsoon. The monsoon processes are dependent upon the global climatic processes and are not yet fully understood or modelled in quantitative terms. Therefore, the rainfall process is considered a random process and very little specific information about spatial and temporal availability of the rainfall is available with a reliable forecast model on which quantitative decisions like cropping areas and possible inflows can be generated well in advance. With this constraint, the role of data becomes invaluable to compare the trends and derive planning decisions therefrom using various stochastic models. In the absence of real time data, trends cannot be discerned and thereby the reliability of food and energy production cannot be ensured.

6.3.2 Data for Water Diplomacy

It is a famously said that the World War 3 would be fought for water. This reality does not seem very distant if we consider the expanse of water scarcity, especially in lesser-developed regions of the world (Al-Shamaa 2020; Wilson 2012). For regions with transboundary river basins, water allocation is decided based on the mutually agreeable water-sharing treaties. Considering the impacts of climate change and other anthropogenic impacts on water resources, cooperative and mutually beneficial strategies for transboundary water management become an urgent priority. To devise and implement such strategies, data is essential to understand the water availability across boundaries and accordingly derive water sharing agreements for transboundary rivers, lakes or aquifers.

Data also plays a crucial role in carrying out water diplomacy amongst regions to resolve the water allocation disputes. Planning for water resources purely on administrative boundaries raises conflicts between the authorities across the boundaries. Negotiations over competing demands can only be resolved in quantitative terms. Neutral unbiased data and analysis enable competing parties to accommodate each other's positions without compromising their core interests.

Moreover, in the backdrop of climate change, the water availability is at further stake and the water-sharing agreements between the riparian states need to be revised to arrive at a consensus for reallocation of water. Thus, availability of good quality data becomes paramount in devising and revising such agreements for water distribution between the parties involved to avoid disputes of any kind. It also shows how data becomes the key factor in unbiased water allocation and conflict resolution (Ganoulis and Fried 2018). Exchange of data between the riparian states which have differing capacities for data collection and analysis also helps provide a complete picture of the basin.

On the other hand, lack of quality assured information poses hindrance to the water diplomacy. This data secrecy impedes the effectiveness of agencies accountable for planning, resource allocation and disaster preparedness. Thus, both the

parties involved must be willing to exhibit equal levels of openness for data sharing which would ultimately provide opportunities for joint development of transboundary basins.

6.3.3 *Reasonability of Demand and Dynamic Water Availability*

Issues related to management of demands and water supply should be tackled with a "whole to part" approach rather than the current approach of resolving atomic issues at the lowest levels of administrative units in a piecemeal manner. For allocation of water resources to various stakeholders, the availability and demand needs to be analysed, since it is a general tendency of the water user to try and maximize its demand. Thus, reasonability of the demand needs to be substantiated through reliable data (such as data on water consumption, water demand for agriculture, industries, municipal uses, environment and so on), so that the probable future plans for increased water demands of individual sectors can be verified and the veracity of these plans on how much can actually be supported and achieved. For example, during planning stages, the crop water demand is shown to be very high compared to their actual crop water requirements.

In dynamic situations of water availability, such as surplus or shortage of water, a mechanism needs to be devised for managing the excess or deficit of water. In case of water shortage, priorities need to be assigned to different sectors for water allocation on the basis of their utility and the impact they face due to water scarcity. Whereas in case of surplus water availability in smaller pockets in any basin, an imbalance may be encountered. With the help of accurate data required for proper planning, long-term interventions may be made for transfer or utilization of water from surplus pockets of the basin to the deficit corners of the basin, for example, concept of interlinking of rivers (South–North Water Transfer Project 2020; NWDA 2020).

Especially in agriculture sector, which consumes nearly 70% share of our freshwater resources (FAO 2012), it becomes imperative to determine the water productivity and maximize its water use efficiency. To achieve this, relevant parameters such as specific crop water requirement, water consumption at farm level, evapotranspiration losses, losses through canal seepage, leakages etc. need to be quantified.

In countries like India, the agriculture sector mainly consists of minor irrigation schemes (area less than 2000 ha) with unorganized information structure as compared to major irrigation schemes (greater than 10,000 ha) with systematic information system. For example, in minor irrigation projects, the information about parameters such as water consumption at farm level, evapotranspiration losses, losses through canal seepage and leakages is available at the operator level, however, it may not be available as a comprehensive database for understanding the complete hydrology of

the river basin. An all-inclusive database with information of minor, medium and major irrigation project in the public domain will help in identifying the hotspots where water-saving interventions are required.

6.3.4 Ensuring Water Security Through Budgeting and Accounting

For efficient management strategies, access to accurate quantitative analysis is required. To this end, data-based tools such as water accounting and water budgeting provide a comprehensive framework for assessing, planning and managing the current reserves of water resources sustainably. They promise impartial avenues for water allocation, regulation and conflict resolution and evidence-informed planning and management. These tools identify the causes of water-related problems and opportunities for solving these problems. It also allows the user to develop and update a common homogenous and open-source information base which provides transparency in water governance at the decision-making level, convenience in water management at the planning level and raises awareness on water scarcity at the community level.

In case of conflicts, the homogeneously processed data also provides a common consensus for both parties on assurance of the data quality. Tools such as water accounting make use of inter-disciplinary information, derived from a wide-range of independent sources. They provide biophysical and societal strategies and plans to the context and demands of different water users and uses in a specified domain. Broadly, among other parameters, water accounting provides information on the water fluxes and flows in the basin, helps in determining water productivity with respect to different water users, information about the consumptive and non-consumptive use of water, evaluation of climate change variations, cost-benefit analysis of water services, assessment of ecosystem and environmental services, meanwhile providing information/knowledge where there is a scope to improve water use efficiency. Additionally, using water accounting, the trends in the water supply and demand can be analysed for current status and future scenarios in specific social, political and institutional contexts.

6.4 Data Collection

The characteristic data required for the river basin development includes physical data of the catchment, hydrometric data, meteorological and climatic data, agricultural, potable and wastewater, industrial, navigation, hydroelectric power, environmental, demographic data, institutional data, economic, recreational, tourism (Molden and Burton 2005). Typically, the data is collected via hydrometric equipment

for measuring, or mapped using remote sensing or GIS mapping, and uses various software simulation for processing, modelling and forecasting the parameters.

Molden and Burton (2005) describe four different types of data collection mechanisms: (i) Direct measurements, e.g. discharge from depth gauge; (ii) Estimated or derived data obtained by calculations using combinations of measured variables, e.g. using Penman-Monteith equation to evaluate evapotranspiration; (iii) Field observations, e.g. canal condition; (iv) Reported—data obtained from secondary sources, using other's observed, estimated or measured data. The relevance of these mechanisms is highlighted with the fact that advanced technology can be made use of to derive data in places with lack of infrastructure. Assurance in a random occurrence scenario requires collection and processing of data at all times to understand the developing situations on ground. With increasing climate uncertainties, parameters such as rainfall, humidity, temperature, evapotranspiration are also becoming unpredictable. Thus, accurate data becomes paramount even for forecasting, monitoring and preparing better for the projected scenarios.

Being a spatially distributed resource, ground-based measurements are needed for raw data over large geographic areas. Occurrence of water is an aggregate response of individual hydrological elements interacting with each other in space and time. However, the measurements have to be point specific in space though at the point of collection, the temporal continuity of observations can be maintained. This requires time coordinated data collection over vast areas. Multiple technologies are available for measurement of flow of water in natural and artificial streams (canals) as well as under the ground surface. The primary measurements are mechanical converted to electrical signals and transmitted as digital data using modern data communication technologies. The sampling intervals depend upon the eventual use of the data. The requirement of the real time data at shorter time steps is acute in view of disaster causing potential of floods that has led to automation in data collection and processing using satellite and terrestrial GSM communications or combinations thereof. The predictions of seasonal availability may be made using relatively longer time step intervals. Remotely sensed data on land use and moisture status of various crops, inundation extents are key augmenting data which lead to comprehensiveness of the information on water regime for a basin or the country (NRSC 2020).

6.5 Role of Data in Project Planning and Management to Make Them Resilient to Increasing Variability of Climate

Data plays a vital role in sound planning and management at each stage of river basin development. A typical river basin development takes place in the following manner (Molden and Burton 2005):

1. In the early greenfield stage of the river basin development, rudimentary information on the water flows and extent of flooding is assessed to demarcate flooded and utilization areas
2. In the development stage of the project, preliminary planning is completed. Initial data collection systems; basin-wide hydrometric stations to gather base data of river flow and quality (climatic data, land use, topographic surveys, aerial photography, land ownership) are established for individual projects
3. In the utilization stage, detailed planning for the river basin is carried out alongside development of a simple model for the river basin. In this phase, standardized procedures are chalked out for data collection and monitoring of the major parameters
4. In the re-allocation and restoration stage, a master plan for the river basin is designed, sophisticated water resource models are generated and various scenarios are analysed to enable participation in decision-making. Information regarding supply and demand of water resources is published.

In India, the relevance of data for sound planning and operations of water resources by the central government is highlighted through the following mechanisms adopted by the Central Water Commission in India (Central Water Commission, Ministry of Jal Shakti, Department of Water Resources, River Development and Ganga Rejuvenation, GoI 2020)

1. *Establishment of Monitoring System:* Installation of hydromet observation networks, water infrastructure and other software to monitor, gather, and process real-time data; establishment of Hydro-Informatics Centres
2. *Information System:* Strengthening the water resources information system (WRIS) for centre and state
3. *Operation and Planning System:* Development of analytical tools and decision support systems; conducting studies and innovative solutions
4. *Institutions Capacity Enhancement:* Establishment of knowledge centres for dissemination knowledge to build capacity of personnel and professional experts, project managers and providing them with operational support.

6.6 Current Challenges and Data Requirement to Address the Challenges for Water Sector

Water sector is under stress from various perspectives. Thus, requirement for data on water is a prerequisite for planning in every sector, i.e. agriculture, industries, municipality, domestic, sanitation and so on. Some of the major challenges include maintaining sustainable food systems, lack of access to water and hygiene, ecosystem health, sharing water resources across provinces and countries, industrial and urban water management, risk mitigation, water pricing and sustainable use of water for energy production.

Several countries where the concept of water pricing is not in play, coupled with the lack of consciousness on the water shortage issues create a false sense of water security among users and thus saving water does not remain a priority. In such cases, raising awareness on issues of water scarcity through mass media would go a long way in creating a water conscious society. Lack of awareness and willingness to adopt integrated water resources management (IWRM) becomes a major challenge in the water sector. Another indirect implication on efficient water management is lack of sufficient data and information or well-documented knowledge base which impacts decision-making at every level.

A glimpse of the data requirement for some of these challenges is listed below:

- Meeting basic needs of water and hygiene: WASH data (drinking water, sanitation and hygiene)
- Sustainable food systems: food production, irrigation requirement, yield, efficiency etc. data
- Ecosystem health: water quality, chemical monitoring data, ecosystem status etc.
- Risk mitigation: flood/drought management data, water pollution and data on other water-related hazards
- Sharing water resources: river basin management data within and—in the case of boundary and transboundary water resources—between concerned states
- Valuing water: economic, social, environmental and cultural price of water
- Water management in urban areas: urban water management, stormwater drainage management, wastewater management data
- Industrial water management: water use and quality data
- Sustainable use of water for energy production: hydropower generation data
- Retaining and updating the knowledge base: data on good water policies and management practices

Considering the vast impact of water in every sector, it can be said that in a way, water, directly or indirectly, impacts all sectors and inadvertently everyone becomes a stakeholder in the water management process. Here, an important point to be noted is that since water resources have multi-disciplinary aspects, they are managed by different public agencies which gather the data from different sources for physical, meteorological and water use data (Government of India 2011). This gives rise to dissonance in data management due to incoherence and inconsistent mechanisms for data collection and validation.

6.6.1 Current and Future Scenario of Water Availability and Demand

With the passage of time, urban areas have seen an unparalleled growth in terms of infrastructure and population, which unfortunately is not in coherence with the water availability and management of effluents. To feed the increasing population, even

agriculture is extensively increased requiring increasing amount of water (Alexandratos and Bruinsma 2012). Thus, for proper assessment and management of these limited resources, utilization and developmental data should be made available, which is a serious constraint in most developing countries.

To remedy this, suitable financial and technical resources for developing the mechanics for assessment of information based on space-based tools as well as other indirect measures coupled with on ground observations are required. Data-based approaches offer solutions for estimating the overall availability in spatial and temporal contexts and integrating the competing demands by simulating different potential future scenarios using sustained basin modelling studies.

While assessing water scarcity, the access to consistent and reliable water utilization data for agriculture and other sectors from various sources has been a constraint, especially in developing countries. Resource data usually has a bias because of the ever-changing utilization factor; in case of water allocation, there is overestimation, which should be avoided by stretching the data in the past without regarding the current prevailing situations. Hence, the accurate data on water demand needs to be assessed by integrating the indirect methods of water consumption and addressing questions such as what is the demand, where and when is this demand occurring?

It is worth mentioning that essentially all assessments are probabilistic while calculating water allocation, hence the water availability every year might be different. In case of extremities such as occurrence of floods or droughts, the availability of resources (surplus/deficit) may differ from provisions laid down earlier. Thus, strong mechanisms should be devised for allocation accounting for the variations brought about by climate change.

In all likelihood, the amount of data required for the river basin development is huge in terms of volume, and so it requires robust system for collection, management, storage and analysis of the hydrological database. This has been a challenge in the past. Another constraint for water data management is inconsistent approach used for data collection and processing, i.e. using different methods for filling-in the missing data.

6.7 Limitations and Resolutions for Data Collection and Processing

Some of the major limitations for data collection and processing are lack of sophisticated infrastructure for utilization measurements, access to cutting-edge technology, availability of trained personnel and policies for transparency in data sharing. Additionally, accounting for climate change projections while processing the data. Some of the issues plaguing the data quality are listed below:

- Improper measurement methodologies
- Lack of personnel and material infrastructure for data collection
- Non-systematic record keeping and lack of archival policy

- Lack of long-term vision about data management and developments in future
- Non-availability of ancillary information to define the context
- Extreme hesitation to report utilization and minor developments data
- Non-availability of tools for transforming the data into consumable forms
- Lack of integration between various types of atomic data elements
- Non uniformity of definitions for the same parameter sets.

To counter these difficulties, robust frameworks need to be implemented with supplemental policies and systematic use of alternate satellite-based/space-derived measurements. The allocation of financial resources needs to be increased for reliable and accurate collection and analysis of hydrological data. Furthermore, investments and training efforts need to be devoted to build the infrastructure and capacity of personnel to make use of these infrastructure to measure, collect and analyse data. Institutional developments should enable smoother governance for the purpose of data sharing. Future projections of climate change scenarios also need to be considered and integrated in water resources project planning and development.

6.8 Data-Based Governance

For generating a realistic picture, quality assured data collection and rigorous processing is a prime requirement. As discussed in this chapter, since data forms the foundation block for the decision-making and subsequent water policies, the quality assurance of data in terms of accuracy and reliability needs to be tested before consumption. Any form of inconsistency in data needs to be identified and corrected by using appropriate tools to process and fill in the gaps, if any. A commonly approved consensual approach on data standardization process should be adopted to arrive at a common assessment.

Data processing methodologies also require special attention in providing the key input to the data-based decision making. Observed data is an idealisation of the complex processes which has generated the response at the observation site. This eventually leads to randomness in the observations. Selection of appropriate data sets for processing and generating the conclusions is a matter of great concern. There are no unique solutions to the processing outcomes. However, the rationality of the outcomes vis-à-vis the situations observed or existing on the ground is an important factor which should be taken into account while evaluating the results of such analysis. Added sophistication and rigor brings with it, additional assumptions and with each additional assumption, the questionability of the outcome increases. The processing methodologies therefore have to strike a balance between the complexity and data availability.

According to Jiménez et al. (2020), the core governance functions include policy and strategy, coordination, planning and preparedness, financing, management, monitoring, evaluation and learning, regulation and capacity development. The responsible authorities need to carry out these core governance functions coherently

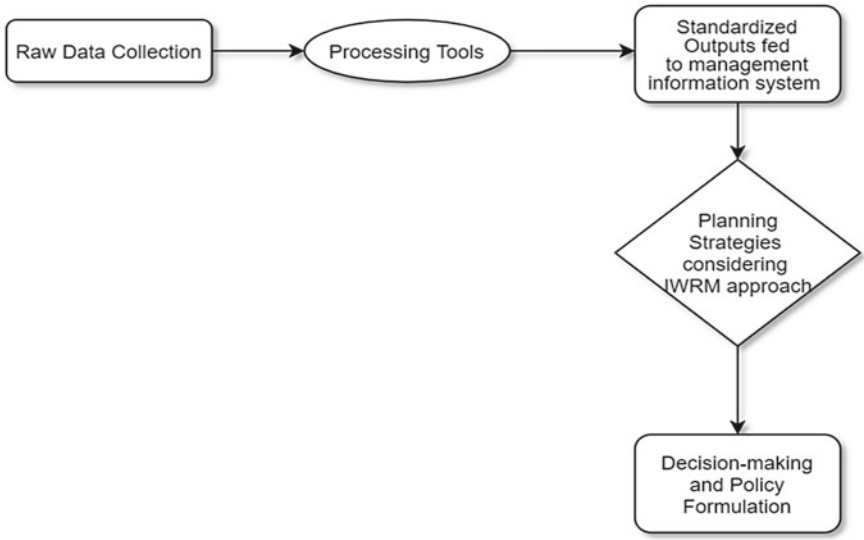

Fig. 6.1 General flowchart highlighting the flow and relevance of data at micro-level to policy formulation at macro level

for the development of the sector (Jiménez et al. 2020) with the help of accurate data, relevant information and the knowledge derived from these respectively. Preconditions for such a pervasive data management system demand smooth exchange of data/information between the stakeholders, a national network, supplemented by the local level agencies. Overall, a well-defined information management system should be established to present a comprehensive evaluation of the resources and demand.

With the advent of advanced technologies and improvements in the database scenario using this extensive system of data and knowledge, future scenario of demand and availability of water resources can be generated and presented to the decision-makers. Planning advisories can be issued for equitable utilizations at various levels through (i) adoption of policy regime to enable sustainable and equitable water resources development, (ii) promotion of exchange avenues for ideas and concerns, and (iii) creation of facilities for institutional and individual capacity building (Fig. 6.1).

6.9 Conclusions and Way Forward

6.9.1 Conclusions

In a nutshell, it can be conclusively said that hydrological data is essential to understand the behaviour of the system and the underlying hydrological and chemical

processes within the system. Increasing water scarcity demands the remaining water to be used more productively. Furthermore, in the face of rapidly changing climate and increased pressure on the water resources, a scientific approach needs to be adopted to carefully assess and thus manage the water resources available. Thus, to mitigate the impacts of climate change, specific measures are required which need to be evaluated based on the accurate data.

Data is integral for decision-making process required for good governance and management. It becomes vital for predictive modelling and evaluating the risk management. Nowadays, advancements in technology such as remote sensing and GIS have provided opportunities to derive data in places where there is unavailability of physical infrastructure.

6.9.2 Way Forward

Some of the most effective methods for optimal utilization and efficient management of water resources place an emphasis on the research on policies and their impact on the society; water resources planning considering impact of the climate change; and impact of external factors such as demography, global economy, changing societal values and norms, technological innovation, laws, financial markets etc. on water resources management. Thus, moving forward, we should promote research and studies on a much larger scale with the objective of identifying alternative ways to address the future challenges of water scarcity and other related issues. Adoption of a unified approach in addressing the water challenges in a coordinated manner with active participation of the stakeholders is necessary.

The data on utilization of water for various purposes should be adequately collected and compiled for consumption by various stakeholders. Availability of this data helps to (i) facilitate generation of future scenario of water availability as well as demand for preparation of basin-wise comprehensive plans in line with IWRM principles; (ii) identify and adopt improved management practices in agriculture as well as other sectors; (iii) monitor and guide to ensure that the project operation achieves highest level of efficiency; (iv) undertake appropriate studies using available information including that in respect of river flow forecast and planning advisories for equitable utilization at various levels; (v) strengthen and streamline the monitoring mechanism for in-depth evaluation of schemes at different stages of implementation and initiating course-correction measures; (vi) promote avenues for exchange of knowledge, relevant concerns and ideas, and (vii) generate awareness on water related issues and management at the atomic level.

However, for efficient and reliable data management, the procedures for data collection, storage, processing and outputs need to be standardized to foster transparency for all the stakeholders and general public. Authenticity of the data is the key here. More investments should be diverted towards data management and improving the quality of hydrological observation and adoption of standard procedures. Also, capacities need to be enhanced at ground level for systematic data collection and

processing. For this, tools such as water accounting and water budgeting present good examples of homogenous and standardized data collection and data processing techniques for transparent governance decisions. Adopting the practice of water accounting gives a clearer picture of the current status and trend analysis of water resources in the region; whereas activities such as water auditing provides avenues for improving the management practices. Another important factor that needs to be considered is ensuring rigorous consistency checks and validation of all data by competent authority before the data is being placed in the public domain for wider consumption.

References

Alexandratos N, Bruinsma J (2012) World agriculture towards 2030/2050. ESA Working Paper No. 12-03. [online] Food and Agriculture Organization of the United Nations. Available at: <http://www.fao.org/3/a-ap106e.pdf> [Accessed 22 July 2020]

AL-shamaa M (2020) Dam talks 'At Crossroads' after egypt rejects ethiopian plea. [online] Arab News. Available at: <https://www.arabnews.com/node/1703346/middle-east> [Accessed 14 July 2020]

Central Water Commission, Ministry of Jal Shakti, Department of Water Resources, River Development and Ganga Rejuvenation, GoI (2020) [online] Available at: <http://cwc.gov.in/> [Accessed 13 July 2020]

FAO WFP, IFAD (2012) The state of food insecurity in the world 2012. Economic growth is necessary but not sufficient to accelerate reduction of hunger and malnutrition. Rome, FAO

Ganoulis J, Fried J (2018) Transboundary water conflicts and cooperation. In: Transboundary hydrogovernance. Springer, Cham

Government of India (2011) Report of the working group on water database development and management. In: 12th Five year plan (2012–2017). Planning Commission, India

Jiménez A, Saikia P, Giné R, Avello P, Leten J, Liss Lymer B, Schneider K, Ward R (2020) Unpacking water governance: a framework for practitioners. Water 12(3):827

Molden D, Burton M (2005) Making sound decisions: Information needs for basin water management. https://doi.org/10.1079/9780851996721.0051

Muir MJ, Luce CH, Gurrieri JT, Matyjasik, M, Bruggink JL, Weems SL, Hurja JC, Marr DB, Leahy SD (2018) Effects of climate change on hydrology, water resources, and soil [Chapter 4]. In: Halofsky JE, Peterson DL, Ho JJ, Little NJ, Joyce, LA (eds) Climate change vulnerability and adaptation in the Intermountain Region [Part 1]. Gen. Tech. Rep. RMRS-GTR-375. Fort Collins, CO: U.S. Department of Agriculture, Forest Service, Rocky Mountain Research Station. pp 60–88

National Remote Sensing Centre (2020) [online] Available at: <http://www.nrsc.gov.in/> [Accessed 13 July 2020]

National Water Development Agency (2020) [online] Available at: <http://www.nwda.gov.in/> [Accessed 13 July 2020]

South–North Water Transfer Project (2020) En.wikipedia.org. 2020 [online] Available at: <https://en.wikipedia.org/wiki/South%E2%80%93North_Water_Transfer_Project> [Accessed 14 July 2020]

The Financial Express (2019) Water scarcity: India's demand may exceed supply two times by 2030. [online] Available at: <https://www.financialexpress.com/opinion/water-scarcity-indias-demand-may-exceed-supply-two-times-by-2030/1691788/#:~:text=By%202030%2C%20India's%20water%20demand,official%20threshold%20for%20water%20scarcity. > [Accessed 22 July 2020]

UN-Water (2020) Water, food and energy| UN-Water. [online] Available at: <https://www.unwater.org/water-facts/water-food-and-energy/> [Accessed 13 July 2020]

UN Water (2013) Water security & the global water agenda. UN-Water Analytical Brief. [online] UN Water. Available at: <https://www.circleofblue.org/wp-content/uploads/2013/03/UNWater_watersecurity_analyticalbrief.pdf> [Accessed 13 July 2020]

Wilson R (2012) Water-shortage crisis escalating in the tigris-Euphrates basin—future directions international. [online] Future Directions International. Available at: <http://www.futuredirections.org.au/publication/water-shortage-crisis-escalating-in-the-tigris-euphrates-basin/> [Accessed 14 July 2020]

Chapter 7
Real-Time Monitoring of Small Reservoir Hydrology Using ICT and Application of Deep Learning for Prediction of Water Level

Tsugumu Kusudo, Daisuke Hayashi, Daiki Matsuura, Atsushi Yamamoto, Masaomi Kimura, and Yutaka Matsuno

7.1 Introduction

A reservoir is an artificial pond to collect water from the catchment area where there are frequent deficits in precipitation or river water. There are more than 150,000 reservoirs in Japan (Matsuno et al. 2019). Seventy per cent of them have been built before the eighteenth century and many of them have deteriorated. Recently, occurrences of natural disasters, such as torrential rains and earthquakes, often bring about floods and the collapse of reservoirs (Japanese Ministry of Agriculture, Forestry and Fisheries 2018). As shown in Fig. 7.1, the annual number of heavy rains has increased over the past decades (Japanese Meteorological Agency). Flooding and collapse of reservoirs caused by these disasters have given rise to an increase in the number of secondary disasters in the downstream basins. In particular, as shown in Fig. 7.2, 73% of the causes of such damage and 98% of the causes of such collapses are heavy rains (Japanese Ministry of Agriculture, Forestry and Fisheries 2018).

There has been an increasing interest in monitoring small reservoirs' hydrologic parameters and predicting the risk of local floods using modern sensing and simulation technologies. For example, Tanihara (2008) created a simulation model estimating an embankment breach of irrigation tanks based on catchment area, spillway and freeboard and rainfall data. This model estimates inflow and outflow volumes and water level and, based on these estimations, predicts flooding risks. However, there is a limitation in accurate prediction with this model as the initial loss was not accounted for when using the general runoff estimation. Generally, there are many advantages in making a prediction model for large dams or major rivers. But for small

T. Kusudo · D. Hayashi · D. Matsuura · A. Yamamoto · M. Kimura · Y. Matsuno (✉)
Department of Environmental Management, Faculty of Agriculture, Kindai University, 3327-204 Nakamachi, Nara 631-8505, Japan
e-mail: matsuno@nara.kindai.ac.jp

© The Author(s), under exclusive license to Springer Nature Singapore Pte Ltd. 2021

A. Pandey et al. (eds.), *Hydrological Aspects of Climate Change*,
Springer Transactions in Civil and Environmental Engineering,
https://doi.org/10.1007/978-981-16-0394-5_7

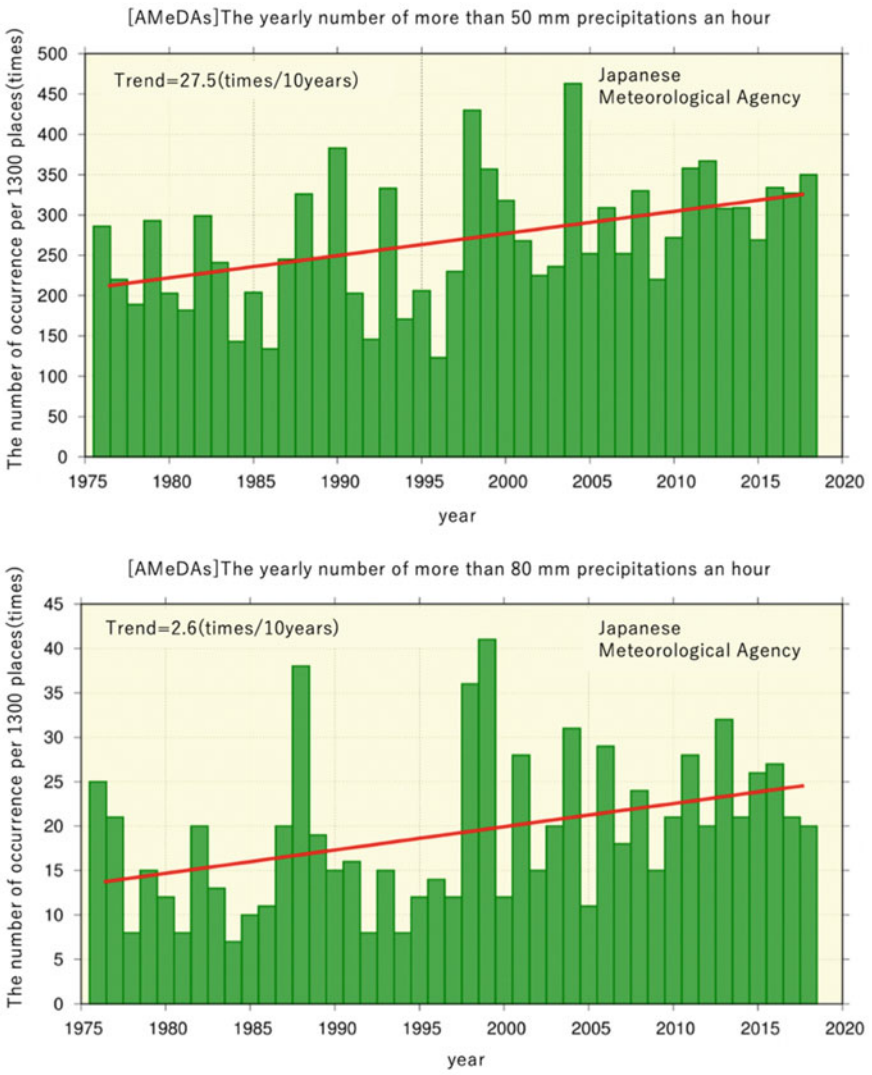

Fig. 7.1 Yearly number of precipitations (Modified from the data by Japanese Meteorological Agency. https://www.data.jma.go.jp/cpdinfo/extreme/extreme_p.html)

reservoirs, the model is a relatively high cost when considering O&M costs for development of a particular water level prediction model. More recently, Hitokoto et al. (2016) predicted a river's water level and a reservoir's water level utilizing the deep learning technique. Although there are researches utilizing deep learning on drought prediction (Agana and Homaifar 2017), urban water level prediction (Assem et al. 2017) and daily reservoir inflow forecasting (Bai et al. 2016), the authors found very few published research on water level prediction of small irrigation reservoirs.

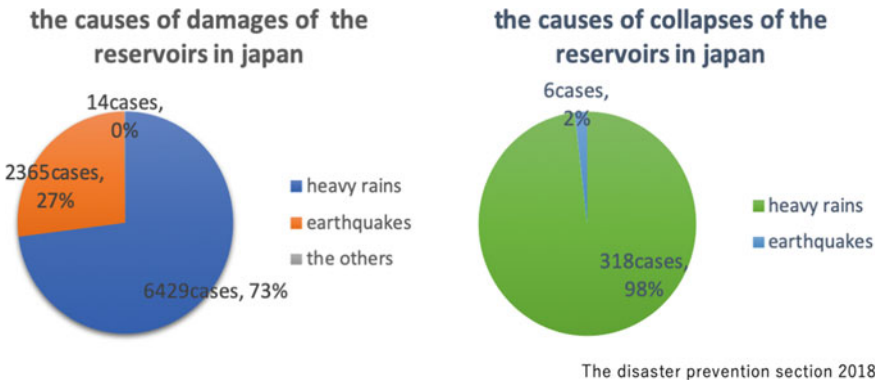

Fig. 7.2 Trend of reservoir's damages in Japan (Created from the information by Japanese Ministry of Agriculture, Forestry and Fisheries. https://www.maff.go.jp/j/nousin/bousai/bousai_saigai/b_tameike/attach/pdf/index-58.pdf)

In this paper, we describe developed low-cost monitoring systems to acquire the hydrologic information utilizing information and communication technologies (ICT), which is coupled with a model that predicts the future water level applying the long short-term memory (LSTM) algorithm as one of the deep learning techniques.

7.2 Material and Methods

7.2.1 Study Site

A survey was conducted at the Takayama Reservoir in Takayama Town, Ikoma City, Nara Prefecture, and at the Kaerumata Reservoir located in Ayameike-Minami Town, Nara City, Nara Prefecture (Fig. 7.3). There are approximately 4300 reservoirs in Nara Prefecture, the majority of which are found in the Yamato Plain. The Yamato Plain region, which occupies two-thirds of the prefecture's agricultural land area, has been plagued by a shortage of water due to low annual rainfall and the absence of large rivers and lakes. The outflow from the Takayama Reservoir flows to the Tomi River, a tributary of the Yamato River basin. The Kaerumata Reservoir flows through the Oike River to the Akishino River, which also belongs to the Yamato River system. Both reservoirs are mainly used for irrigation so that water is released during the irrigation period from early May or late April to mid-September. The specification of the Takayama Reservoir is provided in Table 7.1.

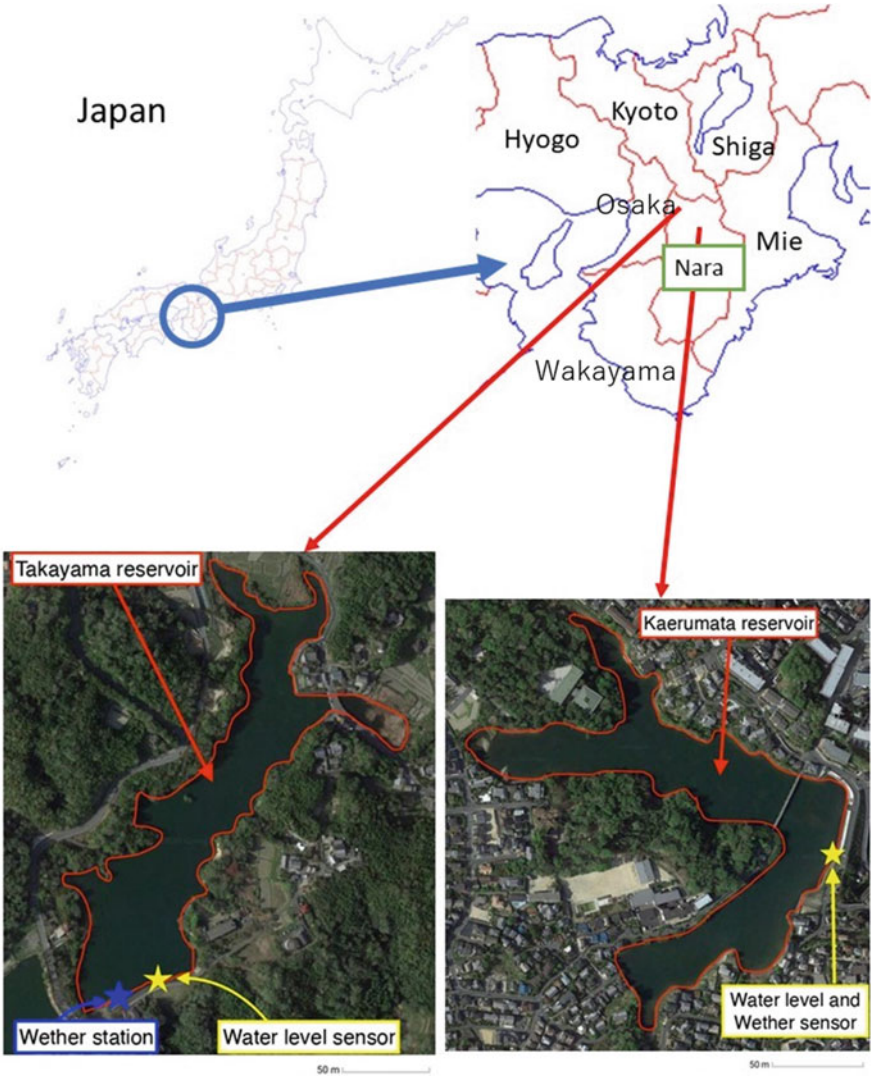

Fig. 7.3 Location of Takayama and Kaerumata Reservoirs

Table 7.1 Specification of Takayama and Kaerumata Reservoirs

	Capacity	Surface area	Catchment area
Takayama	580,000 m^3	90,000 m^2	2.3 km^2
Kaerumata	211,716 m^3	86,300 m^2	0.92 km^2
	Beneficiary area	Embankment height	Embankment length
Takayama	530 ha	23 m	135 m
Kaerumata	38 ha	14 m	

7.2.2 Water Level and Weather Data Monitoring

The sensor was set to monitor water level and water temperature of the reservoir every ten minutes (GSC-01A, Geotech Service) and show them on the web page through the remote data logger (HOBO RX3000, Onset) with the communication channel, SORACOM. Atmospheric pressure, atmospheric humidity, air temperature, solar radiation, precipitation, wind velocity and wind direction were also measured every ten minutes using the KOSEN weather station. A solar panel was attached to the sensing system for electricity supply. Water level data was stored as a CSV data file, while the weather data was stored as a JSON format so that it could be later converted to a CSV data file. Combined data accumulated from July 2018 to September 2019 was used for training and testing of the water level prediction model. The Python program was used to organize and combine the water level and weather data (Fig. 7.4).

For the Kaerumata Reservoir, we installed a different set of IoT devices to monitor real time water level, water temperature, rainfall. In addition, a web camera was set up to observe the reservoir water online. These data were sent to the server once every hour through the LTE mobile line. METER's CTD-10 was used as the water level and water temperature sensor, and METER's ECRN-50 was also used as the rain gauge. The data observed by these was integrated and quantified using Atmel's microcontroller ATMEGA328P-PU, and the data was stored and sent to the server using RS Components' single board computer Raspberry Pi 3B+. Regarding the

Fig. 7.4 Weather station (left), data logger (upper right), water level sensor (lower right)

ATMEGA328P-PU, we designed the circuit board to connect to each sensor and to communicate with the Raspberry Pi 3B+, as shown in Fig. 7.5.

These devices are readily available and can be purchased through online shops in Japan and can be assembled even with a limited knowledge of electronics. Figure 7.6 shows the schematic of the IoT system flow. The solar power supply was used for the system that ensured the supply of sufficient power to run the sensors, web camera and communication devices (Fig. 7.7).

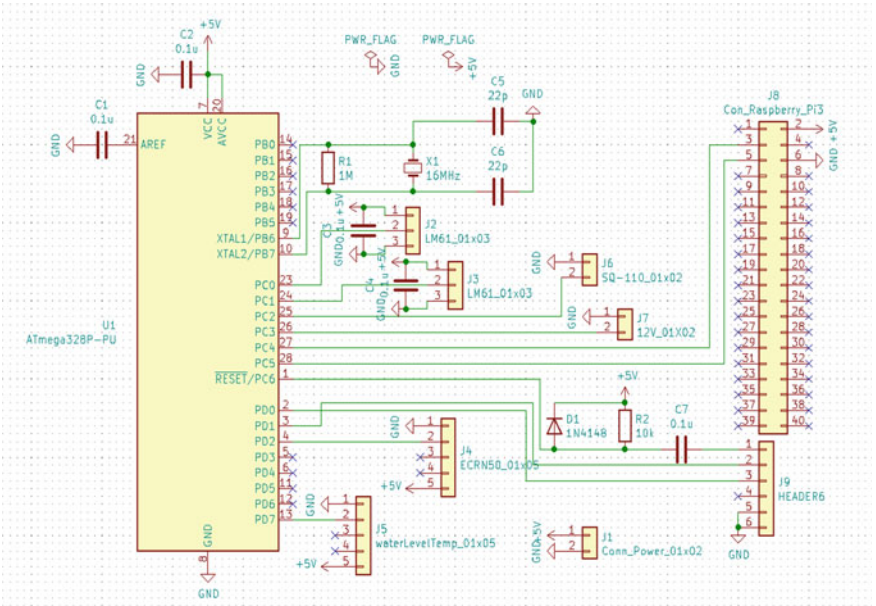

Fig. 7.5 Designed circuit board for connecting ATMEGA328P-PU

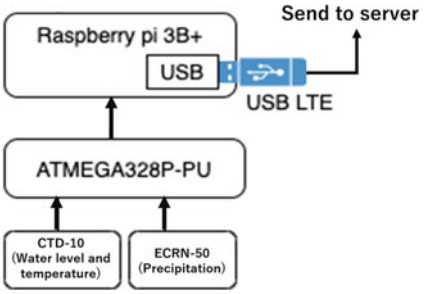

Fig. 7.6 IoT system flow for the Kaerumata Reservoir

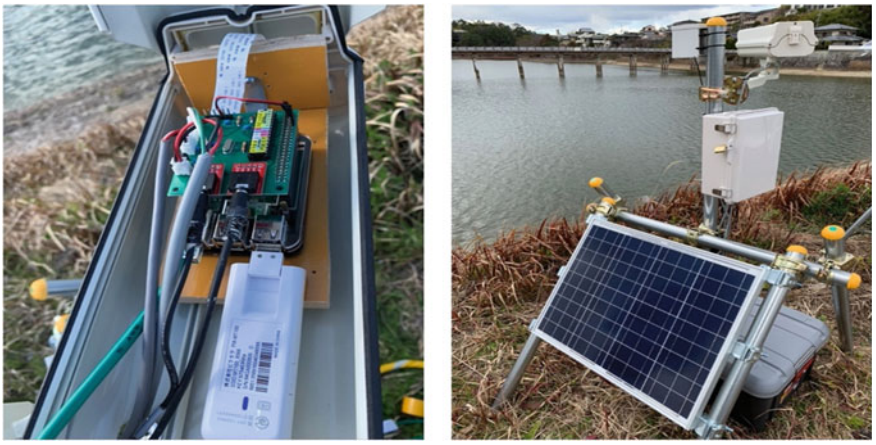

Fig. 7.7 Installed devices and solar panel for the Kaerumata Reservoir

7.2.3 Water Level Prediction Model Using LSTM

The water level prediction model using the deep learning technique was developed using Python with neural network libraries such as TensorFlow and Keras. Deep learning, a kind of neural network, imitates the neural transmission of living things. By assigning a threshold and weight to each unit from a huge number of input and output data groups, it can be expressed similar to a person identifying an event with a lot of information. In recent years, deep neural network models with deeply complicated neural network layers have been successful in fields such as image processing and pre-language processing and their effects are accepted in the fields of hydrology and agricultural engineering (Li et al. 2016; Taniguchi et al. 2019; Xudong et al. 2019).

A neural network is composed of an input layer, hidden layers and an output layer, while past water level, precipitation and discharge are considered as inputs to predict the future water level of the reservoir, as shown in Fig. 7.8.

The model was developed by applying long short-term memory (LSTM) algorism for prediction of the reservoir's water level as it is suitable for handling the time series

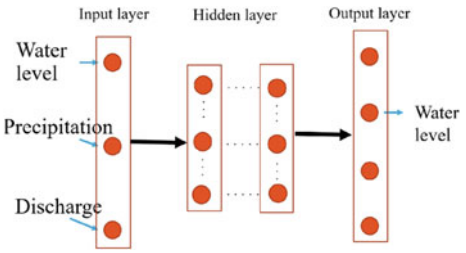

Fig. 7.8 Schematic of deep learning

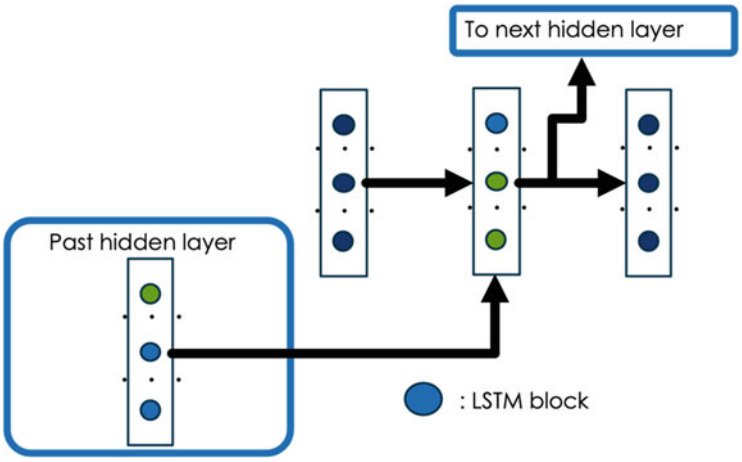

Fig. 7.9 Schematic of long short-term memory (LSTM) algorithm

data. LSTM is considered as a kind of recurrent neural network (RNN) that integrates past hidden layers with present learning data (Fig. 7.9). RNN is a deep learning method often used for natural language processing and time series data analysis. In this study, we treated water level fluctuations as time series data and assumed that future water levels could be predicted by RNN. Simple RNNs, on the other hand, had a problem of disappearing gradients in the past due to long-term memory difficulty and an increase in learning volume. LSTM was adopted to solve these problems because long-term past memory is considered to be significantly involved in learning water level prediction. With LSTM, the vanishing gradient problem encountered in the ordinary RNN is solved because the long temporary dependence vanishes every time the model learns a new.

7.2.4 Layer Setting for LSTM Model Development

Table 7.2 shows the selected parameters and layer setting of the developed model.

Table 7.2 Model parameters and layer

Input layer	Hidden layer	Output layer
Past rainfall intensity Current water level Discharge	Activation: tanh LSTM layer: 1 Unit number: 7 Loss function: RMSE	Water level at 1–11 h future

7.2.5 LSTM Model Evaluation

The difference between predicted and actual water level data was examined by applying Nash–Sutcliffe efficiency (NSE) and per cent bias (PBIAS) for the evaluation. NSE is the normalized statistic to determine the relative magnitude of residual variance for comparison with the variance of measured data that is often used to assess the performance of hydrological models. NSE is expressed as:

$$\mathrm{NSE} = 1 - \left\{ \frac{\sum_{i=1}^{n} \left(Y_i^{\mathrm{act}} - Y_i^{\mathrm{pre}}\right)^2}{\sum_{i=1}^{n} \left(Y_i^{\mathrm{act}} - Y^{\mathrm{mean}}\right)^2} \right\} \tag{7.1}$$

where Y_i^{act} expresses the ith actual water level, Y_i^{pre} expresses the ith predicted water level and Y^{mean} expresses the mean of all data. PBIAS estimates the deviation of data expressed as percentages that is shown in Eq. (7.2):

$$\mathrm{PBIAS} = \left\{ \frac{\sum_{i=1}^{n} \left(Y_i^{\mathrm{act}} - Y_i^{\mathrm{pre}}\right) * (100)}{\sum_{i=1}^{n} \left(Y_i^{\mathrm{act}}\right)} \right\} \tag{7.2}$$

7.2.6 Reservoir Monitoring System and Water Level Prediction Model

PHP, JavaScript, MySQL and Python were used to develop a website to display the hydrologic data of the reservoir in real time. The prediction model was also incorporated into the website to show the future water level with given forecasted precipitation events.

The accuracy of the deep learning model depends on the quality and amount of training and testing data. In the system, the model can automatically update these data by incorporating observed data into the program in real time. It was set to use 70% of the observed data for the training and 30% for the testing. The schematic diagram for building the system is shown in Fig. 7.10.

The rainfall intensity data obtained from KOSEN weather station and the water level data obtained from GSC-01A are saved in HOBO RX3000 and sent automatically to the cloud server. The LSTM model uses the data for prediction of future water levels. At the same time, the observed water level and rainfall data are displayed graphically, together with predicted water levels on the web screen.

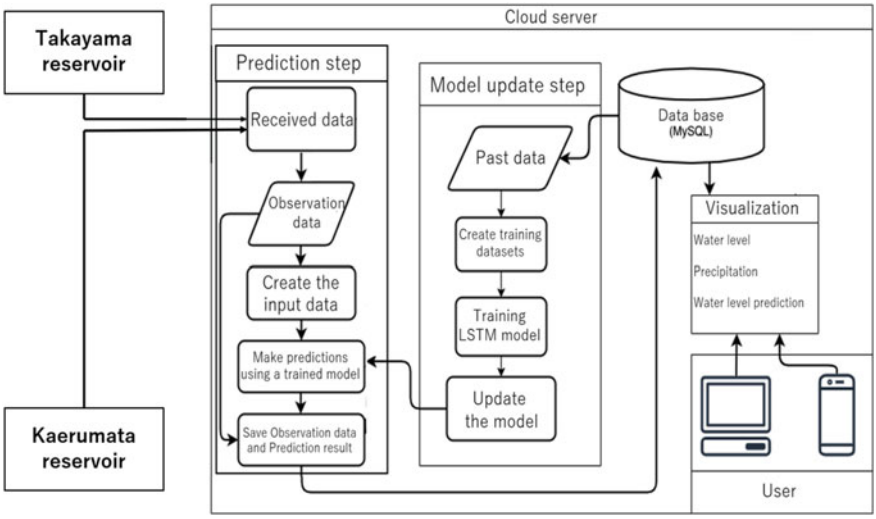

Fig. 7.10 Flow of developed system

7.3 Results and Discussion

7.3.1 Collection and Display of Water Level and Weather Data

With the developed system, the water level of the Takayama Reservoir was successfully monitored. Every ten minutes water level data displayed on the web page of HOBOlink (see Fig. 7.11). The data file was exported as a CSV file from the page to the developed system every hour. The weather data, such as rainfall, ambient temperature, relative humidity, solar radiation, wind speed and wind direction, were also successfully obtained every ten minutes and was shown on the web page of the KOSEN system (Fig. 7.12). The data from HOBOlink and KOSEN was automatically acquired via FTPS communication and API, respectively.

The water level from HOBOlink and the precipitation data from KOSEN system were merged to visualize the relationship between water level and precipitation. The gradual water level changes with changes in climatic variation are shown in Fig. 7.13. The precipitation events from 1 July 2018 through 31 December 2018 shown in this figure indicate the response of the reservoir's water level with rainfall events. An overflow was observed in July as the water level surpassed the spill level of the Takayama Reservoir. The overflow–precipitation relationship is shown in Fig. 7.14.

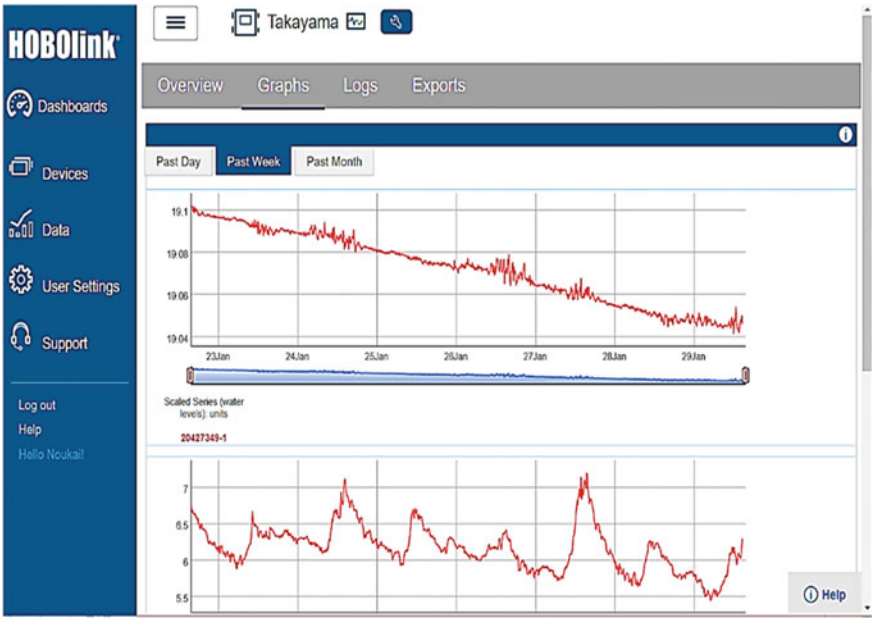

Fig. 7.11 Display of water level on web page of HOBOlink

7.3.2 Reservoir Monitoring by Web Camera

In the Kaerumata Reservoir, a web camera was installed for surveillance of the reservoir water and surroundings that could be useful, especially during heavy rain events, to observe the situation of the reservoir without going to the site. Figure 7.15 shows the location of the installed camera in the reservoir and an image taken and transmitted to the server.

The images can be seen from the mobile phone communication tools, Slack and Line. Figure 7.16 shows the screen display on the Slack application sending the imagery data every hour.

7.3.3 Water Level Prediction Component of the System

The water level prediction model was developed using the aforementioned monitoring data for training and testing of the model. Using the LSTM algorithm, the future water levels of one to 11 h were estimated from the series of observed current and past water levels, rainfall and the forecasted precipitation data. The forecasted precipitation data was received from a commercial weather forecasting service. The model was developed to estimate possible amounts of water storage during a future rainfall event. It could also be used to reduce the risk of the reservoir's collapse and

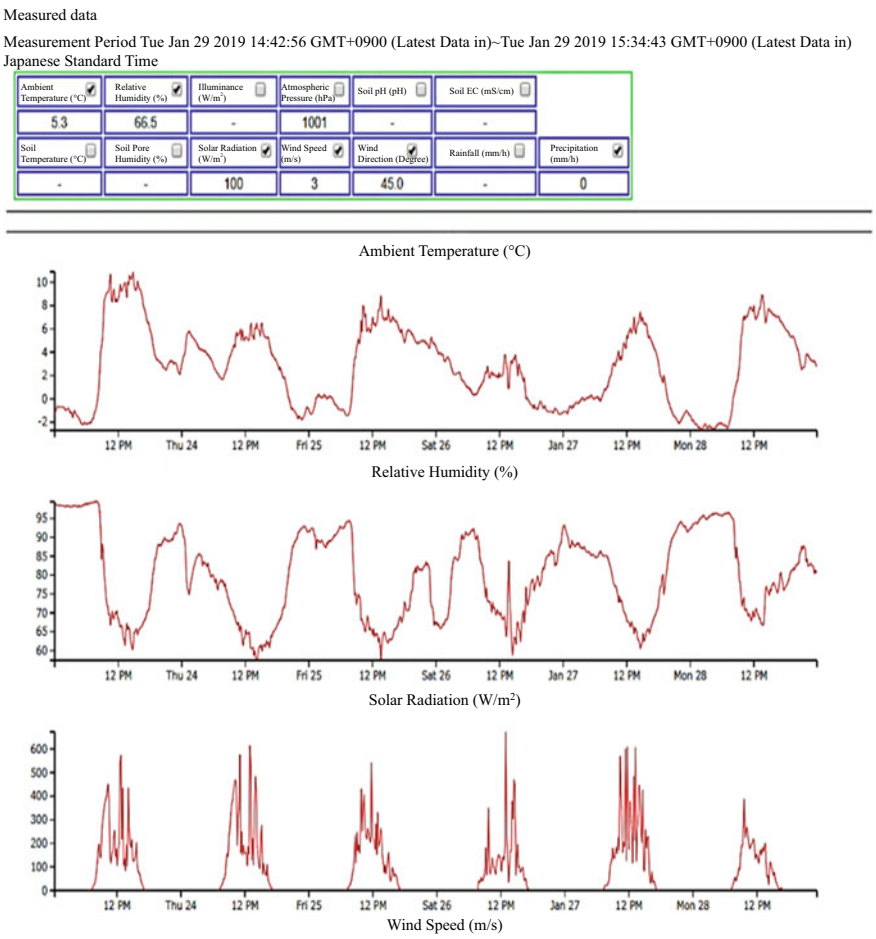

Fig. 7.12 Display of weather data on web page of KOSEN system in Japanese

downstream flooding that occurs with the collapse, while ensuring sufficient water storage for irrigation owing to its ability to decide an appropriate amount of water release from the reservoir prior to rainfall events. The observed data from 1 July 2018 to 31 December 2018 was used for learning and testing of the model.

The performance of the developed model, as indicated by the relation between the epochs of the model**, i.e.** the number of times to learn an absolute error with observed values, is shown in Fig. 7.17. The abscissa of Fig. 7.17 is for the number of epochs. This figure indicates that the error decreases as the epochs increase. The prediction model became accurate sharply when the epoch was around 30.

Prediction of this model was then compared with the observed data obtained from 15 January 2019 to 21 January 2019 as shown in Fig. 7.18. Figure 7.18 shows that the model could respond to precipitation and predict water level, although it reacted

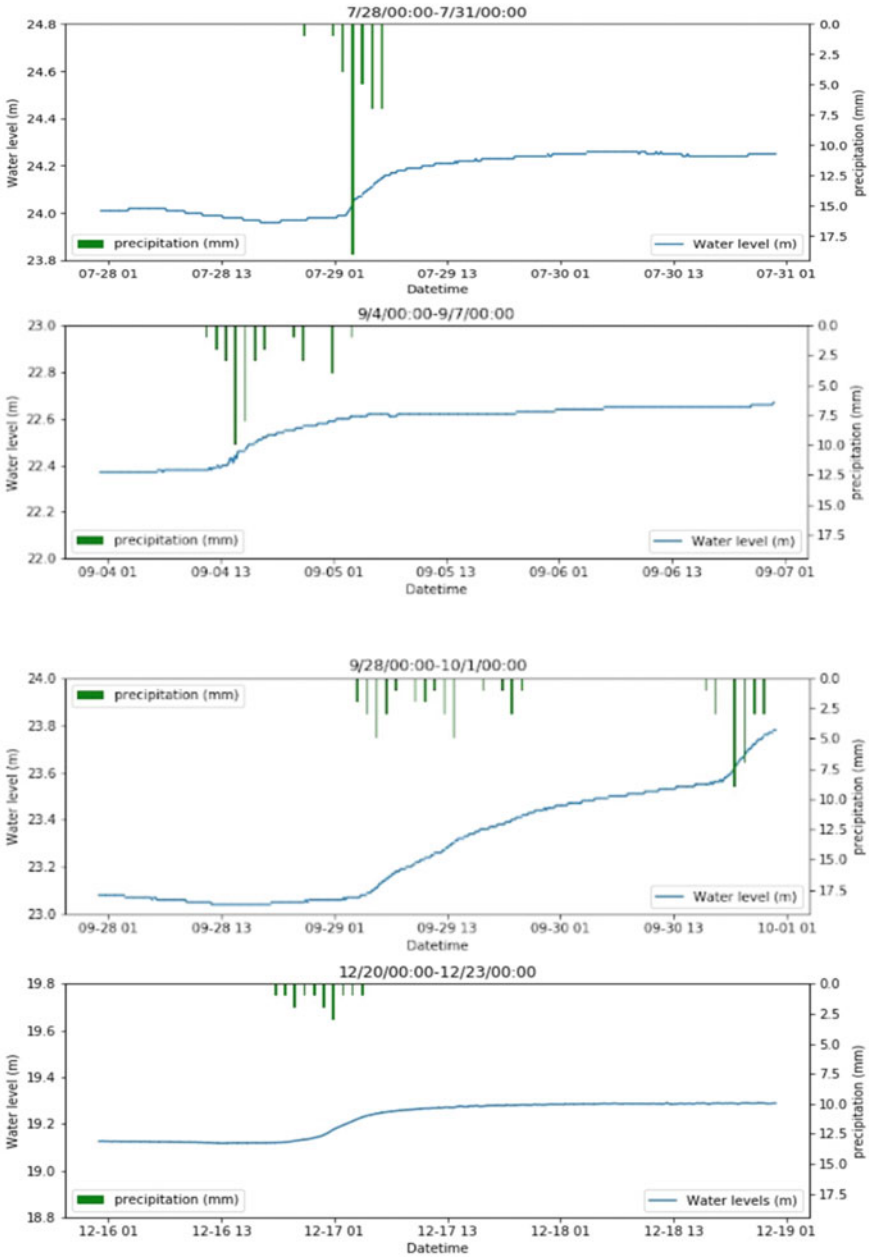

Fig. 7.13 Relationship of water level and precipitation

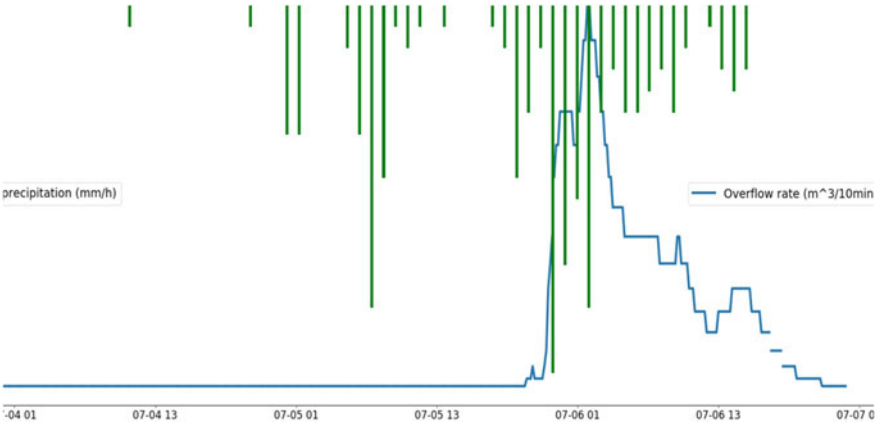

Fig. 7.14 Relationship of overflow and precipitation

Fig. 7.15 Location of web camera and an image taken from the camera

too immediately after the rainfall event. On the other hand, as shown in Fig. 7.19, the difference between observed and predicted water level is about 1 cm.

Figure 7.20 expresses an accuracy of the model, when it compared observed water level with predicted water level data after an hour and after 11 h. Nash–Sutcliffe efficiency (NSE) and per cent bias (PBIAS) were used for model evaluation. Table 7.3 shows the results of the model evaluation. Both NSE values significantly surpass the standard value. Generally, a model is judged as satisfactory if NSE is close to 1 and low values of PBIAS indicate accurate model simulation (Moriasi et al. 2007). Here, both NSE and PBIAS values show satisfactory levels of prediction.

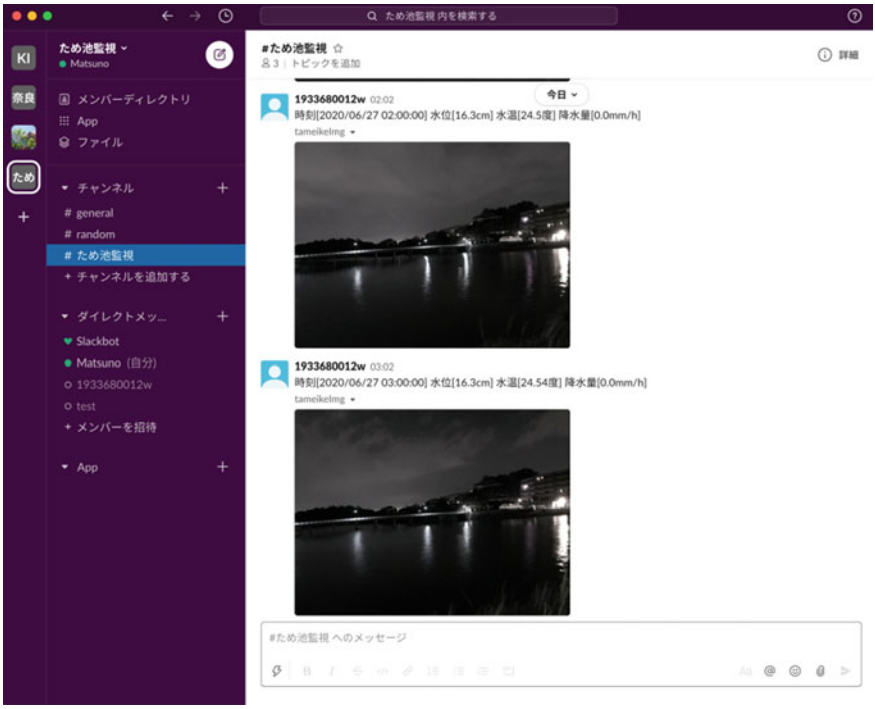

Fig. 7.16 Reservoir images displayed on the screen of Slack during the night time

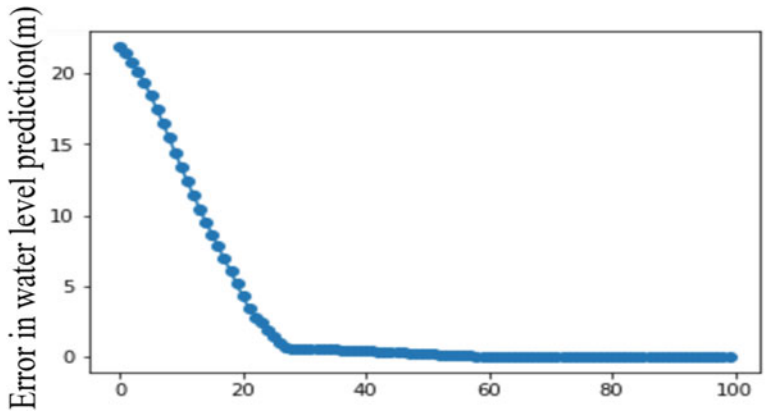

Fig. 7.17 Relation of epochs and absolute error of water level prediction

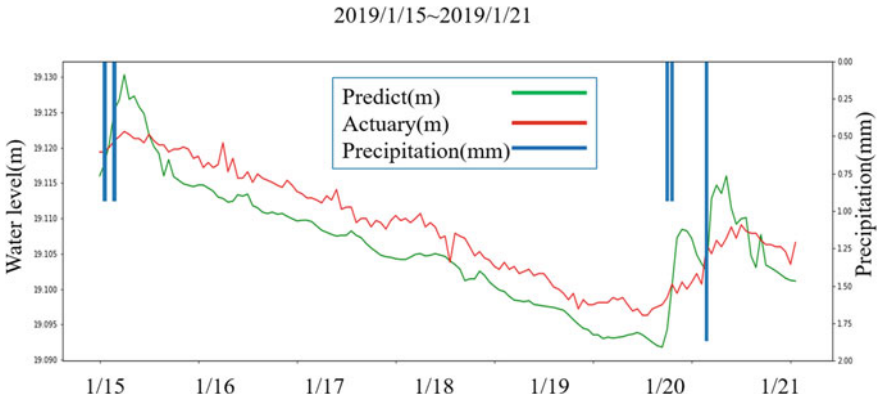

Fig. 7.18 The comparison of predicted and observed water level

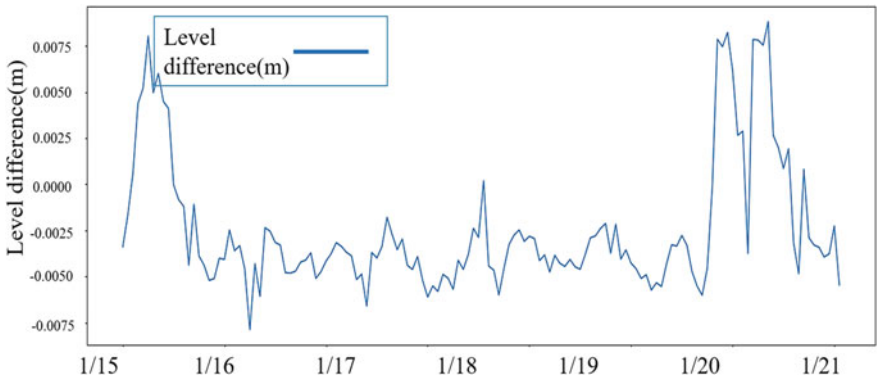

Fig. 7.19 Difference between observed and predicted water level

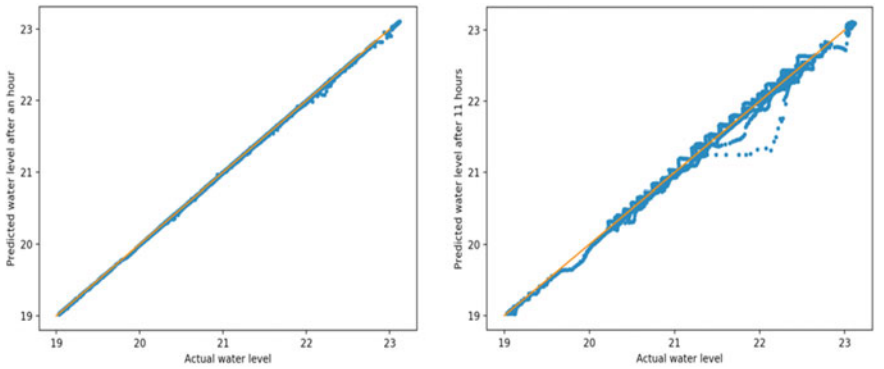

Fig. 7.20 Accuracy of predicted water level after an hour and after 11 h

Table 7.3 Results of NSE and PBIAS values estimated

	One hour later	11 h later
NSE	0.999	0.998
PBIAS	5.0%	8.9%

7.3.4 Visualization of Past, Present, and Future Water Level and Rainfall

The water prediction model was incorporated into the monitoring system for its application to water management of the reservoirs. Figure 7.21 shows the web screen displaying the current observed water levels, future water levels from after an hour to 11 h with forecasted rainfall events in the Takayama (upper figure) and Kaerumata (lower figure) Reservoirs.

It should be noted that, even in the same rainfall event, the prediction results differ due to the difference in the period of training data used in the model. Accuracy is increased with the increased training data period. Consequently, long-term monitoring data has an advantage in the construction of accurate DNN models.

7.4 Conclusions

The water level sensor and the weather station were set in the Takayama and Kaerumata Reservoirs to monitor water level and the other hydrologic parameters. The system was able to obtain the data from a remote location at relatively low cost. However, there are issues that were realized during the process of the development, such as power supply when installing in the area, wireless data transmission cost, versatility and interchangeability of sensing devices.

The developed model predicted the water level changes using past water level and precipitation data but requires more training data to increase its accuracy. Both NSE and PBIAS meet the criteria of prediction. The advantage of the model using LSTM is that it may require a smaller set of hydrologic parameters than the conventional one and the accuracy could be increased with an increased number of training data, even though the basic structure of the model remains the same. On the other hand, the quality of the model outcomes may depend on the availability of training and testing data.

By combining the monitoring system and the prediction model developed in this study, it would be easy to use the model for reservoir water management to decrease the risk of flooding in reservoir downstream and also for irrigation.

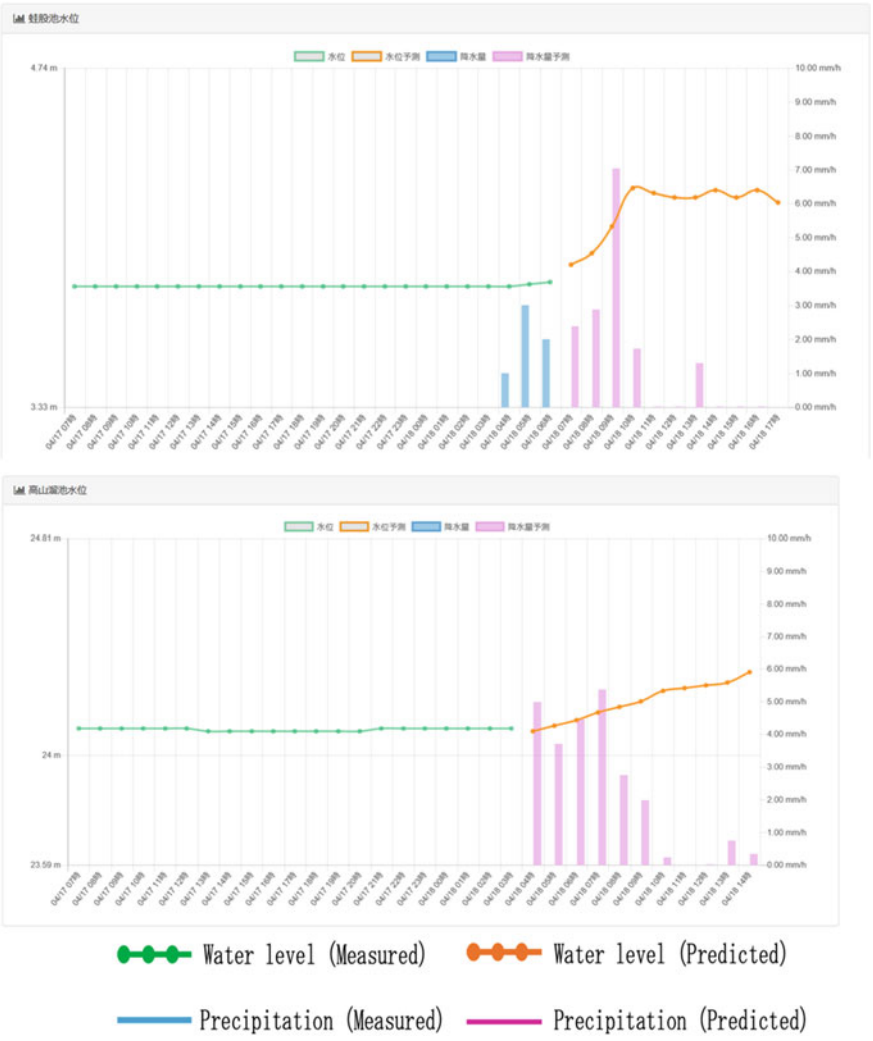

Fig. 7.21 Display of current and predicted future water levels

Acknowledgements Author(s) gratefully acknowledge the support of Agriculture and Forestry Department of Nara Prefectural Government for this study. We also fully acknowledge the information provided by Water Users Associations of the Takayama and Kaerumata Reservoirs.

References

Agana NA, Homaifar A (2017) A deep learning based approach for long-term drought prediction. In: Conference proceedings—IEEE SOUTHEASTCON

Assem H, Ghariba S, Makrai G, Johnston P, Gill L, Pilla F (2017) Urban water flow and water level prediction based on deep learning. In: Altun Y et al (eds) Machine learning and knowledge discovery in databases. ECML PKDD 2017. Lecture notes in computer science, vol 10536. Springer, Cham

Bai Y, Chen Z, Xie J, Li C (2016) Daily reservoir inflow forecasting using multiscale deep feature learning with hybrid models. J Hydrol 532:193–206

Hitokoto M, Sakuraba M, Sei Y (2016) Development of the real-time river stage prediction method using deep learning. Proc Japan Soc Civ Eng B1. 72, I_187-I_192

Japanese Meteorological Agency, The transition of extreme phenomenon such as heavy rains and extremely hot day (2019) https://www.data.jma.go.jp/cpdinfo/extreme/extreme_p.html. Accessed 11 Sept 2019

Japanese Ministory of Agriculture, Forestry and Fisheries (2018) The guidelines of reinforcement of the reservoir's overflow adjustment function. https://www.maff.go.jp/j/nousin/bousai/bousai_saigai/b_tameike/attach/pdf/index-47.pdf. Accessed 11 Sept 2019

Japanese Ministry of Agriculture, Forestry and Fisheries. Circumstance of reservoir's damages (2019) https://www.maff.go.jp/j/nousin/bousai/bousai_saigai/b_tameike/attach/pdf/index-58.pdf. Accessed 11 Sept 2019

Li C, Bai Y, Zeng B (2016) Deep feature learning architectures for daily reservoir inflow forecasting. Water Resour Manage 5145–5161

Matsuno Y, Kishi Y, Hatcho N (2019) Assessment of water quality in small agricultural ponds in Nara Japan. Paddy Water Environ. https://doi.org/10.1007/s10333-019-00748-9

Moriasi DN, Arnold JG, Liew MW Van, Bingner RL, Harmel RD, Veith TL (2007) Model evaluating guidelines for systematic quantification of accuracy in watershed simulations 50(3):885–900

Qu X, Yang J, Chang M (2019) A deep learning model for concrete dam deformation prediction based on RS-LSTM. J Sens 2019, Article ID 4581672, p 14. https://downloads.hindawi.com/journals/js/2019/4581672.pdf

Taniguchi J, Kojima T, Sota Y, Hukumoto S, Satou H, Machida Y, Mikami T, Nagayama M, Nishikohri T, Watanabe A (2019) Application of recurrent neural network for dam inflow prediction. Adv River Eng 25. https://www.tokencon.co.jp/technology/external_papers/gpvufv0000002lid-att/101.pdf

Tanihara T (2008) Prediction of downpour-induced embankment breach of irrigation tanks, and prevention of rood damage to downstream area. J JSIDRE 76:44–45

Chapter 8
Hydrology: Problems, Challenges and Opportunities

Vijay P. Singh

8.1 Introduction

Hydrology is legitimately regarded as a geophysical science. However, its origin in civil or water resources engineering cannot be overlooked. Indeed, the birth of hydrology occurred because of the need for designing civil infrastructure facilities, such as water supply systems, urban and rural drainage, flood control works, water impoundments, arterial airfields, land reclamation, river training works and agricultural irrigation. The need for appropriate design of such facilities, in turn, gave birth to the development of measurement techniques and tools. The point to be emphasized here is that hydrologic science and hydrologic engineering are inseparable and in fact they are partly complementary and partly complimentary. It serves well to treat hydrology both as a geophysical science and an engineering discipline. One can also justifiably consider hydrology as an environmental science as well as a branch of environmental engineering. It is not important what hydrology is called or where hydrology is placed. What is important is that hydrology is advanced in all aspects and water-related questions impacting the mankind are answered.

For planning, design, operation and management of environmental and water resources systems, some key questions had to be answered, for example, design of an impoundment, a spillway, a drainage facility, an embankment, pavement or a dam called for answering such questions as the following: What is the peak discharge for a given rainfall event? How often does a discharge of a given magnitude occur? What is the volume of discharge resulting from a rainfall event and how is it distributed in time? How much and at what rate does rainwater infiltrate into the ground? These questions fall under rainfall–runoff modelling and frequency analysis which have

V. P. Singh (✉)
Department of Biological & Agricultural Engineering & Zachry Department of Civil & Environmental Engineering, Texas A&M University College Station, Texas 77843-2117, USA
e-mail: vsingh@tamu.edu

© The Author(s), under exclusive license to Springer Nature Singapore Pte Ltd. 2021

A. Pandey et al. (eds.), *Hydrological Aspects of Climate Change*,
Springer Transactions in Civil and Environmental Engineering,
https://doi.org/10.1007/978-981-16-0394-5_8

received much attention for over eight decades. These questions are still being addressed with, of course, more sophisticated tools and greater data availability.

In olden days, land reclamation and irrigation occupied an important place in the society. In the USA, Bureau of Reclamation, a branch of the US Department of the Interior, was established for that reason. Water had to be brought through canals from storage reservoirs to farms. Canals had to be designed using the theory of hydraulic geometry which gave rise to the regime theory in the early part of the twentieth century. This theory was also applied for river training and restoration works. For farm irrigation, it was important to determine the distribution of the infiltrated water into the vadose zone, soil moisture status, evapotranspiration and space–time characteristics of droughts.

Dam construction had started many centuries ago but was not widely prevalent. People depended on groundwater through well construction and pumping. Therefore, it was necessary to determine the discharge of pumping, the rate of groundwater depletion, as well as the rate groundwater recharge.

For dam and canal operation, and river training and restoration, there were issues related to erosion, sediment yield, sediment concentration and sediment transport. Likewise, for domestic water supply, reliable water supply systems had to be designed which would supply pollutant free water. This means that water had to be treated so it was potable.

To answer the relevant questions needed data which led to hydrologic data collection systems. In the USA, several federal agencies were charged with the task of collecting data. For example, the US Geological Survey is responsible for collecting surface and groundwater data, the US National Weather Service is responsible for collecting precipitation data and the US Department of Agriculture is responsible for collecting soil erosion and snow data. Likewise, state government agencies were charged with collecting a variety of data, including water quality data.

The scope of hydrology has vastly expanded and hydrology is now being applied to many new areas which were unknown in olden days. Besides the usual classification of hydrology into surface water hydrology, vadose zone hydrology and groundwater hydrology, many branches of hydrology have therefore taken roots, depending on their emphasis or the nature of watersheds. For example, urban hydrology, agricultural hydrology, forest hydrology, snow hydrology, mountain hydrology, desert hydrology and coastal hydrology are now well developed. Likewise, depending on the methods of analysis or techniques of solution, hydrology is often classified as deterministic hydrology, stochastic or statistical hydrology, and numerical or computational or digital hydrology. Each branch of hydrology has its unique problems and challenges.

Many of the same questions that were addressed a century or many decades ago are being still asked but with a different context and many new questions are being formulated. The objective of this paper therefore is to reflect on the problems, challenges and opportunities in hydrology. It may be instructive to first visualize the anatomy of hydrology which directly connects with the objective.

8.2 Anatomy of Hydrology

The anatomy of hydrology comprises six components, as shown in Fig. 8.1: (1) aspects of water, (2) phases of water, (3) place of occurrence, (4) domain, (5) scale, and (6) processes. Water has two aspects: (i) quantity and (ii) quality, and it has four phases: (i) liquid, (ii) vapour, (iii) solid-snow and ice and (iv) fourth phase. The water occurs over the land surface, below the surface in the unsaturated zone called vadose zone, and below the vadose zone in the saturated zone or aquifers, also called geological zone or groundwater zone. The processes of water occur in three domains: (1) space, (2) time and (3) frequency, and the scales at which hydrologic processes operate are micro, meso, macro and mega. The hydrologic processes can be principally characterized as occurrence, distribution, movement and storage.

Hydrologic processes include water in storage above, on and below the land surface, comprising water (vapour) in the atmosphere, interception storage, depression and detention storage, channel storage, storage in lagoons, lakes, and reservoirs, storage in wetlands, and snow, ice and glaciers. Water moves on or above the land surface horizontally or vertically upward or downward. It comprises precipitation (downward), evaporation (upward), transpiration (upward), and throughflow (downward). Water moving horizontally as overland flow, channel flow, snowmelt runoff and glacial movement.

Water flows below the land surface in the unsaturated zone as infiltration (normally vertically downward but also laterally), percolation (usually vertically downward) and interflow (horizontally). Water also flows below the land surface in the saturated zone as baseflow (usually horizontally) and groundwater flow (horizontally as well as vertically).

Hydrologic processes are parts of the hydrologic cycle which at a large scale connects atmosphere, land surface, pedosphere, lithosphere and hydrosphere. These sphere are interconnected and are interactive. The degree of interconnectivity depends

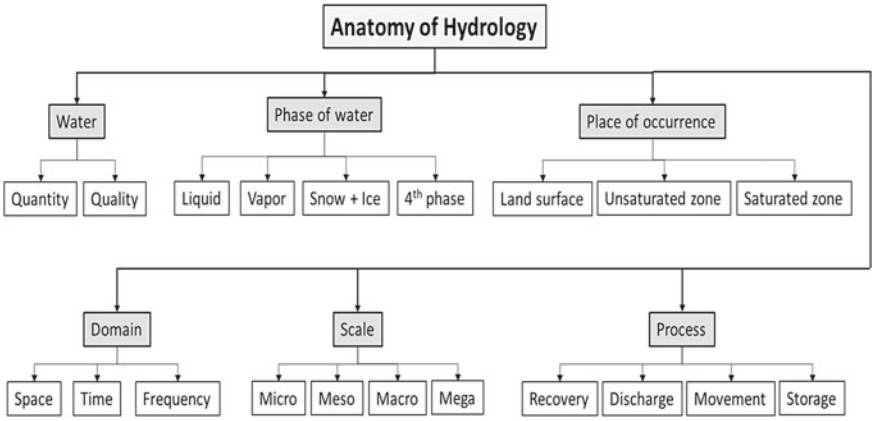

Fig. 8.1 Anatomy of hydrology

on the space and time scales. As a consequence, the role of different hydrologic processes varies with space–time scaling. For example, at a large scale, the most important hydrologic processes are precipitation, evapotranspiration and streamflow which includes groundwater flow. On the other hand, at smaller scales, infiltration, percolation interception, overland flow and snowmelt runoff also become important.

Each component and each hydrologic process present unique problems and challenges and hence offer new opportunities to advance hydrologic science and engineering and in turn serve the mankind.

8.3 Grand Challenges

The twenty-first century is facing a number of grand challenges and hydrology plays a fundamental role in meeting these challenges. The grand challenges, as shown in Fig. 8.2, can be enumerated as food security, water security, energy security, health security, climate security, environmental security, ecosystem sustainability, and water–energy–food–environment nexus. Indeed, the survival of humanity might

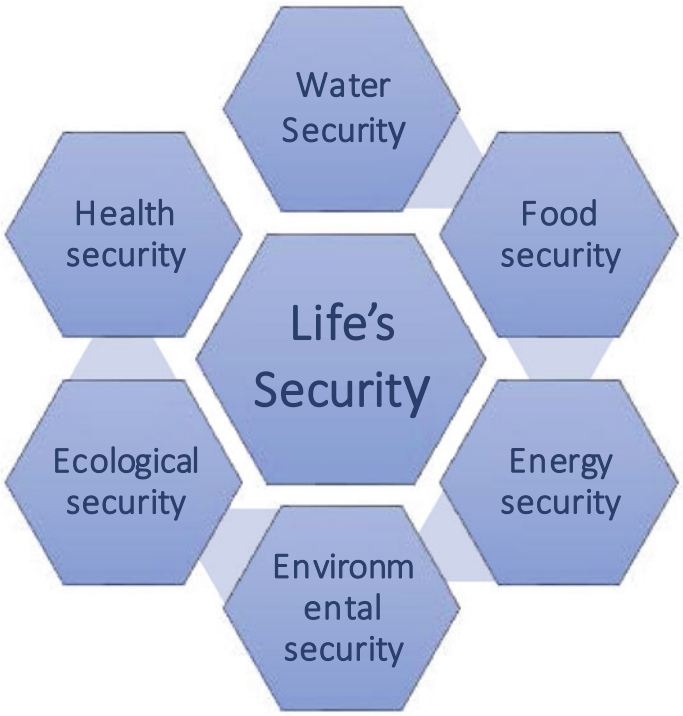

Fig. 8.2 Grand challenges

be at risk unless these challenges are met and the full scope of hydrology can be brought to bear on meeting the challenges. Each challenge involves a unique set of hydrologic problems.

8.4 A Glimpse of History of Hydrology

The beginning years of hydrology entailed the development of component models. Surface runoff modelling started with the development of rational method for determining peak discharge (Mulvany 1850; Imbeau 1892) and then evolved with the development of the unit hydrograph method for determining the runoff hydrograph (Sherman 1932), overland flow analysis for describing the space–time history of overland flow (Keulegan 1944; Izzard 1944), unit hydrograph theory (Nash 1957; Dooge 1959), geomorphologic unit hydrograph combining the laws of geomorphology with the unit hydrograph theory (Rodriguez-Iturbe and Valdez 1980) and kinematic wave theory for flow routing (Lighthill and Whitham 1955). One of the key problems when determining the runoff hydrograph is the determination of storm runoff amount which led to the development of the SCS-CN method (Soil Conservation Service 1956). Snow modelling began with the development of snow hydrology (US Army Corps of Engineers 1956) and kinematic wave theory of snowmelt movement (Colbeck 1972, 1974).

In forested watersheds and humid zones, part of streamflow is generated by subsurface flow whose modelling involves the discovery of subsurface flow mechanisms (Lowdermilk 1934; Hursh 1936, 1944; Hursh and Brater 1944; Hoover and Hursh 1943; Roessel 1950; Hewlett 1961a, b; Nielsen et al. 1959; Remson et al. 1960). Part of infiltrated rainwater gives rise to interflow which is also subsurface flow. Different mechanisms of subsurface flow, including Horton mechanism, Dunne-Black or saturated mechanism and subsurface mechanism were formulated. Thus, streamflow generation may entail Horton mechanism-rainfall excess (Horton 1933), subsurface flow mechanism (Lowdermilk 1934), or saturation excess or Dunne-Black mechanism (Dunne and Black 1970). In the process, the concepts of partial area and variable source area were developed.

A major portion of rainfall usually infiltrates into the soil. The theory of infiltration started with the Green-Ampt model (1911), Kostiakov model (1932) and Horton Model (1933). The infiltration component has received much emphasis not only in hydrology but also in soil physics. The result is that there are umpteen infiltration equations available these days. Another major development occurred that showed that soils may have macropores which act like pipes or tubes, often called macropore and preferential flow paths, and flow through them is the dominant flow through soil matrix (Beven and Germann 1981).

The determination of runoff hydrograph requires an estimation of abstractions, such as interception (Horton 1919), detention and depression storage (Soil Conservation Service 1956), as well as evaporation. While these abstractions are not pronounced for individual rainfall events, they become considerable in watershed

modelling, especially at large time scales, such as month, season or year. Even at a daily timescale, they are important in continuous watershed simulation as well as soil moisture simulation. Frequent occurrences of droughts and global warming have given new impetus to evapotranspiration modelling. The theory of evaporation began with the development of energy method (Richardson 1931; Cummings 1935) and the combination method (Penman 1948). The evaporation component has received a lot of emphasis in the past five decades.

Perennial rivers are sustained by groundwater and a significant portion of a runoff hydrograph is constituted by baseflow which is also derived from groundwater. Groundwater modelling started with Darcy equation (1854), hydraulic conductivity relation (Fair and Hatch 1933), well response to pumping (Theis 1935) and correlation between ground water and precipitation (Jacob 1943, 1944). The groundwater area is highly developed, triggered by the digital revolution.

For flood control, construction of dams and reservoirs, as well as river training works, channel flow needs to be routed through channels and reservoirs. This need led to the development of Puls method (US Army Corps of Engineers 1936) and modified Puls method (US Bureau of Reclamation 1949) for reservoir Routing, and Muskingum method (U.S. Army Corps of Engineers 1936), modified Puls method (US Bureau of Reclamation 1949), and diffusion wave method (Lighthill and Whitham 1955) for channel routing.

In agricultural watersheds, erosion was a major environmental issue which led to the development of Universal Soil Loss Equation (Wischmeier and Smith 1960) for determining watershed sediment yield, delivery ratio (Dendy 1968), sediment rating curve (Campbell and Bauder 1940), sediment unit graph (Rendon-Herrero 1974; Williams 1978) and kinematic wave theory (Hjelmfelt et al. 1975; Singh 1983; Singh and Regl 1983). Now erosion modelling has become an integral part of environmental and watershed modelling. The watershed is the primary source of sediment that rivers transport. For any kind of river-related work, sediment transport is needed and this led to the development of Duboys bed load equation, Einstein's bed load formula, Schoklitsch equation, Yalin's transport capacity equation, Yang's total load formula, among others. There is a vast body of literature on sediment transport which also constitutes a major subject in hydraulics. With the growing concern for environmental and water quality, pollutant transport has received a great deal of attention in the past fifty years. Solute transport modelling involves Fick's law, isotherms and advection–dispersion equation.

Beginning with Horton's laws of geomorphology, the field of basin geomorphology has received much emphasis in the past half a century, leading to the law of geometric similarity (Strahler 1958), Horton–Strahler ordering scheme (Horton 1945; Strahler 1952), Horton's laws of stream numbers and lengths (Horton 1945), Schumm's law of stream areas (Schumm 1956), Yang's law of stream slope (Yang 1971), length–area relation (Gray 1961), law of basin relief (Maxwell 1960), law of drainage density (Horton 1945) and hypsometric curve (Strahler 1952). These laws play a fundamental role in watershed and river management.

With the advent of computers in the 1960s, hydrologic modelling took a giant leap forward. It was possible to model the entire hydrologic cycle, which began with the

development of the Stanford Watershed Model (Now in its new incarnation BASINS) (Crawford and Linsley 1966). A large number of watershed models have since been developed all over the world. Examples include HSPF-IV, USDA-HL Model, PRMS, NWS-RFS, SSARR, SWMM; HEC-HMS, KINEROS, ANSWERS, CREAMS, EPIC, SWRRB, SPUR, AGNPS, WATFLOOD, UBC, SHE, TOPMODEL, IHDM, SHETRAN, WBNM, RORB, THALES, LASCAM, Tank Model, Xinanjiang Model, HBV Model, ARNO Model, TOPIKAPI Model, HYDROTEL, WBNM 1994), ARNO model, Soil and Water Assessment Tool (SWAT) model, Macro-PDM, topographic kinematic approximations and integration (TOPKAPI) model, and BTOP model and SWAM. These models have been described in Singh (1995, 2018), Singh and Frevert (2002a, b, 2003, 2006), Singh et al. (2006), and Singh and Woolhiser (2002) and will not be repeated here. One of the limitations of many of these models (with the exception of a few) is that they do not invoke the power of GIS technology. After all, watershed hydrology is a spatial science and GIS technology offers a tremendous power of combining analytical or computational component of modelling with spatially distributed nature of the science which is at the very heart of hydrology of large areas.

8.5 Evolution of Hydrologic Models

Watershed models evolved along four lines in the USA (Donigian and Imhoff 2002): (1) models and support tools, (2) model science, (3) legislation and (4) computing technology. In the decade of the 1960s, watershed and water quality models were developed. During this period, there was a great deal of emphasis on incorporating hydrologic science in watershed modelling. The Water Quality Act was passed by the US Congress. During this period, the computing power was increasing by leaps and bounds. In the decade of the 1970s, watershed and water quality models were further developed, perhaps because the Environmental Protection Agency (EPA) was created, and Fresh Water Pollution Control Act was passed and environmental awareness reached a new high. At the same time, watershed and water quality needs were being more clearly defined. Minicomputers were just beginning to be commercialized. The development and refinement of watershed models have continued since then. In the decade of the 1980s, sediment and pollutant transport were integrated with watershed models. New laws for pollution abatement were being enacted. On the other hand, database management systems were being developed and personal computers were becoming available. The decade of the 1990s witnessed the inclusion of wetlands and forest lands, TMDL, expert systems, graphical software, GIS and database management systems in watershed models. In the decade of the 2000s, surface water and groundwater and their interactions were integrated. Windows were developed and were being used, which altered the entire computing scenario.

8.6 Recent Advances

8.6.1 Data Collection and Processing Technology

With the increasing need for more comprehensive watershed models and meeting more complex societal needs on the one hand and exponentially growing computing needs on the other, the need for a variety of data, such as hydrometeorologic, hydrologic, topographic, geomorphologic, pedologic, land use, lithologic and hydraulic, started to grow. The data needs led to the development of new hydrologic data acquisition tools, such as remote sensing, satellite technology, radar technology, digital terrain and elevation models, and chemical tracers. Some of these tools became possible because of the availability of sophisticated computers. To handle large volumes of data, data processing and management tools were developed, such as geographical information systems (GIS), and database management systems (DBMS).

The impediments are being gradually removed with the development and refinement of globally gridded datasets. Such datasets are expected to evolve further in the future providing new opportunities for researchers in various fields to investigate wide ranging issues related to water availability, water management, climate change, etc. Such investigations will either support or challenge the various posits given in different agency and governmental reports whose peer-review process can sometimes be questioned.

8.6.2 Spatial Hydrologic Variability

For distributed hydrologic modelling, space–time variability of precipitation and watershed characteristics were needed. With the radar and satellite technologies, it became possible to describe precipitation variability, including storm movement, spatial variability, temporal variability and rainfall field description. For hydrologic forecasting, methods for rainfall forecasting were developed.

With the development of digital elevation models (DEM), it became possible to define the spatial variability of watershed characteristics, such as hydraulic roughness, hydraulic conductivity, steady infiltration and mean infiltration. It was then feasible to quantify the spatial variability of these characteristics on runoff dynamics and hydrograph, and formation of shocks.

8.6.3 Scaling and Variability

Another major advance that hydrology has witnessed is the incorporation of scaling and its impact on hydrologic modelling. For example, it is known that watershed characteristics are heterogeneous in space and the same applies to hydrologic processes. However, the degree of heterogeneity depends on the size of scale. It is this physical spatial scale that led to the concepts of representative elementary area, hydrologic response unit or even computational grid size. In a similar vein, hydrologic processes vary in time and the need to incorporate led to the concept of time interval of observations and computational grid size.

8.6.4 Model Calibration

Model calibration has witnessed a number of advances, including the development of new parameter estimation algorithms which require definition of an objective function, optimization algorithm, termination criteria and calibration data. New tools have been developed for handling data errors, determining data needs-quantity and information richness, representing the uncertainty of calibrated models, and the use of artificial neural networks for model calibration.

8.6.5 Emerging Tools

Recent years have witnessed a variety of tools for hydrologic modelling, such as water resources system analysis and decision-making, mechanistic models, data mining models, uncertainty analysis, entropy theory, risk analysis, multivariate stochastic analysis (copula theory), intelligent systems (ANN, fuzzy, etc.) and deep learning tools, optimization algorithms, decision support systems, GIS and data collection and mining.

8.7 Hydrologic Modelling Challenges

Challenges for hydrologic modelling include integration with biogeochemical models, geochemistry, environmental biology, environmental chemistry, earth sciences, meteorology, climatology, oceanography, social sciences, economics, decision-making, climate models as well as ecosystems models. Decision-making entails social, political, economic, legal, administrative and environmental factors. More hydrologic data at finer spatial resolutions, regional scale models, uncertainty analysis, long-term forecasting (ahead of time), probable maximum precipitation

(PMP) and probable maximum flood (PMF) are challenges to be reckoned with. These challenges become even greater challenges with climate change.

8.7.1 Environmental Sustainability

In order to sustain our way of life, it is vital to sustain the environment and indeed for the sustainability of society/human civilization. However, it is subject to a number of constraints, such as population rise, demographic changes, climate change, land use change, urbanization, rising standard of living, rising human expectations, rising energy demand and food security.

8.7.2 Modelling Challenges

Modelling challenges include making models user-friendly, and defining model choices and credibility. This calls for scoping out hydrology.

8.8 Future Outlook

The question is where we go from here. First, there is increasing emphasis on increasing societal demand for models. Second, there should be increasing emphasis on linking models to environmental and ecosystems models. Third, there should be emphasis on user-friendliness. Fourth, modelling should incorporate information technology, computer-based design, artificial intelligence and space technology. Models should have a clear statement of uncertainty and reliability. Also, models should be competitive.

8.9 Reexamination and Reflection

It is now clear that water is fundamental to food security and energy security. Therefore, the water–energy–food security system must become part of the hydrologic education. There must be a partnership among academia, government sector, non-governmental organizations (NGOs) and private sector. The educational system requires restructuring and should aim at training the trainers and teaching the teachers.

The question is: Where are we headed as a society? There is renewed emphasis on the shift from development to management. Hence, there should be a paradigm shift. There has been a great deal of scientific and technological progress in the past century. However, under social progress, the value system has changed. There

are changes in global demographic landscape. Human nature has changed. These days there are conflicts and wars and there is competition. There is convergence or divergence of opinions. This is time for the integration of engineering, technology, and socio-economic-political science.

8.10 Summation

It is important to take a stock of the current situation and recognize social and cultural constraints, taking account of looming global changes, re-examine and re-evaluate our social values and value systems. Our future can be bright or dark-it is all in our hands.

References

Beven K, Germann P (1981) Water flow in soil macropores, 2. A combined flow model. J Soil Sci 32:15–29

Campbell FB, Bauder HA (1940) A rating-curve method for determining silt discharge of streams. Trans Am Geophys Union 21, Part II:603–607

Colbeck SC (1972) A theory of water percolation in snow. J Glaciol 11:369–385

Colbeck SC (1974) Water flow through snow overlying an impermeable boundary. Water Resour Res 10:119–123

Crawford NH, Linsley RK (1966) Digital simulation in hydrology: Stanford Watershed Model IV. Tech. Rep. No. 39, Stanford Univ., Palo Alto, California

Cummings NW (1935) Evaporation from water surfaces: status of present knowledge and need for further investigations. Trans Am Geophys Union 16(Part 2):507–510

Dendy FE (1968) Sedimentation in nation's reservoirs. J Soil Water Conserv 23(4):135–137

Dooge JCI (1959) A general theory of the unit hydrograph. J Geophys Res 64(2):241–256

Donigian AS, Imhoff J (2002) History and evolution of watershed modeling derived from the Stanford Watershed Model. In: Singh VP, Frevert DK (eds), Chapter 2, Watershed models. CRC Press, Boca Raton, Florida, pp 21–46

Dunne T, Black RG (1970) Experimental investigation of runoff production in permeable soils. Water Resour Res 6:478–490

Fair GM, Hatch LP (1933) Fundamental factors governing the streamline flow of water through sand. J Am Water Works Assoc 25:1551–1565

Gray DM (1961) Interrelationships of watershed characteristics. J Geophys Res 66(4):1215–1223

Green WH, Ampt CA (1911) Studies on soil physics: 1. Flow of water and air through soils. J Agric Sci 4:1–24

Hewlett JD (1961a) Some ideas about storm runoff and base flow. U.S.D.A. Forest Service, Southeast Forest Experiment Station, Annual Report, pp 62–66

Hewlett JD (1961b) Soil moisture as a source of base flow from steep mountain watersheds. U.S.D.A. Forest Service, Southeast Forest Experiment Station, Paper No. 132

Hjelmfelt AT, Piest RP, Saxton KE (1975) Mathematical modeling of erosion on upland areas. In: Proceedings, XVI congress of the international association for hydraulic research, vol 2, Sao Paulo, Brazil, pp 40–47

Hoover MD, Hursh CR (1943) Influence of topography and soil-depth on runoff from forest land. Trans Am Geophys Union 24:693–697

Horton RE (1919) Rainfall interception. Mon Weather Rev 147:603–623
Horton RE (1933) The role of infiltration in the hydrologic cycle. Trans Am Geophys Union 145:446–460
Horton RE (1945) Erosional development of streams and their drainage basins: hydrophysical approach to quantitative geomporphology. Geol Soc Am Bull 56:275–370
Hursh CR (1936) Storm water and absorption. Trans Am Geophys Union 17(Part II):301–302
Hursh CR (1944) Appendix B-report of the subcommittee on subsurface flow. Trans Am Geophys Union 25:743–746
Hursh CR, Brater EF (1944) Separating hydrographs into surface- and subsurface-flow. Trans Am Geophys Union 25:863–867
Imbeau ME (1892) La Durance: regime, crues et inundations. Annales des Ponts et Chaussees, Memoires et Documents, 7 Series, III (I):5–18 (French)
Izzard CF (1944) The surface profile of overland flow. Trans Am Geophys Union 25(VI):959–968
Jacob CE (1943) Correlation of groundwater levels and precipitation on Long Island, New York: 1. Theory. Trans Am Geophys Union 24:564–573
Jacob CE (1944) Correlation of groundwater levels and precipitation on Long Island, New York: 2. Correlation of data. Trans Am Geophys Union 24:321–386
Keulegan GH (1944) Spatially variable discharge over a sloping plane. Trans Am Geophys Union 25(Part VI):959–965
Kostiakov AM (1932) On the dynamics of the coefficient of water percolation in soils and of the necessity of studying it from a dynamic point of view for purposes of amelioration. Trans Sixth Commun Int Soil Sci Soc Russian, Part 1:17–29
Lighthill MJ, Whitham GB (1955) On kinematic waves: 1. Flood movement in long rivers. Proc Royal Soc London, Ser A 229:281–316
Lowdermilk WC (1934) Forests and streamflow: a discussion of Hoyt-Trozell report. J For 21:296–307
Maxwell JC (1960) Quantitative geomorphology of the San Dimas Experiment Forest, California. Department of Geology. Technical Report, Columbia University, New York
Mulvany TJ (1850) On the use of self-registering rain and flood gauges. Proc Institution Civ Eng 4(2):1–8, Dublin, Ireland
Nash JE (1957) The form of the instantaneous unit hydrograph. Hydrol Sci Bull 3:114–121
Nielsen DR, Kirkham D, van Wijk WK (1959) Measuring water stored temporarily above the field moisture capacity. Soil Sci Soc Am Proc 23:408–412
Penman HL (1948) Natural evaporation from open water, bare soil and grass. Proc Royal Soc London. Ser A Math Phys Sci 193(1032):120–145
Remson I, Randolf JR, Barksdale HC (1960) The zone of aeration and ground water recharge in sandy sediments at Seabrook, New Jersey. Soil Sci 89:145–156
Rendon-Herrero O (1974) Estimation of washload produced by certain small watersheds. J Hydraul Div ASCE 109(HY7):835–848
Richardson B (1931) Evaporation as a function of insolation. Trans Am Soc Civ Eng 95:996–1011
Rodriguez-Iturbe I, Valdez JB (1980) The geomorphologic structure of hydrologic response. Water Resour Res 15(6):1409–1420
Roessel BWP (1950) Hydrologic problems concerning the runoff in headwater regions. Trans Am Geophys Union 31:431–442
Schumm SA (1956) The evolution of drainage systems and slopes in Badlands at Perth Amboy, New Jersey. Geol Soc Am Bull 67:597–646
Sherman LK (1932) Stream flow from rainfall by the unit graph method. Eng News Rec 108:501–505
Singh VP (ed) (1995) Computer models of watershed hydrology, Water Resources Publications, Littleton, Colorado, p 1130
Singh VP (1983) Analytical solutions of kinematic equations for erosion on plane: II. Rainfall of finite duration. Adv Water Resour 6:88–95
Singh VP (2018) Hydrologic modeling: progress and future directions. Geosci Lett 5(15):5–15

Singh VP, Frevert DK (eds) (2002) Mathematical modeling of small watershed hydrology and applications. Water Resources Publications, Littleton, Colorado, p 950
Singh VP, Frevert DK (eds) (2002) Mathematical modeling of large watershed hydrology. Water Resources Publications, Littleton, Colorado, p 891
Singh VP, Frevert DK (2003) Watershed modeling. In: Proceedings, world water & environmental resources congress 2003, ASCE, June 23–26, Philadelphia
Singh VP, Frevert DK (eds) (2006) Watershed models. CRC Press, Boca Raton, Florida
Singh VP, Frevert DK, Rieker JD, Leverson V, Meyer S, Meyer S (2006) The hydrologic modeling inventory-A cooperative research effort. J Irrig Drainage Eng ASCE 132(2):98–103
Singh VP, Regl R (1983) Analytical solutions of kinematic equations for erosion on a plane: 1. Rainfall of infinite duration. Adv Water Resour 6:2–10
Singh VP, Woolhiser DA (2002) Mathematical modeling of watershed hydrology. J Hydrol Eng ASCE 7(4):270–292
Soil Conservation Service (1956) National engineering handbook, supplement A, Section 4, hydrology. Chapter 10, U. S. Dept. Agric., Washington, D. C.
Strahler AN (1952) Hypsometric (area-altitude) analysis of erosional topography. Geol Soc Am Bull 63:1117–1142
Strahler AN (1958) Quantitative slope analysis. Geol Soc Am Bull 67:571–596
Theis CV (1935) The relation between the lowering of the piezometric surface and the rate and duration of discharge of a well using ground-water storage. Trans Am Geophys Union 16:519–524
U. S. Army Corps of Engineers (1936). Method of flow routing. Report on survey for flood control, Connecticut River Valley, vol 1, Section 1, Appendix, Providence, Rhode Island
U. S. Army Corps of Engineers (1956) Snow hydrology: summary report of snow investigations. U.S. Army Engineers, North Pacific Division, Portland, Oregon
U. S. Bureau of reclamation (1949) Flood routing. Chapter 6.10 in Flood hydrology, Pt. 6. In: Water studies, vol IV, Washington, D. C.
Williams JR (1978) A sediment graph model based on an instantaneous unit sediment graph. Water Resour Res 14(4):659–664
Wischmeier WH, Smith DD (1960) A universal soil loss equation to guide conservation farm planning. In: 7th international congress of soil science, vol 1, pp 418–424
Yang CT (1971) Potential energy and stream morphology. Water Resour Res 7(2):311–322

Chapter 9
Flood Modelling, Mapping and Monitoring of Sparsely Gauged Catchments Using Remote Sensing Products

Biswa Bhattacharya, Maurizio Mazzoleni, Reyne Ugay, and Liton Chandra Mazumder

9.1 Introduction

River basins are increasingly managed using information generated by hydrological and hydraulic models. Models are used in planning, decision support, forecasting and scenario studies. There have been significant improvements in various aspects of modelling such as in coupled modelling, parameter estimation, automatic calibration, uncertainty assessment and data assimilation. However, due to data limitation in many catchments developing even a simple rainfall–runoff model is often problematic. For large number of basins, availability of hydrometeorological data is limited. Additionally, the data required for the representation of the physical domain in the model such as digital elevation data, which is required for identifying river networks, is also an issue. In many cases even if data is available, data sharing principles lead to data accessibility restrictive to the wider audience.

The concurrent advances in remote sensing have provided a number of alternative data sources. Remotely sensed rainfall estimates, referred to in this paper as Satellite Precipitation Products (SPPs), provide rainfall estimates at global scales at increasingly finer spatial and temporal resolution. For example, Tropical Rainfall Measuring

B. Bhattacharya (✉) · R. Ugay · L. C. Mazumder
IHE Delft Institute for Water Education, Delft, The Netherlands
e-mail: B.Bhattacharya@un-ihe.org

M. Mazzoleni
Department of Earth Sciences, Uppsala University, Uppsala, Sweden

Centre of Natural Hazards and Disaster Science (CNDS), Uppsala, Sweden

R. Ugay
National Irrigation Administration, Diliman, 1104 Quezon City, Philippines

L. C. Mazumder
Institute of Water Modelling, Dhaka, Bangladesh

© The Author(s), under exclusive license to Springer Nature Singapore Pte Ltd. 2021

A. Pandey et al. (eds.), *Hydrological Aspects of Climate Change*,
Springer Transactions in Civil and Environmental Engineering,
https://doi.org/10.1007/978-981-16-0394-5_9

Mission (TRMM) provided rainfall estimates at $0.25^{\circ} \times 0.25^{\circ}$ spatial resolution every three hours for the region 50° N to 50°S (Huffman et al. 2007). In more recent time, since the launching of satellites for the Global Precipitation Measurement (GPM) in 2014, some SPPs are available every hour at $0.1^{\circ} \times 0.1^{\circ}$ spatial resolutions (Mastrantonas et al. 2019). The Shuttle Radar Topography Mission (SRTM) launched by NASA and Japanese Space Agency JAXA in 1997 collected digital elevation data at 3 arc-seconds resolution (later version is of 1 arc-second), which has been used in numerous hydrological studies. Similarly, other remotely sensed datasets of temperature, evapotranspiration, etc., are available to be used in hydrological studies. These datasets, which are mostly collected from satellite-borne instruments, occasionally corrected with in situ data and publicly available at global scales, are referred to as global datasets (Bhattacharya et al. 2019a).

The availability of global datasets has contributed to the success of simulation modelling in sparsely gauged catchments (Xu et al. 2014). Collischonn et al. (2008) used TRMM rainfall data in hydrological modelling of the Amazon basin at daily time step. Gu et al. (2010) and Li et al. (2015) used TRMM rainfall data for the Yangtze basin. Zhao et al. (2017) for the Nanlu river basin and He et al. (2017) for a mountainous basin evaluated the usefulness of TRMM rainfall. Wang et al. (2016) used satellite rainfall and gauge data in a hydrological study of the Mekong basin. Xue et al. (2013) used TRMM rainfall for the mountainous Wangchu basin in Bhutan. Arias-Hidalgo et al. (2013) used TRMM rainfall data to complement gauge rainfall in the hydrological modelling of Vinces basin in Ecuador. Most of these studies focused on complementing in situ data with remotely sensed data to improve modelling results.

Hydrological and hydraulic modelling using global datasets is subject to uncertainty. This is primarily due to the use of imprecise data in model calibration and validation. See, for example, Moradkhani et al. (2006) for estimating uncertainty of hydrological models due to remotely sensed rainfall estimates and Islam et al. (2019) for probabilistic flood mapping. Uncertainties may originate from input data, model parameters, model formulations and calibration data. Among these sources, uncertainties in hydrological and hydraulic models due to imprecise boundary condition have not been extensively studied (Mukolwe et al. 2014; Bhattacharya et al. 2019b). This issue is particularly important for large basins as due to the limited availability of gauge data hydrological models are often calibrated with discharge data estimated from imperfect rating curve(s) usually at the outlet of the catchment. For large basins, this may lead to uncertainty in simulated variables such as flow, water depth and water extent (on floodplains), which during flood events may lead to uncertain flood inundation maps.

The objective of this paper is to investigate the potential of flood mapping of the sparsely gauged large-scale Brahmaputra basin primarily using global datasets for model calibration and validation. The hydrological model is calibrated using a rating curve at the outlet of the basin. An uncertainty assessment of the imprecise boundary data used in the modelling framework is provided to investigate the consequent uncertainty in flood maps.

9.2 Case Study

Brahmaputra River is one of the largest rivers of the world. It starts its journey from the Kailash range of southern Tibet (China) at an elevation of over 5000 m. The river flows through China, India and Bangladesh. In Bangladesh, the river joins another mighty River Ganges to form Padma River, which joins Meghna River and ends up in Meghna Estuary for eventually discharging in the Bay of Bengal. The total length of the river is about 2880 km out of which more than half (1625 km) flows through China (Banerjee et al. 2014). The length of the river in India and Bangladesh is about 918 and 363 km, respectively. This is a perennial river fed with snow melt during the spring and with huge monsoon rainfall during the wet period.

The catchment (Fig. 9.1) is rather large with an area of about 580,000 km^2 and spreads over China (~50%), India (34%), Bhutan (~8%) and Bangladesh (~8%) (Mirza 2003). As the long river flows through this large land mass, there are vast changes in topography, climate and land use. The topography varies from cold dry Tibetan Plateau in the upstream side to the Himalayan Slopes followed by Alluvial Plains in the Assam Province in India and finally to flat plains in Bangladesh. The upper part of the basin is relatively dry and cold and receives snow and rainfall about 1/3rd of the precipitation in the Assam valley. Average basin rainfall is about 1100 mm, which in the valley is more than 2200 mm (Sharma and Paithankar 2014; Parua 2010). The average maximum basin temperature in summer is about 20 °C and in winter is about 9 °C. The basin is not much industrialized, and the forest area

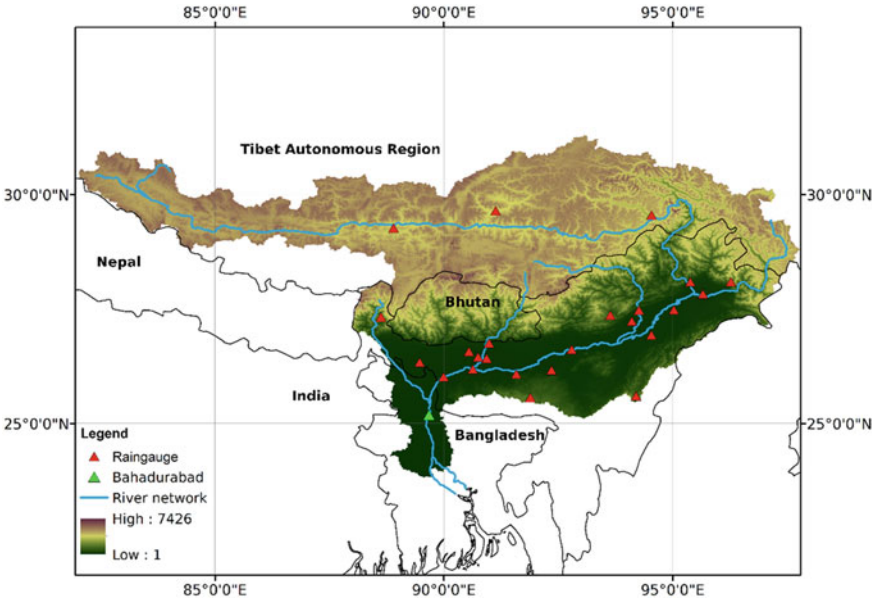

Fig. 9.1 A location map showing the Brahmaputra basin with its outlet at Bahadurabad

plus grassland constitute to 58% of the basin area. The rest of the land use consists of agriculture (14%), cropland (12.6%), barren land (2.5%), water bodies (1.8%) and settlements (0.02%).

Brahmaputra River, as it enters Bangladesh, has a gauging station Bahadurabad, which is considered as the outlet of the basin in this study partly to keep the focus on the hydrological characteristics of the Assam region in India and partly due to the data availability at the gauging station. The peak discharge in Bahadurabad is 102534 m^3/s, whereas the average and minimum discharge is about 22,000 m^3/s and 3280 m^3/s, respectively. The Assam valley of the basin experiences frequent flooding (Sharma and Paithankar 2014; Mahanta et al. 2014). The basin is sparsely gauged and has only a limited number of rainfall stations. Moreover, the basin has also data sharing issues as the collected data is not easily accessible to the wider audience. Due to these reasons, the basin has not been studied well with the help of simulation models. Such studies, for example, involving rainfall–runoff modelling can be used in studying hydrological extremes, seasonality and so on, and the generated knowledge can be used in planning, socio-economic development and decision support. Water allocation modelling can be particularly useful in prioritizing water demands and in planning intervention works. For transboundary rivers, this is particularly important as the lack of quantitative assessment based on simulation studies inhibits fruitful dialogues (Mahanta 2006; Christopher 2013).

In a previous study using lumped conceptual rainfall–runoff modelling of the basin employing tools NAM and MIKE11, Mahanta et al. (2014) concluded that the lack of adequate data was a limitation. Futter and Whitehead (2015) carried out another study of the Ganges and Brahmaputra basin using a semi-distributed rainfall–runoff model using the tool PERSiST. The accuracy of the model was not high. This study was based primarily on gauge data. Schneider et al. (2017) carried out rainfall–runoff modelling of the Brahmaputra basin. Satellite altimetry data was used in updating river cross sections extracted from digital elevation data. All these studies complemented remote sensing data with gauge data. As gauge data is very limited, particularly for the spatial scale of the basin, exploring the possibility of hydrological and hydraulic modelling primarily with remote sensing products is important.

Table 9.1 shows the gauge data that is used in this study. The daily rainfall data was collected from 24 gauging stations (Table 9.1, Fig. 9.1) for 2013 and 2014. Daily discharge data, estimated from a rating curve based on the measured stage, was available from 2000 to 2015 only at the gauging station at Bahadurabad.

Table 9.1 Gauge data of Brahmaputra basin used in this research

Data	Availability	Spatial resolution
Gauge rainfall	2013–2014, daily	24 stations
Discharge data	January 2000–December 2015, daily	Bahadurabad Station

9.3 Global Datasets

Global datasets are increasingly used in modelling ungauged/sparsely gauged catchments. Challenges exist in working with this data as imprecision may lead to uncertainty. Table 9.2 presents the list of global datasets used in this paper.

9.3.1 Digital Elevation Data

Among global datasets, the digital elevation data from the Shuttle Radar Topographic Mission (SRTM) or Advanced Spaceborne Thermal Emission and Reflection Radiometer (ASTER) is well known. This data is used in creating a digital elevation model (DEM) with identified river networks along with their geometrical properties (slope, length, width, depth, etc.) to facilitate the physical representation of a catchment in a model. There are numerous other proprietary datasets, usually of finer resolutions, often with national governments and mostly inaccessible to the wider audience. As a result, SRTM and ASTER are most widely used in creating DEMs of sparsely gauged large catchments. Both datasets have low spatial resolutions (originally 3 arc-seconds, since 2014 with 1 arc-second). The coarse resolution restricts usage of this data primarily to catchments with large rivers with wide floodplains. These datasets are not suitable for small rivers and torrents, particularly in hilly regions. The vertical accuracy of SRTM and ASTER datasets is not high (Rodríguez et al. 2005). The DEM created with these datasets may have errors, and it is necessary to cross-check at least the identified river network with Google Earth, national stream/river database and where possible with field visits.

Table 9.2 Global datasets used in this study

Data type and product	Provider	Data period	Resolution
DEM: SRTM	NASA, JAXA	2000	3 arc-seconds
Water level: Jason-2 altimetry data	NASA	2012–2015	Every 10 days at specific locations, Barpeta for the current study
Land use: GlobCover	European Space Agency	2009	300 m × 300 m
Soil: Harmonised World Soil Database (HWSD)	FAO	2008	1 km × 1 km
Lithology: Global Lithological Map (GLIM, V 1.0)	Hartmann and Moosdorf (2012), PANGAEA	2012	$0.5^{\circ} \times 0.5^{\circ}$
Rainfall: TMPA 3B42 V7	NASA	1998–2015	Daily, $0.25^{\circ} \times 0.25^{\circ}$
Evapotranspiration	FAO	2000–2015	Monthly, 5 km × 5km
Temperature	ERA-Interim	2000–2012	Daily, $0.25^{\circ} \times 0.25^{\circ}$
Temperature	NASA	2002–2015	Daily, $0.25^{\circ} \times 0.25^{\circ}$

9.3.2 Rainfall Data

Rainfall information is vital in flood modelling, mapping and monitoring. In sparsely gauged catchments, availability of rainfall data from gauges and weather radar is limited and modelling largely needs to depend upon SPPs. SPPs are estimated by applying retrieval algorithms to measurements obtained through satellite-borne microwave instruments. Other than the TRMM rainfall mentioned above, Precipitation Estimation from Remotely Sensed Information using Artificial Neural Networks-Climate Data Record (PERSIANN-CDR) (Ashouri et al. 2015) and Climate Prediction Centre MORPHing Technique (CMORPH) (Joyce et al. 2004) are well-known SPPs. Multi Source Weighted Ensemble Precipitation (MSWEP) is a recently prepared dataset by merging diverse SPPs and gauge rainfall (Beck et al. 2017). The merging is done in four stages to get a dataset with accuracy higher than each of the individual products used in merging. It is noteworthy that SPPs are not available at real time and have latency, which varies with products. As a result, real-time computation involving SPPs has limitations.

9.3.3 Other Data

For the representation of the catchment in the model, soil data from the Harmonised World Soil Database (HWSD) from FAO is a popular source. Land use and land cover data GlobCover and CORINE from the European Space Agency and AfriCover from FAO are widely used in hydrological studies. Global Lithological Map (GLIM, Version 1.0) (Hartmann and Moosdorf 2012) is a good source of global lithological data needed to estimate, for example, infiltration and percolation rates. Among other meteorological data monthly average evapotranspiration data from FAO, NASA's EarthData Center and ERA-Interim (from European Centre for Medium Range Weather Forecast), temperature data from NASA's EarthData Center and ERA-Interim is used in flood modelling and mapping of sparsely gauged basins.

9.4 Methodology

In the following, four major methodological steps, namely (1) bias correction, (2) hydrological modelling, (3) hydraulic modelling and (4) uncertainty assessment, are described.

9.4.1 Bias Correction

The remotely sensed information needs to be corrected with in situ data to get a more accurate estimation of the rainfall field. Such a correction, mostly applied to SPPs, is usually known as bias correction (Arias-Hidalgo et al. 2013) and is tricky. A gauge measures a rain field at a point and that measurement is usually used in inferring rainfall over a much larger area. Commonly, there is a higher spatial sampling error in estimation of areal rainfall using different interpolation techniques especially when the network of the gauges is sparse. This has been a major source of uncertainty in hydrological modelling, particularly for sparsely gauged catchments. On the other hand, SPPs are based on measurements of the atmospheric column and provide estimates based on a snapshot of a much larger area determined by the field of view (FOV) of the swath, which often is 240 km (Li and Shao 2010). Hence, it has a better spatial resolution compared to gauges. On the other hand, gauge measurements are continuous. When comparing SPPs with gauges, differences may also be due to differences in measurement techniques, in particular due to continuous measurement at a point to snapshot measurement over a larger area, vis-à-vis the spatial and temporal variability of rainfall at a given location and time. Errors in SPPs decrease with larger spatial and temporal sampling scales (Bell and Kundu 2003). Bias correction therefore leads only to a better approximation and cannot systematically remove all errors. This aspect is at the core of hydrological and hydraulic modelling of sparsely gauged catchments as in such studies limited gauge rainfall is often supplemented with SPPs, usually corrected for bias with limited data and occasionally merged (Mastrantonas et al. 2019) with different data products.

Bias correction methods are statistical in nature, and their usefulness depends, among other things, on the length of gauge data as well as of SPPs. The usefulness also depends upon the variability of rainfall captured in gauges and SPPs, and the spatial and temporal resolution of data collection. One of the popular and easily applicable bias correction methods is known as ratio bias correction (RBC) (Eq. 9.1) (Arias-Hidalgo et al. 2013). This approach can be applied also when there is limited data. The correction method can be applied to compute, for example, bias correction factors for every month. If data length is too short, then RBC may also be applied to compute seasonal bias correction factors.

$$C_{RBC} = \frac{\sum_{i=1}^{N} R_{g,i}}{\sum_{i=1}^{N} R_{s,i}} \tag{9.1}$$

where the correction factor C_{RBC} is computed for a time period with N observations (in a month or season), $R_{g,i}$ and $R_{s,i}$, respectively, stand for gauge rainfall and SPP at time moment i and $i = 1,2,3,\ldots, N$.

The computed bias correction factors, for example, monthly correction factors, can be subsequently used in correcting SPPs (Eq. 9.2).

$$R_{s,i\text{Corrected}} = C_{RBC} * R_{s,i} \tag{9.2}$$

where $R_{s,i\text{Corrected}}$ is the corrected SPP at time step i.

Owing to the climatic variability, such correction factors may rather be approximation if gauge data used in correction is limited. Note that the usefulness of this approach also depends upon the spatial variability (e.g. due to the terrain such as in mountainous regions) and temporal variability of rainfall. The density of gauges and if any interpolation technique has been employed in computing mean areal rainfall also influences the accuracy of bias correction. Moreover, correction to rainfall of small duration events is more problematic as the correction works better for seasons than for hours.

When longer time series of gauge rainfall and SPPs are available, then probabilistic methods are better suited. Quantile mapping works on computing the probability of any value of a SPP in the SPP data sample, finding the gauge rainfall with the corresponding probability within the gauge rainfall data sample and assigning the found gauge rainfall value as the bias corrected value of the SPP (Mastrantonas et al. 2019).

Using a Python script, the daily TRMM data (3B42 V7) at a spatial resolution of $0.25^{\circ} \times 0.25^{\circ}$ was downloaded for the Brahmaputra basin for the entire study period (1 January 2000 to 26 December 2015). The RBC method was used in correcting the TRMM data. The available gauge rainfall data from 24 gauging stations (Fig. 9.1) for the year 2013 was used in computing monthly bias correction factors for the sub-catchments which had a gauge inside it. The approach was validated by comparing the corrected TRMM data with gauge rainfall for the year 2014. Subsequently, the TRMM rainfall data of the entire study period was corrected using the obtained monthly correction factors. TRMM rainfall of the sub-catchments which did not have any gauging station inside was not corrected. The bias correction was indeed limited due to the limited availability of gauge data, and more data should be considered in future for improved bias correction.

9.4.2 Hydrological Modelling

Hydrological modelling of sparsely gauged catchments usually involves lumped conceptual modelling as distributed physically based modelling requires a lot of catchment measurements, which for most catchments are not available. Black box (such as machine learning-based models) or empirical models (such as rational method-based models) can also be built, but their usefulness in catchment studies or in flood forecasting is rather limited.

For the Brahmaputra basin, the DEM was created using SRTM data with 3 arc-seconds resolution in a GIS environment and the catchment was delineated by choosing Bahadurabad as the outlet of the basin (Fig. 9.1). In total, 39 sub-catchments were identified.

In lumped conceptual hydrological modelling, each sub-catchment may be represented as a lumped model. By having several sub-catchments, the model can be treated as a semi-distributed hydrological model. Such a model does not require measured parameter values as parameters are conceptual and cannot be measured in the field. As a result, calibration of these models with measured data is mandatory as otherwise the parameter values cannot be trusted.

In lumped conceptual hydrological modelling of sparsely gauged catchments, the rainfall–runoff process is typically simulated by employing loss, direct runoff and baseflow modelling. In loss modelling the amount of rainfall that is stored in canopy and depressions, and the amount that infiltrates and later is used in evaporation, plant roots and percolation to groundwater is estimated. Typically, separate linear reservoirs for each category of storage are considered, and loss from storages and translation of water are estimated using catchment-specific parameters such as infiltration capacity, percolation rates, storage capacity in vegetation and depressions. Soil Moisture Accounting (SMA) (Bennett and Peters 2000) is a very well-known method to simulate precipitation loss. For short-term forecasting, however, precipitation loss is estimated, for example, by the curve number method, by ignoring changes in soil moisture during the simulation time (Ghadua and Bhattacharya 2019).

For the Brahmaputra basin, the hydrological model was developed using the HEC-HMS tool from the Hydrologic Engineering Center (https://www.hec.usace.army.mil/software/hec-hms/). Precipitation loss was modelled using SMA with the linear reservoirs for canopy, surface storage, soil storage and groundwater (two reservoirs, one for the shallow and the other for the deep groundwater). In the absence of detailed data, the canopy loss was modelled using the simple canopy method with zero storage as the initial condition and with maximum storage capacity as 1 mm in the upper catchments with sparse vegetation, which was gradually increased to 5 mm in the downstream catchments with much higher vegetation. Precipitation loss in the storage was modelled using the simple storage method with zero storage as the initial condition and with the maximum storage varying with topography between 7 and 9 mm. Following Bell et al. (1986) and using the soil data of different sub-catchments from the Harmonised World Soil Database (V1.2) (Hartmann and Moosdorf 2012), the infiltration capacity was estimated between 5.1 and 20.3 mm/hr (one value for one sub-catchment). Similarly, the percolation rates were considered as 0.3 to 1.2 mm/hr and 0.04 to 0.25 mm/hr to the shallow groundwater and deep groundwater, respectively. Groundwater coefficients and indicators of time needed of a water particle from the point of reaching groundwater to the point of returning as baseflow were estimated as 80 to 120 h and 200 to 400 h for the shallow groundwater and deep groundwater, respectively.

The precipitation excess is converted to direct runoff hydrograph ordinates using a chosen unit hydrograph and by calculating properties of the catchment such as time of concentration and other geometrical properties. Snyder Unit Hydrograph, Clark Unit Hydrograph (CUH) and Modified Clark Unit Hydrograph are well-known methods for estimating direct runoff from excess rainfall. For the Brahmaputra basin, the CUH was used. The time of concentration varied between 56 and 128 h. In the baseflow modelling, the flow per unit area was used as the initial condition in the linear

reservoir method and the baseflow coefficient from sub-catchment to sub-catchment was between 8 and 15 h.

The model was simulated using the corrected TRMM data (Eq. 9.2). Additionally, precipitation input from snow melt in the Himalayan sub-catchments during the spring months was modelled using the temperature index method using the temperature data listed in Table 9.2. The monthly average evaporation data (Table 9.2) was used, and it varied from sub-catchment to sub-catchment from 80 to 120 mm, 30 to 50 mm and 60 to 80 mm, respectively, during the summer, winter and spring months.

Calibration of any lumped conceptual hydrological model is a major issue, it requires the availability of measured data, and most commonly discharged time series at the catchment outlet is used for this purpose. These models require a long warming-up time, also to balance the effect of imprecise initial condition, thereby requiring the availability of measured data for several years to calibrate a model. For the Brahmaputra basin, the daily discharge data was estimated using measured stage values and an existing rating curve at the catchment outlet at Bahadurabad. This discharge data was used in the calibration. Based on the availability of data, the calibration and validation periods were chosen as 1 January 2005 to 29 April 2013 and 1 January 2000 to 31 December 2004, respectively. The simulation time step was one day.

9.4.3 Hydraulic Modelling

In a sparsely gauged basin, a hydraulic model may use the simulated discharge from the hydrological model of the catchment as upstream and lateral input to simulate flow in a river. Hydraulic models use Saint–Venant equations (continuity and momentum) to compute water level and flow velocity at every (grid) location of the modelled domain. These models are capable of producing flood inundation maps, which are useful in flood management as they present flood extent, depth and velocities. Although a model can be 1D, 2D or 1D2D, in a sparsely gauged catchments DEMs are often not very accurate and modelling may have to be restricted to 1D only. In this study, we used the hydraulic model HEC-RAS to simulate river flow and flood propagation within the floodplains.

The required geometry data for the representation of the physical domain in the model includes river cross sections, bed slopes, flood plain widths and elevations. This data is mostly proprietary with limited access to the wider audience. On the other hand, most rivers and floodplains do not change frequently and any previously available geometry dataset may serve the purpose as well. In the absence of hydrographic and land surveys in sparsely gauged catchments, the required geometry data may be extracted from elevation data from SRTM, ASTER and similar publicly available datasets.

The Assam region of the Brahmaputra basin suffers from frequent flooding (Mahanta et al. 2014; Sharma and Paithankar 2014) and was chosen as the domain of the hydraulic model (Fig. 9.2) leaving out the vast upstream area, which is

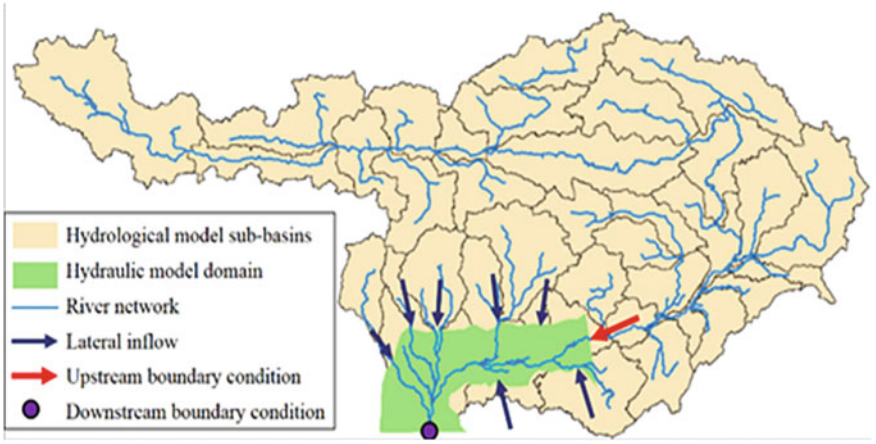

Fig. 9.2 Schematic diagram showing the layout of the hydraulic model of a part of the Brahmaputra River

not frequently flooded and is not much populated. The length of the modelled river was 500 km. The downstream boundary was chosen at the gauging station Bahadurabad, mainly due to the availability of the measured discharge data. The geometry data of the modelled river and floodplain region was extracted from SRTM data (3 arc-seconds resolution, Table 9.2) in the ARC-GIS environment along with the HEC-GeoRAS plug-in (V10.2, https://www.hec.usace.army.mil/software/hec-georas/). The procedure outlined by Domeneghetti (2016) and Gichamo et al. (2012) was followed. The river centreline, bank lines and cross sections (every 500 m) were digitized. The extent of the floodplain was considered far enough and to the higher grounds so that the entire flood extent could be modelled. The processed geometry data was imported from the GIS environment to the hydraulic modelling tool HEC-RAS (Version 5, https://www.hec.usace.army.mil/software/hec-ras/). If a couple of measured cross sections are available, then the imported geometry data, particularly the cross-sectional data, may be validated and, where required, corrected. However, for the Brahmaputra basin we did not have any measured cross sections and we could not make any corrections. Only the channel width was compared to the width estimated from Google Earth.

The upstream boundary of the model was the simulated inflow from the hydrological model (Fig. 9.2). In addition, the flow in the tributaries was used as lateral flows to the hydraulic model. The downstream boundary at Bahadurabad was chosen as the normal depth. The simulated results from the hydrological model were stored in the database HEC-DSSVue (https://www.hec.usace.army.mil/software/hec-dssvue/), which was later automatically read by the hydraulic model. The calibration and validation periods for the model were, respectively, 1 January 2013 to 31 December 2013 and 1 January 2015 to 26 December 2015. During the calibration, the model was simulated with Manning's roughness coefficient for the main channel as 0.03, 0.02 and 0.015, and by comparing the simulated water level with the measured water level

at Bahadurabad the roughness coefficient's value was chosen to be 0.02. Similarly, the roughness coefficient's value for the floodplain was determined to be 0.025, which was determined by considering corresponding values as 0.035, 0.025 and 0.02. In the absence of more elaborate data, the calibration remained limited to considering only a number of possible values of the roughness coefficient.

The hydraulic model was validated using water level estimated from Jason-2 radar altimetry data (https://www.theia-land.fr/). In a previous study, Papa et al. (2012) used Jason-2 data in estimating the river discharge in Ganges–Brahmaputra–Meghna basin. Jason-2 satellite has an observation point (virtual) in the Brahmaputra basin (near Barpeta) from which water level is available once every 10 days. This data was used in validating the hydraulic model.

The simulated inundation maps for two flood events on 29 June 2012 and 23 September 2012 were compared with the satellite imageries of the flood events from Dartmouth Flood Observatory of the Colorado University. The forecast accuracy was estimated using the standard contingency table (Table 9.3) with hits, misses, false alarms and positive rejections, which are defined below:

Hit: When both the simulated map and the satellite image show a pixel to be wet.

Missed: When the simulated map shows a pixel to be dry, whereas the satellite image shows it wet.

False alarm: When the simulated map shows a pixel to be wet, whereas the satellite image shows it to be dry.

Positive rejection: When both the simulated map and the satellite image show a pixel to be dry.

The accuracy of the simulated flood maps is also evaluated using the: (i) probability of detection (POD, showing the flood fraction of the observed events that is correctly simulated); (ii) false alarm ratio (FAR, showing the dry fraction of the flood event that is incorrectly simulated as flooded); and (iii) critical success index (CSI, indicating the goodness of fit between the simulated and observed flood).

$$\mathrm{POD} = \frac{B}{B+C}; \quad \mathrm{FAR} = \frac{A}{A+B}; \quad \mathrm{CSI} = \frac{B}{A+B+C} \tag{9.3}$$

where A is the number of total false alarms, B is the number of total hits and C is the number of total missed alarms. Optimal results of POD and CSI are found when equal to one, while the opposite is valid for FAR.

Table 9.3 Contingency table for accuracy of flood inundation mapping

Simulated	Observed	
	Wet	*Dry*
Wet	Hit	False alarm
Dry	Missed	Positive rejection

9.4.4 Uncertainty Assessment

All hydrological and hydraulic models bear uncertainty, which is likely to be much higher in sparsely gauged catchments. Uncertainty may originate from inputs, model parameters, modelling formulations and calibration data. For the Brahmaputra basin, the hydrological model was calibrated using the discharge data at the outlet, which was estimated from a rating curve. Rating curves can be imprecise and lead to uncertain model parameters. In this research, we investigated the uncertainty in hydrological model due to the use of imprecise rating curves as boundary data and its consequent influence on the simulated flood inundation map.

Errors in rating curve can exist for a number of reasons. One common possibility is due to errors in velocity measurements, which influences the discharge computation. This particularly happens during high velocities. Moreover, rising flood waves due to additional friction result in lower stages than falling waves. As a result, the same discharge results in a lower stage during rising water level than during falling water level, which is known as the hysteresis effect (Bhattacharya and Solomatine 2005). Rating curves also may be influenced by backwater effect. Here, an error in a rating curve has been considered as the difference between the measured discharge and rated discharge, which originate due to the combination of all sources of errors.

A rating curve in a natural river is usually expressed as follows:

$$Q_r = \alpha(h - h_0)^{\beta} \tag{9.4}$$

where Q_r is the rated discharge (m^3/s), h is the stage (m), *h0* is the likely minimum stage at the location and can be found from measured stage values over a long period of time, and α and β are regression coefficients determined from a sample of pairwise measured data of stage and discharge (usually by employing the least square method).

The rating curve used at the gauging station Bahadurabad has the following three segments. The first one (Eq. 9.5) applies to high flows, whereas the second one (Eq. 9.6) applies to medium flows and the third one (Eq. 9.7) is applicable to comparatively low flows (dry period flows).

$$h > 17.86 \text{ m}: \quad Q_r = \alpha_1(h - h_{01})^{\beta_1} \tag{9.5}$$

$$14.66 \text{ m} > h < 17.86 \text{ m}: \quad Q_r = \alpha_2(h - h_{02})^{\beta_2} \tag{9.6}$$

$$h < 14.66 \text{ m}: \quad Q_r = \alpha_3(h - h_{03})^{\beta_3} \tag{9.7}$$

where h_{01}, h_{02}*and* h_{03} stand for the minimum stages for high, medium and low flows; α_1 and β_1, α_2 and β_2 and α_3 and β_3 are the regression coefficients for the high, medium and low flows.

As explained above the error in the rated discharge, Q_e is defined as

$$Q_e = Q_m - Q_r \tag{9.8}$$

where Q_m is the measured discharge.

Considering Q_e to follow a normal distribution with μ and σ as the mean and standard deviation, the upper and lower limits of the rated discharge can be computed as shown below:

$$Q_{r,\text{Upper}} = Q_r + \mu + 3\sigma \tag{9.9}$$

$$Q_{r,\text{Lower}} = Q_r + \mu - 3\sigma \tag{9.10}$$

$Q_{r,\text{ Upper}}$ and $Q_{r,\text{ Lower}}$ present the upper and lower limits of the rated discharge for a given value of stage (h) within which the rated discharge will fall with a 99% likelihood. A Monte Carlo approach was followed in sampling the rating curves. The parameters α_1 and β_1, α_2 and β_2 and α_3 and β_3 were sampled 500 times with equal probability to produce 500 rating curves. The rating curves, due to varying values of the parameters, did not always have Q_r within the limits of $Q_{r,\text{ Upper}}$ and $Q_{r,\text{ Lower}}$. Out of these 500 rating curves, fifty rating curves were chosen (Fig. 9.3) which had the rated discharge Q_r within the limits of $Q_{r,\text{ Upper}}$ and $Q_{r,\text{ Lower}}$ for all possible values of h.

The hydrological model described above was re-calibrated 50 times with the sampled rating curves, thereby ending up with 50 hydrological models. All the models were simulated to produce an ensemble of fifty discharge hydrographs. The hydraulic model was also simulated fifty times with the simulated ensemble discharge hydrographs. Flood depths were assumed to follow normal distribution, and from

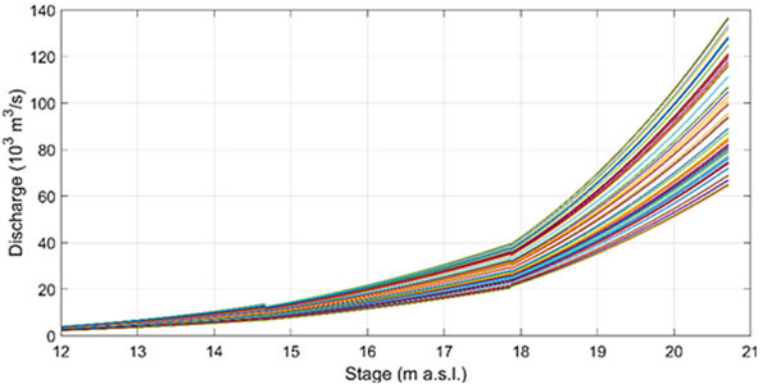

Fig. 9.3 Ensemble of fifty sampled rating curves generated with Monte Carlo simulation and used subsequently in calibrating fifty hydrological models

the simulated flood depths $D_{x,y}$ (at location x,y) the mean flood depth ($\mu_{d,x,y}$) and its standard deviation ($\sigma_{d,x,y}$) were computed. Upper ($D_{x,y,\text{ Upper}}$) and lower ($D_{x,y,\text{ Lower}}$) limits of flood depths along with the mean flood depth were defined as:

$$D_{x,y,\text{Upper}} = D_{x,y} + \mu_{d,x,y} + 3\sigma_{d,x,y} \tag{9.11}$$

$$D_{x,y,\text{Mean}} = D_{x,y} + \mu_{d,x,y} \tag{9.12}$$

$$D_{x,y,\text{Lower}} = Q_{x,y} + \mu_{d,x,y} - 3\sigma_{d,x,y} \tag{9.13}$$

9.5 Results and Discussion

9.5.1 Bias Correction

Using the gauge rainfall data of 2013 and Eq. (9.1), the monthly bias correction factors were computed, which were applied, using Eq. (9.2), to correct the daily TRMM rainfall estimates of 2014. Figure 9.4 presents the annual average TRMM rainfall estimates varying over sub-catchments. The sub-catchments in the Himalayan Slopes, which receive high rainfall (annual average >2200 mm), had the largest correction factors (1.1 to 2.1). Arias-Hidalgo et al. (2013) experienced a similar correction in

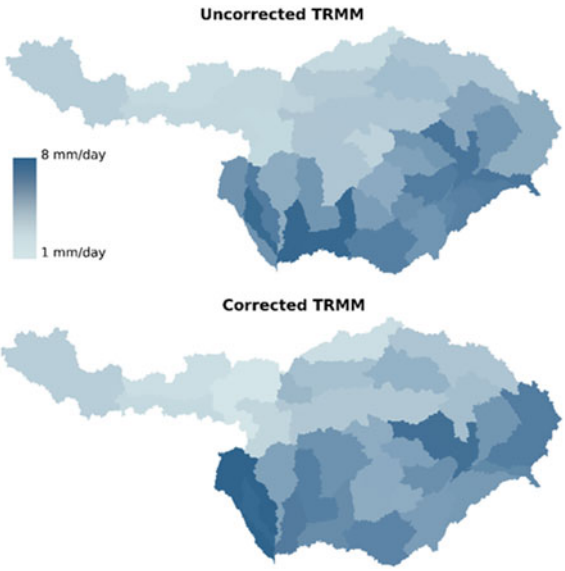

Fig. 9.4 Annual average TRMM rainfall estimates in 2014 in different sub-catchments of the hydrological model of Brahmaputra

the mountainous sub-catchments in the Vinces basin in Ecuador and reported that TRMM underestimates intense rainfall. The sub-catchments, which receive less rainfall, had correction factors less than one (0.91 to 0.58). The corrections applied were approximate as only one year of gauge data was used in determining the RBC correction factors. Owing to climatic variability, these correction factors should ideally be computed based on a much longer time series.

The computed RBC correction factors were further utilized in correcting the daily TRMM rainfall estimates from 2000 to 2015, and the corrected TRMM rainfall estimates were used in the modelling.

9.5.2 Hydrological Modelling

This section presents the results of the hydrological model HEC-HMS when forced with corrected TRMM data. The results show a good agreement between model performance and observed flow value at the gauging station Bahadurabad. As expected, calibration performances outperform the validation one, resulting in a higher Pearson correlation coefficient R^2 as can be seen in Fig. 9.5 and Table 9.4. In particular, R^2 values of 0.9 and 0.88 were obtained, respectively, during the calibration and validation. Such high correlation values justified the use of bias correction for the uncorrected TRMM data. The corresponding RMSE was 9630 and 11,938 m^3/s (Table 9.4). From Fig. 9.5, it can be seen that compared to the calibration phase the hydrological model has slightly higher tendency to overestimate the observed flow during the validation phase.

In order to investigate the hydrological modelling results further, we divided the study period into wet, dry and lean seasons. In this study, we considered that the wet season is between 1 June and 31 October, the dry season is between 1 November and 28 February, while the lean season is between 1 March and 31 May. From the calibration results, it may be observed that the river flow was better simulated during the wet season than during the dry season. For the calibration period, R^2 values were 0.8, 0.54 and 0.84 for the wet, dry and lean periods, respectively. For the validation period, R^2 values were 0.75, 0.47 and 0.89 for the wet, dry and lean periods, respectively.

During further analysis of the results for each season, we observed systematic model behaviour. The hydrological model showed a tendency to overestimate river flows during the wet and lean seasons, while it underestimated the observed flow during the dry season. This can be due to limitations in model calibration. In similar studies, Arias-Hidalgo et al. (2013), Yoshimoto and Amarnath (2017) and Mazzoleni et al. (2019) reported a comparable fit between the observed and simulated flows with TRMM rainfall estimates. These results justify the use of global rainfall datasets for hydrological simulations in data-scarce basins.

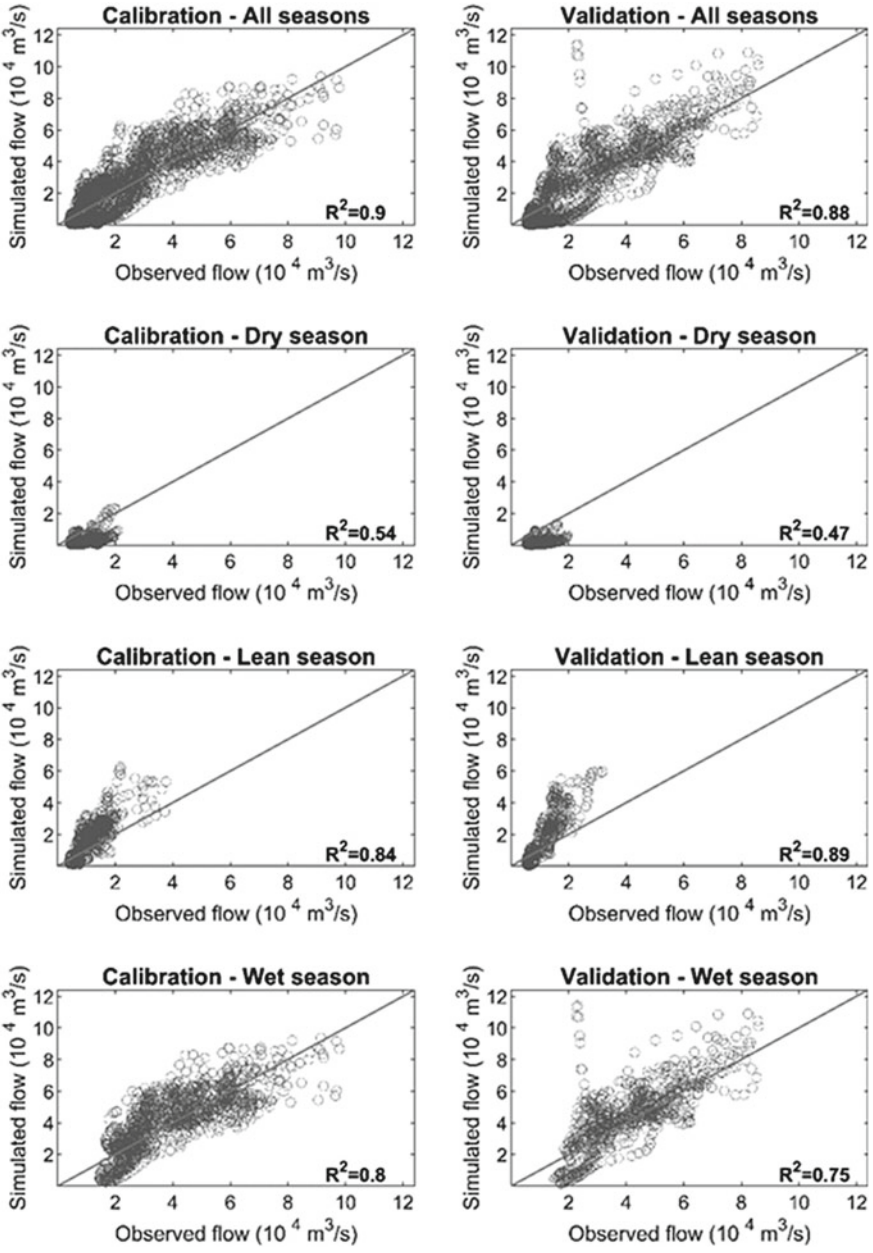

Fig. 9.5 Scatter plots of measured and simulated discharge at Bahadurabad for the model calibration (left column) and validation (right column) for the entire calibration and validation period (first row), dry season (second row), lean season (third row) and the wet season (fourth row)

Table 9.4 Accuracy indices of the hydrological model

	Calibration		Validation	
	R2	RMSE (m^3/s)	R2	RMSE (m^3/s)
All seasons	0.90	9630	0.88	11,938
Dry	0.54	7162	0.47	7756
Lean	0.84	9126	0.89	12,423
Wet	0.80	11,545	0.75	14,151

9.5.3 Hydraulic Modelling

Simulated outflow from the hydrological model was used as input to the hydraulic model based on HEC-RAS, as both upstream boundary condition and lateral inflow along the main river channel. The calibration of the hydraulic model was performed by comparing the observed and simulated river flow at Bahadurabad for the period 1 January 2013 to 31 December 2013. The model was validated for the period 1 January 2015 to 26 December 2015 using water levels estimated from Jason-2 radar altimetry data at the location Barpeta (Fig. 9.6). It may be noticed that observed and simulated water levels have different time steps; the simulated water level was available at a daily time step, while the water level estimated from Jason-2 was available once every 10 days. Overall, a reasonably good agreement between the pattern of simulated and observed water level was found. However, we can see that starting from the beginning of the wet season the model underestimated water levels. Nonetheless, the results were encouraging as they further proved the usefulness of global datasets for hydrological and hydraulic modelling in sparsely gauged basins.

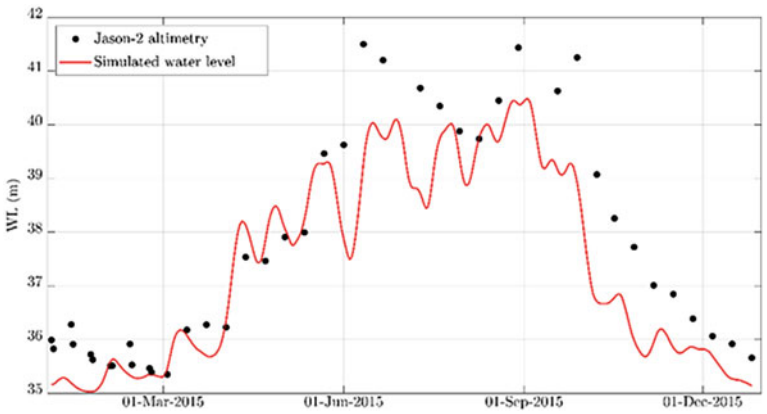

Fig. 9.6 Comparison of simulated water level with water levels estimated from Jason-2 satellite at Barpeta (validation period)

Flood extent maps were generated for two flood events occurred on 29 June 2012 and 23 September 2012. The maximum water surface profiles from the hydraulic model were converted into spatial dataset to extrapolate flood extent. The simulated flood maps were then compared with the satellite imageries of flooded areas from the Dartmouth Flood Observatory (2010). The comparison was carried out for every simulation grid. In particular, we estimated the values for positive rejection, false alarms, misses and hits (as previously described in Table 9.3) between the simulated flood maps and the satellite-based flood maps. The results obtained for the two flood events gave comparable results. Figure 9.7 shows a hit rate of 51% and 47% for the June and September flood event, respectively, followed by a considerable number of false alarm areas. However, it may be observed that for the June flood event false alarms were observed more in areas in the downstream part of the reach, while in the September event more missed alarms were noticed along the entire river reach.

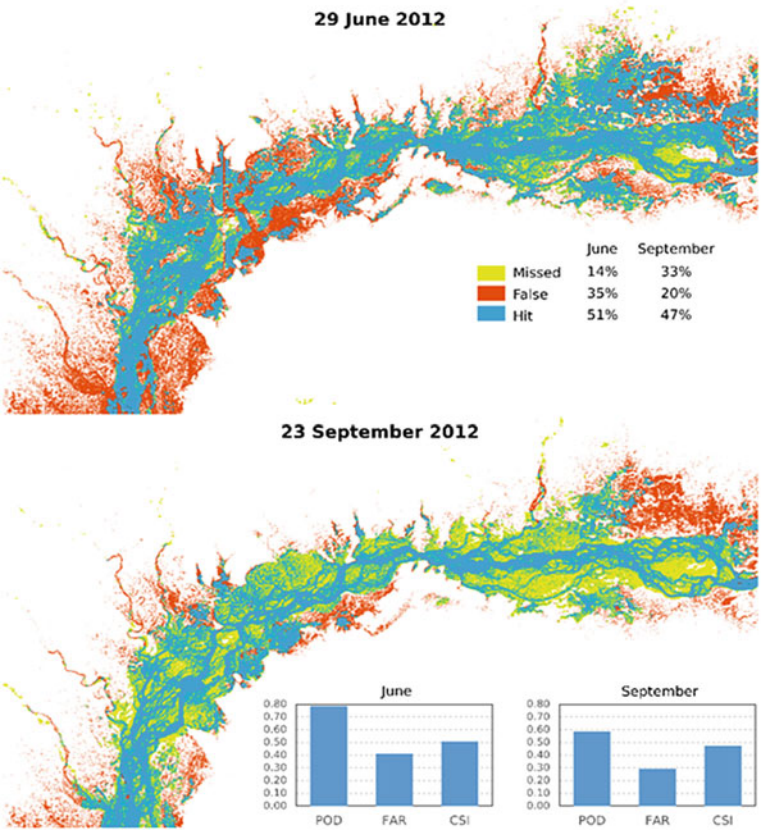

Fig. 9.7 Contingency maps and accuracy indices of simulated inundation map as compared to the satellite observed flood map for the two flood events (29 June 2012 and 23 September 2012)

Results were encouraging considering the simplified hydraulic modelling framework and the scarcity of data to calibrate the model.

Comparing the model accuracy indices POD, FAR and CSI, it may be observed that comparable results were obtained for the two flood events. However, model performance was slightly better for the June event than for the September event. In particular, we found good model performance and high value of POD; i.e. a large number of grid cells were observed to be flooded in the satellite imagery which were also simulated as flooded. Moreover, the model's prediction skills are represented by the reasonably high CSI values obtained for both flood events.

9.5.4 Uncertainty Assessment

Uncertainty in the rating curve used for hydrological model calibration can significantly affect model performance during validation. The hydrological model was calibrated fifty times using fifty sampled rating curves as the boundary condition for the period of 1 January 2005 to 29 April 2013. The outcome was fifty sets of optimized model parameters for fifty models. These fifty models were simulated for the validation period 1 January 2000 to 31 December 2004. Figure 9.8 presents the simulated discharge at Bahadurabad for the validation period of the hydrological model. The ensemble of simulated flows provides an indication of the uncertainty in the simulated discharge. In addition, we have included the deterministic results, as reported in the previous section, obtained without considering the uncertainty induced due to the rating curve.

In general, it can be seen that the pattern of the simulated discharge, with and without uncertainty assessment, matches the measured discharge quite well. As previously described, hydrological model with or without uncertainty assessment

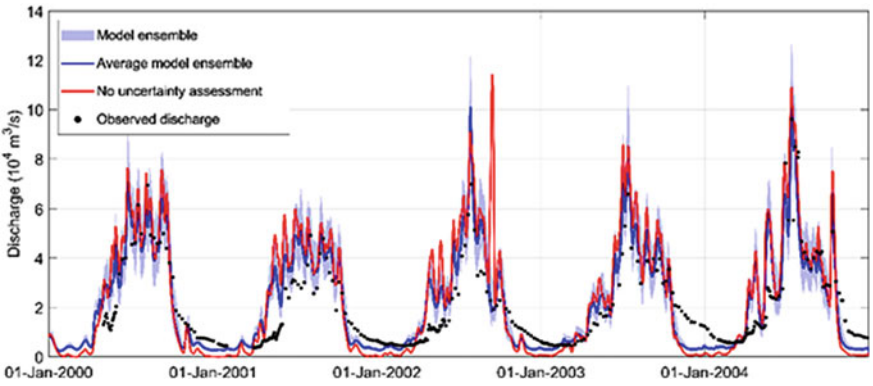

Fig. 9.8 Observed and simulated discharge (with and without uncertainty assessment due to the rating curve used for calibration) from the hydrological model at Bahadurabad for the validation period (2000–2004)

tends to systematically underestimate observed flow during dry seasons while overestimate flows during lean and wet seasons. Moreover, simulated flows with uncertainty assessment mostly showed lower peak values than the deterministic results. Figure 9.8 shows uncertainty, represented by the spread of the ensemble, for peak discharge values. This can be due to the high deviation of the measured discharge from the rating curve during peak discharges, and as a result the fifty rating curves sampled showed large variations in the discharge during the times the flow was high. It is also discernible that during the rising flood the simulated flow was overestimated, whereas during the falling flood it was underestimated.

The results of the hydraulic model are assessed for the year 2000 at Guwahati. Figure 9.9 presents the ensemble of simulated discharge at Guwahati, which is an internal location in the basin. It may be seen that during the falling limb the uncertainty of simulated discharge at Guwahati was low, while during the peak flows higher uncertainty is visible. Unfortunately, no observed flow was available at this location for comparison purposes.

Accuracy of flood inundation maps can be highly affected by different sources of uncertainty. In this study, we assessed uncertainty in flood depth and extent due to uncertainty in the rating curve. The resulting range of variability of water level is shown in Fig. 9.10. In particular, the lower and upper limits, corresponding to the 99th percentile of the simulated flood depths, are depicted. Larger flood extent and water-level values were found when simulating the June flood event. The difference between the upper and lower limits of flood depths at any location, when averaged over the modelled domain, was 1.04 m and 0.87 m for the June and September events, respectively. Such variations demonstrate that uncertainty in rating curve can significantly affect flood mapping and can significantly influence the identification of critical hotspots for emergency management and urban planning.

When comparing the contingency maps of Figs. 9.7 and 9.11, it can be noticed that higher missed alarms and lower false alarms were achieved for both June and September flood events for the simulation with uncertainty assessment. On the other

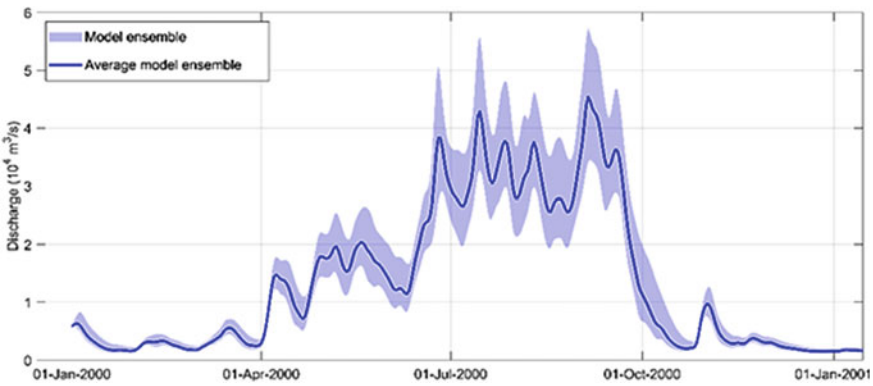

Fig. 9.9 Ensemble and average of simulated discharge with the hydraulic model at Guwahati

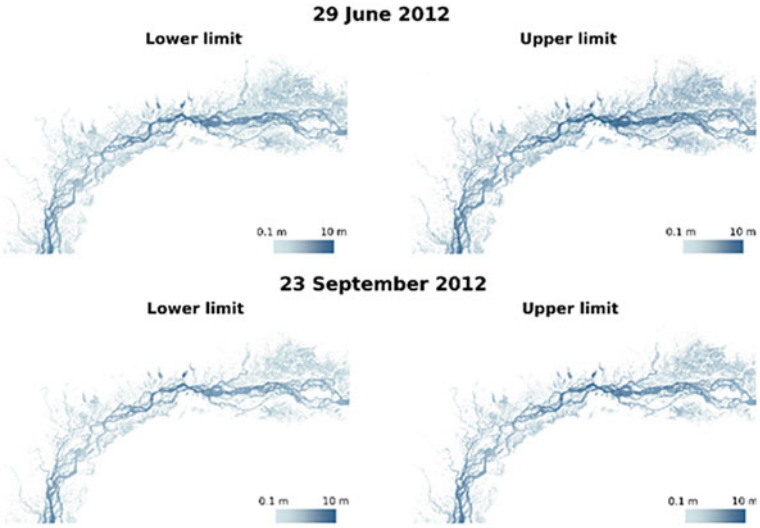

Fig. 9.10 Simulated flood depth maps for the lower and upper limit of the uncertainty estimation for the two flood events (29 June 2012 and 23 September 2012)

hand, similar hit values were noticed. Missed alarms showed an increase in the lower part of the river reach during both flood events. In a similar fashion, false alarm showed a decrease in the same area. The simulation considering the uncertainty due to the rating curve resulted in a smaller flood extent compared to the case without considering the uncertainty. This may be due to the lower flow values estimated with the hydrological model. Because of the lower false alarms and higher missed alarms, both POD and FAR values were lower for the June and September flood events. The CSI value obtained with the simulated results considering the uncertainty due to the rating curve was slightly better than the one without the influence of uncertainty in the rating curve, and it demonstrated the goodness of fit between the simulated and observed flooded areas. In particular, slightly higher hit areas and CSI index were found with simulation considering the uncertainty due to the rating curve for the June flood event.

9.6 Conclusions and Recommendations

Global datasets can provide useful information for hydrological and hydraulic modelling in large-scale data-scarce basins. In this study, we demonstrate the usefulness of remote sensing products for flood mapping of the sparsely gauged Brahmaputra basin. We demonstrated that using remote sensing information in a cascade of hydrological and hydraulic models can be helpful in flood modelling, mapping and monitoring.

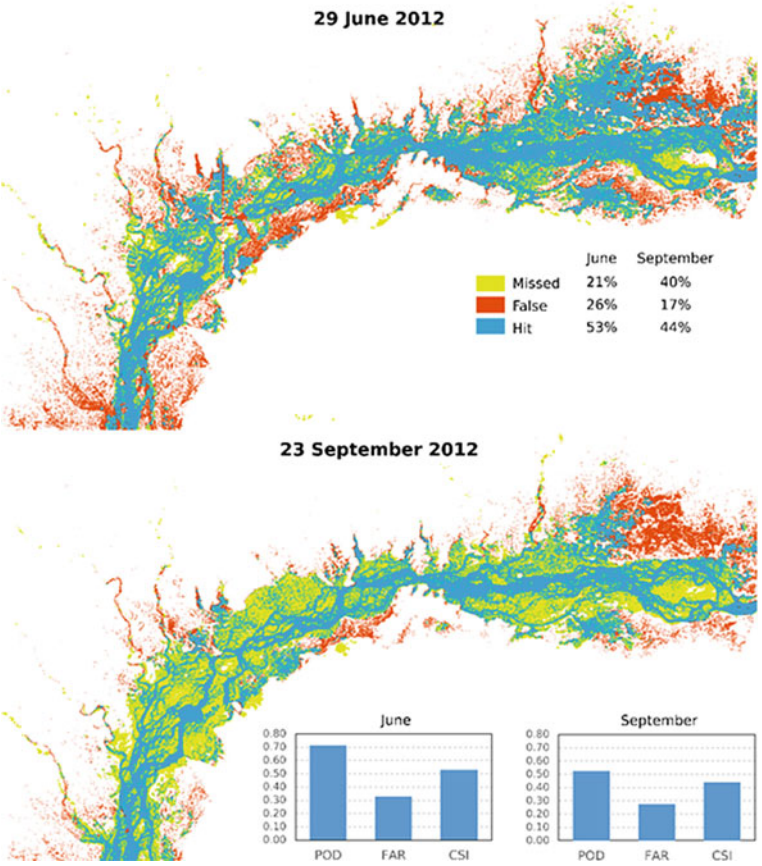

Fig. 9.11 Contingency maps and accuracy indices of simulated inundation map with mean flood depths (mean simulated flood depths considering the uncertainty due to uncertainty in the rating curve) as compared to the satellite observed flood map for the two flood events (29 June 2012 and 23 September 2012)

A coupled modelling framework made by a cascade of hydrological and hydraulic models was calibrated and validated with different remote sensing products providing hydrometeorological information of the basin. In particular, TRMM precipitation dataset, corrected for bias, was used as the main forcing of the hydrological model developed with HEC-HMS. The outputs of this model were then used as upstream and lateral boundary conditions for the hydraulic model developed with HEC-RAS. The hydraulic model was used to estimate water level along the main river channel and consequent flood extent in the floodplains. Calibration of the hydrological and hydraulic models was performed by comparing model results with the observed data at Bahadurabad Station. In particular, both deterministic and probabilistic approaches for the estimation of the rating curve at the Bahadurabad Station were used to calibrate the hydrological model to account (or not) for data uncertainty. Finally, simulated

flood extents were compared with satellite images for two different flood events to assess the ability of the model to predict flooded areas.

The results show that the hydrological model forced with the TRMM data correctly represents peaks and timing of the flood, while underestimation of flow was noticed during the dry season. The usefulness of using remote sensing data in hydraulic modelling was also demonstrated by the good agreement between simulated and satellite observed water levels along the Brahmaputra River. However, overestimation of flood extent was found mainly in shallow areas of the floodplains as possible flood protection structures are not properly represented in the low resolution of the DEM. Modelling results when including rating curve uncertainty show a smaller flood extent and a consequent higher missed alarms and lower false alarms for both flood events. However, similar hit values were found. This can be due to the lower flow values estimated with the hydrological model when considering uncertain rating curve from model calibration.

Similar to other research studies, our study also has its limitations. One of the main limitations is the scarcity of gauge rainfall to properly correct TRMM data. Moreover, calibration of the hydrological model was performed only at the outlet station at Bahadurabad due to lack of discharge data at any other location inside the basin. This causes an imprecise parametrization of the semi-distributed hydrological model within the basin, which in turn may affect the distributed representation of important hydrological variables, which are important for flood assessment, such as soil moisture. Moreover, as the SRTM was used as the main source of topographic information and bathymetric data was estimated from the imprecise SRTM data so more precise digital elevation data and geometry data should be included in future studies. The uncertainty was estimated only due to the uncertainty in the rating curve used in calibration. The influence of uncertainties in meteorological input and topographic data may also be ascertained. Finally, more complex hydrodynamic modelling approaches should be used to better represent flood propagation in shallow areas of the floodplains of the Brahmaputra River.

This study proved that global datasets of remote sensing can be integrated with a cascade of hydrological and hydraulic models for flood mapping and identifying hotspot areas prone to flooding for a better flood risk management. We also showed that uncertainty in the rating curve can significantly affect flood mapping and, consequently, can influence identification of critical hotspots for emergency management and urban planning.

References

Ashouri H, Hsu K-L, Sorooshian S, Braithwaite DK, Knapp KR, Cecil LD, Nelson BR, Prat OP (2015) PERSIANN-CDR: daily precipitation climate data record from multisatellite observations for hydrological and climate studies. Bull Am Meteor Soc 96(1):69–83

Arias-Hidalgo M, Bhattacharya B, Mynett AE, Av G (2013) Experience in using the TMPA-3B42R satellite data to compliment rain gauge measurements in the ecuadorian coastal foothills. Hydrol Earth Syst Sc 17:2905–2915

Banerjee P, Salehin M, Ramesh V (2014) Water management practices and policies along Brahmaputra River Basin: India and Bangladesh. SaciWaters, available online at: https://brahmaputrariversymposium.org/wp-content/uploads/2017/09/report_12-05-2014_v16.pdf. Accessed on 19 Apr 2020

Beck HE, van Dijk AIJM, Levizzani V, Schellekens J, Miralles DG, Martens B, de Roo A (2017) MSWEP: 3-hourly 0.25° global gridded precipitation (1979–2015) by merging gauge, satellite, and reanalysis data. Hydrol Earth Syst Sci 21:589–615. https://doi.org/10.5194/hess-21-589-2017

Bell FG, Cripps JC, Culshaw MG (1986) A review of the engineering behaviour of soils and rocks with respect to groundwater. Engg Geol Spec Pubs 3:1–23

Bell TL, Kundu PK (2003) Comparing satellite rainfall estimates with rain gauge data: optimal strategies suggested by a spectral model. J Geophys Res 108(D3):1–115

Bennett TH, Peters JC (2000) Continuous soil moisture accounting in the hydrologic engineering center hydrologic modeling system (HEC-HMS). Proceeding of joint conference on water resource engineering and water resources planning and management 2000

Bhattacharya B, Solomatine DP (2005) Neural networks and M5 model trees in modelling water level-discharge relationship. NeuroComputing J 63:381–396

Bhattacharya B, Mazzoleni M, Ugay R (2019a) Flood inundation mapping of the sparsely gauged large-scale Brahmaputra basin using remote sensing products. Remote Sens 11(5):501

Bhattacharya B, Mazzoleni M, Mazumder LC (2019b) Uncertainty assessment of hydrological models of large basins with limited data—experiences with the Brahmaputra basin. Proceeding of 38th IAHR world congress, Panama

Christopher M (2013) Water wars: the Brahmaputra River and Sino-Indian relations. New Port, Rhode Island

Collischonn B, Collischonn W, Tucci CM (2008) Daily hydrological modelling in the amazon basin using TRMM rainfall estimates. J Hydrol 360(1–4):207–216

Dartmouth Flood Observatory (2010) Retrieved from dartmouth flood observatory. Available online at: https://floodobservatory.colorado.edu/index.html. Accessed on 17 Apr 2020

Domeneghetti A (2016) On the use of SRTM and altimetry data for flood modeling in data-sparse regions. Water Resour Res 52:2901–2918. https://doi.org/10.1002/2015WR017967

Futter MN, Whitehead P (2015) Rainfall runoff modelling of the upper ganga and Brahmaputra Basins using PERSiST. Environ. Sc., Processes and Impacts

Ghadua Z and Bhattacharya B (2019) Improving flash flood forecasting with a bayesian probabilistic approach: a case study on the Posina. Int J Environ Ecol Eng 13(5)

Gichamo ZG, Popescu I, Jonoski A, Solomatine DP (2012) River cross section extraction from ASTER global DEM for flood modeling. Environ Modell Softw 31(5):37–46

Gu H, Yu Z, Yang C, Ju Q, Lu B-J, Liang C (2010) Hydrological assessment of TRMM rainfall data over Yangtze river Basin. Water Sci Eng 3(4):418–430

Hartmann J, Moosdorf N (2012) The new global lithological map database GLiM: a representation of rock properties at the earth surface. Geochem, Geophys, Geosyst 13(12):1–37

He Z, Hu H, Tian F, Ni G, Hu Q (2017) Correcting the TRMM rainfall product for hydrological modelling in sparsely-gauged mountainous basins. Hydrol Sci J 62(2):306–318

Huffman G, Bolvin D, Nelkin E, Wolff D, Adler R, Gu G (2007) The TRMM multisatellite precipitation analysis (TMPA): quasi-global, multilayer, combined-sensor precipitation estimates at fine scales. J Hydrometrology 8(1):38–55

Islam MF, Bhattacharya B, Popescu I (2019) Flood risk assessment due to cyclone induced dike breaching on coastal areas of Bangladesh. NHESS 19:353–368

Joyce R, Janowiak JE, Arkin PA, Xie P (2004) CMORPH: a method that produces global precipitation estimates from passive microwave and infrared data at high spatial and temporal resolution. J Hydrometeorol 5:487–503

Li M, Shao Q (2010) An improved statistical approach to merge satellite rainfall estimates and raingauge data. J Hydrol 385:51–64

Li Z, Yang D, Gao B, Jiao Y, Hong Y, Xu T (2015) Multiscale hydrologic applications of the latest satellite precipitation products in the Yangtze river Basin using a distributed hydrologic model. J Hydrometeorology 16(1):407–426

Mahanta C (2006) Water resources on the northeast: state of the knowledge base, Indian institute of technology Guwahati, available online at: https://siteresources.worldbank.org/INTSAREGTOPWATRES/Resources/Background_Paper_2.pdf. Accessed on 19 Apr 2020

Mahanta C, Zaman AM, Shah Newaz SM, Rahman SMM, Mazumdar TK, Choudhury R, Borah PJ, Saikia L (2014) Physical assessment of the Brahmaputra River, 2014, international union for conservation of nature (IUCN), available online at: https://portals.iucn.org/library/sites/library/files/documents/2014-083.pdf. Accessed on 19 Apr 2020

Mastrantonas N, Bhattacharya B, Shibuo Y, Rasmy M, Espinoza-Dávalos G, Solomatine D (2019) Evaluating the benefits of merging near real-time satellite precipitation products: a case study in Kinu Basin, Japan. J Hydrometeorology https://doi.org/10.1175/JHM-D-18-0190.1

Mazzoleni M, Brandimarte L, Amaranto A (2019) Evaluating precipitation da-tasets for large-scale distributed hydrological modelling. J Hydrol 578:124076

Mirza M (2003) Three recent extreme floods in Bangladesh: a hydrological analysis. Nat Hazards 35–64

Moradkhani H, Hsu K, Hong Y, Sorooshian S (2006) Investigating the impact of remotely sensed precipitation and hydrologic model uncertainties on the ensemble streamflow forecasting. Geophys Res Lett 33:L12401. https://doi.org/10.1029/2006GL026855

Mukolwe M, Di Baldassarre G, Werner MGF, Solomatine DP (2014) Flood modelling: parameterization and inflow uncertainty. Proc ICE-Water Manage 167:51–60

Papa F, Bala SK, Pandey RK, Durand F, Gopalkrishna VV, Rahman A, Rossow WB (2012) Ganga-Brahmaputra river discharge from Jason-2 radar altimetry: an update to the long term satellite-derived estimates of continental freshwater forcing flux into Bay of Bengal. J Geophys Res 117:1–13

Parua PK (2010) Water use in the Indian subcontinent. Springer

Rodríguez E, Morris CS, Belz JE, Chapin EC, Martin JM, Daffer W, Hensley S (2005) An assessment of the SRTM topographic products, jet propulsion laboratory D-31639 (Report), NASA, available online at: https://www2.jpl.nasa.gov/srtm/SRTM_D31639.pdf. Accessed on 19 Apr 2020

Schneider R, Godiksen PN, Villadsen H, Madsen H, Bauer-Gottwein P (2017) Application of CrySat-2 altimetry data for river analysis and modelling. Hydrol Earth Syst Sci 751–764

Sharma JR, Paithankar Y (2014) Brahmaputra basin report. Ministry of Water Resources, Government of India

Wang W, Lu H, Yang D, Sothea K, Jiao Y, Gao B, Peng X, Pang Z (2016) Modelling hydrologic processes in the Mekong river basin using a distributed model driven by satellite precipitation and rain gauge observations. PLoSOne 11(3):e0152229

Xu X, Li J, Tolson BA (2014) Progress in integrating remote sensing data and hydrologic modeling. Progress Phys Geogr: Earth Environ 38(4):464–498. https://doi.org/10.1177/0309133314536583,2014

Xue X, Hong Y, Limaye AS, Gourley JJ, Huffman GJ, Khan IK, Dorji C, Chen S (2013) Statistical and hydrological evaluation of TRMM-based multi-satellite precipitation analysis over the Wangchu basin of Bhutan: are the latest satellite precipitation products 3B42V7 ready for use in ungauged basins? J Hydrology 499:91–99

Yoshimoto S, Amarnath G (2017) Applications of satellite-based rainfall estimates in flood inundation modeling—A case study in Mundeni Aru River Basin, Sri Lanka. Remote Sens 9(10):998. https://doi.org/10.3390/rs9100998

Zhao Y, Xie Q, Lu Y, Hu B (2017) Hydrological evaluation of TRMM multisatellite precipitation analysis for Nanliu river in humid southwestern China. Sci Rep 7(1):2045–2322

Chapter 10
Ground and Satellite Observations to Predict Flooding Phenomena

Tommaso Moramarco

10.1 Introduction

Flooding is complex phenomena involving many factors as the interaction between the atmosphere, the hydrogeological structure of the basin, land use, climate change and, last but not the least, anthropogenic activities. As regards the climate, Milly et al. (2008) made a focus on the stationarity stressing that observations show that stationarity is dead. Positive and negative trends in temperature and rainfall, respectively, are observed worldwide. Based on Milly et al. (2008) analysis of 12 climate models, considering the IPCC's SRES A1B scenario, there is an expectation of ±40% runoff changing at global scale, with severe consequence in terms of water resources management. Looking at temperature and daily precipitation data recorded in central Italy last century, a trend was observed for both variables which should lead decision makers to cope with the climate change and preserve the water resources (Pierleoni et al. 2014). However, Papalexiou and Montanari (2019) showed that although the trend of daily precipitation is overall negative, an increase of extreme precipitations is observing under global warming. Based on more than 8730 high quality daily rainfall data for the period 1964–2013, screened from more than 100,000 rain gauges across the world, an analysis was conducted at 5° × 5° grid scale identifying the trend of extreme precipitations. Unlike the trend of daily precipitation, mean trend in extreme daily precipitations for the period 1964–2013 is found increase worldwide (Papalexiou and Montanari 2019). Therefore, a positive trend in temperature and in extreme precipitations has being observing. This would entail an increase in flooding. However, Wasko and Sharma (2014) investigated this aspect and they found that a positive increase in heavy rainfall events at higher temperatures does not result in

T. Moramarco (✉)
Research Institute for Geo-Hydrological Protection, CNR, Via Madonna Alta 126, 06128 Perugia, Italy
e-mail: t.moramarco@irpi.cnr.it

© The Author(s), under exclusive license to Springer Nature Singapore Pte Ltd. 2021

A. Pandey et al. (eds.), *Hydrological Aspects of Climate Change*,
Springer Transactions in Civil and Environmental Engineering,
https://doi.org/10.1007/978-981-16-0394-5_10

similar increases in streamflow worldwide; conversely data showed flooding decrease with higher temperatures. Indeed, previously Sharma et al. (2018) showed that over a large number of catchments in USA, only few large extreme precipitations turned in flooding and this was depending on the antecedent wetness conditions of soil. As regards floods, Blöschl et al. (2019), using more than 2300 gauged river sites, stressed that the observed regional trend of discharges in Europe for the period 1960–2010 varies showing increasing trend in (north) western Europe due to increasing precipitation, and decreasing in eastern and northern Europe due to increasing temperatures. Therefore, this has an impact on flood frequency curves at gauged sites and on the return period value which changes in comparison to the one estimated in 1960. As a consequence, hydraulic works designed in the past for the risk mitigation in Europe may be oversized or undersized according to the location where the work is located. In this context, it is fundamental that discharge time series be reliable, for whatever analysis in terms of risk mitigation and water resources management. Based on the above insights, it is evident that soil moisture and discharge are essential variables to analyse processes underpinning the floods formation. Therefore, it is of paramount importance to identify how ground and satellite observations of these two variables may be representative in terms of spatial–temporal resolution and accuracy, so that the hydrological processes can be correctly identified and represented. In this context, even the technology to adopt unfolds a crucial role in monitoring of processes characterizing flooding at different spatial-time scales. These aspects represent the focus of this work and they are preparatory to the analysis to identify which process controls the triggering of a flooding event, its frequency, duration and intensity.

10.2 Soil Moisture Monitoring and Antecedent Wetness Conditions

Soil moisture (SM) is identified by the Global Climate Observing System (GCOS) program (https://www.wmo.int/pages/prog/gcos/) as an Essential Climate Variable technically and economically feasible for systematic observations aimed to investigate the hydrological processes underpinning geo-hydrological risks in terms of floods and landslides. Therefore, the monitoring of the water content in the soil is fundamental for the study of processes tied to the runoff formation, as can be inferred by: (i) the numerous measurement campaigns carried out in recent years in hill slopes and river basins in the national and international context using techniques based on time domain reflectometry also integrated by geophysical instrumentation (Calamita et al. 2012), (ii) the proliferation of soil moisture monitoring stations, such as the International Soil Moisture Network (https://ismn.geo.tuwien.ac.at/) as well as (iii) space missions aimed at observing water content, such as ESA's SMOS and NASA's SMAP.

Based on these observations, many important findings are inferred for the spatial–temporal variation of soil moisture in basins (Brocca et al. 2007). Figure 10.1 shows

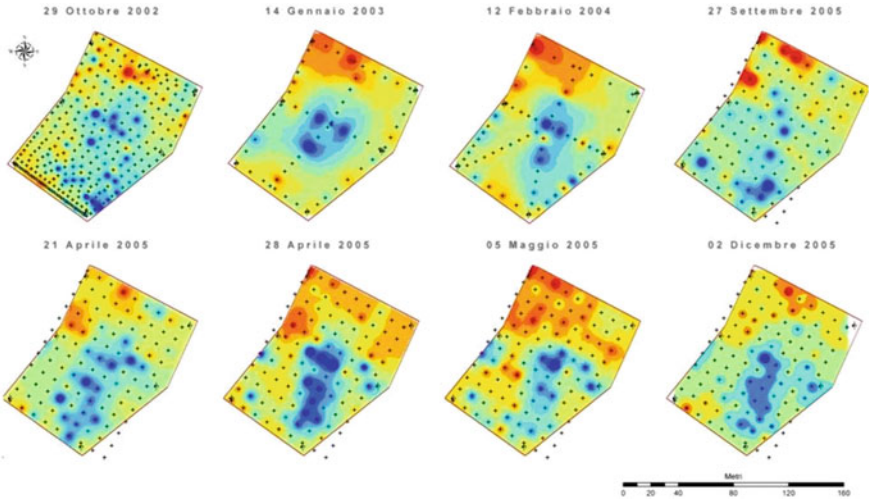

Fig. 10.1 Spatial distribution of soil moisture observed during different campaigns of measurements by TDR carried out in the parcel of Colorso experimental catchment

campaigns of soil moisture monitoring over a parcel located inside the small experimental Colorso catchment of area 12.9 km^2 set up for studying the rainfall–runoff relationship. The plot has an extension of 9000 m^2 (110 m $\times$ 80 m), and a mean slope of 12% (maximum 70%). The area is vegetated mostly with natural grasses (permanent pasture) and it is used for grazing of beef cattle.

The near-surface soil moisture measurements were carried out on a regular grid and were repeated six times from October 2002 to December 2005 and resampled to 10 m. The analysis showed a general decreasing trend of variance with increasing the mean moisture content in accordance with the previous analyses carried out in humid and semi-humid climates. Through these campaigns, the importance of topography in the determination of soil moisture spatial pattern and hence of the lateral redistribution process was confirmed (Brocca et al. 2007; 2009).

Along on the basis of the monitoring of this quantity, by analysing the humidity conditions prior to flood events observed in various experimental basins of the Tiber River, among them the Colorso basin too, it was verified that the initial degree of saturation, θ, of the basin before the event is highly correlated (R = 0.94) to the maximum potential soil retention capacity, S, of the SCS-CN method, and this correlation is higher than that obtained with parameters such as the antecedent precipitation index (R = 0.68) (see Fig. 10.2) and the base flow index (R = 0.69), both using ground and satellite data (Brocca et al. 2008). The analysis was extended to larger basins with an area up to nearly 140 km^2 and the same findings were found, as can be inferred from Fig. 10.2 where the correlation between θ and S was also shown for two basins: Reschio (104 km^2) and Migianella (137 km^2). Likewise, Brocca et al. (2009) using ERS/METOP soil moisture products available at https://www.ipf.tuwien.ac.at/radar/ers-scat/home.htm found a robust correlation between the antecedent soil wetness

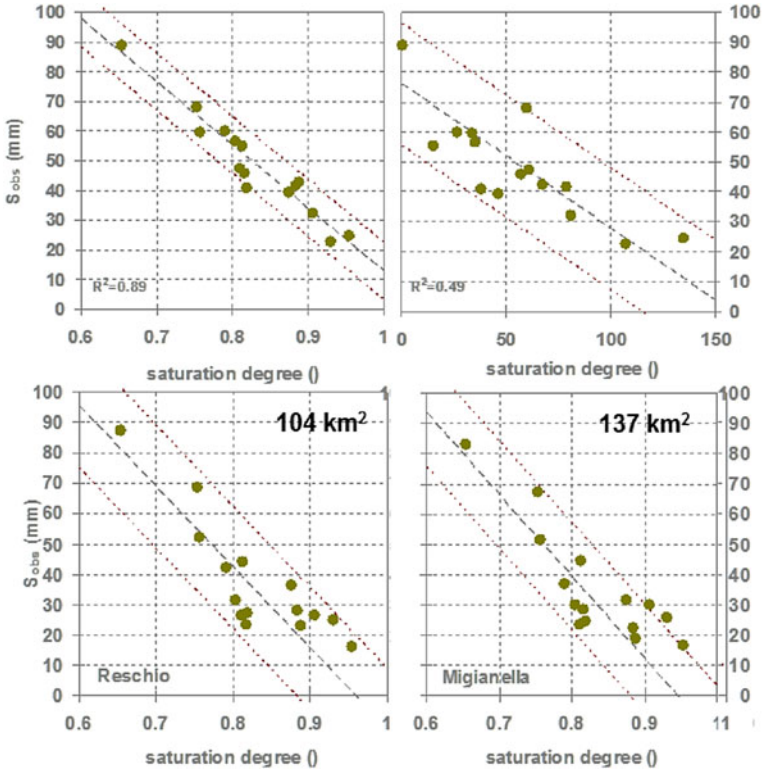

Fig. 10.2 Comparison between the correlation of the initial saturation degree and S **a** and API **b** for the Colorso catchment (13 km^2), and the correlation initial degree of saturation—S for Reschio and Migianella catchments, all belong the Tiber basin

index (*SWI*), proxy of soil moisture, and the maximum soil retention capacity, S, for flood events occurred in sub-catchments of Tiber basin, central Italy, whose areas range from 130 km^2 up to 4100 km^2. *SWI* is a variable depending on the average soil water content given by satellite observation and the characteristic time length, which, in principle, depends on soil properties including soil depth and moisture state and whose value is obtained by calibration (Brocca et al. 2009) (Fig. 10.3).

Therefore, a linear relationship between the initial degree of saturation, θ, and S can be surmised. This important insight led Brocca et al. (2011) to develop the continuous semi-distributed hydrological model, MISDc, based on two components: (i) the soil water balance model that provides the antecedent degree of saturation of soil, θ, and (ii) the event-based rainfall runoff model that routes the runoff along the drainage area and channels. These two components are linked by the linear relationship θ-S, of which the first component provides θ and hence, through the linear relationship, S from which AWC is identified and applied for the component of the event-based rainfall runoff model. Interestingly, Massari et al. (2014) proposed to replace in MISDc the soil water balance component with satellite or ground soil

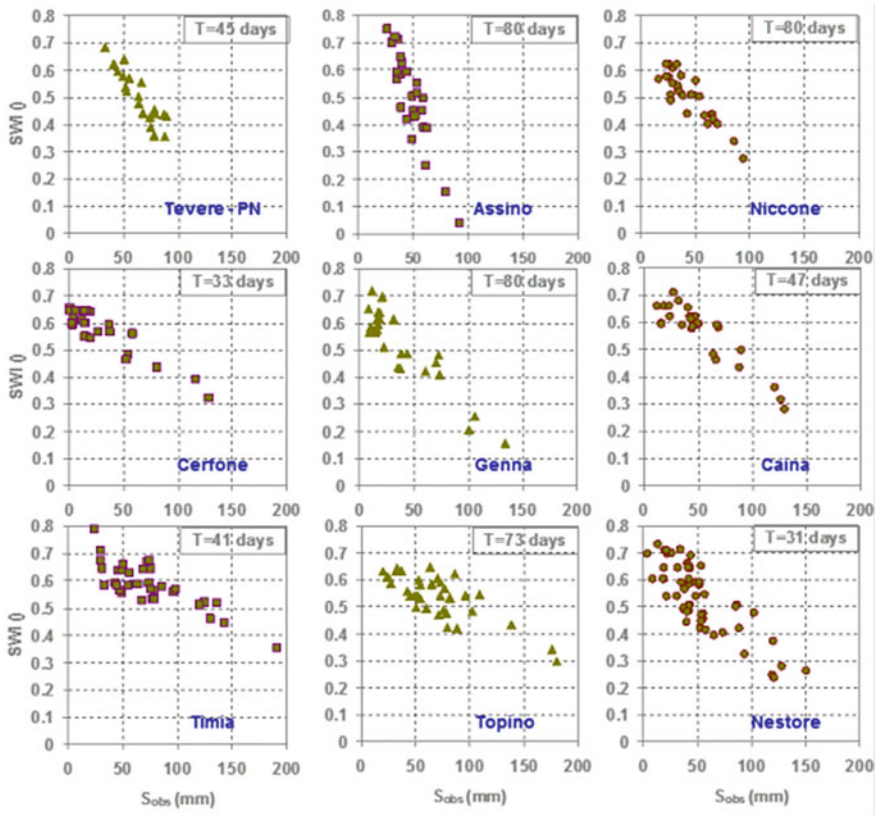

Fig. 10.3 Comparison between the correlation of the initial degree of saturation and S for different sub-catchments of Tiber basin

moisture observations developing a new model named simplified continuous runoff model, *SCRRM*, and shown in Fig. 10.4. The advantage to apply SCRRM is linked to reduced parameters as soil moisture data (ground or satellite observations) becomes an input to the model together with the precipitation. Therefore, no need of continuous temperature and evapotranspiration datasets are necessary and can be very useful for poorly gauged areas and operational purposes as shown by Massari et al (2014, 2015).

In this direction, two further aspects should be highlighted. The first is linked to the benefit that can derive from the assimilation of the water content data in the hydrological modelling, as demonstrated for some basins of different sizes of the Tiber River, where the assimilation of the daily ASCAT data allowed to improve the performance on the forecast of outflows (Massari et al. 2015). The second aspect concerns the potential of the water content to be a "driver" for the estimation of precipitation on a global scale, as demonstrated by the recent innovative method, called *SM2RAIN*, which determines rainfall from soil water content data (Brocca et al. 2011), with important scientific and applicative developments.

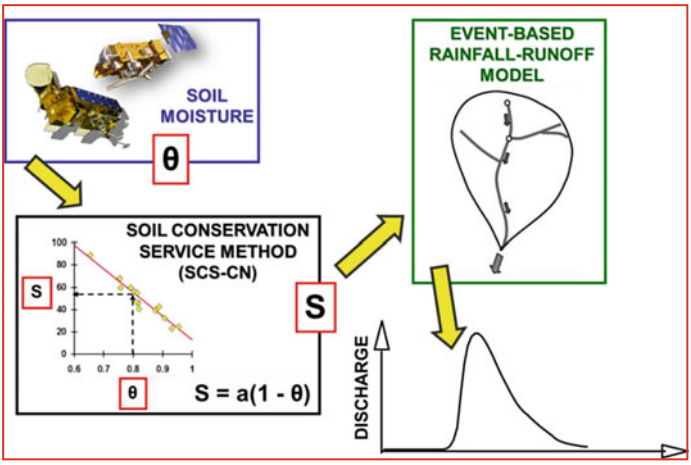

Fig. 10.4 Structure of the SCRRM model where the satellite/ground soil moisture observations, θ, replace the soil water balance model and together with the precipitation initializes the event-based RR model

10.3 Discharge Monitoring and Advanced Technology for Flood Prediction

The discharge variable is another Essential Climate Variable for analysing hydrological cycle processes fundamental to address water resource management, hydraulic risk, drought and impact of climate change. All these aspects can be evaluated if accurate discharge time series are available at gauged river sites through rating curves (Herschy 1985). For this, there is an increasing interest in improving the discharge monitoring for whatever flow conditions at river sites, particularly for high flow, and this may be accomplished by leveraging advanced technologies developed for ground (Corato et al. 2015) and satellite observations (Tarpanelli et al. 2013 at catchment scale. Indeed, the uncertainty in the estimation of the rating curve at river site generally derives from the difficult to carry out velocity measurements during high floods when, e.g. velocity points cannot be sampled by conventional techniques which are costly, time-consuming, and dangerous for operators. As a consequence, discharge estimate for high levels is characterized by errors which affect the hydrological analyses, also in terms of modelling calibration and validation as well as for data assimilation. Therefore, the main issue is how the discharge is estimated for high flow when the measurements are limited to low flow, with high uncertainty in the extrapolation of the rating curve. For this reason, the monitoring of discharge in natural channels is more and more addressed through different techniques such as the Acoustic Doppler Current Profilers (Oberg et al. 2005) and the large-scale particle image velocity (Tauro et al. 2014) which, however, have limitations of use for measurement reliability during particular flow conditions (Wagner and Mueller

2011). Based on ADCP measurements, large dataset is available for hydraulic analysis at river sites (Bjerklie et al. 2020). Currently, the latest technology based on "no-contact" radar sensors to measure the surface flow velocity (Surface Velocity Radar-SVR) has had a significant boost (Alimenti et al. 2020) and could be a fundamental support in monitoring the discharge, especially during high magnitude events (Corato et al. 2011). Another aspect, that needs to be further considered, is the likely absence of infrastructures across the river site of interest for which the discharge monitoring can be done by sensors onboard of drones or satellite. In this case, the no-contact approach would allow to retrieve the distribution of surface flow velocity from which the cross-sectional mean flow velocity and, hence, the discharge may be estimated if the river site topography is known. For this purpose, Moramarco et al. (2017, 2004) developed an entropy-based model that allows to assess the 2D flow velocity distribution just starting from the observed surface velocities and the flow area corresponding to the hydrometric level of observations. The approach is a simplification of the entropy model developed by Chiu (1987, 1988, 1989), who can be considered the pioneer in applying the entropy theory (Shannon 1948) in streamflow measurements. Likewise, Marini et al. (2017) applied the same theory for streamflow analysis in natural channels. Therefore, Moramarco et al. (2017) entropy-based model can be applied to identify the 2D velocity distribution in whatever flow condition even whether secondary currents are present by sampling the surface velocity across the river and using one parameter, Φ, which can be estimated on the basis of velocity dataset as the ratio between mean and maximum flow velocity (Moramarco and Dingman 2017; Moramarco and Singh 2010). A similar approach was proposed by Fulton et al. (2020) for 10 gauged river sites in USA with different geometric and hydraulic characteristics with Φ values ranging from 0.52 up to 0.78. The entropy-based mean flow velocities starting from the surface velocity measured by radar sensor were compared with the ones obtained using the conventional technique of sampling as current metre and ADCP and shown in Fig. 10.5. As can be seen, there is a good agreement among all measurements, showing that using the radar sensor and exploiting the entropy model one is able to carry out fast and accurate measurements during high floods and in full safety for workers safely.

Therefore, the possibility of estimating the average flow velocity in a simple and accurate way during high floods would allow to monitor the velocity both with the conventional techniques (current metre), by means of a sampling of velocity limited to the upper portion of the flow area with reduction of measurement times and dangers to which the operators themselves are subjected, and with new generation "no-contact" sensors, by sampling only the surface velocity. Figure 10.6 shows the comparison between the rating curve and discharge hydrograph obtained at the gauged site of Paglia River, tributary of Tiber River in central Italy, during the flood event 14–20 November 2019, using conventional stream flow measurements by current metre and the entropy model developed by Moramarco et al. (2017) using surface velocities measured by a fixed radar sensor installed on a bridge crossing the gauged site. Interestingly, the entropy model was able to reproduce discharge for high flow along with the effect of unsteady flows, as can be inferred from loops shown in Fig. 10.6. This is explained because the model leverages the measurements of surface velocities

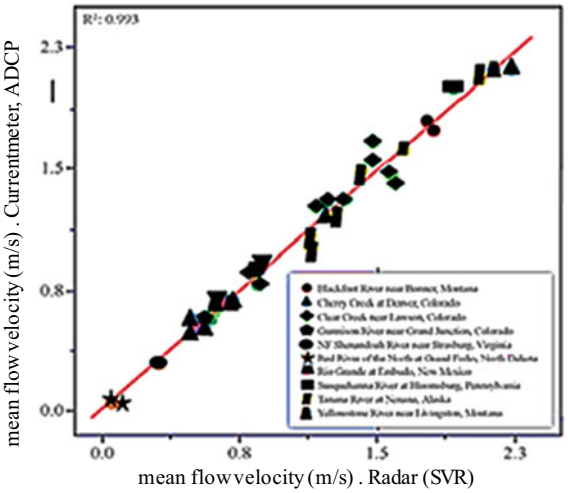

Fig. 10.5 Comparison between the mean flow velocity estimated by using the entropy-based model applied to the y-axis and measuring max surface velocity by SVR and the one obtained by conventional techniques, i.e. current metre and ADCP different sites USGS—Refer to Fulton et al. (2020)

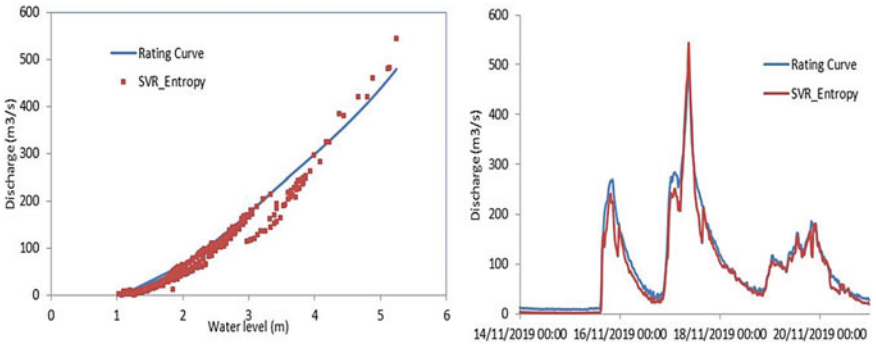

Fig. 10.6 Comparison between the rating curve and discharge hydrograph obtained at the gauged site of Paglia River, central Italy, during the flood event 14–20 November 2019, using conventional stream flow measurements and the entropy model initialized by the surface velocities measured by radar

that may be different for the same water level, unlike the rating curve that being a one to one discharge—water level relationship is not able to consider for the same level different velocities.

The use of no-contact measurements is exacerbated from the growing interest towards the use of unmanned aerial vehicle (UAV) for survey applications, and considering their capability, UAV may be of considerable interest for the hydrological monitoring and in particular for stream flow measurements (Fulton et al.

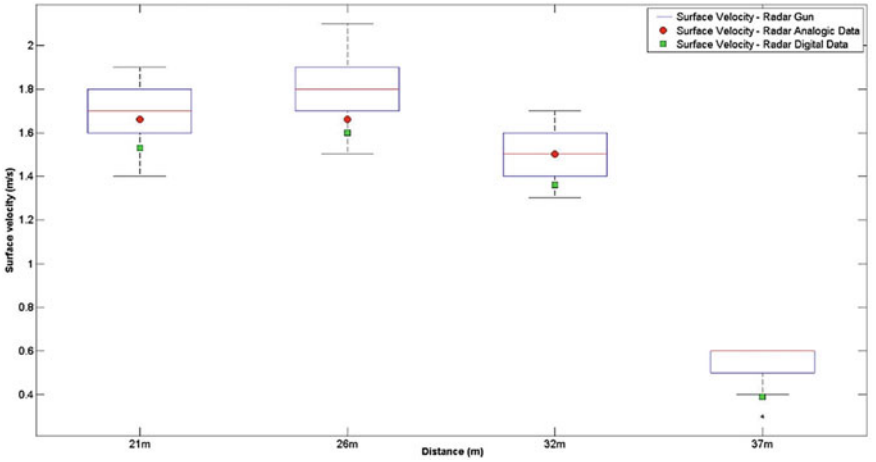

Fig. 10.7 Comparison between the surface velocity measurements carried out by the developed lightweight radar sensors and the trade sensor (Decatur) at Montemolino gauged site along the Tiber River

2020). Indeed, UAV may give information in terms of surface velocity and water surface level, whether on board there is a radar sensor able to monitor both hydraulic variables. This is the aim of the enterprising project funded by the Italian Ministry of University and Research (MUR) which is also addressed to develop a lightweight radar sensor for surface velocity measurements to be used also on board of drone (Alimenti et al. 2020). In this context, Fig. 10.7 shows the box plot of the comparison between the surface velocity measurements carried out by the developed lightweight radar sensors and a trade sensor (Decatur) at Montemolino gauged site along the Tiber River, central Italy. The box plot refers to the number of measurements of Decatur in 1 min. As can be seen, there is a good agreement between the two sensors, with the difference that the developed sensor is lightweight and does not exceed 200 g, making it suitable to be used onboard drone.

Ultimately, using the entropy-based 2D velocity distribution model initialized by surface velocity measurements, the discharge for high flow can be assessed satisfactorily.

10.3.1 Evaluating the Potential for Measuring River Discharge from Space

In this context, the interest of programs of ESA and NASA that have invested in satellite missions for the monitoring of inland waters at global scale is noticeable (e.g. Sentinel by ESA and SWOT by NASA).

This has encouraged studies to evaluate the potential for measuring river discharge from space (Bjerklie et al. 2003) and on the use of sensors such as Moderate Resolution Imaging Spectroradiometer (MODIS) that provides useful data for the estimation of satellite river flow. Indeed, Brakenridge et al. (2007) used daily AMSR-E data at 37 Ghz to globally infer river discharge by using as proxy of cross-sectional mean flow velocity, the ratio between the brightness temperature measured for a pixel unaffected by the river and a pixel centred over the river itself, respectively. Tarpanelli et al. (2013), for four gauged river sites along the Po River in Italy, found a good correlation between the observed average velocity, u_m, at river sites and the daily MODIS's reflectance ratio of two pixels (250 m), one located near an urban centre, named C, where the reflectance signal is expected to be constant, and the other on the river site, named M, where the signal varies according to the flood level. For the four gauged sites, the correlation between observed flow velocity, u_m, and the brightness ratio C/M was addressed for the period 2005–2012 obtaining a coefficient of determination 0.72, on average. This permitted to identify a linear relationship between u_m and C/M to be used for operational purposes, i.e. $u_{m\_\mathrm{MODIS}} = \mathrm{a\ C/M} +$ b, with a and b parameters obtained by best fitting. Based on this relationship, and considering the flow area, A_{obs}, corresponding to the observed water level temporally available for the gauged sites, the discharge was easily estimated for the four gauges sites as the product $Q_{\_\mathrm{MODIS}} = u_{m\_\mathrm{MODIS}} {}^{*}A_{obs}$ with a Nash–Sutcliffe efficiency equal to 0.78, on average. Therefore, MODIS observations can be used with ground measurements of water level recorded by, e.g. ultrasonic or radar sensors. Likewise, MODIS can be coupled with radar altimetry on board satellites (ENVISAT, CryoSat-2, SARAL/Altika, to quote a few) able to monitor water levels even at ungauged sites (Tourian et al. 2016) and which, despite a sub-monthly time resolution, also has high potential for the calibration of hydraulic models (Domeneghetti et al. 2015). This fostered the use of altimeter data in simplified hydrological models (Birkinshaw et al. 2010) and the combined use of MODIS and Altimeter for the estimation of discharge (Tarpanelli et al. 2015). Therefore, the discharge estimation can be done by leveraging ground and satellite observations even for river sites where the bathymetry is unknown (Moramarco et al. 2013), as shown in Fig. 10.8.

Assuming that the bathymetry is absent and the information available is only the measurement of the water level and the surface velocity, it is possible to estimate the cross-section mean flow velocity and therefore the discharge by applying the entropy-based bathymetry model developed by Moramarco et al. (2019). The Monte Carlo technique is used to analyse the uncertainty in estimating the initial conditions of the four parameter set linked to the bathymetry distribution at river site, i.e. roughness, hydraulic gradient, channel bottom level and entropy parameter. As an example, Fig. 10.9 shows the simulated bathymetry for two current measurements carried out in the hydrometric site of Pontelagoscuro on the River Po and Ponte Nuovo on the Tiber River, both in Italy, considering the generation of 1000 scenarios of initial conditions of the set of parameters, starting from the measurement of the surface velocities across the river, and the water level referred to the hydrometric zero. The figure also shows the 5–95% percentiles of the 1000 realization of bathymetry together with the expected value. As can be seen, there is a good agreement between the expected

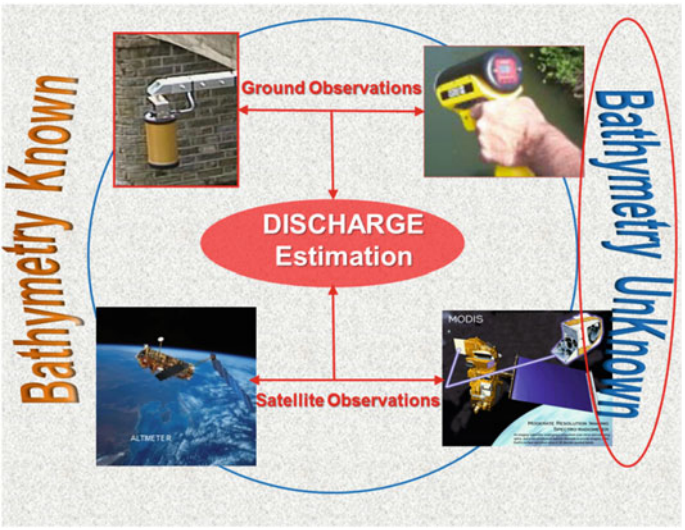

Fig. 10.8 Ground and satellite sensors for water level and flow velocity observations to be used in discharge estimation at river site also when the bathymetry is unknown

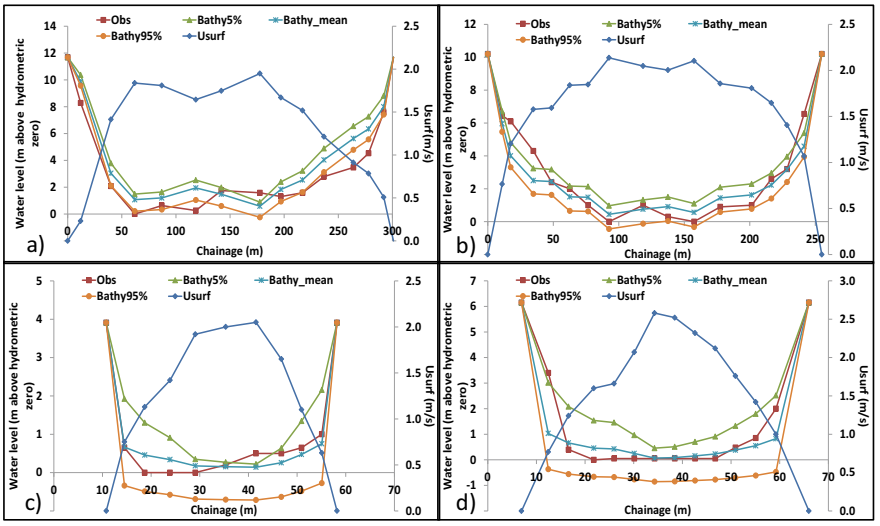

Fig. 10.9 Entropy-based river bathymetry (Bathy_mean) using surface velocity measurements (Usurf) carried out in 8 May 1991 (**a**) and 13 October 1992 (**b**) at Pontelagoscuro site on Po River and in 2 Jan 1996 (**c**) and 16 Dec 1999 (**d**) at Ponte Nuovo site on Tiber River. Comparison with the bathymetry surveyed during the measurement along with the percentiles, 5–95% of 1000 realizations of bathymetry are also shown

entropy-based bathymetry and the observed one. Therefore, once the bathymetry is estimated, the discharge can be estimated as the product between the entropy-based flow area and the mean flow velocity obtained by using the entropy approach developed by Moramarco et al. (2017). In this context, Table 10.1 summarizes the errors in flow area and discharge using the entropy-based model for bathymetry and mean flow velocity estimation.

The same procedure can be applied using satellite data. In this context, the proposed entropy-based methodology may be applicable for the ESA and NASA programs that have invested in satellite missions for the monitoring of inland water on a global scale. Indeed, considering that MODIS and altimetry radar can provide

Table 10.1 Comparison between cross-sectional flow area and discharge observed and expected by the entropic approach using streamflow measurements at Pontelagoscuro and Ponte Nuovo gauged river site. The percentage error in estimating both quantities is also illustrated

	Date	Area_obs	Area_Entr	Err A (%)	Q_obs	Q_Entr	Err Q (%)
Pontelagoscuro	Feb 24, 87	1853	1730	−7	1779	1732	−3
	Apr 23, 87	1570	1379	−12	1199	1216	1
	Jan 30, 91	1284	1249	− 3	887	970	9
	May 08, 91	1974	2006	2	3218	3005	−7
	Oct 13, 92	2830	2446	−14	4000	3304	−17
	Oct 14, 92	2711	2472	−9	3738	3372	−10
Ponte Nuovo	Oct 22, 92	204	195	−5	341	299	−12
	Jan 02, 96	157	155	−1	210	203	−3
	Mar 04, 97	76	80	5	39	38	−3
	Jun 03, 97	278	271	−3	506	461	−9
	Nov 29, 99	80	89	12	54	57	6
	Dec 16, 99	290	298	3	438	492	12
	Nov 07, 2000	150	144	−4	228	214	−6
	Jan 30, 2001	166	162	−3	270	256	−5

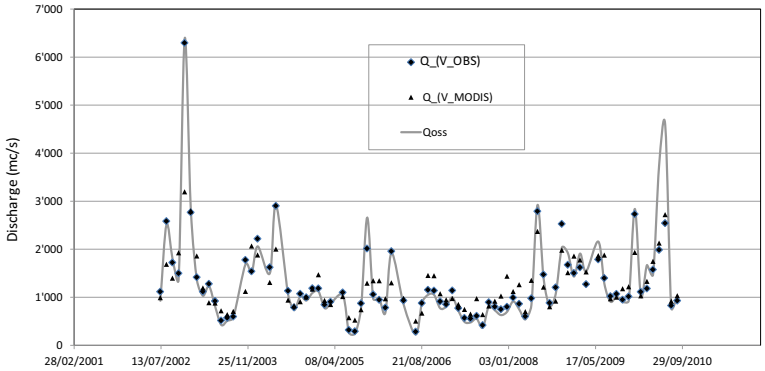

Fig. 10.10 Pontelagoscuro—Po River: comparison between observed discharge, Q_obs, and expected value from the bathymetry using Modis + Altimeter (Q_(V_MODIS)) and observed velocity + Altimetro (Q_(V_OBS))

information on mean flow velocity and water level, respectively, all information are available to apply the entropy-based bathymetry model.

Figure 10.10 shows the comparison between the discharge time series observed at Pontelagoscuro for the period 2002–2010 and the entropy-based expected value (average scenario) in the hypothesis of absence of bathymetry for the entire time series. For the reconstruction of the bathymetry scenarios, in addition to the average velocity inferred by MODIS, the one observed on the ground in correspondence of the altimeter passage was also used. As can be seen, using the ground velocity data in place of one obtained by MODIS and the water level observed by the altimeter, the performance of the entropy-based bathymetry model improves, above all in the estimation of the higher flow rate values, unlike to using the altimeter and MODIS coupled for which the performance decreases. The velocity data provided by MODIS still allows for the estimation of quite satisfactory discharge values, however highlighting the need for a more in-depth analysis between the reflectance ratio and flow velocity for highest values of water level.

10.4 Conclusions

The response of a hydrographic basin to a weather stress is strictly linked to the initial saturation conditions of the basin itself. The ground and satellite monitoring of the water content thus allows the identification of the degree of saturation of the basin and this information can be directly integrated / assimilated into a hydrological model, effectively improving the accuracy in estimating the outflows. Similarly, the limit of river flow monitoring for extreme events can be overcome by, on the one hand, the measurement of the surface velocity by using no-contact radar technology, possibly

even aboard drones and, on the other hand, by satellite observations such as the radar altimeter and MODIS directing the estimation of outflows also in non-instrumented river sites.

Acknowledgements I would like to express my gratitude to the hydrologists of IRPI's Hydrology group. Without them, this research would never have been possible. In particular, my sincere thanks to Silvia Barbetta, Luca Brocca, Stefania Camici, Luca Ciabatta, Christian Massari and Angelica Tarpanelli. It is also acknowledged the activity of Enterprising PRIN Project's team, funded by the Italian Ministry of Research and University.

References

Alimenti F, Bonafoni S, Gallo E, Palazzi V, Vincenti Gatti R, Mezzanotte P, Roselli L, Zito D, Barbetta S, Corradini C, Termini D, Moramarco T (2020) Non-contact measurement of river surface velocity and discharge estimation with a low-cost doppler radar sensor. IEEE Trans Geosci Remote Sens https://doi.org/10.1109/TGRS.2020.2974185

Birkinshaw SJ, O'Donnell GM, Moore P, Kilsby CG, Fowler HJ, Berry PAM (2010) Using satellite altimetry data to augment flow estimation techniques on the Mekong River. Hydrol Process 24:3811–3825

Bjerklie DM, Dingman LS, Vorosmarty CJ, Bolster CH, Congalton RG (2003) Evaluating the potential for measuring river discharge from space. J Hydrol 278(1–4):17–38

Bjerklie DM, Fulton JW, Dingman SL, Canova MG, Minear Justin T, Moramarco T (2020) Fundamental hydraulics of cross-sections in natural rivers: preliminary analysis of a large data set of acoustic doppler flow measurements. Water Resour Res https://doi.org/10.1029/2019WR025986

Blöschl G, Hall J, Viglione A et al (2019) Changing climate both increases and decreases European river floods. Nature 573:108–111. https://doi.org/10.1038/s41586-019-1495-6

Brakenridge GR, Nghiem SV, Anderson E, Mic R (2007) Orbital microwave measurement of river discharge and ice status. Water Resour Res 43:W04405

Brocca L, Morbidelli R, Melone F, Moramarco T (2007) Soil moisture spatial variability in experimental areas of central Italy. J Hydrol 333(2–4):356–373

Brocca L, Melone F, Moramarco T (2008) On the estimation of antecedent wetness conditions in rainfall-runoff modelling. Hydrol Process 22(5):629–642

Brocca L, Melone F, Moramarco T, Morbidelli R (2009) Soil moisture temporal stability over experimental areas in central Italy. Geoderma 148(3–4):364–374

Brocca L, Melone F, Moramarco T (2011) Distributed rainfall-runoff modelling for flood frequency estimation and flood forecasting. Hydrol Process 25:2801–2813

Calamita G, Brocca L, Perrone A, Piscitelli S, Lapenna V, Melone F, Moramarco T (2012) Electrical resistivity and TDR methods for soil moisture estimation in central Italy test-sites. J Hydrol 454–455:101–112

Chiu CL (1987) Entropy and probability concepts in hydraulics. J Hydr Eng ASCE 113(5):583–600

Chiu CL (1988) Entropy and 2-D velocity distribution in open channels. J Hydr Engrg ASCE 114(7):738–756

Chiu CL (1989) Velocity distribution in open channel flow. J Hydr Engrg ASCE 115(5):576–594

Corato G, Moramarco T, Tucciarelli T (2011) Discharge estimation combining flow routing and occasional measurements of velocity. Hydrol Earth Syst Sci 15:2979–2994

Corato G, Moramarco T, Tucciarelli T, Fulton JW (2015) Continuous discharge monitoring using non-contact methods for velocity measurements: uncertainty analysis. Eng Geol 3:617–621

Domeneghetti A, Castellarin A, Tarpanelli A, Moramarco T (2015) Investigating the uncertainty of satellite altimetry product for hydrodynamic modelling. Hydrol Process 29(23):4908–4918. https://doi.org/10.1002/hyp.10507

Fulton JW, Mason C, Eggleston J, Nicotra M, Chiu CL, Henneberg M, Best H, Cederberg J, Holnbeck S, Lotspeich R, Laveau C, Moramarco T, Jones M, Gourley J, Wasielewski D (2020) Remote sensing of surface velocity and river discharge using radars and the probability concept at 10 USGS streamgages. Remote Sens 12(8):1296. https://doi.org/10.3390/rs12081296

Herschy RW (1985) Streamflow measurement. Elsevier, London, UK

Marini G, Fontana N, Singh VP (2017) Derivation of 2D velocity distribution in watercourses using entropy. J Hydrol Eng 22(6)

Massari C, Brocca L, Barbetta S, Papathanasiou C, Mimikou M, Moramarco T (2014) Using globally available soil moisture indicators for flood modelling in mediterranean catchments. Hydrol Earth Syst Sci 18:839–853

Massari C, Brocca L, Ciabatta L, Moramarco T, Gabellani S, Albergel C, de Rosnay P, Puca S, Wagner W (2015) The use of H-SAF soil moisture products for operational hydrology: flood modelling over Italy. Hydrology 2(1):2–22

Milly PCD, Falkenmark JBM, Hirsch RM, Zbigniew Kundzewicz WD, Lettenmaier DP, Stouffe RJ (2008) Stationarity Is Dead: Whither Water Management? Science 319(5863):573–574

Moramarco T, Dingman SL (2017) On the theoretical velocity distribution and flow resistance in natural channels. J Hydrol https://doi.org/10.1016/j.jhydrol.2017.10.068

Moramarco T, Singh VP (2010) Formulation of the entropy parameter based on hydraulic and geometric characteristics of river cross sections. J Hydrol Eng 15(10):852–858

Moramarco T, Saltalippi C, Singh VP (2004) Estimation of mean velocity in natural channels based on Chiu's velocity distribution equation. J Hydrol Eng 9(1):42–50

Moramarco T, Saltalippi C, Singh VP (2011) Velocity profiles assessment in natural channel during high floods. Hydrol Res 42(23):162–170. https://doi.org/10.2166/nh.2011.064

Moramarco T, Corato G, Melone F, Singh VP (2013) An entropy-based method for determining the flow depth distribution in natural channels. J Hydrol 497:176–188

Moramarco T, Barbetta S, Tarpanelli A (2017) From surface flow velocity measurements to discharge 2 assessment by the entropy theory. Water 9(2):120. https://doi.org/10.3390/w902012

Moramarco T, Barbetta S, Bjerklie DM, Fulton JW, Tarpanelli A (2019) River bathymetry estimate and discharge assessment from remote sensing. Water Resour Res https://doi.org/10.1029/2018WR024220

Oberg KA, Morlock SE, Caldwell WS (2005) "Quality-assurance plan for discharge measurements using acoustic Dopplercurrent profilers." U.S. geological survey scientific investigations report 2005–5183, Denver

Papalexiou SM, Montanari A (2019) Global and regional increase of precipitation extremes under global warming. Water Resour Res 55(6):4901–4914

Pierleoni A, Camici S, Brocca L, Moramarco T, Casadei S (2014) Climate change and decision support systems for water resource management. Procedia Eng 70:1324–1333

Shannon CE (1948) A mathematical theory of communication. Bell Syst Tech J 27(379–423):623–656

Sharma A, Wasko C, Lettenmaier DP (2018) If precipitation extremes are increasing, why aren't floods? Water Resour Res 54:8545–8551

Tarpanelli A, Brocca L, Melone F, Moramarco T, Lacava T, Faruolo M et al (2013) Toward the estimation of river discharge variations using MODIS data in ungauged basins. Remote Sens Environ 136:47–55

Tarpanelli A, Brocca L, Barbetta S, Faruolo M, Lacava T, Moramarco T (2015) Coupling MODIS and radar altimetry data for discharge estimation in poorly gauged river basin. IEEE Appl Earth Observations Remote Sens 8(1):141–148

Tauro F, Porfiri M, Grimaldi S (2014) Orienting the camera and firing lasers to enhance large scale particle image velocimetry for streamflow monitoring. Water Resour Res 50:7470–7483

Tourian MJ, Tarpanelli A, Elmi O, Qin T, Brocca L, Moramarco T, Sneeuw N (2016) Spatiotemporal densification of river water level time series by multimission satellite altimetry. Water Resour Res 52:1140–1159. https://doi.org/10.1002/2015WR017654

Wagner CR, Mueller DS (2011) Comparison of bottom-track to global positioning system referenced discharges measured using an acoustic doppler current profiler. J Hydrol 401:250–258

Wasko C, Sharma A (2014) Quantile regression for investigating scaling of extreme precipitation with temperature. Water Resour Res 50:3608–3614

Chapter 11
Indices for Meteorological and Hydrological Drought

John Keyantash

11.1 Overview

Drought is a deceptively difficult phenomenon to quantify. Drought is most basically defined as a deficiency in water supply, which is occurring with an uncommon frequency and/or severity. It is a natural disaster that is plainly comprehended by farmers, fishermen and the general public, but this simplicity belies the variety of forms in which drought may manifest itself. First, there is the issue of which natural reservoir is deficient in water: surface water, groundwater and/or the root water zone? Due to the interconnectedness of the hydrological cycle, a water shortage in one reservoir (e.g. soil growing zone) is usually mirrored by a deficiency in another (e.g. surface runoff), although the shortages may be time-lagged. For example, groundwater droughts typically lag surface water droughts by several months to years. Nonetheless, delineating the principally affected reservoir is a common approach to simplify drought description. This isolationist approach has led to the recognition of several drought forms.

11.1.1 Drought Forms

There are four primary forms of drought. A shortage of precipitation is known as *meteorological* drought, while a shortage of soil moisture is termed *agricultural* drought. A decrease in surface water (streams, lakes and/or impounded reservoirs) or groundwater levels is known as *hydrological* drought. Finally, *socio-economic*

J. Keyantash (✉)
Department of Earth Science and Geography, California State University, Dominguez Hills, Carson, CA, USA
e-mail: jkeyantash@csudh.edu

© The Author(s), under exclusive license to Springer Nature Singapore Pte Ltd. 2021

A. Pandey et al. (eds.), *Hydrological Aspects of Climate Change*,
Springer Transactions in Civil and Environmental Engineering,
https://doi.org/10.1007/978-981-16-0394-5_11

drought is the consequence of multiple water deficiencies upon society. It is measured not only in terms of various water supplies, but also in terms of monetary cost to the economy.

11.1.2 The Metric for Deficiency

Aside from associating the water deficiency with a specific natural reservoir—and therefore a form of drought—another rudimentary consideration is how to quantify the shortage. For example, a hydrological drought could result in the reduced water supply within an unconfined aquifer. How might the groundwater deficiency be best described? There is no universal answer: metres of water table decline, megatons of absent water or the per cent change in the storativity of the aquifer are all valid metrics. Furthermore, once a direct measure is adopted, how does its value reflect the statistical unusualness of the situation? The desire to interpret the water deficiency in terms of its probability of occurrence is a fundamental property of drought studies. As we will see, this probabilistic component is at the heart of some of the most widely used drought indices.

11.1.3 Timescale Considerations

The statistical analysis of probabilities inevitably involves the consideration of time: over which time frame is the water deficiency occurring? For example, over months or decades? The timescale is commonly considered with respect to the typical expected dryness for the location, that is, the local climate. For example, a meteorological drought in India's Western Ghats would be entirely different than drought in Algeria, in terms of the length of the dryness interval (e.g. months versus years, respectively) and the absolute water deficiency: metres in India to scant millimetres in North Africa.

11.1.4 The Drought Index Approach

For these complicated reasons, the scientific community commonly uses indices to describe drought, rather than direct observations of the water quantity (which are easy to comprehend but do not provide a broader context for the deficiency). But just like there is no single form of drought, there is no single drought index which works best in all circumstances. Instead, various drought indices have been developed which target each physical form of drought: agricultural, meteorological and hydrological (as well as some composite versions). Highlights for a broad suite of indices may

be found in WMO and GWP (2016), while Keyantash and Dracup (2002) and Heim (2000) expand upon selected drought indices in more depth.

It bears mention that socio-economic drought does not have a distinct index to describe it, other than financial damages (for example, dollars or rupees). Due to this abstraction from the physical world, socio-economic drought will not be discussed further, and agricultural drought will also be omitted, as this chapter is primarily concerned with the meteorological and hydrological forms of drought.

11.2 Meteorological Drought Indices

This section discusses four indices of meteorological drought: Palmer drought severity index, rainfall deciles, standardized precipitation index and the related standardized precipitation evapotranspiration index.

11.2.1 Palmer Drought Severity Index (PDSI)

In 1965, Wayne C. Palmer published a U.S. Weather Bureau report titled *Meteorological Drought*, in which he outlined the methodology for the calculation of what came to be known as the Palmer drought severity index (PDSI). In subsequent decades, the PDSI went on to become the most widely used index of meteorological drought in the USA. The enthusiasm for this index was related to its attempt, as Palmer put it, of "measuring the cumulative departure of moisture supply" (Palmer 1965). The integrative nature of this approach is at the heart of all drought studies. The PDSI is a dimensionless number typically ranging between 4 and −4, with negative quantities indicating a shortage of water. Near-normal conditions are ± 0.5, while drought occurs when the PDSI is <-1.

The PDSI incorporates a two-layer soil model and calculates water balance within the soil, depending upon observed meteorological conditions. The fluctuations in the hypothetical moisture supply are compared to a reference set of water balance terms. This comparison leads to computation of the dimensionless PDSI. Index values are calculated on an ongoing basis by the US National Centers for Environmental Information (NCEI) (formerly known as the National Climatic Data Center [NCDC]), and monthly PDSI values extend back to 1900 (NCEI 2020). Computation of the PDSI is complicated; for an in-depth discussion of the numerical steps, see Alley (1984).

The PDSI was intended to be a standardizing measure of moisture conditions across different geographic regions and time. However, it was empirically calibrated using various soil types in the Midwestern United States, which are not necessarily representative of other regions. Guttman et al. (1992) determined that routine climatological conditions tend to yield more severe PDSI measures in the Great Plains of the USA than other regions. Thus, there exist regional biases.

The PDSI is also imprecise in its water balance accounting. The two-layer soil model is constructed such that no water may migrate to the underlying layer until the surface layer is at its full water holding capacity, set at the arbitrary level of 25 mm (Alley 1984). There is also no consideration for the delayed hydrological availability of snowfall, which is instead treated as immediately available liquid water. On the positive side, the PDSI does factor in antecedent conditions and is calculable from basic observational data. But its empirical nature, coupled with the fact it was developed for US agricultural regions, limits its broad applicability, and as a result the PDSI is not widely used internationally.

11.2.2 Rainfall Deciles

Precipitation distributions are decidedly non-normal, featuring asymmetry with positive skewness. For example, a comprehensive study of precipitation time series in the USA found that the Pearson type-III and kappa distributions best describe precipitation records for hundreds of sites, although the two-parameter gamma distribution has been widely used to characterize precipitation probabilities (Ye et al. 2018). Since the mean does not lie in the centre of an asymmetric (probability distribution) function, meteorological drought assessments involving variations from the mean precipitation are not equally comparable in their positive (wet) and negative (dry) phases. These imbalances can be circumvented by judging precipitation totals with respect to the median rather than the mean. Such an approach utilizes precipitation quantiles as proxies for direct precipitation measurements.

An established quantile methodology is the usage of ten quantiles, or *deciles*. A decile-based system for monitoring meteorological drought in Australia was proposed by Gibbs and Maher (1967), and adopted by the Australian Bureau of Meteorology (BOM) to monitor drought conditions in that nation. The BOM-adopted characterizations of decile levels are shown in Table 11.1 (Kinninmonth et al. 2000).

Despite having five categories, this is indeed a decile rather than a quintile system, as the bin width of each characterization is not constant. It should also be noted that "average" in Table 11.1 actually implies the median (50th percentile) rather than the arithmetic mean, as a fundamental purpose of the quantile approach is to avoid

Table 11.1 Characterization of rainfall deciles

Decile(s)	Characterization
1	Very much below average
2–3	Below average
4–7	Average
8–9	Above average
10	Very much above average

the distorted values of the mean, which results from Australia's erratic precipitation climatology.

The rainfall decile methodology begins by assembling three-month (or longer) precipitation totals, which are ranked against climatological records. If the precipitation sum falls within the lowest decile (tenth percentile or lower) of the historical distribution of totals sharing that timing (i.e. those particular months of the year) and duration (viz. 3 months or longer [as drought is not validly recognized for briefer periods in Australia]), then the location is considered to be experiencing a "rainfall deficiency" (drought). The first-decile totals are parsed into two characterizations: *serious* (drought) if the precipitation total is between the 10th and 5th percentiles and *severe* if it is below the 5th percentile (Kinninmonth et al. 2000). A decile map of 12-month precipitation totals is shown in Fig. 11.1.

It is interesting that BOM also examines monthly rainfall totals from the decile perspective, even when drought characterization is not the objective; see Fig. 11.2. Thus, deciles are a useful probabilistic lens with which to view precipitation, particularly within a region of naturally high climatic variability, such as Australia.

The *severe* or *serious* forms of meteorological drought are considered to persist until either of two termination criteria occur (Kinninmonth et al. 2000). These termination criteria can be thought of as forward-looking or backward-looking triggers, which are practically employed using a three-month window of inspection:

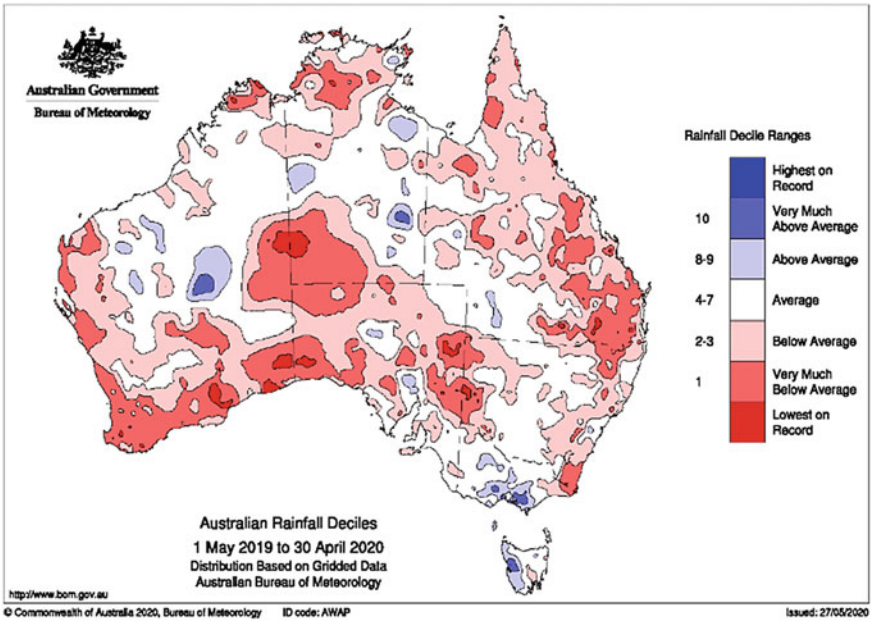

Fig. 11.1 Decile map of 12-month precipitation totals in Australia, through April 2020. Meteorological drought in Australia may be assessed across a variety of timescales, but the duration must be a minimum of three months. *Source* BOM 2020

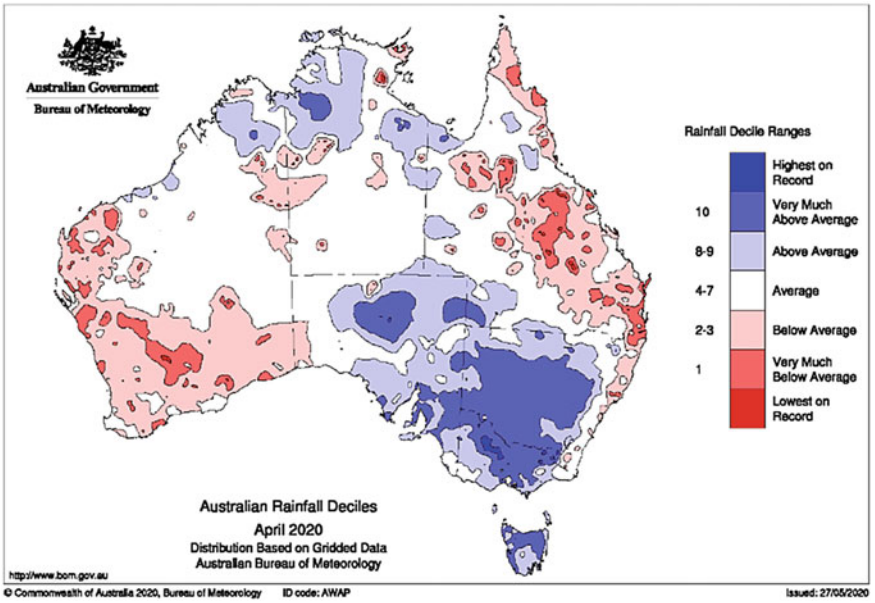

Fig. 11.2 Monthly precipitation deciles across Australia. Red regions are not necessarily experiencing drought (for drought identification, refer to Fig. 11.1), but the decile perspective is useful for judging precipitation deficiencies. *Source* BOM 2020

1. Forward-looking: The precipitation measured during the past month already places the new, forward-looking three-month total in the 4th decile or higher. That is, the three-month total will be "average" (median) or higher (per Table 11.1), even if no further precipitation falls in the next two months. The drought is therefore broken by an unusually wet month. (*But see following* **Rule restriction** *sect.*)
2. Backward-looking: The precipitation total for the past three months is in the 8th decile or higher. Thus, to exit a sustained drought, the three-month rainfall must be above or very much above average.

Rule restriction

In regions with highly seasonal precipitation, it is mathematically possible for a slight amount of precipitation at the start of a typical dry season to trigger the forward-looking drought-stopping condition. In this case, a further rule restriction is applied: the drought does not terminate unless the total precipitation for all months since the drought began exceeds the first decile (G. S. Beard 2000, personal communication).

For example, consider a hypothetical ongoing drought in its eleventh month. The eleventh month of the drought occurs during the start of the typical dry season, and it happens to be a relatively wet month. On its own merits, the eleventh month

precipitation would result in the forward-looking precipitation total (i.e. months 11–13) being in the fourth (or higher) decile, which would activate the forward-looking trigger to indicate that the meteorological drought—*serious* or *severe*—had ended. However, before declaring the drought over, BOM would inspect the eleven months since the start of the drought to verify that the 11-month precipitation total was in the second (or higher) decile. In all cases, the termination criteria require the precipitation quantities to exit the lowest deciles and shift to higher deciles.

11.2.3 Standardized Precipitation Index (SPI)

Despite the nonparametric simplicity and utility of rainfall deciles, the scientific world values parametric distributions, as they provide the ability to extrapolate the probabilities of events beyond the observational record. In particular, the widespread usage of normal (Gaussian) statistics motivates data transformations which can re-express skewed, unimodal precipitation data into normal distributions.

The data transformations may involve raising the original data to various exponential powers within specific mathematical functions, with the form of each function depending upon the sign of the exponent. This approach is referred to as a *power transformation*, as an exponential power is involved in performing the transformation. The Box–Cox transformation (Box and Cox 1964) is a classic approach which involves scaling the original data and exponentiating it to the *transformation parameter* λ (lambda). A simpler variant is given by Wilks (1995):

$$T(P) = \begin{cases} P^{\lambda} & \lambda > 0 \\ \ln(P) & \lambda = 0 \\ -P^{\lambda} & \lambda < 0 \end{cases} \tag{11.1}$$

where

P = observed precipitation
T = transformed precipitation
λ = transformation parameter

Obviously, the choice of λ will fully dictate the resulting distribution of the transformed data T. Positively skewed data (i.e. data with a pronounced right tail, such as precipitation) will shift leftwards towards normality when $\lambda < 1$, while negatively skewed data redistributes rightwards when $\lambda > 1$ (Wilks 1995). The precise choice for the value of the transformation parameter that produces the optimal transformation requires some data exploration, and guidance is given in other references (e.g. Box and Cox 1964; Wilks 1995).

In 1993, McKee et al. proposed the standardized precipitation index (SPI) as a way to measure the intensity of drought—in a probabilistic perspective—across multiple timescales. The SPI is anchored upon defined probabilities for each SPI value, in

particular the probabilities associated with a Gaussian (normal) distribution of SPI values. Precipitation is not normally distributed, but as discussed in the previous paragraph, it may be transformed to a normal distribution. McKee et al. (1993) considered precipitation data to follow the gamma (Γ) distribution and performed the appropriate transformation. The gamma distribution is one of several recognized extreme value distributions for precipitation (such as Gumbel, Pearson type-III and generalized extreme value [GEV] distributions, among others; refer to Ye et al. (2018) and Guttman (1999) for more thorough discussion), and it benefits from wide acceptance in hydrology and related fields.

The SPI is the standardized precipitation anomaly, *after* the precipitation data have been transformed from their original distribution (nominally gamma) to the normal distribution:

$$SPI = \frac{P - \bar{P}}{\sigma_P} \tag{11.2}$$

where

P = precipitation datum
$\bar{P}$ = mean precipitation
σ_P = sample standard deviation of precipitation

Effectively, the SPI is the expression of the normalized precipitation data as Gaussian variates. Each SPI value has an associated probability of occurrence, given by the routine Gaussian cumulative distribution function, shown in Fig. 11.3. For example, Fig. 11.3 shows that an SPI value of -1 or lower occurs approximately 15% (9% + 4% + 2%) of the time (absent rounding approximations, the actual probability is 15.87%). Per the given SPI categories, these would comprise the "dry", "moderately dry" and "extremely dry" sub-classifications of drought. As shown on the right

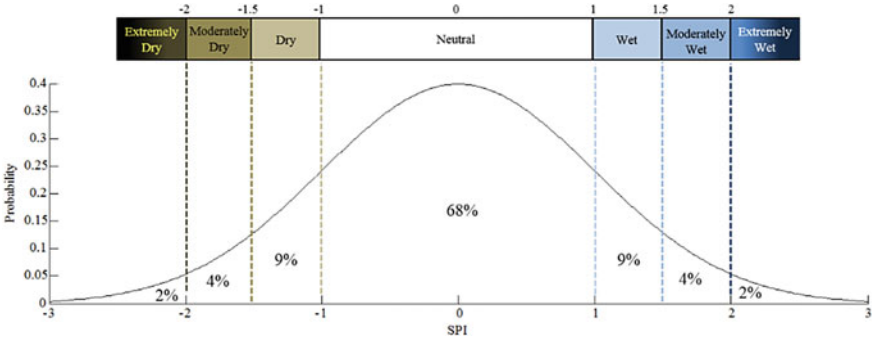

Fig. 11.3 Normal curve and its associated probabilities. The given probabilities represent the likelihood of falling strictly within the dashed boundaries. The sum of the probabilities is less than 100% due to rounding. The colour bar along the top indicates the associated drought labels for the SPI. *Source* Keyantash and NCAR 2018

side of Fig. 11.3, we also see that the SPI is equally suited to represent wet spells (*pluvials*).

A critical benefit of the SPI is that it can be used to characterize droughts across multiple timescales. Specifically, the P value in Eq. 11.2 may be the precipitation total from any particular timescale: one month, three months, 18 months, 72 months or any other desired interval. This grants the SPI the ability to assess dryness across a sliding range of perspectives. For example, a recent wet month might be embedded within a seasonal moderate drought, which in turn is a portion of a multi-year severe drought. The basic question, *"Are we in a drought, and if so, how severe is it?"* produces a complex answer, dependent upon the timescale of interest. The SPI is able to provide quantitative responses across multiple timescales.

The probabilistic foundation for the SPI, coupled with its multi-scale flexibility, has led to its international acceptance. In 2009, at a conference hosted at the University of Nebraska-Lincoln, an international panel of drought experts decreed that among the variety of available meteorological drought indices, the SPI was recommended as the international standard. This statement was known as the Lincoln Declaration on Drought Indices and is detailed more fully by Hayes et al. (2011).

11.2.4 Standardized Precipitation Evapotranspiration Index (SPEI)

A related variant of the SPI is the standardized precipitation evapotranspiration index (SPEI [Vicente-Serrano et al. 2010]), which includes temperature in its computation. The purpose of this inclusion is to recognize that the true deficiency of water depends upon evaporative demand—a reduced water input is less deleterious in a cool climate than a region which is warm and arid. For example, 5 cm of precipitation could produce strong or weak drought relief, depending upon not only the precipitation climatology, but also the evaporative conditions. For the SPEI, monthly mean temperature is used to compute potential evapotranspiration via a Thornthwaite model, and it is the difference of the precipitation and potential evapotranspiration which undergoes transformation to a normal distribution, using a log-logistic distribution (Vicente-Serrano et al. 2010). But once the SPEI is computed, the interpretation of the index follows the same track as the SPI; the inclusion of temperature data results in a different index value (and probability) than the SPI, but the same underlying merits guide the interpretation of SPEI and SPI values alike: direct probabilities across multiple timescales.

11.3 Hydrological Drought Indices

Hydrological drought indices look at water supply conditions, with *water supply* being represented by surface water and groundwater. Due to the transport and storage aspects between surface water and groundwater, hydrological drought indices represent drought over longer timescales than meteorological drought indices. The hydrological drought indices discussed here are the total water deficit and the surface water supply index.

11.3.1 Total Water Deficit

Total water deficit is a straightforward concept. During the course of prolonged drought, there is an accumulated shortage of water. In *meteorological* drought studies, this would be known as the *cumulative precipitation anomaly* and would be the sum of monthly or annual precipitation deficiencies (where each anomaly is the difference between the observed value and its mean). For *hydrological* drought studies, the cumulative anomaly is termed the *total water deficit*. It is the cumulative volume of water which is deficient over the examination period, expressed plainly in units of volume.

The total water deficit may be represented graphically. Figure 11.4 shows a time series depiction of the total water deficit, in which the water supply fluctuates over time. The cumulative deficiency—the drought severity *S*—is represented by the total

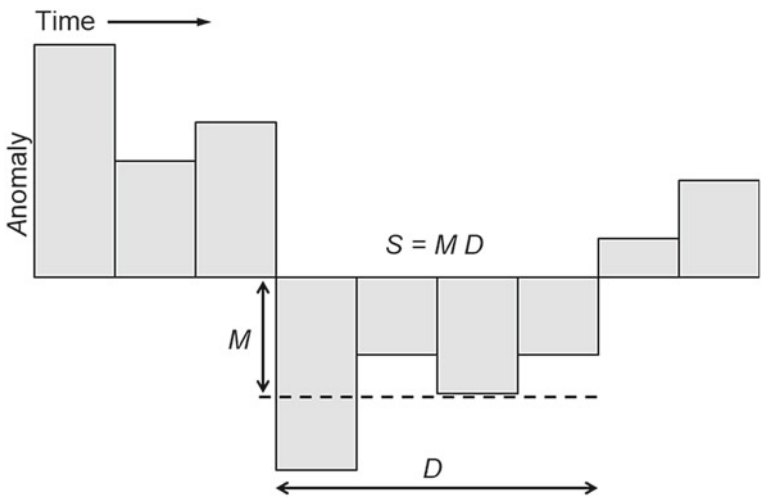

Fig. 11.4 Drought severity represented as the product of drought duration and its average magnitude. When the severity represents a volume of surface or groundwater, the severity is known as the *total water deficit*. Modified from Keyantash and Dracup 2002

barred area beneath the horizontal axis (which is set at the hydroclimatic mean). The water-deficient portion of the time series has a duration D and an average drought magnitude M (Dracup et al. 1980). It should be noted that drought severity, duration and magnitude alternatively appear in the research literature as the run sum, run length and the run intensity,[1] respectively (e.g. Yevjevich 1967). These are fully synonymous terms.

For surface water bodies, such as lakes or reservoirs, the total water deficit is determined by summing the storage anomalies (which may have positive or negative sign). Each anomaly, in turn, is computed by knowing the depth of the reservoir and referencing a depth–volume (or *hypsographic*) curve for the water body. The mean storage is subtracted to reveal each anomaly:

$$V'(t) = V(y(t)) - \bar{V} \tag{11.3}$$

where

V = volume (e.g. km^3 or hm^3)
t = time
y = depth
$\bar{V}$ = mean reservoir volume

Primed quantity is the anomaly.

The total water deficit is the sum of the anomalies during the n months (or years) of the hydrological drought:

$$\text{Total water deficit} = \sum_{t=1}^{n} V'(t) \tag{11.4}$$

The concept of total water deficit also applies to a flowing surface water body, such as a river. However, instead of volume, the principal variable is the discharge Q, possessing units of volume per time (e.g. cubic metres per second). Each discharge value requires multiplication by a time conversion factor T—which relates the denominator of the discharge to the duration of each t—to produce the familiar volumetric units of the total water deficit. For example, if annual mean discharge were expressed in cubic metres per second, and we were tracking a water deficit over n years, $T = 31{,}536{,}000$ s per year. For annually averaged discharge data,

$$\text{Total water deficit} = \sum_{t=1}^{n} V'(t) = \sum_{t=1}^{n} Q'(t) \cdot T$$

[1] Take special note to not inadvertently exchange the words *intensity* and *severity*, as they are distinct terms. Intensity implies the average strength, while severity indicates the cumulative effect. To wit, PDSI does not stand for the Palmer drought *intensity* index.

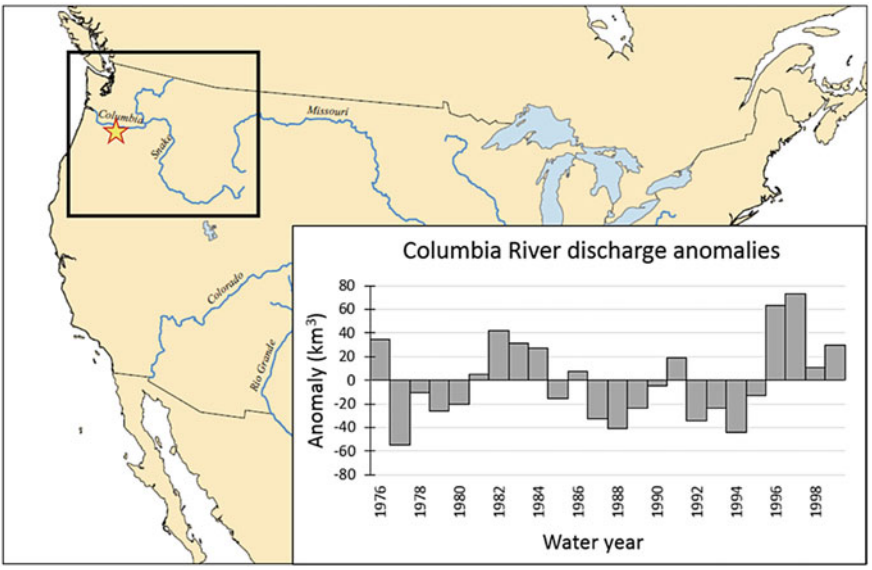

Fig. 11.5 Annual discharge anomalies for the Columbia River, 1976–1999. Modified from Keyantash and Dracup 2002

$$= T \sum_{t=1}^{n} [Q(t) - \bar{Q}] = T \sum_{t=1}^{n} Q(t) - Tn\bar{Q} \tag{11.5}$$

Equation 11.5 is suitable for annual data only. For monthly (or even daily) data, modifications must be made to the summation indices in Eq. 11.5, as the monthly/daily means vary from one datum to the next (i.e. $\bar{Q}$ is not constant across all t).

An example of the total water deficit is given for the Columbia River, a major waterway in the northwest portion of the USA, shown in Fig. 11.5.

At the starred measurement location in Fig. 11.5, the Columbia River has a mean discharge of 5150 m^3/s or 163 km^3 per year. The river experienced three prolonged hydrological droughts during the 24-year period from 1976 to 1999. Each drought had a duration of four years, and all were comparable in terms of severity: the first drought had a total water deficit of 112 km^3, the second had a water deficit of 102 km^3, and the third was the most severe, at 115 km^3. The third drought had a magnitude of 28.8 km^3/yr, and over the four-year duration its total water deficit represented 71% of the mean annual discharge. Thus, the effect of the 1992–1995 hydrological drought was as if the perennial Columbia River stopped flowing for over eight months.

11.3.2 Surface Water Supply Index (SWSI)

Much of the environment in the Western United States is mountainous and/or arid, including a large number of locations subject to rain shadow effects. There is also a seasonal precipitation regime, and the mountains receive a large fraction of their annual precipitation as snowfall, which is redistributed to lower altitudes during the spring and early summer months. In these landscapes, surface water reserves are particularly precious, and several major rivers—such as the Columbia, Colorado and San Joaquin—are in fact *exotic* streams, transporting water from distant environs subject to higher precipitation rates. Without aqueducts and large reservoirs, it would be difficult to support large populations in the region (e.g. Los Angeles, Phoenix and Las Vegas). For these reasons, large dams and surface water reservoirs are critical to the livelihood of the Western United States.

The surface water supply index (SWSI) was developed by Shafer and Dezman (1982) for the Western United States, as a method to judge the availability of surface water supplies. The SWSI is computed for major river basins. In each basin, the typical values of four hydrologic components are used to estimate the overall abundance/deficit of surface water resources. The hydrologic variables are snowpack, precipitation, streamflow and reservoir storage, and are expressed in the following manner (Garen 1993):

$$\mathrm{SWSI} = \frac{\mathrm{aP_{snow}} + \mathrm{bP_{precip}} + \mathrm{cP_{streamflow}} + \mathrm{dP_{storage}} - 50}{12} \tag{11.6}$$

In the above equation, the P values are the percentiles of each hydrological variable, based on the current water conditions. The coefficients *a-d* are the average contributions of each component to the surface water supply, and their sum is unity. The subtraction of 50 centers the data about the median (the 50th percentile), and the division by 12 is an arbitrary scaling which produces index magnitudes that are comparable to the PDSI. In particular, it theoretically bounds the SWSI between + 4.17 and −4.17 (Garen 1993).

The SWSI undergoes different computational procedures in several Western states. For example, in the state of Colorado there are two sets of weights (i.e. values for *a-d*), depending upon the season, while Oregon has coefficients which change on a monthly basis. Garen (1993) thoroughly critiqued the different approaches in which SWSI is computed. He made the cogent argument that if the SWSI is intended to assess surface water supply, perhaps it makes less sense to *directly* include precipitation and snowpack, as those variables will naturally transition to surface water, but are not yet surface water. Instead, Garen (1993) recommended a revised version of the SWSI which was only dependent upon streamflow and reservoir storage, i.e. *actual* surface water. However, he does not discount the value of the four hydrologic variables of the SWSI, for they play a role in river forecasting performed by the National Weather Service of the USA. But he argued that those variables are best utilized as inputs to a hydrological model, which a hydrological drought index, such as the SWSI, surely is not.

Furthermore, Garen (1993) suggested that it makes sense to input model predictions (for future key seasons [e.g. the agricultural growing seasons which require irrigation from surface water supplies]) into the SWSI computation, rather than the actual observational data. For example, a November assessment of the current surface water supply is probably less relevant than a November prediction of the upcoming June water supply, when the surface water resources will need to be tapped to irrigate farmland.

Keyantash (2005) analysed the SWSI values for a 23-year period (1983–2005) in adjacent river basins in Oregon and Idaho; see Fig. 11.6. The climatologies of the two basins are highly similar, but different computational procedures between Oregon and Idaho resulted in somewhat dissimilar SWSI values, which had a correlation of 0.78 during the examination period. In contrast, the SPI values in the two basins exhibited a correlation coefficient of 0.93. Keyantash (2005) concluded that the inter-state comparability of the SWSI is compromised by its non-standardized computational scheme. For these complex reasons, the SWSI has not found broad adoption outside of the region for which it was developed, the Western United States.

Fig. 11.6 Malheur and Weiser basins are adjacent, with highly similar climates (i.e. temperature and precipitation patterns). Nonetheless, their SWSI values differ noticeably due to different computational rules. Modified from Keyantash 2005

11.4 Composite Drought Indices

Composite drought indices consider water deficiencies across multiple compartments of the hydrological cycle. They are germane here because they include both meteorological and hydrological droughts (as well as agricultural drought). Discussed here are two examples, the U.S. Drought Monitor and the aggregate drought index.

11.4.1 U.S. Drought Monitor (USDM)

The U.S. Drought Monitor (USDM) is a weekly drought assessment map produced by scientific experts representing several branches of the US government. This composite index has been in existence since 1999. It is a semi-quantitative analysis of drought conditions across the USA, based on multiple drought indices (such as the SPI, SWSI, PDSI and PDSI variants), percentiles from measured site data (including soil moisture and streamflow), satellite vegetative health imagery, plus field reports from over 450 observers nationwide (USDM 2020). National experts from the National Oceanographic and Atmospheric Administration (NOAA), National Centers for Environmental Prediction (NCEP), National Weather Service (NWS) and the Climate Prediction Center (CPC) weigh in on observational data during weekly meetings and collectively assess US drought conditions. Their findings are compiled into a national map for each week. The processes involved in the weekly creation of the USDM are detailed by Svoboda et al. (2002). Figure 11.7 shows a drought monitor map for US drought conditions on 18 February 2020.

The USDM drought assessments contain four categories of drought intensity, all prefixed with the letter "D" (for dry/drought):

0. Abnormally dry
1. Moderate drought
2. Severe drought
3. Extreme drought
4. Exceptional drought.

The integer ranks of these classifications were originally selected as public-friendly analogues to the familiar Fujita (tornado) and Saffir–Simpson (hurricane) intensity scales (Svoboda et al. 2002). Semi-quantitatively, these numerals can be viewed as roughly representing the integer values of the PDSI and/or SWSI. Similarly, the associated labels bear strong similarity to verbal descriptions attached to the PDSI, rainfall deciles, SPI and SWSI. However, it should be noted that the percentiles associated with the relative classifications do not perfectly match across the various indices, so the non-exceedance probabilities associated with each category should not be assumed to be identical. Svoboda et al. (2002) provide a useful comparison of the various USDM index values with the PDSI and SPI, among others.

While the drought monitor does not explicitly distinguish between agricultural, meteorological and hydrological droughts, it does so implicitly through the use of the

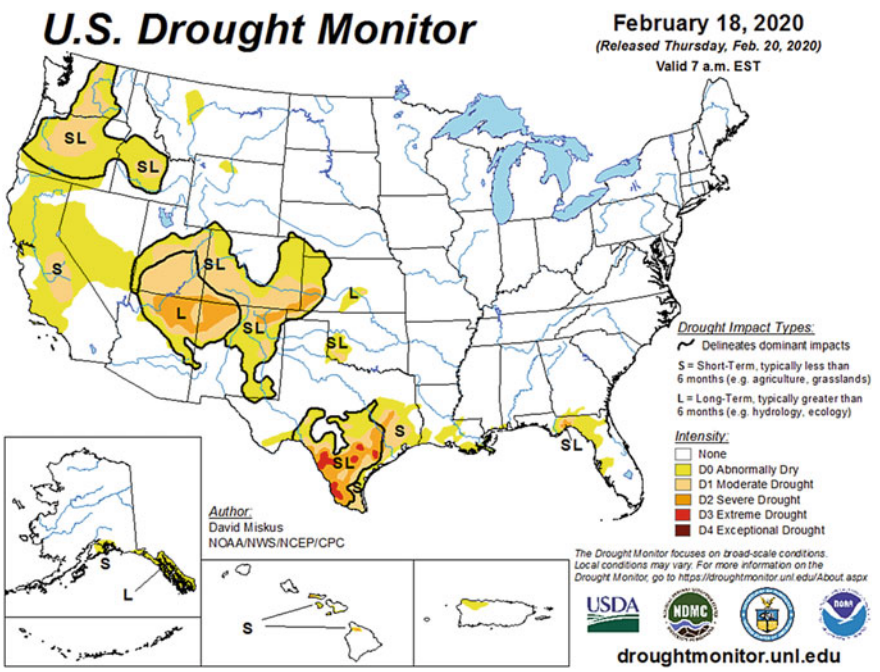

Fig. 11.7 USDM for 18 February 2020

prefixes "S" and "L" to distinguish between short- and long-term impacts, respectively. The "S" is associated with agricultural drought and the "L" with hydrological drought, and both letters could potentially imply meteorological drought, which can occur from short to long time intervals. Furthermore, both letters may appear in the same region, to indicate that there are distinct short-term and long-term drought impacts. Ultimately, USDM data is used to make national agricultural decisions in the USA on farm relief payments, farmer tax deferral decisions, livestock foraging and agricultural loans (USDM 2020).

11.4.2 Aggregate Drought Index (ADI)

The aggregate drought index (ADI; Keyantash and Dracup 2004) is a comprehensive drought index that, in the spirit of SPI, takes a standardized statistical perspective to assess drought. The ADI utilizes diverse observations of water availability in a region of hydroclimatic uniformity, such as a climate division or a river basin. It incorporates observed hydrological data from various geophysical compartments—such as precipitation, evaporation, streamflow and reservoir volume, among other possibilities (viz. soil moisture and snowpack levels; see Fig. 11.8)—to construct a multi-variate assessment of water availability. The anomalies of each variable

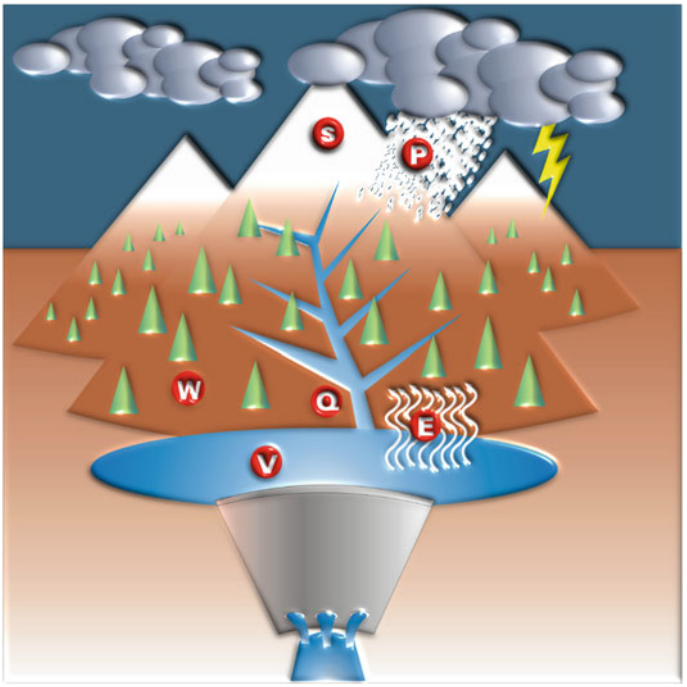

Fig. 11.8 Hydrological variables included in the ADI are precipitation (P), snowpack (s), evaporation (E), soil moisture (W), streamflow (Q), and reservoir storage (V). *Source* Keyantash and Dracup 2004

are subjected to correlation-based principal component analysis (PCA) to extract a common signal of water abundance/deficit from the suite of hydrological observations. In this manner, the ADI extracts the "essential" signal from all of these components, which are all physically related by their participation in the hydrological cycle.

In mathematical terms, the ADI is the standardized anomaly of the first PC of the hydrological data. It is given as:

$$\mathbf{a} = \frac{\mathbf{z}_1}{\sigma_{z_1}}, \quad \mathbf{z}_1 = \mathbf{X}\mathbf{e}_1 \tag{11.7}$$

where

$\mathbf{a}$ = ADI time series for select month (e.g. February)
$\mathbf{z}_1$ = first PC times series (for February)
σ_{z_1} = standard deviation of first (February) PC
$\mathbf{X}$ = (year $\times$ variable) matrix of (February) observational data, expressed as standardized anomalies (mean of zero, unit standard deviation)
$\mathbf{e}_1$ = first eigenvector of the PCA.

The ADI for a selected region is separately computed for each month in the time series (i.e. 12 separate analyses). The monthly segregation allows the observational data anomalies to be judged with respect to the hydroclimatic norm for each month. The monthly ADI values are then recombined into a single chronological time series. More detailed computational instructions are given in Keyantash and Dracup (2004).

The ADI uses only the first principal component due to the unique, advantageous properties of PCA. Principal component analysis produces an alternate expression of the original dataset, possessing as many alternate variables (known as the "principal components" [which are linear combinations of the original variables]) as the original dataset. For example, if six hydrological variables underwent PCA, there would be six created PCs. The full variance—i.e. "information"—of the original dataset is completely replicated by the PCs, with the vital distinction that the bulk of the variance is maximally apportioned to the first PC, with decreasingly less variance in subsequent PCs.

Furthermore, each PC is fully uncorrelated with every other PC (i.e. their correlation coefficients are zero), such that information expressed in one PC is not duplicated by another. Thus, PCA can be a powerful data reduction technique, as latter PCs contribute vanishingly less information to the problem at hand (in this case, water supply across the study region). In the ADI study of three climate divisions in California, Keyantash and Dracup (2004) found that the first PC described an average of 60 per cent of the variance across the 5–6 hydrological variables illustrated in Fig. 11.8 (snowpack was not relevant for all divisions).

A comparison of the ADI and SPI for the San Jacinto river basin of Southern California is shown in Fig. 11.9 for the month of September for years 1943–1998 (Keyantash and Sakata 2012). The ADI values have been composited into 12-month sums to match the 12-month timescale of the SPI (i.e. October through September).

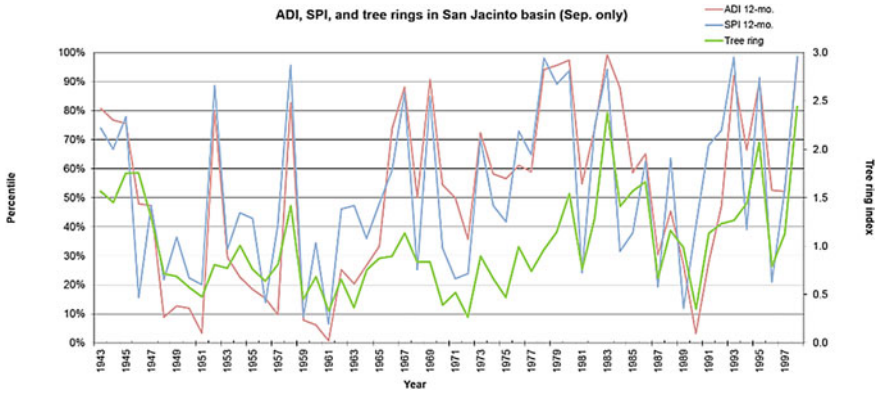

Fig. 11.9 ADI compared to the SPI and a tree ring chronology for a 12-month period, ending in September, for water years 1943–1998 in the San Jacinto river basin of Southern California. Note that the tree ring index values are not percentiles (i.e. the left ordinate is not accurate for the tree ring index). *Source* Keyantash and Sakata 2012

Due to fundamentally different index values, the ADI and SPI values are expressed as percentiles to aid comparability.

Also shown in Fig. 11.9 is a tree ring chronology of bigcone Douglas fir (*Pseudotsuga macrocarpa*) from the same basin. Low values of the tree ring index presumably indicate limited growth due to water deficiency/drought. Overall, the ADI and SPI exhibit tight correlation ($r = 0.81$) for the examined interval, and both qualitatively agree with the tree ring chronology.

Summary

Drought is a complex phenomenon to characterize. There are multiple aspects of water deficiency (such as soil moisture, rainfall and streamflow, to name a few) which are associated with different forms of drought (agricultural, meteorological and hydrological, respectively). These water shortages occur on different minimum timescales, so the lens to assess drought intensity may need to broaden or contract to discern between various drought forms. Yet these timescales may also overlap during droughts of extended duration—a region may simultaneously experience short-term and long-term drought.

Furthermore, the measure of water "deficiency" depends upon the native climate of the region. For example, drought conditions in England would bear little resemblance to a recognized drought in Australia. The anthropological demand for water is another important factor that can exacerbate the impacts of natural drought events.

These latent complexities lead to a variety of research indices to describe drought. For the sake of brevity, this chapter has focused on widely accepted drought indices for meteorological and hydrological drought. It also discussed some composite indices which jointly assess meteorological, hydrological and agricultural drought conditions.

Meteorological drought was discussed in the context of the PDSI, rainfall deciles, SPI and SPEI. Hydrological drought indices were explored through the concepts of the total water deficit and SWSI. The USDM and the ADI were introduced as examples of composite drought indices, with data for the latter being compared to the SPI and a tree ring chronology.

References

Alley WM (1984) The Palmer drought severity index: limitations and assumptions. J Clim Appl Meteorol 23:1100–1109

Australian Bureau of Meteorology (BOM) (2020) Drought: rainfall deficiencies and water availability. http://www.bom.gov.au/climate/drought/. Accessed 27 May 2020

Box GEP, Cox DR (1964) An analysis of transformations. J Royal Stat Soc: Ser B 26(2):211–243

Dracup JA, Lee KS, Paulson EG Jr (1980) On the definition of droughts. Water Resour Res 16:297–302

Garen DC (1993) Revised surface-water supply index for the western United States. J Water Res Plan Man 119:437–454

Gibbs WJ, Maher JV (1967) Rainfall deciles as drought indicators. Bull 48, Australia Bureau of Meteorology, Melbourne

Guttman NB (1999) Accepting the standardized precipitation index: a calculation algorithm. J Amer Water Resour Assoc 35:311–322

Guttman NB, Wallis JR, Hosking JRM (1992) Spatial comparability of the Palmer drought severity index. Water Resour Bull 28:1111–1119

Hayes M, Svoboda M, Wall N et al (2011) The Lincoln declaration on drought indices: universal meteorological drought index recommended. Bull Amer Meteor Soc 92(4):485–488. https://doi.org/10.1175/2010BAMS3103.1

Heim RR Jr (2000) Drought indices: a review. In: Wilhite DA (ed) Drought: a global assessment. Routledge, New York, pp 159–167

Keyantash J (2005) Hydrological and meteorological drought severity in Oregon: comparisons between the surface water supply index (SWSI) and standardized precipitation index (SPI). Eos Trans AGU 86(52), Fall Meet Suppl, Abstract H33B-1384, presented at 2005 Fall Meeting of AGU, San Francisco, CA, 5–9 Dec 2005

Keyantash J, Dracup JA (2002) The quantification of drought: An analysis of drought indices. Bull Amer Meteor Soc 83(8):1167–1180

Keyantash JA, Dracup JA (2004) An aggregate drought index: assessing drought severity based on fluctuations in the hydrologic cycle and surface water storage. Water Resour Res 40:W09304. https://doi.org/10.1029/2003WR002610

Keyantash JA, Sakata C (2012) Multiple timescale comparison of the aggregate drought index (ADI), the standardized precipitation index (SPI), and tree rings in Southern California. Abstract H41B-1178, presented at 2012 Fall Meeting of AGU, San Francisco, CA, 3–7 Dec 2012

Keyantash J, National Center for Atmospheric Research (NCAR) staff (eds) (2018) The climate data guide: Standardized precipitation index (SPI). https://climatedataguide.ucar.edu/climate-data/standardized-precipitation-index-spi. Last modified 7 Aug 2018

Kinninmonth WR, Voice ME, Beard GS et al (2000) Australian climate services for drought management. In: Wilhite DA (ed) Drought: a global assessment. Routledge, New York, pp 210–222

McKee TB, Doesken NJ, Kleist J (1993) Drought monitoring with multiple timescales. Proc Eighth Conf on Applied Climatology, Amer Meteor Soc, Anaheim, CA, pp 179–184

National Centers for Environmental Information (NCEI) (2020) Historical Palmer drought indices. https://www.ncdc.noaa.gov/temp-and-precip/drought/historical-palmers/. Accessed 26 July 2020

Palmer WC (1965) Meteorological drought. Research paper no. 45, Weather Bureau, U.S. Dept. of Commerce, Washington, D.C

Shafer BA, Dezman, LE (1982) Development of a surface water supply index (SWSI) to assess the severity of drought conditions in snowpack runoff areas. Proc 50th Western Snow Conf, Reno, NV, p 164–175

Svoboda M, LeComte D, Hayes M et al (2002) The drought monitor. Bull Amer Meteor Soc 83(8):1181–1190

United States Drought Monitor (USDM) (2020) What is the U.S. drought monitor? https://droughtmonitor.unl.edu/About/WhatistheUSDM.aspx. Accessed 26 July 2020

Vicente-Serrano SM, Beguería S, López-Moreno JI (2010) A multiscalar drought index sensitive to global warming: the standardized precipitation evapotranspiration index. J Clim 23:696–1718. https://doi.org/10.1175/2009JCLI2909.1

Wilks DS (1995) Statistical methods in the atmospheric sciences: an introduction. Academic Press, San Diego

World Meteorological Organization (WMO) and Global Water Partnership (GWP) (2016) Handbook of drought indicators and indices (Svoboda M, Fuchs BA). Integrated Drought Management Programme (IDMP), Integrated Drought Management Tools and Guidelines Series 2, Geneva

Ye L, Hanson LS, Ding P et al (2018) The probability distribution of daily precipitation at the point and catchment scales in the United States. Hydrol Earth Syst Sci 22:6519–6531. https://doi.org/10.5194/hess-22-6519-2018

Yevjevich VM (1967) An objective approach to definitions and investigations of continental hydrologic droughts. Colorado State University, Hydrology Paper 23, Fort Collins, CO

Chapter 12
Water Resources Management—An Indian Perspective

K. Vohra and M. L. Franklin

12.1 Background

12.1.1 Water Availability

India has an agricultural economy and remains the principal source of livelihood for about 54.6% (MSPI 2018) of the population. Every year, the precipitation in India is about 4000 BCM. The average annual water availability is 1999 BCM, of which 1123 BCM is the total utilizable water resources due to various constraints of topography, distribution, etc. India has a population of 1.31 billion (about 17.7% of the world's population) (NABARD and ICRIER (2018a), and the annual per capita water availability is 1,526 m^3/person (NABARD and ICRIER (2018b)), making India a water-stressed country.

12.1.2 Water Demand

The estimated requirements of water for various purposes, including irrigation as per the National Commission on Integrated Water Resources Development (NCIWRD) Report, 1999, are given in Table 12.1. Water demand by 2050 is expected to increase to 1180 BCM, surpassing the utilizable water resources.

K. Vohra (✉) · M. L. Franklin
Department of Water Resources, River Development and Ganga Rejuvenation, Ministry of Jal Shakti, India
e-mail: kush.vohra@gov.in

M. L. Franklin
e-mail: mlfranklin-cwc@gov.in

© The Author(s), under exclusive license to Springer Nature Singapore Pte Ltd. 2021

A. Pandey et al. (eds.), *Hydrological Aspects of Climate Change*,
Springer Transactions in Civil and Environmental Engineering,
https://doi.org/10.1007/978-981-16-0394-5_12

Table 12.1 Water demand for various purposes in India

Sector	Water demand in BCM			
	2010	%	2050	%
Irrigation	553.8	78	802.4	68
Domestic	42.6	6	112.1	9.5
Industry	35.5	5	82.6	7
Power	21.3	3	70.8	6
Others	56.8	8	112.1	9.5
Total	710		1180	

12.1.3 Use of Water for Irrigation

The annual water withdrawal for irrigation is 553.8 billion cubic metre (BCM). In paddy irrigation alone, there is a yearly withdrawal of 248.31 BCM water in 25.354 million hectares (Mha) (in 15 major rice-producing states) out of 26.524 Mha under paddy irrigation in India (NABARD and ICRIER 2018b). In other words, 45% of the irrigation water withdrawal is used for paddy, which occupies 26% of the gross irrigated area of the country.

The average farm applied irrigation water for paddy in India is about 980 mm. FAO has estimated the crop water requirement for paddy as 400–700 mm (average: 550 mm) (FAO 1986). An average of 550 mm of water to irrigate 25.345 Mha of paddy would require only 139.40 BCM of water (56% of what is presently being used). Thus, an annual saving of 108.91 BCM could irrigate an additional 19.80 Mha with paddy (at 550 mm application) that could potentially yield an additional production of 71.28 MT (taking the average yield of paddy as 3.6 ton /Ha) (NABARD and ICRIER 2018b), adding over 25% to the food grain production. That is only an example of additional paddy that could be produced by saving as above. If judicious cropping pattern is used, the increase in production of various food grains could be much more if water consumption in paddy field is rationalized.

12.1.4 Irrigation Potential Created (IPC) and Irrigation Potential Utilized (IPU)

Out of India's 328.7 Mha geographical area, agricultural land /cultivable land is 182 Mha, the net sown area is 139.9 Mha and gross cropped area is 194.4 Mha with a cropping intensity of 138.9% (SIA 2016). Out of the net sown area of 139.9 Mha, the net irrigated area is only 68.383 Mha (SYBI 2017) with the gross irrigated area being 95.772 Mha (SYBI 2017) (140% irrigation intensity).

The ultimate irrigation potential (UIP) in India is about 139.9 Mha. According to the National Perspective Plan of the Ministry of Jal Shakti, an additional potential of

35 Mha (Planning Commission 2009) may be created through the implementation of Inter-Basin Water Transfer (IBWT) taking the UIP to 174.9 Mha. Against this, the irrigation potential created (IPC) is 112 Mha (SIA 2016) (as on 2015-16) and the irrigation potential utilized (IPU) or gross irrigated area is just 95.772 Mha leaving a gap of 16.228 Mha (14.5%) between IPC and IPU which needs to be bridged. The main reasons for such gap are improper maintenance of canal systems, changing pattern of land use, lack of participatory management, no /inadequate command area development, absence of field channels for last-mile connectivity, deviation from planned initially cropping pattern, more utilization by farmers in upper reaches, etc.

12.1.5 Water Use Efficiency

The irrigation efficiency for surface and groundwater stands at about 25–35% (SIA 2016) and 60–75% (NABARD and ICRIER 2018b), respectively. Low irrigation efficiency leads to excess water use in irrigation and thereby a low irrigation water productivity in agriculture (CWC 2014). Increasing efficiency in the irrigation sector can make significant gains in water availability.

Micro-irrigation is a growing popular technique to save water. Unlike flood irrigation, where water is lost through seepage in conveyance and evaporation, micro-irrigation leads to water saving, aids soil health management and prevents water logging. Micro-irrigation potential in the country is estimated to be 69.5 Mha, whereas only about 10 Mha has been covered under micro-irrigation so far, leaving enormous scope for its expansion. The use of underground pipelines instead of open channels increases the water use efficiency by cutting off evaporation losses. Automation in water distribution systems also serves to enhance water use efficiency.

12.1.6 Participatory Irrigation Management

Participatory irrigation management (PIM) is the cornerstone in effective water management by involving the stakeholder farmers in planning, operation and maintenance of irrigation systems and associating them right from planning of irrigation in the command area, canal maintenance, levying water tax and settlement of disputes through the formation of Water Users' Association (WUA). So far, seventeen states in India have enacted PIM-related acts. 84,779 WUAs have been formed in the country for water management in about 17.84 Mha command area. However, the performance of PIM in India is yet to reach the level to be effective.

12.1.7 Traditional Water Harvesting Systems

Water harvesting has been in India since antiquity. Various structures and conveyance systems specific to the culture and region are prevalent since time immemorial. Some of the notable features were:

- Direct collection of rain from rooftops and open community lands and stored in tanks or artificial wells
- Harvesting rainfall–runoff by diverting water from swollen streams to store in various water bodies.

Some of the region-specific water harvesting systems are:

Paar system: This is a popular practice of harvesting water in west Rajasthan, which faces frequent drought. The paar is a structure where the rainwater from the catchment of the structure percolates into sandy soil. Usually, six to ten structures are constructed in a paar. Rainwater, so harvested by this system, is known as Patali paani.

Saza Kuva: Saza kuva is a well which is owned and used by a community (saza means partner), and is a popular irrigation source in the Aravalli hills of eastern Rajasthan. The soil excavated in making the well pit is used to construct a platform that serves as a foundation to accommodate the water lifting equipment. Farmers mostly take up the construction of saza kuva with adjacent landholdings.

Johad: These are earthen check dams to hold and conserve rainwater, thus promoting percolation and groundwater recharge. From 1984 onwards, about 3000 such structures in over 650 villages in Rajasthan were revived resulting in an overall rise in groundwater level by about 6 metres and an increase in the forest cover by 33%. Five rivers that used to go dry immediately following the monsoon have now become perennial, like the River Arvari.

Talab/Bandhis: Talabs or reservoirs may be natural or man-made. A reservoir with a low water spread is termed talai; a medium-sized lake is a bandhi or talab, and sagar or samand for bigger lakes. These reservoirs are used for irrigation and drinking purposes. When these reservoirs dry up, rice is grown on the pond beds.

Pat: This system essentially diverts water from hill streams into irrigation channels called pats which are designed according to the terrain. The pat system is widely used in Jhabua district of Madhya Pradesh.

12.2 Traditional Irrigation Systems

India has been an agrarian country through the ages, and the agricultural sector has always been the main concern for water management. Irrigation systems have been developed over the years and notable among these are:

Irrigation systems of Indus Valley Civilization took advantage of the flood season by promoting rainwater harvesting. This technology was used extensively at that time but nearly forgotten in the twentieth century.

The Rigvedas mention a system of ring wells where wells once dug never run dry. The water was lifted and fed into channels and further into field distributaries. Extracts from the Maurya Empire era in the third century BCE mention that the state charged farmers for irrigation services, indicating water usage accountability.

Araghatta system /Persian wheel was used to lift water from open wells and is cited in the Panchatantra (third Century BCE). Men, bullocks, elephants or camels were employed to lift water by the Araghatta system.

Cholan tank irrigation system was an effective system of water management through tanks at the village level. A large tank called Solagangam was built by Rajendra Chola in his capital city Gangaikonda Cholapuram. At nearly 26 km long, it had sluices and canals for irrigating the surrounding region. Another large lake of this era, a vital irrigation source even today, was the Viranameri in South Arcot district founded by Parantaka Chola.

The Western Yamuna Canal excavated and renovated during 1335 CE is still used for irrigation today.

Kakatiya tank irrigation system brought irrigation facilities to the Deccan. The Kakatiya kings themselves constructed some tanks apart from the thousands of others built by ministers and subordinate chiefs. The most important piece of work in the construction of a tank was always the erection of an embankment strong enough to withstand the water's pressure impounded in it. One of the most revolutionary features was the interlinking of tanks to form a network of tanks where surplus tanks would supply to downstream tanks through a canal network.

12.3 Green Revolution in India

The Green Revolution marks the period between 1960 and 1980 when agriculture in India became industrialized with the adoption of technology and high-yielding variety (HYV) seeds, pesticides, fertilizers and irrigation facilities. As a result, food grain production increased significantly.

The revolution pioneered in helping the country to produce necessary crops within the country instead of depending on imports with often biased foreign policies.

12.3.1 Water Scenario Post the Green Revolution

After the Green Revolution period, the nation witnessed a continued increase in agricultural water use. On average, India receives about 1200 mm of rainfall every year, which cannot be termed as less than the general requirement. However, its

spatial and temporal variation makes many areas witness extreme water stress conditions. About 78% of the freshwater available in the country is used up by agriculture. A mismatch in the cropping patterns with available water resources in various states causes most water-related issues, including depletion of the groundwater tables. According to a study by Indian Council for Research on International Economic Relations (ICRIER), water-guzzling crops like paddy and sugarcane are grown in states like Maharashtra, Uttar Pradesh (UP) and Punjab, where water availability is low. Maharashtra produces 22% of India's total sugarcane, while Bihar produces only 4% despite having a better water resource position. Further, nearly all of the sugarcane crop in Maharashtra irrigated, despite the severe water crisis in various parts of the state. The ICRIER study shows that from a perspective of irrigation water productivity, the relatively water-surplus states like Bihar and eastern Uttar Pradesh should be growing more sugarcane than Maharashtra, Andhra Pradesh, Tamil Nadu and Karnataka.

A similar scene emerges with the other water-guzzling crop, paddy. Nearly 100% of the paddy cultivated in Punjab is irrigated. It uses more than twice the amount of water used in West Bengal and three times the water than Bihar, to produce each kg of rice. Further, in Punjab, 80% water for paddy irrigation is extracted from groundwater. This has resulted in the groundwater of 76% of administrative blocks in Punjab being overexploited.

Keeping in view that 82% of Punjab blocks are overexploited /critical /semi-critical, we need to look for various solutions for irrigation to be sustainable in the long run. The traditional practice of flood irrigation should be replaced by micro-irrigation. Using a seed variety that requires less water, employing conventional and eco-friendly farming methods requiring less water, and changing to low water-intensive crops in regions of low rainfall, are some steps that need to be taken to reduce overconsumption of water in agriculture.

Additionally, efforts to augment groundwater table, viz. rainwater harvesting, artificial groundwater recharge, etc. need expansion. Percolation tanks, farm ponds, man-made reservoirs and dams also contribute to increase groundwater recharge. The various traditional water conservation practices have proven to be a saving grace at this stage.

12.4 Present-Day Relevance of Traditional Water Conservation Practices

12.4.1 Jal Mandir (Gujarat)

Jal Mandirs or stepwells are wells constructed across Gujarat from the eleventh through the sixteenth century CE, in which water is made accessible by descending a set of steps. It can have multiple levels, and water is raised across the levels as a bullock turns the water wheel. A primary difference between stepwells and tanks or

conventional wells was that people could reach the groundwater and carry out the well's maintenance. Deep trenches were dug into the ground in areas with abundant groundwater. These trenches' walls are lined with stone blocks, which also served as stairs towards the water. The stepwells allowed water access for general public for various purposes.

The step wells are usually recharged from surrounding surface water sources, viz. reservoirs, rivers, streams, canals, etc. One highlight of the wisdom prevalent back then was that even during dry spells, most wells still had water in them. Many wells are linked to phreatic aquifers of different formations like basaltic, phyllite, alluvial, etc.

The concept of Jal Mandirs is very pertinent in those areas where groundwater table is high and municipal supply is not assured. In places where electric supply is a limitation, stepwells prove to be a reliable source of water for the people.

Some examples of Jal Mandirs are:

- Khodiayar Mata ki Vav—in Bareja village, Daskroi Taluk of Ahmedabad District
- Tintoi Jal Mandir in Tintoi village, Modasa Taluk, Aravalli District
- Kohivav Jal Mandir in Moti Mori village, Meghraj Taluk, Aravalli District.

In view of their architectural heritage along with their role in water conservation, the Gujarat government undertook a drive from 2007-08 to 2011-12, to clean, revive and rejuvenate these "Jal Mandirs". About 1200 Jal Mandirs were identified across the state, and several stepwells were renovated under the Jal Mandir Yojna.

12.4.2 Khatri, Kuhl (H.P., J&K)

Khatris are pits with a spread of around 10 × 12 feet and 6 feet deep carved into hard rock mountains. The cost of construction is about Rs. 10,000–20,000 per pit. Khatris are found in Mandi, Kangra and Hamirpur districts of Himachal Pradesh.

Under the Mahatma Gandhi National Rural Employment Guarantee Act (MGNREGA), 2005, many of these traditional structures have been renovated, which have yielded benefits like increase in agricultural revenue and the prevention of flash flood soil erosion in various villages of Himachal Pradesh and Jammu and Kashmir.

12.4.3 Zabo (Nagaland)

In Nagaland, the word zabo implies impounding runoff and is also termed the ruza system. The system is a combination of water conservation with afforestation and cultivation.

Zabos are found even today, in villages like Kikruma which are situated on a high ridge. Although the area receives good rainfall, drinking water is still an issue as when the rain falls, the water runs off along the slope. However, with the construction of

zabos the rainfall–runoff is made to pass through a series of terraces where water is collected in pit-like structures and then towards the foothills where paddy fields are located.

In the Nagaland State Action Plan on Climate Change, the pivotal thrust for storing surplus water made available on account of excess precipitation during extreme events is to explore the possibility and effectiveness of expanding various traditional water harvesting practices like the zabo.

12.4.4 Eri, Ooranis (T.N.)

About a third of the irrigation in Tamil Nadu is by eris or tanks. Their role is crucial to the maintenance of ecological balance and serves as flood-mitigation measure by reducing soil erosion and runoff during high rainfall. The eris also help in replenishing groundwater in the nearby region. Without eris, paddy could not have been cultivated in the water-deprived state.

Ooranis are tanks in regions of non-uniform topography to contain just sufficient water to cultivate small parcels of land surrounding them. These tanks are usually much smaller in size than the eri.

Recognizing the importance of these structures in the water-scarce state, Government of Tamil Nadu has partnered with universities and organizations in rejuvenating eris and ooranis through creation of micro-finance groups. Similar activities are also being taken up by Madras Atomic Power Station and other organizations as part of their Corporate Social Responsibility.

12.4.5 Dongs (Assam)

Dongs are ponds constructed in Assam that are used for water harvesting and irrigation. The dong system is vital for hundreds of villages situated on the Indo-Bhutan border in Baksa district of Assam. Community-managed committees are looking after the dong system and follow traditional water management practices to ensure judicious distribution of the water.

12.4.6 Katas, Mundas and Bandhas (Odisha and M.P.)

These were the primary irrigation sources in the earlier tribal kingdom of the Gonds during the fourteenth and fifteenth century CE (now in Madhya Pradesh and Orissa). A kata is constructed by forming an earthen embankment across a stream to create some pondage. The undulations of the topography usually determine its shape.

12.4.7 Surangam (Kerala)

In the terrain of Kasargod district of Kerala, the river discharge is high during the monsoon and low in the dry period. Hence, apart from groundwater, people here depend on a water harvesting structure called surangam.

Excavation of surangam is carried out in hard laterite rock formations which continues until sufficient water is struck. Once water seeps out it flows out of the tunnel and fills a pit dug outside the surangam.

The width of a surangam is around 0.45–0.70 m with a depth of about 1.8–2.0 m. Depending on the terrain, its length ranges from 3 to 300 m. Sometimes, secondary surangams are excavated within the primary. If the length of the surangam is high, several vertical air vents /shafts of size 2 m $\times$ 2 m with varying depths are provided with a pitch distance of 50–60 m to ensure atmospheric pressure inside.

12.4.8 Bawdi /Jhalara (Gujarat /Rajasthan /Karnataka)

These are square-shaped stepwells with arches, motifs, rooms and other elaborate structures which not only serve for water storage but also used for water sports. These stepwells usually last for about 20–30 years.

Renovation of these structures in Rajasthan, Karnataka and Gujarat has restored their water storing capacity, and during the dry periods, water is drawn using electric pumps.

12.5 Water Management Initiatives in Recent Times

Technological interventions such as use of Underground Pipelines in Prioritized Projects under PMKSY-AIBP, Solar Panels Over Open Channel Canals, Canal Automation, Command Area Development and Water Management (CADWM) Works and Extensive Use of Micro Irrigation under Per Drop More Crop (PDMC) are being implemented by the GoI and state governments. Details of these interventions are available in Vohra and Franklin (2020).

12.6 Initiatives by Various States

Restoration of Tanks under Mission Kakatiya of Telangana State, Jalyukt Shivar Abhiyan of Maharashtra State and Management Approach in Madhya Pradesh State are some notable initiatives by the state governments (Vohra and Franklin 2020).

12.6.1 Sujalam Sufalam Jal Abhiyan (SSJA) in Gujarat

The Government of Gujarat launched the Sujalam Sufalam Jal Abhiyan (SSJA) in 2018 to increase the state's water holding capacity and decrease the dependence on groundwater. In addition to creating more sources for storing rainwater, the campaign provides employment to the poor under MGNREGA. Further, the soil obtained after deepening of check dams, reservoirs and ponds under SSJA is provided free of cost to farmers so that they can use it as manure for their fields. A number of works like deepening of ponds, desilting and repairing of check dams and desilting of reservoirs, etc., are undertaken under this campaign every year. In 2020, the SSJA was flagged off on 20 April and ended on 10 June. Despite the crisis due to the novel coronavirus, 11,072 works were completed with a generation of 30.4 lakh man-days of employment and creation of 52 thousand cubic metre additional storage.

12.6.2 Mukhyamantri Jal Swavlamban Abhiyan of Rajasthan State

Rajasthan has 10% of India's geographical area and about 5.5% of its population but only 1% of the water resources. Excess withdrawal of groundwater caused a rapid decline of groundwater tables. Over 90% of the 249 blocks in the state are categorized as unsafe or dark zones with excess salinity and fluoride in the groundwater making it unfit for consumption. In 2014, the state government started a pilot project on the Four Waters concept in select villages of Jhalawar district of Rajasthan. The concept involves adoption of inexpensive technology that increases recharge of fourfold and provides three times the benefit as conventional models. The concept focuses on conserving the available runoff in by proper preparation of catchment areas, extensive implementation of water harvesting structures, and the creation of new structures and renovation of non-functional ones. In the pilot project, many percolation tanks were made in the watershed areas to trap the rain runoff. This helped in checking erosion and increasing soil moisture, making it more productive. Groundwater increased significantly, and the villages had sufficient water for drinking and irrigation even for several months after the monsoon. Agricultural output increased and so did the income of the farmers.

To extend the model's success across the state, the state government started "Mukhyamantri Jal Swavlamban Abhiyan (MJSA)" in 2016. It aims at making villages self-sufficient in terms of water by providing a sustainable solution. This was achieved through renovation of non-functional rainwater harvesting (RWH) structures and the creation of new ones along the rainwater runoff route. The mission also included intensive afforestation and pasture development near villages. In the first year, works were carried out in 3529 villages and over 6000 villages were included every year for the next three years benefitting 21000 villages of the state. MJSA

was truly a people's mission encompassing local residents, servicemen, government officials, students, social and religious groups and people from all walks of life volunteering in large numbers through cash, kind and service out construction works.

12.6.3 Pani Bachao, Paise Kamao in Punjab

The Punjab state government announced the "Pani Bachao, Paise Kamao" Scheme or the Save Water Earn Money project on the 14 June 2018. It is a unique scheme that will enable farmers to save water and earn money for every unit for electricity they save. It will in turn cut down power shortage in the state. The Pani Bachao Paise Kamao Scheme is targeted towards proper utilization and conservation of water and electricity. Some of the key features of the scheme are:

- Installation of metre by state government.
- No fee for the farmers.
- Two hours of extra electricity supply for those people who will enrol under this water-saving scheme.
- The farmers will receive Rs. 4 for every unit of electricity that they save as subsidy.
- The state government will transfer the money into the bank account of agricultural workers.
- The state will fix an optimum limit of power that every farmer will be expected to use each day.

12.6.4 Mera Pani Meri Virasat in Haryana

To save water for our future generations, Haryana's government has launched "Mera Pani Meri Virasat" Scheme for diversification from maize /cotton /millet /pulses /horticulture crops in 1.00 lakh hectares of land. Farmers receive at least 50% of the paddy area (maize /cotton /bajra /pulses) in at least 50% of the area in last year's paddy area in eight blocks (Ratia, Sirsa, Sewn, Guhla, Pipli, Ismailabad, Babain and Shahabad/Horticulture) to grow and adopt diversification. The objective of crop diversification through the above scheme is to promote two latest technologies with sustainable farming, increase production and choose crop options to increase the farmer's income.

The objectives of the scheme are:

- To reduce the area under high demand for crops in Haryana
- Promoting alternative crops for sustainable farming and motivating the latest technologies
- Promoting conservation of resources
- Maintaining the groundwater level

- To save soil health from the ill effects of the paddy–wheat cycle and to maintain the balance of micronutrients in the soil
- To give the farmer an alternative to the crops that are more profitable, by removing them from the paddy–wheat cycle cultivation.

To promote mechanization under the Mera Pani Meri Virasat Scheme and for maize crop sowing, the department has ensured adequate availability of maize planter, multi-crop planter and pneumatic planter. Under various mechanization schemes, grants of 40–50% are also being given on these devices.

12.7 Participatory Irrigation Management (Pim) and Initiatives by Communities and Individuals

12.7.1 Ralegan Siddhi

Ralegan Siddhi is an arid region of Maharashtra which receives an annual rainfall of about 450–650 mm. In 1975, this place was poverty-stricken where water conservation was neglected leading to excessive runoff resulting in soil degradation. This led to drying up of wells up to depths of 400 m, severely impacting cultivation. This drove 70% of the households below poverty line. Availability of drinking water and fodder for livestock were also impacted. People migrated out and many who stayed back resorted to alcoholism causing the poverty situation to escalate.

A revolution was brought about by Shri Baburao Hazare or "Anna" (big brother). He focused on water conservation and harvesting and spread his ideas with the community to get the villagers involved. With a resolve for restoration of water, he undertook a community project for the construction of nalla and contour bunds, trenches and percolation tanks to minimize runoff.

Digging wells near the tanks was a challenge as the people did not have much money. To tide over this issue, Anna drew 16 poor farmers holding continuously adjacent plots, and they dug a mutually shared well. Labour was offered voluntarily by the farmers, and Anna borrowed funds for materials. The well provided a steady water supply to 35 acres, and subsequently, eight such community wells were constructed over the following two years. After all the wells were constructed along with the water harvesting structures, an annual irrigation was possible in 700–800 acres. To secure even more water for the village, gully plugs and contour trenches were built, and extensive afforestation was carried out all over the village.

Ralegan Siddhi today is free from water shortage, and crops can be grown year round. Production of milk increased fourfold, and the economy of the area has grown manyfold.

12.7.2 Hiware Bazar

Hiware Bazar in Ahmednagar district of Maharashtra receives very low rainfall (below 380 mm) every year. Realizing the need for water conservation, the village Sarpanch, Mr. Popatrao Pawar gave thrust to rainwater harvesting and set up water conservation and management programme from 1990 onwards. In 1993, the panchayat and the villagers undertook the regeneration of catchment areas of the village wells along with that of 70 ha of forest area that was completely degraded. Forty thousand contour trenches were built around hilly terrain to preserve runoff from slopes, thus recharging groundwater. A massive plantation drive of 45,000 trees was carried out spread over 30 ha, which could hold 15 lakh litres of water. The entire forest area of 150 ha was brought under continuous contour trenching (CCT) to conserve about 225,000 cu. m of water (Vohra and Franklin 2020).

As a result of these efforts, the village's water table rose from 70–80 feet to 20–25 feet. The monthly per capita income increased from Rs. 830 in 1995 to Rs. 30,000 today as employment opportunities also increased (Vohra and Franklin 2020).

12.8 Efforts Towards Water Conservation—Initiatives by Central Government

12.8.1 Pradhan Mantri Krishi Sinchayi Yojana (PMKSY)

GoI launched Pradhan Mantri Krishi Sinchayee Yojana (PMKSY) during 2015–16 to bring convergence of investments in irrigation by integration of the following four components:

- Accelerated Irrigation Benefits Programme (AIBP)
- Har Khet Ko Pani (HKKP)
- Per Drop More Crop (PDMC)
- Integrated Watershed Management Programme (IWMP).

The focus is on improving water use efficiency at farm level and bridging the gap between irrigation potential and utilization.

The funding of AIBP projects was devised through creation of a Long Term Irrigation Fund (LTIF). Approval was given to draw funds under LTIF for both central and state shares as per requirements from time to time to avoid any delay on account of financial requirements (Vohra and Franklin 2020).

12.8.2 Mahatma Gandhi National Rural Employment Guarantee Act (MGNREGA), 2005

Mahatma Gandhi Employment Guarantee Act, 2005, aims to guarantee the "right to work". It aims to assure security of livelihood in rural areas by providing at least 100 days of wage employment a year to every household whose adult members volunteer to do unskilled manual work.

Another aim of MGNREGA is to create rural infrastructure assets like roads, canals, ponds and wells. If an applicant does not get a job within 15 days of application, they would receive unemployment allowance.

Since its enactment, MGNREGA has contributed in the creation of a multitude of assets in water conservation. Under MGNREGA, micro- and minor irrigation works and creation, renovation and maintenance of irrigation canal and drains, etc., works related to renovation of traditional water bodies, desilting, etc., are taken up. During 2014-19, a total of Rs. 40,434.36 crore was spent on renovation of water bodies, desilting works and construction and repairs of minors and farm ponds.

12.8.3 Jal Shakti Abhiyan

Hon'ble Prime Minister of India wrote letters to Sarpanch (Village Head) of more than 2,30,000 villages in India for taking various measures for water conservation. Hon'ble Prime Minister also appealed to the nation for water conservation in his "Mann Ki Baat" on 30 June 2019. Water Conservation Campaign "Jal Shakti Abhiyan" was launched on 1 July 2019 to cover 1592 water-stressed blocks in 256 districts in two phases, viz. Phase I (1 July to 15 September 2019) and Phase II (1 October to 30 November 2019) through the involvement of central and district officials along with people's participation in five intervention areas:

- Water Conservation and Rainwater Harvesting
- Renovation of Water Bodies /Tanks
- Reuse and Recharge Structures
- Watershed Development
- Intensive Afforestation.

The Jal Shakti Abhiyan (JSA) has resulted in the creation of over 3.5 lakh water conservation measures in 256 districts. Out of these, 1.54 lakh are of water conservation and rainwater harvesting measures, 20,000 related to the renovation, rejuvenation and restoration of traditional water bodies, over 65,000 are reuse and recharge structures and 1.23 lakh are watershed development projects. About 2.64 crore people participated in the campaign making it a Jan Andolan.

12.8.4 Catch the Rain

National Water Mission's (NWM) campaign "Catch the Rain" with the tagline "Catch the rain, where it falls, when it falls" is to nudge the states and stakeholders to create appropriate Rainwater Harvesting Structures (RWHS) suitable to the climatic conditions and subsoil strata before monsoon.

Under this campaign, drives to make check dams, water harvesting pits, rooftop RWHS, etc.; removal of encroachments and desilting of tanks to increase their storage capacity; removal of obstructions in the channels which bring water to them from the catchment areas, etc.; repairs to stepwells, and using defunct borewells and unused wells to put water back to aquifers, etc., are to be taken up with the active participation of people.

To facilitate these activities, states have been requested to open "Rain Centres" in each district—in collectorates/municipalities or GP offices. During this period, these Rain Centres will have a dedicated mobile phone number and will be manned by an engineer or a person well trained in RWHS. This centre acts as a technical guidance centre to all in the district as to how to catch the rain, as it falls, where it falls.

Efforts should be made so that all buildings in the district should have rooftop RWHS and that maximum quantity of rainwater falling in any compound should be impounded within the compound itself. The basic aim should be that no or only limited will water to flow out of the compound. This will help in improving soil moisture and rasing groundwater table. In urban areas, it will reduce water gushing onto roads, damaging them, and will prevent urban flooding.

Under the "Catch the Rain" initiative, all water bodies in the districts are to be enumerated (checked with revenue records) and encroachments to be removed.

All District Collectors, Heads of institutions like IIMs, IITs, Central Universities and Private Universities, Chairmen of Railways, Air Port Authority, PSUs, DGs of Central Armed Police Force, etc., having large tracts of lands with them have been requested to take steps to "Catch the Rain".

12.9 Conclusion

From the above discussion, it is seen that India has had a rich tradition of water conservation, but lately, water has been taken for granted and used indiscriminately in agriculture. However, the realization of this fact is gradually setting in due to various initiatives taken by central /state governments, communities and individuals to achieve improvement in water use efficiency and agricultural productivity. A synergetic integration of initiatives by government along with public participation can significantly help in achieving many benefits even in non-irrigated areas. Realizing the limitations imposed on the supply side, focus now needs to switch towards demand-side management. Judicious demand-side water management would not only alleviate the stress on the prevailing infrastructure but also lead to increase in

agricultural productivity. This would also go a long way in keeping the water demand below the availability. As evidenced in the various case studies above, the presence of water has always brought about an upliftment of the community, both socially and economically, which in turn contributes to the nation's economic growth.

Government schemes solely cannot give the solutions to the envisioned goals for water and food security. People's participation in water management becomes crucial to achieve these goals. People's participation stimulates a sense of ownership and responsibility in the public. It is encouraging that many irrigation projects executed by different state governments have been taken up by WUAs for operation and maintenance of water distribution network, and this should be the way forward for all ongoing projects.

The micro-irrigation technology is a staple in bringing about reforms in demand-side water management to effect reduction in agricultural water wastage. As farmers are now realizing the importance of saving water, crops like sugarcane and paddy, which were conventionally flood irrigated, are now being irrigated by micro-irrigation techniques in various drought-prone states.

References

Central Water Commission (2014) Guidelines for improving water use efficiency in irrigation, Domestic and Industrial Sectors, November

FAO (1986) Irrigation water management: training manual No. 3- Irrigation Water Needs, Chapter 2: Crop Water Needs

Ministry of Statistics and Programme Implementation (MSPI) (2018) Statistical year book india, 2.8—Projected Population. New Delhi, India

NABARD, ICRIER (2018a) Water productivity mapping of major indian crops, (Annual per capita availability of water in India was taken as 1544 m^3/person based on the 2011 census population of 1.21 billion). pp xix, 14, 26, 60, 62

NABARD, ICRIER (2018b) Water productivity mapping of major Indian crops, 2018, p 26

National Bank for Agriculture and Rural Development (NABARD), (ICRIER) (2018a) Water productivity mapping of major indian crops, pp xix: Annual per capita availability of water in India was taken as 1544 m3/person based on the 2011 census population of 1.21 billion. New Delhi, India

National Bank for Agriculture and Rural Development (NABARD), (ICRIER) (2018b) Guidelines for improving water use efficiency in irrigation. New Delhi, India, Domestic and Industrial Sectors

Planning Commission (2009) Report of the task force on irrigation, Government of India, May

State of Indian Agriculture (SIA) (2016) Department of Agriculture, Cooperation & Farmers Welfare, Ministry of Agriculture & Farmers Welfare, Government of India, New Delhi, 2015–16). pp 49, 50, 223, 224

Statistical Year Book India, (SYBI) (2017), 8.2 – Gross area under principal crops;12.1 - Net area under irrigation; 12.2 – Gross area under irrigation, Ministry of Statistics and Programme Implementation (MoSPI)

Vohra K, Franklin ML (2020) Reforms in the irrigation sector of India. Irrigation and Drainage. pp 1–10, https://doi.org/10.1002/ird.2500

Working Group on Major, Medium Irrigation and Command Area Development for the XII Five Year Plan (2012–2017). 2011. New Delhi, India. http://www.imdhyderabad.gov.in/tssite/tsrfnormals.htm

Chapter 13
Overview of Water Resources Management in India

Rajendra Kumar Jain

13.1 Introduction

Water is essential for almost all activities on the planet. It is required for drinking, cleaning, agriculture, transportation, recreation, animal husbandry, electricity production and various other industrial and commercial activities. The water cycle also called as hydrological cycle moves enormous quantity of water around the globe and makes the water available on the earth (land mass).

Geographical area of India is 329 million hectares which is about 2.4% of the world's land area. India has an annual average precipitation of about 3880 BCM which is about 4% of renewable water resource of the world. After consumption in various natural processes such as evapotranspiration from forests, rainfed agriculture and barren lands and also after accounting for the transboundary waters flowing from the neighbouring countries, average annual availability of water in India has been assessed as 1999 BCM by Central Water Commission (CWC 2019). The renewable water resources of India are more than the world's average, but due to the huge population (about 18% of world's population) the per capita annual average availability is very low (about 1460 m^3 per annum in 2019) (CWC 2019). The per capita availability is decreasing continuously due to continuous increase in population.

13.2 Challenges in Water Management

India faces a lot of challenges in the field of water resource management due to large spatial variation in the availability of water resources across the country, as well as large temporal variation which is not only within a year but also across the years.

R. K. Jain (✉)
Central Water Commission, Government of India, New Delhi, India

© The Author(s), under exclusive license to Springer Nature Singapore Pte Ltd. 2021

A. Pandey et al. (eds.), *Hydrological Aspects of Climate Change*,
Springer Transactions in Civil and Environmental Engineering,
https://doi.org/10.1007/978-981-16-0394-5_13

These variations are likely to further increase due to climate change impact. Out of total annual precipitation of 3880 BCM, about 75% of the precipitation occurs during the southwest monsoon period from June to September (CWC 2019).

To tackle these challenges being faced in the water sector, a huge infrastructure of large storage reservoirs, canals, treatment plants, etc., is required to evenly distribute water resources in space and time to ensure supply of good quality water, where and when required. Creation and maintenance of such infrastructure require huge capital investment and involve significant environmental costs. In addition, increased hydrological uncertainty under climate change scenarios is also likely to have huge financial, social and environmental implications. Due to uneven distribution of water, many water disputes crop up from time to time at different levels starting from a small locality to the disputes between the states and the nations. It is, therefore, imperative that water resources are managed in most efficient and judicious manner.

13.3 Water Sector Governance in India

India is union of states and thus has federal structure of the government. The constitutional provisions in respect of allocation of responsibilities between the state and centre fall into three categories (https://cwc.gov.in/sites/default/files/constitutional-provisions-and-central-water-laws.pdf): The Union List (List I), the State List (List II) and the Concurrent List (List III), which are given in 7th Schedule of Constitution of India (CWC 1997, Vol-I).

In the Constitution, water is a matter included in entry 17 under List II (State List) which provides that:

> Water, that is to say, water supplies, irrigation and canals, drainage and embankments, water storage and water power subject to the provisions of Entry 56 of List I.

Entry 56 of List I provides that:

> Regulation and development of inter-state rivers and river valleys to the extent to which such regulation and development under the control of the Union is declared by Parliament by law to be expedient in the public interest.

Almost all the rivers and river basins (river valleys) in India are inter-state barring few smaller ones. Although central government has powers under the Constitution to regulate and develop inter-state rivers (which form the majority of water resources of the country), water has become practically a state subject and the development and management of water resources are done by the state governments themselves on the basis of their own priorities without much regard to the interests of other co-basin states.

Significant water resources of India are borne by international river basins. In view of their strategic importance, separate provision for development and regulation of international river basins by the centre is required in the Constitution, which is not there at present.

Experience shows that there are fewer conflicts and better management of water resources when the centre is at the helm of affairs in management of water resources of inter-state river basins. There are few cases where centre is managing water resources of an inter-state basin or part of it like Tungabhadra Board, Bhakra Beas Management Board (BBMB), Damodar Valley Reservoir Regulation Committee (DVRRC), Narmada Control Authority (NCA), etc. Centre is supposed to play active role in management of water resources of inter-state basins but could not do so due to resistance from the state governments. The examples of Krishna River Management Board (KRMB) and Godavari River Management Board (GRMB) are worth mentioning. The central government constituted KRMB and GRMB in 2014 in accordance with the provisions contained in the Andhra Pradesh Reorganization Act (APRA), 2014, which is an Act of Indian Parliament that bifurcated the erstwhile state of Andhra Pradesh into Telangana and the residuary Andhra Pradesh.

The functions of each board, namely GRMB and KRMB, include the regulation of supply of water and power from the projects to the successor states. As per the APRA, the boards were to exercise jurisdiction on Godavari and Krishna rivers within these two states in regard to any of the projects over headworks (barrages, dams, reservoirs, regulating structures), part of canal network and transmission lines necessary to deliver water or power to the states concerned, as may be notified by the central government. However, the jurisdiction is yet to be notified due to dispute on this issue between the two states and the boards have remained practically non-functional, for a long time.

This act also declares that it is expedient in the public interest that the union should take under its control, the regulation and development of the Polavaram Project, which is a mega project on River Godavari in Andhra Pradesh involving huge investment of about Rs. 60,000 crores (about US$ 8 billion). Accordingly, central government constituted Polavaram Project Authority (PPA) for execution of the project. However, on insistence of the Government of Andhra Pradesh, the central government handed over execution of the project to them. PPA has a little control over the execution of the project except passing on the central funds and monitoring the progress in spite of the fact that major funding for the project is being provided by the centre.

To sum up, in spite of constitutional provisions and best intentions, the centre has not been able to play significant role in regulation and development of water resources of inter-state river basins in India.

13.4 Inter-state and Other Conflicts in Water Sector

Planning and development of water resources need to be done at basin scale which is mostly lacking, particularly in case of inter-state basins. The projects are planned, developed and managed by the states according to their own priorities and needs, ignoring the needs of other co-basin states which leads to conflicts. There is lack of trust between co-basin states, resistance to transparency and data sharing. States, sometimes, defy advice and directions of central government, tribunals and even

Supreme Court. There are about 160 inter-state river water agreements made in the past, which play significant role in management of water resources of the country. It shows that spirit of cooperation has been prevailing in the past. However, with passage of time, spirit of conflict has replaced spirit of cooperation. There are now conflicts not only between co-basin states, but between various types of water users, between environmentalists and project proponents, between government and people (mostly project displaced persons), etc. All these conflicts need to be addressed in comprehensive manner for optimum development and management of water resources of the country (CWC 2015 Part one, 2015 Part two, 2018).

Many a times, the projects are planned on political grounds rather than on techno-economic considerations which leads to sub-optimal utilization of resources. Even the operation of projects is sometimes governed by extraneous considerations rather than scientific principles. For example, it is well-established principle that dams should be filled up in a phased manner as per prescribed rule curves so as to provide trade-off between flood moderation benefits and conservation benefits. However, many dam owners/ authorities either have not devised such rule curves at all or do not follow the same while filling up the dams endangering life and property of the people.

13.5 Financial sustainability of Water Resources Development

At present, the water charges, especially for the agriculture sector, are very low and subsidized. Owing to subsidized water charges and lack of volumetric metering, there is no motivation among the water users to use water efficiently and judiciously. The water use efficiencies are, therefore, generally low, and there is no cost recovery, even to meet the O&M costs (CWC 2017). Further, in many irrigation projects farmers having land at tail end of canals do not get water for their crops as farmers in upstream of canal grow water-guzzling crops and over utilise or wastewater. There is no provision or mechanism to force the farmers to stick to cropping pattern which was planned while constructing the projects to ensure that all farmers in the command shall get equitable share of waters. Due to low water charges, there is mismanagement of water resources including its wastage, thus depriving the needy of the same. Low water charges lead to inefficient and irregular supplies which further motivate the water users to resist even reasonable level of hike in water charges, thus creating a vicious cycle. The following diagram demonstrates the same.

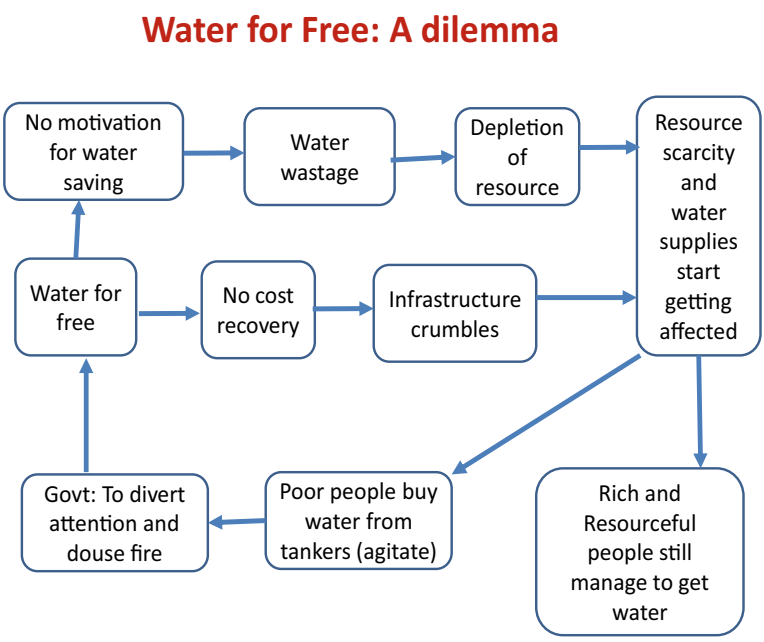

Involvement of private sector in development and management of water resources can ensure that only economically viable projects are constructed, and they are prioritized based on their economic efficiency rather than on any extraneous considerations. However, private sector participation in the management of water sector in India is almost negligible except for hydropower development in spite of the fact that the National Water Policy (2012) of India says that "private sector participation should be encouraged in planning, development and management of water resources projects wherever feasible". Apart from cost recovery issues, the time and cost overruns due to litigations, agitations and various other reasons are also deterrents for private sector participation.

13.6 Conclusion

The centre needs to play proactive role in the development and regulation of water resources of the country particularly in inter-state river basins. It will ensure that resources are better managed, conflicts are reduced, and decisions are taken and implemented based on prescribed principles rather than on extraneous factors.

In order to achieve most efficient and judicious utilization of water resources of the country, there is need of creating empowered river basin organizations led by central government for inter-state basins. These basin authorities may be given enough power to regulate the uses of water. The centre should have more control on water resources of international river basins due to their strategic significance.

There is also a need to create environment for increased private sector participation. It will ensure that projects are planned and developed in judicious manner on techno-economic considerations with full capital and operation cost recoveries ensuring financial sustainability and better water use efficiencies. The deserving groups may be provided subsidies separately, funded by the government. Private sector participation will ensure that projects are prioritized according to their economic efficiencies. The viability gap funding, where required and justified, may be provided.

References

Central Water Commission (CWC) (1997) Legal instruments on Rivers in India, vol-I constitutional provisions, Central Laws and Notifications

Central Water Commission (CWC) (2015 Part One) Legal instruments on Rivers in India, vol-III: agreements on inter state rivers part one, Inter State Matters Directorate, CWC, New Delhi

Central Water Commission (CWC) (2015 Part Two) Legal Instruments on Rivers in India, vol-III: agreements on inter state rivers part two, Inter State Matters Directorate, CWC, New Delhi

Central Water Commission (CWC) (2017) Pricing of water in public system in India, Information System Organisation Hydrological Data Directorate, Water Planning & Projects Wing, CWC

Central Water Commission (CWC) (2018) Legal instruments on Rivers in India, vol-II: awards of inter-state water disputes tribunals, Inter State Matters Directorate-I, CWC, New Delhi

Central Water Commission (CWC) (2019) Reassessment of water availability in basins using space inputs. Report No: CWC/BPMO/BP/WRA/June *2019*/Main Report.

National Water Policy (2012). https://jalshakti-dowr.gov.in/sites/default/files/NWP2012Eng6495132651_1.pdf

Chapter 14
Adaptation to Climate Change in Agriculture: An Exploration of Technology and Policy Options in India

N. K. Tyagi

14.1 Introduction

Climate change is a global phenomenon impacting everything on planet earth, but it impacts them differently. Agriculture being a highly weather-dependent enterprise is impacted most. There are already significant observed adverse impacts, and the projections are that it may reduce the global agricultural yields up to 30% by 2050 (Global Commission on Adaptation 2019). The irony is that the most affected would be the 500 million small farms across the world. Climate change impacts agriculture, but it also gets impacted by the activities involved in various processes in agriculture and food system, which contribute to about a quarter of the global greenhouse emission (IPCC 2014). Thus, it is a two-way relationship. Greenhouse gas (GHG) emission from agriculture may grow up to 70% of the remaining allowable emissions from all human sources by 2050 (Searchinger et al. 2019), and most of it is likely to come from developing countries in Asia and Africa. Though linked to the general global changes, which are largely the consequences of the development activities pursued in the developed part of the world, the climatic regime in South Asia has significant departures from the global mean in terms of changes and the impact on agriculture (Schellnhuber et al. 2013). The need for adaptation to climate change arises because of the changes, which have been introduced in the natural systems in the process of the development.

N. K. Tyagi (✉)
Formerly Member, ICAR-Agricultural Scientists Recruitment Board, New Delhi, India

© The Author(s), under exclusive license to Springer Nature Singapore Pte Ltd. 2021

A. Pandey et al. (eds.), *Hydrological Aspects of Climate Change*,
Springer Transactions in Civil and Environmental Engineering,
https://doi.org/10.1007/978-981-16-0394-5_14

14.1.1 Climate Change Impact on Agriculture

Agriculture and water resources (availability and distribution) are highly dependent on specific climate conditions. The climate change will have a universal, but differentiated impact depending upon the location of the countries. Projections for climate impact on agriculture for South Asia are quite alarming, particularly when weighed together with adaptive capacity and the population growth. In India, because of its size, different regions experience differentiated effects. Cline (2007) has projected that by 2080, agricultural output in India may fall between 19 and 39% with benefits of carbon fertilization and 29–44% without benefits of carbon fertilization in different parts of the country. It may be added that irrigation requirements have significant correlation with temperature and for every 1 °C rise in temperature, the irrigation requirements go up by 10% (Cline 2007). The recent projections on impacts on production are much more alarming. The report of Indian Network for Climate Change Assessment (INCCA), which has been established to study the impact of climate change and advise the government (INCCA 2010), projected a fall in yield of rice in the order of 4–20% under irrigated condition and 35–50% under rainfed condition as early as 2030 (Table 14.1). These projections tally with Cline's estimates of 30–40% (Cline 2007). The only difference is that what was expected to happen in 2080 may happen in 2030. How to minimize the adverse outcomes and build on the positive ones remains the issues to be resolved.

Addressing issues introduced by climate change in agriculture, which supports livelihood of about 58% population in India, assumes urgency (GoI-MoSPI 2014). The two major mechanisms to turn down the heat, and to enable it to keep operating within safe space of resource boundaries, are mitigation and adaptation (GCA 2019). The mitigation processes take care of the causes of climate change, while adaptation tries to moderate the adverse impacts and establish resilience in the system. The resilience to agriculture, which is defined as the capacity of an ecosystem to tolerate disturbance without collapsing into a qualitatively different state, is imparted by both, the adaptation and the mitigation. Understanding this inter-relationship would help develop an optimized mix to maximize benefits and minimize cost. The low-carbon technologies employed for mitigation, being patent protected in developed countries, are costly. But technologies in adaptation have no such constraints and are readily available, and this makes technology transfer easier (Irfanullah et al. 2011). Further, investment in adaptation to bring resilience is highly profitable, because as per the report from Global Commission on Adaptation, the rate of return ranges from 2:1 to 10:1, and in dryland agriculture, it was about 5:1 (GCA 2019). But there are limits on adaptation in terms of technology, finance and social and cultural norms. Though adaptations are largely technology-driven, soft interventions like risk transfer and capacity building, to take advantage of the technology development, also play a very important role in adaptation process (Mobarak and Rosenzweig 2013; Tyagi and Joshi 2019a, b).

In developing countries like India, stress due to climate change is only an additional factor, as the farmers face a large number of non-climatic stresses with high

Table 14.1 Impact of climate change in different sectors and regions of India by 2030

Sector	Himalayan region	Northeast	Western Ghats	Coastal region
Crops	Apple-Overall negative impact	Irrigated rice: +5% to −10% Rainfed rice: +5% to −35% Yield reduction Maize: up to −40%	Yield reduction Rice: −4% Maize: −50% Yield increase Coconut: +30%	Yield reduction Irrigated rice: −(10–20)% Rainfed maize: −35% Irrigated maize: −(15–50)% Coconut: up to −40% (West Coast) Yield increase Coconut: + (10–30) % (in parts east coast)
Fishery	–	–	–	Positive impact
Livestock		Negative impact	Negative impact	Negative impact
Water	Increase	Decrease	Variable	General reduction
Biodiversity (in terms of natural plant productivity (NPP)	NPP increase by 57%	NPP increase by 23%	NPP increase by 20%	NPP increase by 31%

Source Indian Network for Climate Change Assessment (INCCA) 2010. Climate Change and India: A 4 × 4 Assessment: A sectoral and regional analysis for 2030s

damaging potential. These stresses arise due to limited access to assets, capital, technology infrastructure and markets (Vyas 2007; Hazell et al. 2010; World Bank 2008). Among these stresses, lack of human capital is the most constraining, in so far as adaptation capacity is concerned. For example, in the northern states of Bihar and Uttar Pradesh, where human development in terms of health, education and income is low; the potential to assimilate new knowledge and the capacity to interact with input suppliers, bankers and traders is also low.

Thus, there are multiple issues involved in planning, implementing and assessing the adaptation in agriculture, as it has multiple inter-sectoral implications. The key issues addressed herein are: some intricacies of adaptation concept, mapping of India's vulnerability to climate change, biophysical adaptations which would help ensuring food and nutrition security with minimum tradeoffs between increased production and the environment (health of soil and water resources systems), and risk transfer through agricultural insurance and the policies to promote adoption of climate-smart technologies.

14.2 Understanding the Adaptation

Adaptation to climate change in agriculture means adjusting to the changed set of climatic attributes like increased floods, droughts, heat waves, etc., to take care of the biophysical and socio-economic vulnerabilities of natural and built environments by building capacity and using it to implement desired interventions (IPCC 2014; Tompkins et al. 2010; Smit and Skinner 2002). The resilience to agriculture, which is defined as the capacity of an ecosystem to tolerate disturbance without collapsing into a qualitatively different state, is imparted by both, the adaptation and the mitigation. So, it requires mitigation as well as adaptation to keep the climate change impacts within acceptable limits. Mitigation and adaptation are sometimes considered interchangeable, as many interventions serve both the purposes. Understanding the interrelationship between them would help develop an optimized mix to maximize benefits and minimize cost.

Improved agricultural production and sustainable management of natural resources also have considerable mitigation potential as well (Nin-Pratt et al. 2011; Tyagi et al. 2019). For example, carbon sequestration in agricultural soils reduces GHGs, creates an economic commodity for farmers (sequestered carbon) and improves soil productivity by improving soil health. Similarly, stopping the existing practices of straw burning in Indo-Gangetic plain, shifting cultivation in Northeast India, wetland cultivation of rice and traditional tillage practices offer opportunities for conserving the resource base and reducing emission of greenhouse gasses (GHGs). It may however be noted that mitigation has global benefits with some ancillary benefits which can be realized at local or regional level, whereas adaptation mostly works on the scale of an impacted system (Klein et al. 2007).

14.2.1 Classification of Adaptations

Adaptations have been classified in multiple ways depending upon the purpose, mechanism and time sequence. In agriculture, farmers have been adapting to gradual changes since long, albeit unconsciously, in response to ecological changes in the production system or market forces. These are called autonomous or spontaneous adaptations (IPCC 2001). On the other hand, adaptations resulting from deliberate policy guided action to achieve a desired state are called planned adaptations. Depending upon the time (before or after the impact of climate change), adaptations are classified as anticipatory (e.g. early weather warning system) or reactive (adjustment in date of sowing in response to late monsoon), respectively. Planned adaptions can be both anticipatory and reactive.

The adaptation requirements depend on the vulnerability in terms of loss in production and/or income from agriculture under the given set of biophysical and socio-economic factors (Howden et al. 2010). As the degree of climate change increases, the efficacy of the adaptation measures goes down, and so do the benefits requiring change from incremental adaptations to systemic adaptations and finally to transformational adaptations. Further, there are limits on effectiveness of the measures arising from biophysical factors (the ecological tipping points) which create absolute limits for adaption, social limits (how much is acceptable) and economic limits (how much is affordable) (Schipper and Lisa 2009). A partial list of adaptation measures with varying intensity of climate change is given in Table 14.2.

In agriculture, opportunities for adaptation, which connotes adjustment to moderate the impacts of climate change, are higher than mitigation. Adaptations are required to deal with vulnerabilities associated with climate variability, in human health, coastal settlements, infrastructure and food security. The resilience of most sectors in Asia to climate change is very poor. Expansion of irrigation will be difficult and costly in many countries. For most developing countries in Asia, climate change is only one of the many other problems to deal with, including nearer term

Table 14.2 Adaptations in relation to degree of climate change and benefits from adaptation

Degree of climate change	Nature of adaptation	Benefit/cost tradeoff
Moderate	**Incremental**: Crop varieties, planting dates, spacing, nutrient management, canopy management, irrigation scheduling, etc.	No regret
High	**Systemic**: Climate ready crops, precision agriculture, crop diversification, crop insurance, micro-finance and risk management, early warning systems	Income-environment tradeoff
Extreme	T**ransformational**: Land-use changes and distribution, ecosystem services, migration	High

needs such as hunger, water supply, pollution and energy. Resources available for adaptation to climate are limited, and the priority areas for adaptation are land and water resources, food productivity and disaster preparedness.

14.2.2 Strategies for Adaptation Planning

Adaptation responses are closely linked to development activities, which should be considered in evaluating adaptation options. Early signs of climate change are already observed and may become more prominent over 1 or 2 decades. If this time is not used to design and implement adaptations, it may be too late to avoid upheavals. Long-term adaptation requires anticipatory actions. A wide range of precautionary measures are available at the regional and national level to reduce economic and social impacts of disasters. These measures include awareness building and expansion of the insurance industry. Development of effective adaptation strategies requires local involvement, inclusion of community perceptions and recognition of multiple stresses on sustainable management of resources. Adaptive capacities vary between countries, depending on social structure, culture, economic capacity and level of environmental disruptions. Limiting factors include poor resource and infrastructure bases, poverty and disparities in income, weak institutions and limited access to technology. The challenge in India lies in identifying opportunities to facilitate sustainable development with strategies that make climate-sensitive sectors resilient to climate variability. Adaptation strategies would benefit from taking a more system-oriented approach, emphasizing multiple interactive stresses, with less dependence on climate scenarios.

Apart from addressing the climate *risks,* adaptation offers multiple social, economic or environmental co-benefits (Hallegatte 2009). The important dividends of adaptation in agriculture include: reduction in crop yield losses, improved economy and livelihood, and better environment due to avoided deforestation (Tyagi et al. 2019). But there are barriers and limits on effectiveness of adaptation responses. In certain situations, adaptation may become impossible for lack of strategies, high cost and unacceptable consequences. The limit to adaptation may be due to socio-economic, ecological, physical and technological factors.

14.2.3 Adaptations in Agriculture Are Water-Centric

Agriculture, which is the nature's carbon and water-based industry, globally accounts for 70% of all water withdrawals, and its share in consumptive water use is even higher (World Bank 2020; Hoekstra and Mekonnen 2012). In India, agricultural water use is as high as 85% (NITI Aayog 2015). Agriculture being a carbon and water-dependent sector, it is but natural that the impacts of climate change would be largely transmitted in terms of water-related stresses like increased floods and droughts. The observed

data over a period of 1951–2015 shows a significant increase in frequency and spatial extent of droughts, particularly in Indo-Gangetic Plains of India (Mujumdar et al. 2020). A similar trend is found in the frequency of heavy rainfall events, which cause floods. Projections for the future indicate a rise in extreme rainfall events of short duration on rise of global temperature between 1.5 and 2.0 °C (Ali and Mishra 2018). Whereas short-lived and localized floods are also an important source of risk in agriculture, it is the widespread river inundation in flood plain areas in low-lying deltaic regions in Eastern India, which is a major concern. The flooding is a widespread phenomenon, and the floods in river basins of Brahmaputra and Barak Basin, Ganges and Mahanadi create serious problem for agriculture. For example, the state of Bihar, which is one of the most flood-vulnerable states to floods, the average annual crop loss from 2004 to 2013 (Fig. 14.1) was assessed at Rs. 1580 million per year with peak value at Rs. 7084 million in 2007 (Government of Bihar 2014). It is a matter of great concern that at the river basin level, the multi-day frequency is also projected to increase significantly under changing climate (Ali et al. 2019).

Apart from floods, a major concern is the trending reduction in summer monsoon rainfall during last 100 years in Central and East India, which is of the order of 10–20%, having very severe potential socio-economic implications (Roxy et al. 2015). By introducing shifts in rainfall pattern, rainfall intensity and thereby more runoff and less groundwater recharge and increasing evaporation, climate change introduces unprecedented changes in water system.

Uncertainties in water cycle shifts have undermined the concept of stationarity which, in the past, has been the concept used in managing water availability variability (Milly et al. 2008). Further, water, because of its systemic nature, is embedded in all sectors of economy and, therefore, an effective tool of adaptation (Smith et al. 2019). Aligning water management practices and policies with changing climate scenarios remain important, but challenging (Smith et al. 2019).

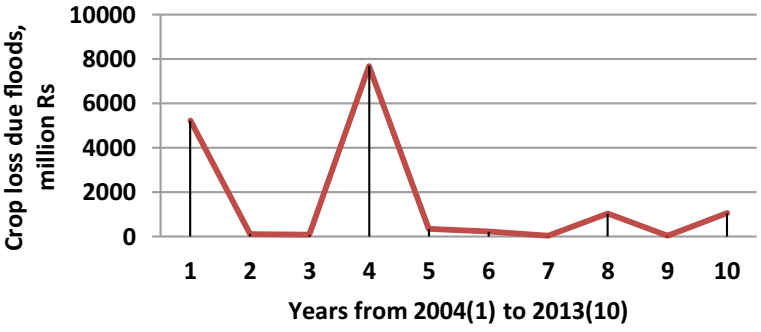

Fig. 14.1 Crop damage due to floods in Bihar-2004–2013 (Source: Based on data from Flood Report-2013 Govt. of Bihar, 2014. https://fmis.bih.nic.in/aboutus.html)

14.3 Vulnerability Mapping of Indian Agriculture

In relation to climate change, the IPCC (2007) defined vulnerability as "the degree to which a system is susceptible to, and unable to cope with, adverse effects of climate change, including climate variability and extremes." Accordingly, in agriculture, vulnerability to climate in agriculture would mean the loss of production or income, when faced with climate shocks, and is impacted by both biophysical and socio-economic factors. The three components of vulnerability are sensitivity, exposure and adaptive capacity, and there are a number of determinants reflecting these components, which combinedly decide the level of vulnerability. These determinants, which are dynamic in nature, are location and the system-specific and also change with climatic stimuli (Smit and Wandel 2006). The capacity of farming communities to manage the impact of climate change varies with social status, ethnicity and class; and the impact is greater on the poor small farm holders (Adger et al. 2009; Joshi and Tyagi 2019).

Various attempts have been made to map the agricultural vulnerability in India, the important ones being those by Kavi Kumar et al. (2007) and Ravindranath et al. (2011). The other two, more recent and comprehensive assessments, are due to Sehgal et al. (2013) for Indo-Gangetic plain and the other by Rama Rao et al. (2013) for the entire country under the auspices of National Initiative on Climate Resilient Agriculture (NICRA). In a large country like India, vulnerability being location-specific is bound to vary in a wide range. As observed in Joshi and Tyagi (2019), the following is the picture of relative level of vulnerability status for 572 districts in the country, developed by Rama Rao et al. (2013).

1. The highest incidence of districts, in very high and high category of vulnerability, occurs in Rajasthan (31),[1] Uttar Pradesh (30), Madhya Pradesh (30), Bihar (21), Gujarat (20), Karnataka (19) and Maharashtra (17).
2. The major exposure factors in Rajasthan and Uttar Pradesh were the projected rise in minimum temperature and decrease in July rainfall, whereas the increase in drought years was an additional factor in Madhya Pradesh and Karnataka, besides the first two factors. In Bihar, major exposure factor was only the decrease in July rainfall. In Maharashtra, the rise in minimum temperature and the increased number of drought years were the factors of exposure.
3. Low rainfall followed by high net sown area were the two major sensitivity factors across the states with a sprinkling of drought proneness.
4. The low net irrigated area and low groundwater availability were the major constraints to adaptive capacity across the vulnerability classes.
5. In case of Punjab, the vulnerability was compounded by low livestock density, while in Uttar Pradesh and Bihar, the culprit was high level of poverty.

[1] Values in parenthesis are numbers of districts.

The observed data for India indicates 8–10% decrease in monsoon seasonal rainfall in Eastern Madhya Pradesh, Northeastern India and parts of Gujarat and Kerala over the past century (Lal et al. 2010). The sea level has risen between 1.06 and 1.75 mm per year (IPCC 2007). The projections of climate change for the next 40–80 years are more frightening.

14.3.1 Quantitative Estimation of Vulnerability

Indian agriculture is essentially a smallholders' farming; 85% of the farms fall in this category, and a very large number of these farms (54%) lie in Indo-Gangetic Plain (GoI-MoA 2014a, b). As discussed in earlier section, the adaptive capacity of farmers in this region is very much constrained by non-climatic factor. For this region, a quantitative analysis of exposure, sensitivity and adaptive capacity on a scale of 0–5 has been performed by Sehgal et al. (2013). The analysis showed that as one traversed from west to east, the exposure and sensitivity increased, whereas adaptive capacity decreased, resulting in increased vulnerability (on 0–4 scale) (Fig. 14.2). But in Punjab and Haryana, the two states which had high irrigation intensity (more than 90%), the adaptive capacity was high. Higher use of chemical fertilizers, greater degree of electrification and improved rural road network were the other contributory factors for their low vulnerability.

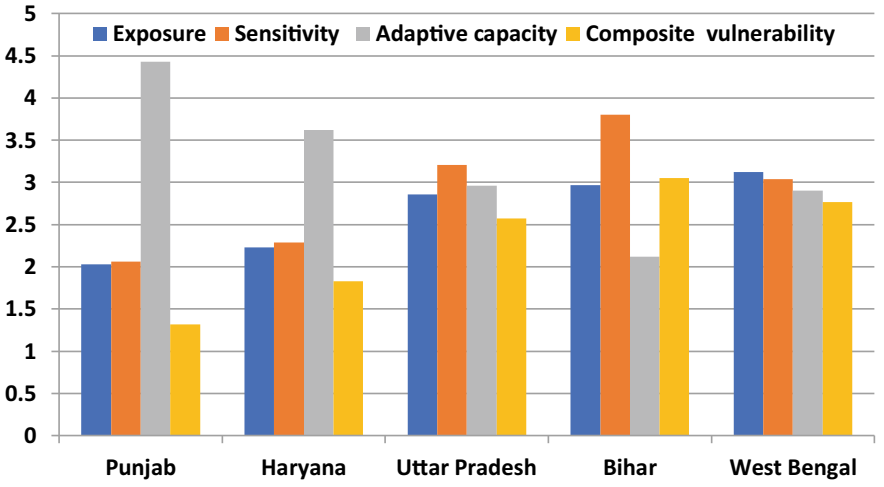

Fig. 14.2 Exposure, sensitivity, adaptive capacity and composite vulnerability of agriculture across Indo-Gangetic Plain (Based on data from Sehgal et al. 2013)

14.4 Adaptation Actions in India

Farmers in India, or for that matter everywhere in the world, have been adapting to climatic and non-climatic factors, since ancient times. But a break from the past occurred in the seventh decade of twentieth century with introduction of seed, fertilizer and water-based productivity enhancing Green Revolution period interventions. These biophysical adaptations were not planned with climate lens, but aimed at increasing food production to feed the teeming millions. Adoption of incremental agro-technologies like improved seeds, higher doses of fertilizers and irrigation helped achieved higher productivity and reduced production cost, resulting in 15–20% higher income (Tyagi et al. 2019).

The dawn of twenty-first century saw adoption of two parallel approaches similar to the ones' mentioned in the 3rd SCAR Foresight Report of European Union (Freibauer et al. 2011). Whereas most farmers continued with the existing Green Revolution period technologies, progressive farmers of upper and middle Indo-Gangetic Plain and parts of Southern India started experimenting with climate-smart low-carbon technologies like zero till, laser levelling and micro-irrigation systems (Tyagi and Joshi 2019a, b). Though a major driver for acceptance of the new technologies was the rapidly declining groundwater, extension activities, like Climate-Smart Village under Climate Change, Agriculture and Food Security (CCAFS), Accelerated Irrigation Benefit Programme (AIBP) and National Horticulture Mission, etc., (GoI-MoA&FW 2019) under which financial support was extended to the farmer, were also quite helpful. According to some estimates, the laser levelling has modified more 20 million ha land surface effecting about 20% increase in water use efficiency, and zero/reduced tillage has gone into 3 million ha, saving both energy and water, while micro-irrigation has changed the way farmers practiced agriculture bringing in more crop per drop, per unit of energy and per unit of GHG emission in about 8 million ha (Tyagi and Joshi 2019a; Global AgriSysrem 2017). But we need to add more technologies and out scale them at country level.

14.4.1 Case-I: Adaptation and Adaptation-Led Mitigation with Green Revolution Technologies

The adoption of Green Revolution technologies (the term was coined in 1968 by former USAID director William Gaud) got initiated in India in late nineteen sixties and reached its peak by 1990. The main ingredients of GRTs in India were improved seeds (mostly rice and wheat crops), large-scale expansion of irrigation and dramatic increase in use of chemical fertilizers. Starting with 1.9 million ha in the initial stage, the coverage of GRTs reached 75 million by 1995 (Swaminathan 2017; Kanolkar ND).

14.4.1.1 Data and Methodology

As reported in Tyagi et al. (2019), a span of two decades from 1990–2010 was selected for analysing the impact of Green Revolution technologies on adaptation, mitigation, resilience and sustainability through the observed reported data on crop area, irrigated area, fertilizer consumption, the resulting production and productivity etc. Simultaneously, using standard procedure on data from FAO for the respective years (FAOSTAT 1990, 2010), the green GHG emissions from each activity were also estimated (Table 14.3).

An empirical framework, explained in detail in Tyagi et al. (2019) to compute adaptation, mitigation and sustainability aspects of out-scaling surface and groundwater irrigation, micro-irrigation technology and fertilizer consumption, was developed. Changes in land productivity, food availability, deforestation, water resources exploitation and emission balance capture impacts of interventions. Indices for mitigation and adaptation were constructed to provide a quantitative basis for assessing the net mitigation or intensification by each technical intervention. The evaluation was performed under "with and without" incremental adaptation situations, to design policy initiatives.

14.4.1.2 Results

The two-decadal change in technology adoption brought an increase of 40% in production, 46% in productivity and 35% in per capita FG availability. The contributions of irrigation and fertilizers to these positive changes were 40 and 20%, and the remaining 40% was attributed to seed and other factors. The most encouraging effect of increased productivity was saving of 56 million ha of forests from being brought under cultivation. Increased land productivity and avoided deforestation achieved through technology implementation had significant impact on potential greenhouse

Table 14.3 Impact of incremental adaptation of Green Revolution period technologies (seed, water and fertilizer) on production, productivity, food grain availability and carbon footprints (Adapted from Tyagi et al. 2019)

Item	1990	2010	Change (%)
Area under food grain production (Mha)	127	122	−3.90
Irrigated area (MHa)	67	85	+ 26.9
Fertilizer consumption (Kg/ha)	68	115	+ 69.1
Food grain production (Mt)	151	212	+ 40.4
Land productivity (T/Ha)	1.19	1.74	+ 46.2
Food grain availability at 1990 population base (kg/cap/year)	203	274	+ 35
Food grain (FG) carbon footprints (TCO_2e/TFG)	1.196	0.907	−24.2

MHa = million-hectare, MT = million-ton, Kg/Ha = kilograms per hectare, CO_2e = carbon dioxide equivalent (Data Sources: GoI-MoC&F 2012; Chand and Pandey 2008; and GoI-DoE&S 2011)

gas mitigation and food security. The carbon footprints of food grain (FG) production, in terms tons of carbon dioxide equivalent emission per ton of FG (TCO_2e/TFG), decreased from 1.2 to 0.91 over period of 20 years (Table 14.3). Total emission from food grain production which was 181 million TCO_2e, in 1990, increased to only 193 million TCO_2e, by 2010 (Fig. 14.3). Estimates indicated that in the absence of incremental GRT technologies, greenhouse gas emissions would have increased to 430 million TCO_2e. Thus, an adaptation-led virtual mitigation of 237 million TCO_2e was achieved due to increased productivity (Tyagi et al. 2019).

The increased agricultural intensification, which saved about 56 million ha of forest land from being brought under the plough, was largely dependent of groundwater. The over exploitation of surface and groundwaters has made the management of irrigation systems difficult and has implications for long-term sustainability of irrigated agriculture. As seen from Table 14.4, the degree of development of surface water (DDS), a ratio of water diverted from the river system and average river flows

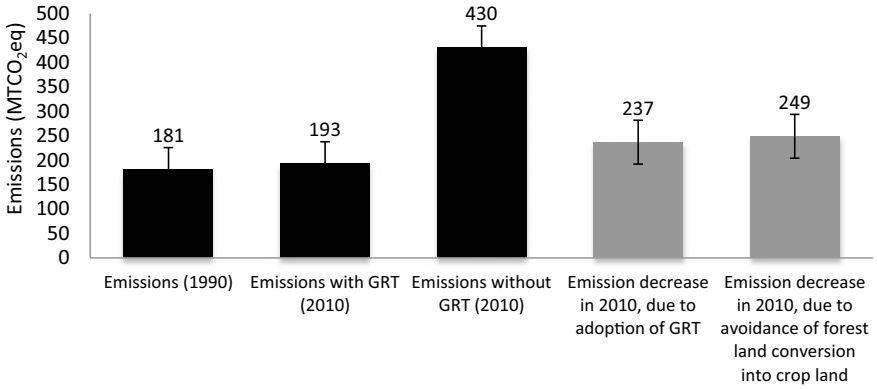

Fig. 14.3 Estimated annual GHG emissions from land under food grains under two scenarios—(i) with adoption of GRTs and (ii) without adoption of GRTs (Source: Tyagi et al. 2019)

Table 14.4 Water resources and sustainability indices of water resource development in India

Item	Level of development (BCM)		
	2000	2010	2050
Surface water	360 (690)[a]	404	647
Groundwater	210 (396)[a]	260	396
	Degree of stress		
DDS	0.522 (high)	0.586 (high)	0.938 (extremely high)
GWAR	0.530 (normal)	0.657 (high)	1.00 (extremely high)

[a]Source—Water resources data are from NCIWRD Report (1999)

during non-monsoon period, stood at about 0.59 in 2010, while the projected value of DDS in 2050 was 0.95, which according to Alcamo et al. (2000) was extremely high value. Similarly, the groundwater abstraction ratio (GWAR), the ratio of groundwater abstracted and the annual recharge, was 0.657 in 2010 and is projected to be >1 in 2050. It may be added that development is considered safe up to a GWAR of 0.65, moderately stressed between 0.65 and 0.85 and unsafe beyond 0.85 (CGWRE 2009).

14.4.1.3 Inferences

1. Out scaling of incremental Green Revolution technologies (GRT) in India not only translated into increased food security by way of increased productivity and more income, but also provided a buffer against climate-induced fluctuations.
2. There was significant adaptation-led virtual mitigation, which saved more 50 million forest land being brought under cultivation, proving Borlaug's hypothesis that increased productivity saved land (Borlaug 2007).
3. The policies promoting GRT out scaling led to evolution of cropping patterns which caused overexploitation of water resources. This calls for urgent action and required corrections in crop area allocation, introduction of water smart technologies and the enabling policies.

14.4.2 Case-II: Adaptation Through Diversification and Climate-Smart Technologies

This case study pertains to the state of Haryana in upper Indo-Gangetic Plain, which has been one of the most significant beneficiary's Green Revolution technologies leading to food grain sufficiency. But the tremendous increase in rice and wheat production, which brought food grain sufficiency, has been traced to the excessive development of groundwater, setting in an ecological crisis (World Bank 2001; Tyagi and Joshi 2019a). Most parts of the state being arid and semi-arid, there was dominance of low water requiring crops like millets, pulses (mostly gram) and oilseeds under rainfed conditions till 1970 (Fig. 14.4). However, 1980 onward, the situation has dramatically changed, and in 2015, rice, wheat and cotton had become the dominant crops, turning into a cropping system which is not ecologically sustainable as the annual groundwater draft was 13.05 billion cubic metre (BCM), against the annual utilizable recharge of 9.79 BCM (CGWB 2017; GoH 2011). Of the total 108 administrative blocks in the state, 55 are overexploited, 11 are critical and 5 are in semi-critical stage (CGWB 2017), as the groundwater table is falling at the rate of 0.65 m/year from 2001–2015.

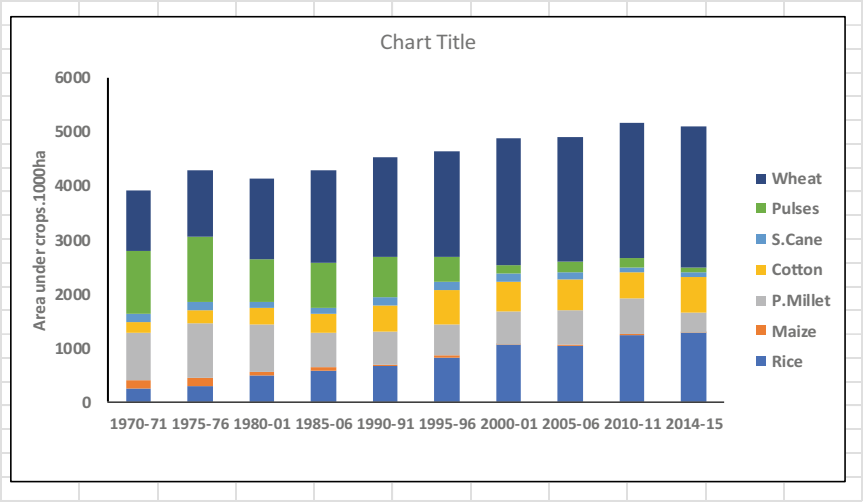

Fig. 14.4 Dramatic changes in cropping pattern during 1970–2015 in Haryana (based on data from GoH 2017)

14.4.2.1 The Emerging Issues

1. Continuous fall in groundwater table requires frequent deepening of tube wells, because of well failures. As a result, the farmers incur heavy cost leading to increased cost of production and decline in farm income.
2. In countryside, the demand for electricity far exceeds the supply, leading to power cuts and putting extra burden on public exchequer, as the electricity charged from farmers is much below the production and distribution cost, rendering the electricity board bankrupt.
3. Coal-based thermal power stations supply 70% of electricity. About 25% of this energy is used to extract groundwater for irrigation, adding significant amount of GHG emissions from agriculture sector.
4. Establishing a balance between food–water–energy security nexus is an urgent issue.

This study investigated the possibilities of achieving the stated objective at farm level through water and energy smart technologies and crop diversification.

14.4.2.2 Methodology and Data

It is important that India transits to new production patterns that keep land, water and other resources within safe limits. The study is based on designing a cropping system based on the combination of ecologically compliant crop mix and experimentally tested technologies, which have out scaled at mesoscale. In India, concerted research

Table 14.5 Average change in important agricultural adaptation parameters over traditional methods and practices (Tyagi and Joshi 2019a)[a]

Attribute	Laser levelling	Zero tillage+	Micro-irrigation
Improvement in irrigation efficiency (%)	15(70)	15(70)	25(85)
Increase in crop yields	15	−5	30
Decrease in energy use (Mj/Ha)	−15	−20	−30
Increase in income (%)	15	15	30

( )Values in parenthesis are the average values under improved methods
[a]Based on data from Naresh et al. (2016), Tyagi and Joshi (2017), Pathak and Aggarwal (2012), IAI and FICCI (2016)

efforts during the last two decades have been made to test and recommend the resource conservation technologies, ranging from micro-irrigation, zero tillage, laser land levelling, salt, drought and heat-tolerant crop varieties for different regions across the country (ICAR 2015). It would be appropriate to mention that zero tillage, laser levelling and micro-irrigation, which were found to increase irrigation efficiencies and crop yields and reduce energy requirements in the range of 15 to 30% (Table 14.5), at research farms (Naresh et al. 2016; Pathak et al. 2011; Tyagi and Joshi 2017), have been adopted by farmers on millions of hectares.

A very important project to reduce energy consumption in groundwater irrigation has been launched by the government under the programme 'Ag Demand Side Energy Management'. Under this programme, the poorly performing irrigation pump sets are being replaced with Bureau of Energy Efficiency (BEE) labelled pumps (BEE 2009; Vasudevan et al. 2011). The energy audit of more than 20,000 pump sets across eight states was undertaken by Bureau of Energy Efficiency. The energy audit indicated that as a result of this improvement, a saving in energy use in the range of 28–49% with an average value of 40% was achieved (Saini 2011).

14.4.2.3 Results

A diversified cropping pattern along with water and energy smart agro-technologies described in this section showed that it was possible to harmonize the water–energy–food security nexus to keep operating within safe natural resource boundaries. The suggested biophysical interventions would yield a reduction in irrigation requirement in the order of 10 BCM and also save about 2200 million kWh of energy on annual basis (Table 14.6). Along with these monitory benefits, the country would get GHG reduction of 3.38 million-ton CO_2e for meeting national GHG mitigation commitments.

Table 14.6 Water and energy saving through crop diversification and introduction of energy-efficient Bureau of Energy Efficiency (BEE) labelled pump sets (Tyagi and Joshi 2019a)

Interventions	Reduction in groundwater draft (BCM)	Energy (million kWh)	GHG reduction (million-ton CO_2e)
Diversification through reduction in rice, wheat cotton area &increase in pulses, oilseeds and arid horticulture	5.33 (53.4%)	Energy saving: With the existing pump sets = 1434 With BEE labelled pump sets = 2213	With the existing pump sets = 1.5 With BEE labelled pump sets = 3.38
Introduction of zero till and laser levelling in entire area	2.27 (23%)		
Micro-irrigation in sugarcane, wheat, cotton, fruits and vegetables	2.27 (23%)		
Area reduction (%) & reallocation: Rice–30% (Reallocated to Maize: Pearl millet: 80:20); Wheat–15% (Reallocated to Veg: Pulses & Oilseeds: 12.5:87.5); Cotton–23% (Reallocated to Arid zone fruits: Pulses: 67:23)			

14.4.2.4 Inferences

1. Diversification of cropping pattern by relocation of crop areas is necessary to make it ecologically compatible. The proposed reallocation would reduce irrigation demands by about 10 BCM, arrest fall in groundwater table and economize energy consumption by 28%, without compromising on food security.
2. Adoption of the diversified cropping through change in cropping mix in order to promote ecologically compliant cropping would require a level playing field, which at present favours water-intensive crops like rice and wheat. The inclusive pricing policy would have to bring the horticultural crops under the regime of minimum price support.
3. Groundwater management is highly political in nature, and it would require generating strong empirical evidence to indicate resource use efficiency, adoption challenges and economics of adoption for end users.

14.4.3 Risk Transfer as Mechanism for Promoting Adaptation

In the past, weather risk management focused more on engineering responses and the ex-post response like compensation. But in recent years, the importance of "soft measures" such as planning, regulations, early warning systems and the risk transfer through insurance is growing. Efficient risk transferring mechanism like crop insurance can enable them to take substantial risks without much hardship. Insurance itself does not directly reduce any damage and the consequent financial losses. But it

provides much-needed financial support and, under certain circumstances, promotes other aspects of flood risk management in the form of risk-reducing interventions (Crichton 2008). A series of agriculture insurance schemes have been implemented in India, and there have been progressive improvements in successive insurance schemes starting from Comprehensive Crop Insurance Scheme (CCIS), through National Agricultural Insurance Scheme (NAIS) and the Modified National Agricultural Insurance Scheme (MNAIS) which were index-based and the one Weather Index-Based Scheme (WBCIS), which were implemented during 1985–2013 (GoI-MoA 2004, 2011, 2013). These improvements were attempts to address the technical, institutional, financial and operational challenges, which cropped up during implementation. The most recent addition to these insurance schemes is Prime Minister Fasal Bima Yojana (PMFBY) and the Revised Weather Index-Based Scheme (RWBCIS) launched in 2016 (GoI-MoA&WF 2019).

Weather index insurance overcomes the defects traditional crop insurance schemes and addresses the problems of moral hazard, adverse selection, high administrative costs, etc., as this financial product is linked to measurable weather parameters, which correlate with crop yield (AFC 2011; Odening et al. 2007). The pilot WIBCIs with varying weather indices, experimented in India, are given in Table 14.7.

A pilot Weather Based Crop Insurance Scheme (WBCIS) was launched in 20 states (as announced in the Union Budget 2007–08) and was implemented as a full-fledged component scheme of National Crop Insurance Programme (NCIP) from Rabi 2013–14 season to Rabi 2015–16. WBCIS intended to provide insurance protection to the farmers against adverse weather incidence, such as deficit and excess rainfall, high or low temperature, humidity, etc., which are deemed to adversely impact crop production. It is planned to set up 5000 automatic weather stations (AWS) in public–private partnership (PPP) mode. The WBCIS component of the above scheme also has a provision for add-on/index plus products for horticultural crops to compensate perils of hailstorm' cloudburst etc.

Table 14.7 Weather index-based insurance products experimented in India (Tyagi and Joshi 2019b)

Weather index parameter	Promoted by
Weighted rainfall	ICICI Lombard-2003 and AIC-2004 and IFFCO Tokyo-2005
Total seasonal rainfall	AIC during Kharif 2005
Multiple phase weather rainfall	ICICI Lombard 2004
Multiple phase weather rainfall	ICICI Lombard 2004
High temperature/low temperature	AIC-IARI-2007, ICICI Lombard-2010

AIC—Agricultural Insurance Corporation, ICICI—Industrial Credit and Investment Corporation of India, IARI—Indian Agricultural Research Institute

Recently, the scheme has further been restructured on the basis of premium structure and administrative lines of Prime Minister Fassal Binma Yojana PMFBY and has become operative from Kharif 2016 as restructured WBCIS (GoI-MOA&FW 2019) and has covered. With a view to increase efficiency, speed in getting data and improved communication, this new scheme envisages use of innovative technologies like satellite imagery, vegetation indices, smart phones/handheld devices and digitization of land records.

14.4.3.1 Performance of Weather Index-Based Crop Insurance Scheme

With a small beginning in 2007, the scope of WIBCS was expanded, and by 2013, it was competing with the earlier MNAIS. During 7 years of its operation (2007–2013), the WIBCIS covered 63.2 m ha lands, progressing at an averaging rate of 9.7 m ha/year and insured 46.94 million farmers (7.2 million farmers per year) (Tyagi and Joshi 2019b). Except for one season, the claims were less than the amount of premium, and claim ratios ranged between 0.51 and 1.06 with an average of 0.76 for all the crops insured (Fig. 14.5), whereas the loss cost remained in the range of 6–12% (GoI-MoA 2014a, b; Tyagi and Joshi 2019b). The PMFBY and RWIBCS together covered 51.94 million ha, benefitting 52.08 million farmers in 2017–18, and the payout was Rs 20.16 billion against a premium of Rs 25.49 billion (GoI-MoA 2014a, b).

In spite of several modifications in WIBCS, there still remain some issues to be resolved. The most important is the basis risk as there is not only non-homogeneity in insurance unit area in terms of weather, but in farming techniques. The second issue is of de-trending (removing the effects of accumulating data sets from a trend to show only the absolute changes in values and to allow potential cyclical patterns to be identified) to minimize effect of inadequate historical weather data. Further,

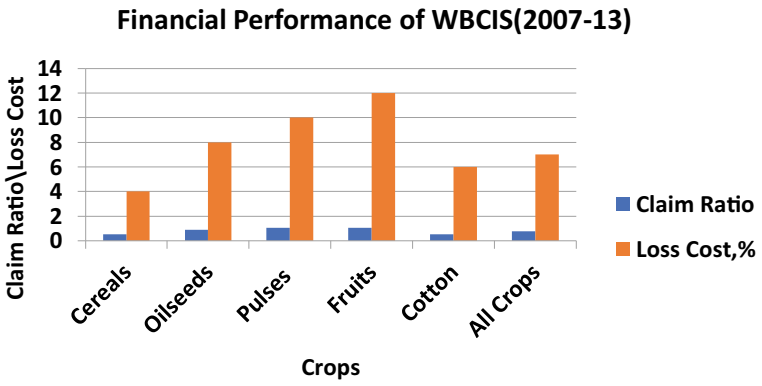

Fig. 14.5 Premium–claim ratio and loss cost (claim/sum insured) for WBCIS during 2007–2013 (Data from GoI 2014)

awareness and appreciation of the beneficial aspects of crop insurance programme hinder its out scaling, and as a result, the degree penetration is still very low. Organized efforts have to be strengthened to educate farming community for expansion of the programme.

14.5 Policies and Institutions

Most adaptation interventions require an enabling environment for action, which is provided by government policies. Unless mainstreamed into development programmes of the governments, large-scale implementation of action programmes is not possible. In India, smallholder farms constitute the backbone of agriculture, and except for some autonomous adaptations, which the poor rural farming communities can take by themselves (or might have already undertaken in response to the gradual changes which have been occurring all the time), large-scale planned adaptations were beyond their capacity. In developing countries, the performance of adaptation process through intensification by adoption of yield increasing technologies has been only 16% (Thornton et al. 2018), even though the technologies were available. The food-insecure regions, as observed by Cline (2007) and Lobell et al. (2008), would require more expensive adaptation measures including the development of new crop varieties and introduction of new irrigation technologies along with related infrastructure. Further, agricultural production takes place under open sky and is subject to damage from weather vagaries like floods, droughts, hail, storms, hurricanes, etc. This requires additional expenses on risk sharing and transfer.

14.5.1 Green Revolution Period Policies

The Indian agricultural policies during Green Revolution period focused on modernization of agriculture sector by focusing on seed–fertilizer–irrigation-based interventions through subsidies and the mechanism of minimum support price (MSP) for selected crops. Though greenhouse gases were not specifically targeted in this effort, modernization had effect on total GHG emissions as well (Climate Policy Initiative 2013; Tyagi et al. 2019). A major advantage of these productivity enhancing policies was the saving of forest land from being brought under the plough, thereby proving Borlaug hypothesis (Borlaug 2007). The MSP and very nominal charges for water and electricity (in some cases free power) policy, weighed as it was in favour of rice and wheat, made them economically remunerative crops. Thus, traditional crops got substituted by water-intensive crops at the cost of diversification (Johal 2002; Sharma et al. 2015).

Box 1: Some Common Features of Climate Policy in India/South Asia

Unlike global climate policy, in India and the South Asian countries, emphasis on adaptation to climate change in agriculture remains in focus. In the absence of legislation, there may not be direct mention of policy, and adaptation strategies are sometimes called action plans. These are currently the most common policy instrument for adaptation (Satpathy et al. 2011).

Climate policy document of all the South Asian countries makes a special mention of attending to concerns of farming community and rural poor as one of the guiding principles of climate policy.

Subsidy has been the main mechanism for mainstreaming adaptation in development programmes.

Policy statement is very elaborate, but the mechanisms to put them into practice are missing. This is particularly true of funding the adaptation programmes.

14.5.2 Post-Green Revolution Policies

The national policies in respect of climate change are reflected in documents on national climate policy, national communications on climate change to United Nations Framework Convention on Climate Change (UNFCCC) and National Action Plan(NCP), which deal with laws, regulations strategies that guide course of action at national and international forums (GoI-PMCCC 2008; GoI-MoEF 2012; GoI-MoWR 2012). The current agricultural development programmes to increase adaptation capacity are: the Mahatma Gandhi National Rural Employment Guarantee Act (MGNREGA), Prime Minister Krishi Sinchai Yojana (PMKSY), Rastriya Krishi Vikas Yojana (RKVY) and National Mission on Micro Irrigation (NMMI). These programmes not only help achieve production targets, but also provide livelihood support by generating employment (GoI-MoACFW 2019). The mission on micro-irrigation has made major headway, as micro-irrigation has been implemented in 8.6 million ha by 2017 (NITI Aayog 2015).

As groundwater has become a major source of irrigation, low electricity tariff and price support to water-intensive crops like rice and sugarcane are leading to drying of aquifers. The recent initiative—Atal Bhujal Yojana (GoI-MoJS 2019)—is the corrective action, but it will succeed only if ecologically compliant cropping is introduced. In agriculture, irrigation is a major consumer of energy. Inefficiency in more than 20 million of these agricultural pump sets results in huge wastages of energy, inflates the energy demand and generates additional greenhouse gas emission. The government has initiated a drive for replacement of inefficient agricultural pumps, under Ag. Demand Side Management (AgDSM) programme (BEE 2009).

This is a climate friendly step in right direction. Speeding up and scaling out of this programme would require creation of appropriate business model like the Domestic Efficient Lighting Programme (DELP).

14.6 Concluding Remarks and Way Forward

There are ample opportunities for agricultural systems to adapt to climate change impacts through biophysical and socio-economic interventions. In India, adaptations in agriculture have been largely productivity enhancing biophysical incremental interventions. The effectiveness of incremental adaptations is getting reduced due to the combined effect of climatic and non-climatic stress. It is reported that globally, adaptation to climate change impacts is lagging behind, as against the projected required growth rate of 1.8% in crop yields, to meet the food demands in 2050, it was growing only at the rate of 1.2% (Aggarwal et al. 2019).

It is therefore important that India transits to a new production system that not only targets yield, but also keeps land, water and other resources within safe limits. To achieve this goal, India would have to go for transformative options such as changes in cropping pattern and resource allocation for harmonization of water–energy–food security nexus (Tyagi and Joshi 2019b). But as there are cost and income tradeoffs, carefully crafted policies and institutions (access to technology, finance and markets) have to put in place.

It would require implementation of both biophysical and socio-economic adaptations to take care of the entire set of vulnerabilities. The major non-climatic factors, which constrain adoption, are: credit, risk, information and access to markets. In India, agro-technical adaptation measures dominate the scene. Though a number of socio-economic, safety nets like crop insurance, short-term crop season loans and incentives for organic farming are included in the basket, the coverage is very low.

Transformative adaptation requires higher investment, watersheds and irrigation infrastructure, advanced water technologies and risk transfer instruments. Most adaptations need additional investment, and adoption of technologies lags behind in the absence of investment. This is particularly true of small farms, which have limited capacity for infrastructure development (de Janvry and Sadoulet 2019).

Information and its communication are the basic elements for adaptive actions. Digital technologies have proved their potential in data gathering at fast speed and communicating to the farming community. India has established a good weather advisory service, and there exists a vast network of Krishi Vigyan Kendra, which remain in direct contact with farming community. There is however need to strengthen their capacity through better training and equipment.

Water has now been recognized as a major enabler of adaptation, and this is reflected in the government policies (PMKSY, NMMI, Atal-Bhujal, etc.) in respect of climate change. Adaptation planning under climate change would need information on water resources, and to capture change at micro-scale, monitoring network would have to be intensified. Further, water interconnects agriculture with other

sectors, and therefore, it would require better coordination between agriculture, water, energy, industry etc., as adaptation in one sector can impact other sectors. At present, the required level of coordination is missing and needs strengthening for improved governance (Tyagi and Mehta 2018).

Like cross-sector linkages of climate impacts, the impacts of climate policies in one sector affect another sector adversely or positively as water is embedded in most sectors. For example, sectors like biodiversity, forestry, disaster management, etc., are the areas outside agriculture, but the policies in these sectors affect the food security of vulnerable people, both positively and negatively (tradeoffs and conflict situations). Therefore, it is not only the technology, but also the inter-sector risk management and risk reduction that should also be incorporated into adaptation planning in agriculture.

Industry is moving towards fourth-generation technologies, and a similar change may be needed to drive systemic and transformative adaptation in production and production supporting services in agriculture. The new precision agriculture technologies that allow us to maximize yields by controlling different farming variables including soil moisture levels, pest stress, nutrient deficiency, micro-climates etc. Progress in these inputs, energy and cost saving technologies would require steep increase in investment in research.

References

Adger WN, Dessai S, Goulden M, Hulme M, Lorenzoni I, Nelson D, Naess LO, Wolf J, Wreford A (2009) Are there social limits to adaptation to climate change? Clim Change 93(3–4):335–354

Aggarwal PK, Vyas S, Thornton P, Campbell BM (2019) How much does climate change add to the challenge of feeding the planet this century? Environ Res Lett 14(4):043001. https://doi.org/10.1088/issn.1748-9326

Alcamo J, Henrich T, Rosch T (2000) World water in 2025: global modelling and scenario analysis for the world commission on water for the 21st century. Kassel World Water Series Report No, Kassel, p 2

Ali H, Mishra V (2018) Increase in sub-daily precipitation extremes in India under 1.5 and 2.0 °C warming worlds. Geophys Res Lett 45 (14):6972–6982

Ali H, Modi P, Mishra V (2019) Increased flood risk in Indian sub-continent under the warming climate. Weather Clim Extrems 25:100212. https://doi.org/10.1016/J.WACE.2019.100212

BEE (Bureau of Energy Efficiency) (2009) Schemes for promoting energy efficiency in India during the XI Plan, Bureau of Energy Efficiency, Ministry of Power, Government of India, New Delhi. https://www.beeindia.nic.in/down1.php?f=schemes_for_promoting_energy_efficiencyin_Indi_during_the_%20XI_Plan.pdf. Accessed 14 Aug 2009

Borlaug N (2007) Feeding a hungry world. Science 318(5849):359. https://doi.org/10.1126/science.1151062

CGWB (Central Ground Water Board) (2017) Ground water year book of Haryana State (2015–2016), North Western Region Chandigarh, Ministry of Water Resources, River Development and Ganga Rejuvenation Government of India. https://www.cgwb.gov.in/Regions/GW-year-Books/GWYB-2015-16/GWYB%20NWR%20%20Haryana%202015-16.pdf. Accessed 12 Nov 2017

CGWRE (Committee on Ground Water Resources Estimation) (2009) Report of the Groundwater Estimation Committee. Ministry of Water Resources, Government of India, New Delhi

Chand R, Pandey LM (2008) Fertilizer growth, imbalances and subsidies: trends and implications. National professor project discussion paper, National Centre for Agricultural Economics and Policy Research 02/2008, New Delhi

Cline W (2007) Global warming and agriculture: impact estimates by country, Washington D.C.: Centre for Global Development and Peterson Institute for International Economics

Crichton D (2008) Role of insurance in reducing flood risk. The Geneva Papers. 33:117–132, https://www.genevaassociation.org/media/246244/ga2008_gp33(1)_crichton.pdf

de Janvry A, Sadoulet E (2019) Transforming developing country agriculture: Removing adoption constraints and promoting inclusive value chain development. https://hal.archives-ouvertes.fr/hal-02287668/document. Accessed on 4 Mar 2020

FAO (Food and Agriculture Organization) (1990, 2010, 2014). FAOSTAT [Online]. Available at: https://faostat3.fao.org/faostat-gateway/go/to/download/G1/*/E. Accessed 22 July 2014

FAO (Food and Agriculture Organization) (2015) AQUASTAT—FAO's global information system on water and agriculture. https://www.fao.org/nr/water/aquastat/data/query/results.html Accessed on 18 Apr 2020

Freibauer A, Mathijs E, Brunori G, Damianova Z, Faroult E, Gomis JG , O´Brien L, Treyer S (2011) Sustainable food consumption and production in a resource-constrained world, European Commission—Standing Committee on Agricultural Research (SCAR)—The 3rd SCAR Foresight Exercise. https://ec.europa.eu/research/scar/pdf/scar_3rd-foresight_2011.pdf. Accessed on 1 Apr 2020

Global AgriSysrem (2017) Impact evaluation study national mission on micro irrigation (NMMI). Report submitted to Ministry of Agriculture, Government of India, New Delhi. https://pmksy.gov.in/microirrigation/Archive/IES-June2014.pdf. Accessed 15 Nov 2017

Global Commission on Adaptation (GCA) (2019) Adapt now: a global call for leadership on climate resilience, world resources institute and the global center on adaptation, Final Report. https://reliefweb.int/sites/reliefweb.int/files/resources/GlobalCommission_ReportFINAL.pdf. Accessed on 31 Mar 2020

GoH (Government of Haryana) (2011) Haryana State Action Plan on Climate Change. http://www.moef.nic.in/sites/default/fles/sapcc/Haryana.pdf. Accessed 26 Nov 2017

GoH (Government of Haryana) (2017) Statistical abstracts of Haryana 2015–16. Department of Economics and Statistical Analysis, Haryana

GoI-Directorate of Economics and Statistics (2011) Agricultural statistics at a glance, Department of Agriculture and Cooperation, Ministry of Agriculture, Government of India [Online]. Available at: https://eands.dacnet.nic.in/latest_20011.htm. Accessed 07 July 2014

GoI Ministry of Agriculture (2004) Report of the joint group on crop insurance, Department of Agriculture & Cooperation. Government of India, Ministry of Agriculture New Delhi

GoI-Ministry of Agriculture (MoA) (2011) Agricultural statistics at a Glance, Department of Agriculture and Cooperation, Directorate of Economics and Statistics. [Online] Available at: http://eands.dacnet.nic.in/latest_20011.htm [Accessed 07 July 2014]

GoI-Ministry of Agriculture (2013) Implementation of national crop insurance proqramme (NCIP) durinq Xll Plan—issue of Administrative lnstructions, Department of Agriculture & Cooperation Ministry of Agriculture. https://agricoop.nic.in/Credit/ncipletter.pdf. Accessed on 20 Aug 2014

GoI-Ministry of Agriculture (2014a) Agriculture census 2010–11. Phase 1. All India report on number and area of operational holdings provisional. New Delhi: Government of India, https://www.agricoop.nic.in/publication/agriculture-census

GoI-Ministry of Agriculture (2014b) Report of the committee to review the implementation of crop insurance schemes in India. Department of Agriculture & Cooperation, Ministry of Agriculture, New Delhi

GoI-Ministry of Agriculture & Farmers Welfare (2019) Annual report 2018–19 Department of Agriculture, Cooperation & Farmers Welfare. https://www.agricoop.nic.in/sites/default/files/AR_2018-19_Final_for_Print.pdf. Accessed on 15 Apr 2020

GoI-Ministry of Chemicals and Fertilizers (2012) Annual Report 2011–12, Department of Fertilizers, Government of India New Delhi. https://fert.nic.in/sites/default/files/Annual%20Report%202011-12%20English.pdf. Accessed on 10 Aug 2014

GoI-Ministry of Environment and Forest (2012) Second national communication to the UNFCCC, Government of India, New Delhi. https://unfccc.int/resource/docs/natc/indnc2.pdf

GoI-Ministry of Jal Shakti (2019) PM Modi Atal Jal Yojana 2020 to Manage Ground Water Resources (Bhujal) by Central Govt. https://sarkariyojana.com/atal-jal-yojana/

GoI-Ministry of Statistics and Programme Implementation (2014) Key indicators of situation of agricultural households in India, NSS 70th Round. https://mospi.nic.in/sites/default/files/publication_reports/KI_70_33_19dec14.pdf

GoI-Ministry of Water Resources (2012) National Water Policy, Government of India New Delhi

GoI-Prime Minister's Council for Climate Change (2008) National action plan on climate change. Government of India, New Delhi

Hallegatte S (2009) Strategies to adapt to an uncertain climate change. Global Environ Change 19(2):240–247

Hazell P, Poulton C, Wiggins S, Dorward A (2010) The future of small farms: trajectories and policy priorities. World Dev 38(10):1349–1361

Hoekstra AY, Mekonnen MM (2012) The water footprint of humanity. PNAS 109(9):3232–3237. https://doi.org/10.1073/pnas.1109936109

Howden SM, Crimp S, Nelson RN (2010) Australian agriculture in a climate of change. In: Jubb I, Holper P, Cai W (eds) Managing climate change: papers from GREENHOUSE 2009 conference. Melbourne CSIRO Publishing, Clayton, pp 101–112

IAI (Irrigation Association of India) and FICCI (Federation of Indian Chamber of Commerce and Industry) (2016) Accelerating growth of Indian agriculture: micro irrigation an efficient solution Strategy paper—future prospects of micro irrigation in India. https://www.grantthornton.in/globalassets/1.-member-firms/india/assets/pdfs/micro-irrigation-report.pdf. Accessed 10 June 2019

ICAR-Indian Council of Agricultural Research (2015) Vision-2050, Indian Council of Agricultural Research, New Delhi. https://www.icar.gov.in/files/Vision-2050-ICAR.pdf. Accessed on 19 Apr 2020

INCCA (Indian Network for Climate Change Assessment) (2010) Climate change and India: A 4 x 4 assessment-A sectoral and regional analysis for 2030s. New Delhi: INCCA Report 2, Ministry of Environment and Forest, Government of India. https://www.indiawaterportal.org/sites/indiawaterportal.org/files/Climate%20Change%20%26%20India_Sectoral%20%26%20Regional%20Analysis%20for%202030s_INCCA_2010.pdf

IPCC (Intergovernmental Panel on Climate Change) (2001) Climate change: impacts, adaptation and vulnerability. In: McCarthy JJ, Canziani OF, Leary NA, Dokken DJ, White KS (eds) Contribution of working group II to the third assessment report of the intergovernmental panel on climate change. Cambridge University Press, Cambridge, UK, and New York, USA, 2001, pp 1032. ISBN 0-521-01500-6

IPCC (Intergovernmental Panel on Climate Change) (2007) Summary for policymakers. In: Parry ML, Canziani OF, Palutikof JP, van der Linden PJ, Hanson CE (eds) Climate change 2007: impacts, adaptation and vulnerability. Contribution of working group II to the fourth assessment report of the intergovernmental panel on climate change. Cambridge University Press, Cambridge, United Kingdom

IPCC (Intergovernmental Panel on Climate Change) (2014) Summary for policymakers. In: climate change 2014: mitigation of climate change. Contribution of working group III to the fifth assessment report of the intergovernmental panel on climate change. Cambridge University Press, Cambridge, United Kingdom and New York, NY, USA, p 1000

Irfanullah HM, Adrika A, Ghani A, Khan ZA, Rashid MA (2011) Introduction of floating gardening in the north-eastern wetlands of Bangladesh for nutritional security and sustainable livelihoods. Renew Agric Flood Syst 23(2):89–96

Jat ML, Malik RK, Saharawat YS, Gupta R, Bhag M, Paroda R (2012) Proceedings of regional dialogue on conservation agricultural in South Asia, New Delhi, India, APAARI, CIMMYT,

ICAR, p 32. https://www.researchgate.net/publication/274707220_Regional_Dialogue_on_Conservation_Agriculture_in_South_Asia. Accessed on 15 June 2015

Johal SS (2002) Report of the expert committee on agricultural production pattern adjustment programme in Punjab for productivity and growth. Government of Punjab, Chandigarh

Joshi PK, Tyagi NK (2019) Small farm holders and climate change: overcoming the impacts in India. In: Pal et al (eds) Climate smart agriculture in South Asia technologies, policies and institutions. Springer Nature Singapore Pvt Ltd., Singapore, pp 49–71. ISBN 978–981–10–8170–5

Kanolkar R (ND) Essay on green revolution in India. From Internet. https://www.economicsdiscussion.net/essays/green-revolution-essays/essay-on-green-revolution-in-india/17559. Accessed on 19 Apr 2020

Kavi Kumar KS, Richard JT, Klein CI, Jochen H, Rupert K (2007) Vulnerability to poverty and vulnerability to climate change: conceptual framework, measurement and synergies in policy, Working Paper 19/2007, Madras School of Economics, p 35

Klein RJT, Huq S, Denton F, Downing TE, Rachels R.G, Robinson JB, Toth FL (2007) Interrelationships between adaptation and mitigation. Climate change 2007: impacts, adaptation and vulnerability. Parry ML, Canziani OF, Palutikof JP, van der Linden PJ, Hanson CE (eds) Contribution of working group II to the fourth assessment report of the intergovernmental panel on climate change, Cambridge University Press, Cambridge, UK, pp 745–777

Lal R, Sivakumar M, Faiz S, Rahman A, Islam K (2010) Climate change and food security in South Asia. Springer, Dordrecht, Heidelberg, New York, London

Lobell D et al (2008) Prioritizing climate change adaptation: needs for food security in 2030. Science 319(5863):607–610

Milly PCD, Betancourt J, Falkenmark M, Hirsch RM, Kundzewicz ZW, Lettenmaier DP, Stouffer RJ (2008) Stationarity is dead: whither water management? Science 319(5863):573–574. https://doi.org/10.1126/science.1151915

Mobarak AM, Rosenzweig MR (2013) Risk, insurance and wages in general equilibrium. Yale University Economic Growth Centre. Discussion Paper No. 1035, Yale Economics Department Working Paper No. 127. Available: SSRN: https://ssrm.com/abstract=236650

Mujumdar M, Ramarao MVS, Uppara U, Goswami M, Borgaonkar H, Chakraborty S, Ram S, Mishra V, Rajeevan M, Niyogi D (2020) Droughts and floods. In: Krishnan R, Sanjay J, Gnanaseelan C, Mujumdar M, Kulkarni A, Chakraborty S (eds) Assessment of climate change over the Indian region. Springer, Singapore. https://doi.org/10.1007/978-981-15-4327-2_6

Naresh RK, Singh SP, Dwived I, Kumar P, Kumar L, Singh V, Kumar V, Gupta RK (2016) Soil conservation practices for sustainability of rice-wheat system in subtropical climatic conditions: a review. Int J Pure App Biosci 4(1):133–165

NCIWRD (National Commission Integrated Water Resources Development) (1999) Integrated water resources development: a plan for action, report, vol I. Ministry of Water Resources, Government of India, New Delhi

Nin–Pratt A, Jonhson M, Magalhaes E, You L, Diao X, Chamberlin J (2011) Yield gaps and potential agricultural growth in West and Central Africa. In: International Food Policy Research Institute (IFPRI), Report 0896291820, Washington, DC, USA, 158 pp 14, 2019. https://www.researchgate.net/publication/254417035_Yield_Gaps_and_Potential_Agricultural_Growth_in_West_and_Cent. Accessed on June 15, 2015

NITI Aayog (National Institution for Transforming India Aayog) (2015) Raising agricultural productivity and making farming remunerative for farmers, An occasional paper. http://www.niti.gov.in/writereaddata/files/document_publication/RAP3.pdf. From Internet Accessed on18 April, 2020

Pathak H, Aggarwal PK (Eds) (2012) Low carbon technologies for agriculture: a study on rice and wheat systems in the Indo-Gangetic Plains. Indian Agricultural Research Institute, p xvii + 78

Pathak H, Saharawat YS, Gathala M, Ladha JK (2011) Impact of resource-conserving technologies on productivity and greenhouse gas emissions in the rice-wheat system. Greenh Gas Sci Technol 1:1–17

Rama Rao CA, Raju BMK, Subba Rao AVM, Rao KV, Rao VUM, Ramachandran K et al (2013) Atlas on vulnerability of Indian agriculture to climate change. Hyderabad, Central Research Institute for Dryland Agriculture, p 116

Ravindranath NH, Rao S, Sharma N, Nair M, Gopalakrishnan R, Bala G (2011) Climate change vulnerability profiles for North East India. Curr Sci 101(3):384–394

Roxy M, Ritika K, Terray P, Murtugudde R, Ashok K, Goswami BN (2015) Drying of Indian subcontinent by rapid Indian Ocean warming and a weakening land-sea thermal gradient. Nat Commun 6:7423. https://doi.org/10.1038/ncomms8423

Saini SS (2011) Mitigation initiatives through agriculture demand side management, Bureau of Energy Efficiency, Government of India, New Delhi. https://www.iitk.ac.in/ime/anoops/for12/7%20-%20Mr.%20Sarabjot%20Singh%20Saini%20-%20BEE%20-%20%20AGDSM%20-%20IIT%20K.pdf. From Internet: Accessed 11 Nov 2017

Satapathy S, Porsché I, Künkel N, Manasfi N, Anna K (2011) Adaptation to climate change with a focus on rural areas and India. Government of India, Ministry of Environment and Forests and GIZ, India, New Delhi

Schipper E, Lisa F (2009) Adapting to climate change in developing countries: institutional and policy responses for urbanizing societies, Background paper World Economic and Social Survey 2009 https://www.un.org/en/development/desa/policy/wess/wess_bg_papers/bp_wess2009_schipper.pdf. Accessed on 8 Apr 2020

Schellnhuber HJ, Hare B, Serdeczny O, et al (2013) Turn down the heat: climate extremes, regional impacts, and the case for resilience, World Bank, Washington, DC. https://documents.worldbank.org/curated/en/2013/06/17862361/turn-down-heat-climate-extremes-regional-impacts-case-resilience-full-report

Searchinger T, Waite R, Hanson C, Ranganathan J, Dumas P, Matthews E (2019) Creating a sustainable food future. World Resources Institute. https://wrr-food.wri.org/sites/default/files/2019-07/WRR_Food_Full_Report_0.pdf. Accessed on 31 Mar 2020

Sehgal VK, Singh MR, Chaudhary A, Jain N, Pathak H (2013) Vulnerability of agriculture to climate change: district level assessment in the Indo-Gangetic Plains. New Delhi, Indian Agricultural Research Institute, p 74

Sharma S, Tripathi S, Mourinho T (2015) Rationalizing energy subsidies in agriculture: a scoping study of agricultural subsidies in Haryana, India September 2015, International Institute for Sustainable Development (IISD) and Global Subsidies Initiative (GSI), Winnipeg, Canada. https://www.iisd.org/sites/default/files/publications/rationalizing-energy-subsidies-agriculture-in-haryana-india.pdf. Accessed 15 Nov 2017

Smit B, Skinner MW (2002) Adaptation options in agriculture to climate change: a typology. Mitig Adapt Strateg Glob Chang 7:85–114. https://doi.org/10.1023/A:1015862228270

Smit B, Wandel J (2006) Adaptation, adaptive capacity and vulnerablity. Global Environ Change 16:228–292

Smit B, Burton I, Klein RJ, Wandel J (2000) An anatomy of adaptation to climate change and variability. Clim Change 45:223–251

Smith DM, Matthews JH, Bharati L, Borgomeo E, McCartney M, Mauroner A, Nicol A, Rodriguez D, Sadoff C, Suhardiman D, Timboe I, Amarnath G, Anisha N (2019) Adaptation's thirst: Accelerating the convergence of water and climate action. Background Paper prepared for the 2019 report of the Global Commission on Adaptation, Rotterdam and Washington, DC. https://www.iwmi.cgiar.org/Publications/Other/PDF/adaptations-thirst-gca-background-paper.pdf. Accessed on 10 Feb 2020

Swaminathan MS (2017) 50 years of green revolution: the quest for a world without hunger, vol 1, M S Swaminathan Research Foundation, India, p 486. https://doi.org/https://doi.org/10.1142/10279

Thornton PK, Kristjanson P, Förch W (2018) Is agricultural adaptation to global change in lower-income countries on track to meet the future production challenge? Global Environ Change 52:37–48

Tompkins EL, Adger WN, Boyd E, Nicholson-Cole S, Weatherhead K, Arnell N (2010) Observed adaptation to climate change: UK evidence of transition to a well-adapting society. Global Environ Change 20(4):627–635

Tyagi NK, Joshi PK (2017) Agro-hydro-technologies and policies for adaptation to climate change: an assessment. In: Belavadi (ed) Agriculture under climate change. Allied Publishers, Bengaluru

Tyagi N, Mehta L (2018) Water energy-food security nexus brief 05. India-UK Water Centre, p 24. https://iukwc.org/sites/default/files/images/Water_Brief_05_Tyagi-Final.pdf. Accessed on 19 Apr 2020

Tyagi NK, Joshi PK (2019a) Harmonizing the water–energy–food nexus in Haryana: an exploration of technology and policy options. INAE Lett 4:251–267. https://doi.org/10.1007/s41403-019-00079-5

Tyagi NK, Joshi PK (2019b) Index-based insurance for mitigating flood risks in agriculture: status, challenges and way forward. In: Pal et al (eds) Climate smart agriculture in South Asia technologies, policies and institutions. Springer Nature Singapore Pte Ltd., Singapore, pp 183–204. ISBN 978–981–10–8170–5, ISBN 978–981–10–8171–2 (eBook)

Tyagi NK, Joshi PK, Agarwal PK, Pandey D (2019) Role of development policies in combating climate change issues in Indian agriculture: an assessment of irrigation and fertilizer policies. In: Pal et al (eds) Climate smart agriculture in South Asia technologies, policies and institutions. Springer Nature Singapore Pte Ltd., Singapore, pp 205–226. ISBN 978–981–10–8170–5

Vasudevan R, Cherail K, Bhatia R, Jayaram N (2011) Energy efficiency in India history and overview, alliance for an energy-efficient economy, New Delhi. http://www.aeee.in/wp-content/uploads/2016/03/AEEE-EE-Book-Online-Version-.pdf [Accessed on 12 October 2017]

Vyas VS (2007) Marginalized sections of Indian agriculture: the forgotten millions. Indian J Labour Econ 50(1):1–16

World Bank (2001) India power supply to agriculture Haryana case study, vol 2, Report No. 22171-IN, Energy Sector Unit South Asia Regional Office. https://siteresources.worldbank.org/INDIAEXTN/Resources/Reports-Publications/PowerAgriculture/casestudyharyana.pdf. Accessed 30 July 2017

World Bank (2008) World development report 2008: agriculture for development, Washington DC. https://doi.org/10.1596/978-0-8213-6807-7

World Bank (2020) Water in agriculture. https://www.worldbank.org/en/topic/water-in-agriculture. Accessed on 8 Apr 2020

Chapter 15
Adapting Improved Agricultural Water Management and Protected Cultivation Technologies—Strategic Dealing with Climate Change Challenge

Kamlesh Narayan Tiwari

15.1 Introduction

15.1.1 The Essence of Food Production

The Food and Agricultural Organization (FAO) of the United Nations has conducted a study and suggested that by the year 2050, the population may increase by 2.3 billion; hence, food production should be increased to meet the growing demand of the estimated population. Standards of living in the developing countries are expected to improve along with the economic growth and uplifting poverty levels, which may tend to increase the food demand in the market continuously. As a basic need, the food supply, according to the demand, is a major concern to all the countries. However, food is a resource that mainly depends on climatic conditions, available natural resources and growers' economic status.

15.1.2 Climate Change and Agriculture

Climate change indicates a change that occurred in global air temperature, the pattern of precipitation and wind and other climatic parameters that took place over a number of decades or longer.

A general increase of average earth temperature affects weather and environmental ecosystem for an extended period due to increasing greenhouse gases in the atmosphere, which causes the greenhouse effect. According to the United Nations' Intergovernmental Panel on Climate Change (IPCC 2001 report), the average global

K. N. Tiwari (✉)
Agricultural and Food Engineering Department, Indian Institute of Technology Kharagpur, West Bengal, Kharagpur 721302, India

© The Author(s), under exclusive license to Springer Nature Singapore Pte Ltd. 2021

A. Pandey et al. (eds.), *Hydrological Aspects of Climate Change*,
Springer Transactions in Civil and Environmental Engineering,
https://doi.org/10.1007/978-981-16-0394-5_15

temperature has increased by 0.8 °C in comparison with the end of the nineteenth century. Researchers expect an increase in average global temperature in the range from 1.5 to 5.3 °C by 2100 due to the current pace of CO_2 emissions. If no action is taken, it would have harmful consequences to humanity and the biosphere.

Agriculture and climate change are inseparably linked with each other, which may affect the yield, pattern and water requirement of crops. The exploitation of fossil fuels is a primary reason for climate change, which affects global temperature, precipitation and hydrological cycles. Constant changes in the rainfall intensity and frequency, waves of heat and other severe events are likely to take place, all of which will influence crop production. Moreover, augmented climate change factors may shrink crop productivity, resulting in an increase in the cost of cultivation for many important agricultural crop production systems. The following are the critical challenges of climate change in the context of agriculture.

- Interruption in the regular farm practice schedule
- May spoil the standing crop
- Upsurge attack of pests and diseases
- The threat of non-availability of water
- Degradation of quality natural resources.

Adoption of both short- and long-term agricultural plans should be the strategy to deal with the effect of climate change. In agriculture, cost-effective water infrastructure, preparedness to mitigate the severe weather conditions, development of drought-resistant crop varieties and modern land use and management practices are required. Effective use of natural resources such as water, solar radiation, other weather parameters and soil using improved irrigation method practices and protected cultivation structures have been presented in this paper to deal with changing climate situations.

15.2 Climate Change Effects on Cultivation Practices

The present agriculture production system has already started facing the effect of projected climate change. To deal with the changing agriculture scenario, suitable crop management practices are of supreme importance. Cropping patterns and crop management practices include adapting different sowing periods in accordance with the thermal time requirements of cultivar to minimize losses of crop yield (Zimmermann et al. 2017).

15.3 Crop Variety and Sowing Time

The amount of radiation required to grow crops is a determinant key to choose the crop variety and sowing date to achieve potential yield levels of a crop. Changes in climate and crop management tend to change in crop phenology and its stages (Craufurd and Wheeler 2009).

A study conducted in Germany on winter wheat shows that the sowing date was advanced by five days. During the study period from 1951 to 2009, Ray et al. (2012) reported that the sowing date was extended by 13 days for the wheat crop. However, the rapeseed sowing date remained almost the same for winter (Rosenzweig et al. 2015). According to Ding et al. (2016), the wheat sowing date might be postponed by 10–20 days for wet as well as for medium years, and for the dry years, it could be postponed by 20–25 days in comparison with the existing sowing date to obtain maximum yield under climate change. This study shows the climate change effect on the date of sowing and varietal choice of a crop. However, other climatic factors, including temperature (e.g. drought threat), influence the choice of variety according to crop and location. Economic factors are also related to the timing of various field operations and crop variety. Hence, climate change impact studies are complex and not a straightforward answer.

15.3.1 Crop Disease and Pests Management

A steep increase in the concentration of carbon dioxide causes variation in temperature and precipitation due to climate change. This may modify crop growth stages and likely to enhance the pathogenic activity. Climate change most likely influences the incidence and occurrence of pest and the severity of plant diseases. Change in climate will influence disease management, such as time of application, choice and the efficacy of chemicals, physical and biological control measures. This will be used as part of integrated pest management (IPM) strategies. Forecasting of the future plant diseases and their management are of larger interest to agriculture-related industries and agricultural extension workers to disseminate information among farmers.

In the present scenario, knowledge on the influence of climate change on disease management is limited and fragmented. Therefore, a comprehensive study of the effects of climate change on plant disease is important. Effective crop protection technologies are required to deal with altered climatic conditions. The longer growing seasons, fog, fewer frosts and shifting precipitation patterns are some of the major consequences of climate change. These changes do affect the incidence and enhancement of containing diseases (Juroszek and Von Tiedemann 2011).

15.4 Agricultural Water Management and Climate Change

The consequence of climate change is probably deepening the risk in the regions where water scarcity is already a significant concern. Efforts to expand or water management strategies in agriculture can manage risk and protect against crop damage. To deal with climate change scenario, planned agricultural water management adaption strategies are required to minimize the risks of crop failure and crop growth dynamics due to climatic fluctuations (Mo et al. 2017). Cultivation of less water-consuming crops and reducing the adaption strategy deal with the water shortage due to climate change.

15.4.1 Improved Irrigation Techniques

Precision irrigation is the need of time as many states in India get severely affected by climate change and facing a continuous drought-like situation and water scarcity. Precision irrigation allows accurate application of water to meet the specific requirements of individual plants without adverse impact on soil and the environment. The information on the quantity of water required for a crop grown at a particular location, crop growth stage and soil condition is needed to communicate with the crop growers at an appropriate time, which is lacking in Indian agriculture. Precision irrigation is the solution to this issue. The precision irrigation involves drip or sprinkler (micro-irrigation) along with sensor-based automation, which ensures an appropriate amount of water application at an appropriate time as per the crop evapotranspiration requirement or available soil moisture status at the crop root zone. Furthermore, micro-irrigation also delivers an appropriate amount of fertilizers along with irrigation depending on the nutrient status of soil within the root zone of a plant(s)/tree. Precision irrigation methods need to be developed and demonstrated at a large scale to deal with climate change issues.

15.4.1.1 Drip Irrigation

Drip irrigation has been recognized as a tool for saving water and increasing crop yield. Drip irrigation is a suitable method of water application to almost all kinds of crops, especially for wide-spaced high-valued crops such as orange, grapes, coconut, banana and mango. This is also suitable for commercial crops like sugar cane, cotton, flowers and chilly. In this method, water is applied at a slow rate near the crop root zone. The results of experimental studies are conducted by the author and his research team at Precision Farming Development Centre, IIT Kharagpur, on establishing the crop water requirement and to study the effect of drip irrigation on yield of different fruit (mango, guava, banana, sapota, litchi, pineapple, cashew nut) crops and vegetable (cabbage, cauliflower, tomato, okra, brinjal, lettuce, capsicum, cucumber

Table 15.1 Water requirement of various fruits and vegetable crops and their response due to drip irrigation

Crops	Water requirement (L Plant^{-1} day^{-1})	Yield increment due to drip (%)	Benefit–cost ratio
Fruit crops			
Mango	16.6–47.4	128.0	6.27
Guava	11.9–34.5	164.0	3.17
Banana	4.0–18.6	39.1	2.55
Pineapple	0.16–0.55	22.8	5.88
Sapota	16.3–36.8	96.7	3.21
Litchi	9.3–33.2	41.0	3.64
Cashew nut	8.2–29.8	46.0	2.02
Vegetable crops			
Cabbage	1.2–1.7	62.5	5.40
Cauliflower	0.7–1.4	22.3	4.20
Tomato	0.9–2.3	44.1	6.42
Okra	0.6–1.9	54.9	2.70
Brinjal	0.8–3.4	25.6	3.27
Broccoli	0.7–1.3	33.5	4.54
Lettuce	0.6–0.9	19.6	2.3
Capsicum	0.5–0.9	36.4	2.6
Cucumber	0.5–0.6	24.6	2.8
Turmeric	0.1–0.5	85.1	4.76

and turmeric) crops. The results are summarized in Table 15.1. The overall water saving is about 40% as compared to the traditional irrigation method. It shows the importance of drip irrigation for the judicious use of water when there will be water scarcity due to climate change.

In another study, Rajwade et al. (2016) conducted a drip irrigation experiment for rice production under climate change scenarios in sub-tropical India. The effect of varying N nutrient levels on crop yield, water productivity and N nutrient use efficiency of rice was experimentally evaluated using subsurface drip irrigation. The field experiments included two different spacings of drip lateral (40 and 60 cm) and four N nutrient levels, i.e. 0 (N0), 50, 75 and 100% of normal N recommendation with three replications. Experiments were conducted at IIT Kharagpur, India, in dry and wet seasons from 2012 to 2014. Both the lateral spacings resulted in similar growth and yield of rice due to uniform distribution and movement of water and N fertilizer through subsurface drip inline lateral system. Under drip irrigation, increasing the N fertilizer level from N0 to N50 and N75 increased the grain yield and water productivity of rice significantly. However, no significant changes were observed with further N fertilizer addition. The drip irrigation saved 32% irrigation water in

the dry season compared to the conventional puddled transplanting with marginally reduced yield (8%) as averaged over two years.

The influence of varied scenarios of climate change on the yield of rice grain for selected places in sub-tropical India was simulated. The CO_2 content was taken as 380 ppm for the base period (1961–1990). The future periods in 2020 (2010–2039), 2050 (2040–2069) and 2080 (2070–2099) were considered as 423, 499 and 532 ppm, respectively, for representative concentration pathway (RCP) 4.5 and 432, 571 and 801 ppm for RCP 8.5 (Rosenzweig et al. 2015). The yield of a dry season rice grain under drip irrigation (DIR) and puddled transplanted rice (PTR) system was simulated using location-specific soil properties, calibrated cultivar genotype parameters and using the standard established crop management practices. For different climate change scenarios, the percentage change in the simulated rice grain yield was estimated in comparison with the yield obtained for both the DIR and PTR systems under the base period. The response of different N nutrient levels (75, 100 and 125% of the normal recommended dose) on the rice grain yield in both DIR and PTR systems was simulated under different climate change scenarios for the selected areas. The effect of different sowing dates on the yield of a rice grain under DIR and PTR was simulated for the selected locations in India. Twenty-one days before and after the existing sowing date (December 22) were chosen for sowing during the dry season. Accordingly, December 1, December 22 and January 15 were the considered sowing dates. The rice grain yield simulations were carried out for the base period (1961–1990) and for future periods (2020, 2050, and 2080), with the above-mentioned sowing dates keeping other management practices constant.

Simulation using the CERES model resulted in a reduction in the rice grain yield by 3–10%, 7–16% and 9–15% in RCP 4.5 and 11–16%, 13–15% and 38–41% in RCP 8.5 scenarios during 2020, 2050 and 2080, respectively, in comparison with base period (1961–1990) rice grain yield using drip irrigation. The combination treatments of 25% increment in the application of N nutrient level in comparison with the normal recommended dose and early sowing were able to compensate for the adverse impact of rising temperature (up to +3.3 °C) in future climate on the rice production (Rajwade et al. 2016).

15.4.1.2 Sprinkler Irrigation

Sprinkler irrigation system sprays water in the form of droplets emerging out of a nozzle attached with a riser pipe connected to a network of pipes. These systems are suitable for irrigating crops where the plant density is very high, where the adaption of the drip irrigation system may not be economical. This system of irrigation has been in vogue in the country for more than forty years. The sprinkler method is technically feasible and economically viable for a large number of crops grown in the country. This method can be adapted in the crops such as cereal, pulses, vegetables, flowers, fruits and plantation crops. Summarized results of sprinkler irrigation experiments conducted by the Precision Farming Development Centres (PFDCs) located in different parts of India are given in Table 15.2. There is considerable water saving

Table 15.2 Saving of water and percentage increase in production using a sprinkler irrigation system

Crops	Water saving (%)	Yield increase (%)	Crops	Water-saving (%)	Yield increase (%)
Bajra	56	19	Gram	69	57
Barley	56	16	Groundnut	20	40
Bhindi	28	23	Jowar	55	34
Cabbage	40	3	Lucerne	16	27
Cauliflower	35	12	Maize	41	36
Chilli	33	24	Onion	33	23
Cotton	36	50	Potato	46	10
Cowpea	19	3	Sunflower	33	20
Garlic	28	6	Wheat	35	24

in comparison with conventional irrigation. Sprinkler system protects crops from fog and frost during winter and also creates a cooling environment surrounding crops during summer.

15.5 Protected Cultivation Technologies

Protected cultivation is a technique used to grow crops with fully or partially controlled micro-climate surrounding plants as per the crop species requirement at their growth period. With the progress in agriculture and horticulture, large numbers of protected cultivation techniques appropriate for a specific type of climatic conditions have emerged.

15.5.1 The State of the Art

15.5.1.1 Low Tunnels

Low tunnels are a tiny form of the greenhouse to protect the crop from extreme rains, winds, cold, frost and another oddity of weather conditions. However, inside low tunnels, completely altering micro-climate artificially is not possible. Inside the low polytunnels, seedlings can be grown in a short duration and can be protected from the rain and storm during the rainy season. The polytunnel seedlings can be transplanted 7–15 days earlier than that of grown in open field conditions. Generally, the cladding film is made up of UV-stabilized LDPE films.

15.5.1.2 Polytunnels

Polytunnels are the protected cultivation structures made from locally available wood or bamboo and covered with UV-stabilized plastic sheet. It facilitates to entrap carbon dioxide and save crops from extreme climatic conditions. Naturally ventilated low-cost polytunnel of the size 9 m long, 3 m wide and 2 m height was constructed with locally available bamboo, and UV-stabilized film was used as a cladding material. An insect-proof net was provided at the side of the structure to prevent the entry of insects. The polytunnels were constructed by the author and his team of researchers at the Precision Farming Development Centre, IIT Kharagpur. These polytunnels were used for the production of off-season vegetables and raising seedlings of vegetables, flowers and hardening of mango grafts. These structures had a working life span of 2.5–3 years. Farmers can fetch annual profit ranging from Rs. 5,000 to Rs 20,000 from 27 m^2 area. Farmers were trained to fabricate and use low-cost greenhouse structures for raising nursery of vegetables, paddy and other seasonal crops and also grow off-season vegetables. The results of a few crops grown under experimental polytunnel structures are given in Table 15.3.

15.5.1.3 Greenhouse/Polyhouse

A greenhouse is a framed structure envelope cladded with a transparent LLDPE film in which crops can be grown in a partially or fully controlled environment. The structure is provided with adequate space to allow entry of person (s) to work and carry out cultural operations. Greenhouse provides favourable micro-climatic conditions to the crop to achieve greater yield and better-quality produce. The structure provides opportunities to grow crops year-round, thereby increasing land productivity. The structure protects plants against biotic (pests, diseases and weeds) and abiotic (temperature, humidity and light) stress grown, especially during off-season.

Table 15.3 Water requirement and crop response in the polytunnel and open field conditions

Sl. No	Name of crop	Water requirement (L day^{-1} $plant^{-1}$)		Average weight (g)		Yield (t ha^{-1})	
		T_1	T_2	T_1	T_2	T_1	T_2
1	Cauliflower	0.74–1.01	0.42–0.63	600	1100	24	44
2	Cabbage	0.76–0.97	0.45–0.60	2000	2750	66	91.66
3	Tomato	0.63–0.82	0.41–0.52	45	80	20	110
4	Broccoli	0.71–0.99	0.46–0.61	730	1400	29	66
5	Capsicum	0.58–0.84	0.37–0.52	170	380	44	124
6	Cucumber	0.29–0.40	0.19–0.25	184	270	35	110
7	Rose	1.28–3.11	0.86–3.00	–	–	12*	19 *

T_1 = Open field; T_2 = Greenhouse
*No. of flowers/plant/year

Table 15.4 Structural design of greenhouses of different floor area and height

Sl. No	Floor area, m^2	Height, m	Gutter height, m	Arch pipes, No	Side sash, No	Columns, No	Polythene area, m^2
1	100	5	2	6	12	–	316.0
2	200	4	2	11	22	–	386.7
3	200	5	2.5	17	34	–	575.0
4	500	4	1.5	45	18	36	1051.7
5	500	4.5	2	88	22	77	2060

15.5.1.4 Design of Greenhouse

A study was conducted to design a greenhouse considering local wind load, live load and dead load. A MATLAB-based programme was developed for the structural design of the greenhouse and to determine the quantity and size of structural component requirement. The programme was run for different wind speeds and for different floor areas of the greenhouse. The results of outer diameter (OD) and thickness (t) of the columns and arches and the number of pipes needed for various positions and sizes of the greenhouse are presented in Table 15.4 (Gupta et al. 2019).

15.5.1.5 Shade Net House

Shade net house is a framed structure made up of GI pipes, angle iron, timber or bamboo. The structure is cladded with a plastic net, which is made of UV-treated LLDPE thread having different shade percentages. Shade net is used to guard the plants against the scorching sunlight, extreme winds, direct impact of rainfall as well as insects and pests. This structure provides the facility to control micro-climate partially by reducing light intensity and provides adequate temperature during day time. Due to these advantages, shade net house structure is used. The structure is also used to produce seasonal and off-season crops. Shading in the structure reduces the crop water requirement and increases water productivity (Moller and Assouline 2007). Shade nets are mainly being used to raise nursery, secondary hardening of tissue-cultured plantlets and cultivation of vegetables and flower crops.

15.5.1.6 Modified Greenhouse

The modified greenhouse is a hybrid concept of shade net house and polyhouse. It is well-framed structure made up of GI pipes covered with nets of different shades and UV-stabilized polyethylene. The poly film is placed beneath shade net (around 1–2 m below shade net), which increases the temperature during winter and creates a favourable environment during the summer season. This structure also protects the

crop from rains and hails storms. The author and his team constructed a modified greenhouse structure to grow Dutch Roses.

15.5.1.7 Micro-climate of Different Protected Cultivation Structures

The cladding of protected cultivation structures (PCS) causes a change in the climatic conditions compared to outside for all the seasons. The debarring entry of rainfall, entrapment of the carbon dioxide within the structures, lesser entry of solar radiation and maintaining higher relative humidity in comparison with open field are the major micro-climatic changes that occur inside PCSs. The change in each of these climatic parameters has its own effect on the crop development, yield and quality of the crop inside the protected cultivation structures.

Temperature

The temperature of a location plays an important role in designing protected cultivation structures and control systems. The temperature has a direct impact on the physiological development phases of the plant. It also regulates plant transpiration rate and plant water status through stomatal control during the photosynthesis. Daily maximum and minimum temperature variation in different PCS were recorded on a daily basis and are presented as monthly average in Fig. 15.1. Air temperature recorded in these structures showed that the use of different covering materials for structure makes an impact on temperature. Air temperature recorded under the shade net house was always lower in comparison with that of temperature at an open field and other types of structures. This is due to the partial passage of solar radiation and the exchange of air by the perforations of the shade net. Shade nets also interrupt the entry of wind flow (Stamps 1994) that influences temperature inside the structure. Higher values of maximum and minimum temperatures were observed inside the polytunnel during summer and monsoon months (April–November) in comparison with other PCS and open field conditions. The cladding of structure with poly film increases the temperature due to the entrapment of solar radiation inside structures (Santosh et al. 2017).

Relative Humidity

Relative humidity (RH), ranging between 60 and 90%, is most optimal for the plants and their growth. Figure 15.2 shows that the monthly average daily RH values are significantly lower for open field conditions compared to the monthly average daily RH values observed in the PCSs. The values of RH in walking tunnels increased by 19–25% in comparison with the open field, which is followed by polyhouse (17–23%), modified greenhouse (15–21%) and shade net house (10–17%).

Solar Radiation

Solar radiation is the most important parameter for the photosynthesis process in plants. The accumulation of plant dry matter linearly reduces with solar radiation values. The monthly average of daily net solar radiation values for different PCS is

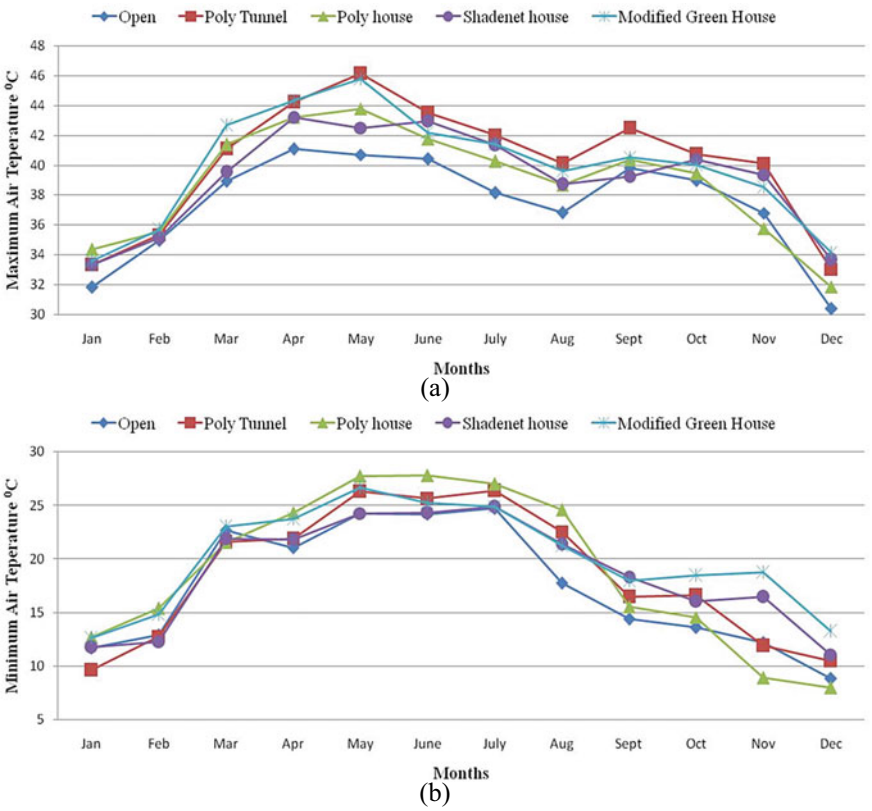

Fig. 15.1 Monthly average of daily maximum **a** and minimum, **b** temperature recorded in different protected cultivation structures and open field condition

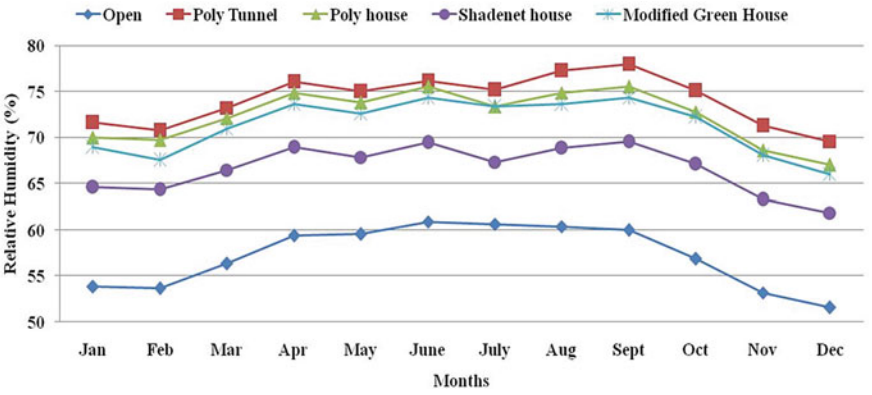

Fig. 15.2 Monthly average of daily mean relative humidity (%) recorded in different protected cultivation structures and open field condition

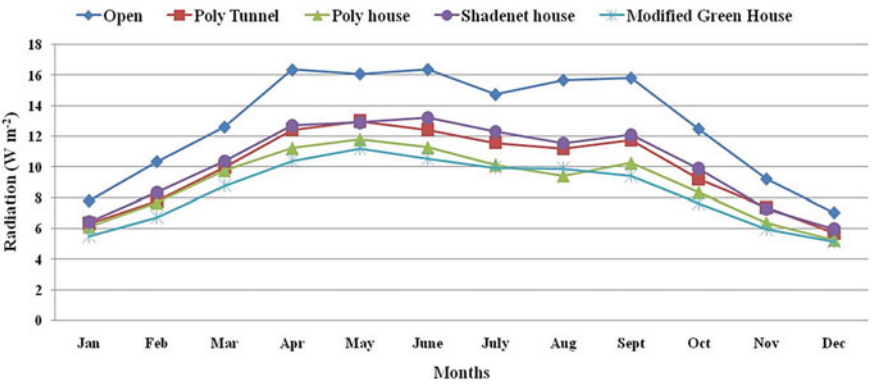

Fig. 15.3 Monthly average of daily net solar radiation (W m-2) recorded in different PCS and open field conditions

presented in Fig. 15.3. The greenhouse film transmits about 60–80% solar radiation depending on the solar intensity, time, season and sunshine hours. The difference in solar radiation values in the PCS and open field during winter months (November to February) was lesser in comparison with summer and monsoon months (March to October). The type of cladding material used in PCS significantly changes radiation balance relative to the external environment. Among all PCSs, the solar radiation transmitted inside shade net house was maximum (74–85%) followed by walking tunnel (71–81%), polyhouse (60–78%) and modified greenhouse (60–73%) in that order (Fig. 15.3). This may be due to the fact that the modified greenhouse cladded with a shade net on the top and UV stabilized at the bottom reduced the transmittance of solar radiation.

Reference Evapotranspiration

The micro-climate formed in PCSs due to different cladding materials influences the evapotranspiration of the crop. The micro-climatic data recorded in the protected cultivation structures was used to estimate the reference evapotranspiration by FAO-56 modified Penman–Monteith (PM) model. The monthly average of daily estimated ET_0 values for all the PCS is presented in Fig. 15.4. The values of reference evapotranspiration (ET_0) under different structures were observed to be lesser in comparison with the open field due to lesser vapour pressure deficit and higher relative humidity in these PCS structures. The values of ET_0 in open field conditions are always higher in comparison with the ET_0 values inside different protected cultivation structures during the entire crop season. The ET_0 values are lesser as there is very less transport of water vapour due to the low entry of wind in these structures.

Crop Water Requirement

Experiments were conducted to determine the water requirement of important crops in the sub-humid climate region of Kharagpur at Precision Farming Development Centre, IIT Kharagpur, under protected cultivation structures and in an open field. The

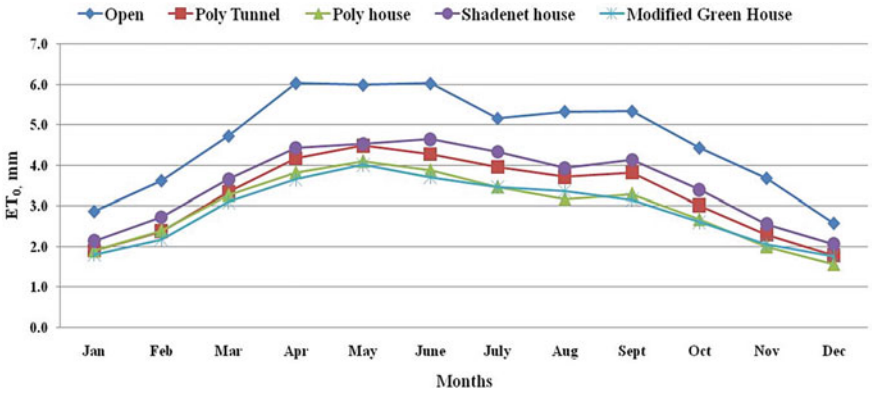

Fig. 15.4 Monthly average of daily reference crop evapotranspiration (mm) estimated for different PCS and open field conditions

Table 15.5 Estimated water requirement of crops in different protected cultivation structures

Sl. No	Crop	Season	Water requirement (L day^{-1} Plant^{-1})		Seasonal water requirement (mm)	
			Polyhouse	Open field	Polyhouse	Open field
1	Capsicum	Nov–Feb	0.37–0.52	0.49–0.84	218.6	339.8
2	Cucumber	Nov–Feb	0.31–0.41	0.50–0.64	201.2	311.9
3	Lettuce	Nov–Feb	0.24–0.33	0.57–0.89	219.1	339.9
4	Gerbera	Year-round	0.18–0.59	0.29–0.91	858.4	1353.0
5	Rose	Year-Round	0.18–0.59	0.32–0.88	991.5	1048.5

monthly average of estimated daily water requirement and seasonal water requirement of the crops under study is presented in Table 15.5. It can be seen from the results that the water requirement of crops inside the greenhouse is always lower than the open field. Hence, there is a considerable saving in water for greenhouse crops. These water requirement values can be used to design in the design water storage structures for cultivating a crop(s) in protected cultivation structures or in open field condition.

15.5.1.8 Mulching

Application of drip irrigation along with plastic mulch film has shown outstanding results in terms of crop productivity, moisture conservation and weed control. Covering soil surface with straw, plants leaves or plastic film is mulching. UV stabilizer is added with the polymer to manufacture UV-stabilized plastic mulch film. These are available in different colours, transparent and silver top and black bottom. It has been found very useful in controlling weed growth and conserving moisture.

Transparent plastic mulch is used for soil solarization to kill soil-borne bacteria. Table 15.6 shows the crops recommended for the use of plastic mulch of different thicknesses.

The yield response of different crops and the corresponding water saving due to plastic mulch are shown in Tables 15.7 and 15.8 (Anonymous 2010).

Table 15.6 Recommended thickness of plastic film suitable for different crops

Thickness (Microns)	Crops recommended
25	Short duration crops, vegetables (3–4 months)
50	Medium duration crops (11–12 months) Early stage of fruit crops, coffee, papaya, sugarcane
100	Mango, citrus fruits and medium-grown trees

Table 15.7 Increase in yield, weed control and water saving due to the application of plastic mulch in different crops

Crop	Weed control (%)	Yield increase (%)	Water saving (%)
Kinnow	55	18	25
Lemon	51	14	30
Cotton	60	25	46
Pineapple	61	32	35
Ginger	99	28	30
Turmeric	94	21	25
Brinjal	90	20	12
Coconut	80	75	25

Table 15.8 Influence of plastic mulch on fruit and vegetable crops

Crop	Increase in yield due to plastic mulch (%)	Crop	Increase in yield due to plastic mulch (%)
Mango	9.90	Cabbage	10.00
Guava	67.13	Tomato	14.82
Pineapple	15.71	Okra	14.92
Banana	23.80	Brinjal	31.05
Litchi	32.80	Broccoli	26.42
Turmeric	28.30	Cucumber	34.70

15.5.2 Role of Protected Cultivation in Mitigating Climate Change Effects

Protected cultivation has tremendous scope to protect crops due to climatic change. Experimental studies have shown about 20% saving in water and a 15% increase in the yield of many crops. These structures protect the standing crop from a sudden wind and rainstorms, high temperature, dew and frost. Due to a controlled and favourable environment, protected cultivation will be one of the most important climate change mitigating tools in the farming operation.

The open field cultivation or natural vegetation such as forest and pasture is highly dependent on climate, unlike crops under protected cultivation. Protected cultivation is less dependent on local climate conditions, and the micro-climate inside structures can be partially or fully controlled by means of appropriate devices. However, the inside climate, energy balance and consequently, the economic models are deeply influenced by external climatic conditions (Boulard et al. 2011). The area of shade net house and naturally ventilated greenhouses in the Mediterranean region and countries with mild climate conditions have been continuously expanding (Gruda et al. 2019) due to favourable climate and economic consideration. The major effect of climate change is a rise in temperature and unexpected high magnitude rains, which are detrimental to the nursery, field crops and high-value commercial crops. The protected cultivation structures have a great future to get fresh and high-value vegetables round the year.

15.6 Conclusion

This research paper presents adaptable technologies to mitigate the effect of climate change on agriculture by giving special attention to agricultural water management and protected cultivation structures. The adaptation of improved irrigation techniques like drip and sprinkler along with the polyhouse, shade net house and modified greenhouse has shown a positive impact on the sustainable production of agriculture and horticulture. The research findings of the Precision Farming Development Centre, IIT Kharagpur, for adapting improved irrigation and protected cultivation techniques are useful and relevant to deal with climate change. The key challenge for the research community is to move beyond the current simplistic understanding of smallholder that is inherently nature-protecting, but unable to adapt to climate change because of their overwhelming vulnerability.

Acknowledgements The author is thankful to the National Committee on Application of Plastics in Horticulture (NCPAH), Ministry of Agriculture and Farmers Welfare, Govt. of India, for providing financial support to the Precision Farming Development Centre, IIT Kharagpur, for conducting research experiments. The author acknowledges researchers working in this area as their researches and literature have provided a path to prepare this manuscript.

References

Anonymous (2010) Annual review meeting reports. Precision Farming Development Centre, IARI, New Delhi

Boulard T, Raeppel C, Brun R, Lecompte F, Hayer F, Carmassi G, Gaillard G (2011) Environmental impact of greenhouse tomato production in France. Agron Sustain Dev 31:757–777. https://doi.org/10.1007/s13593-011-0031-3

Craufurd PQ, Wheeler TR (2009) Climate change and the flowering time of annual crops. J Exp Botany 60:2529–2539.https://doi.org/10.1093/jxb/erp196

Ding DY, Feng H, Zhao Y, He JQ, Zou YF, Jin J (2016) Modifying winter wheat sowing date as an adaptation to climate change on the loess plateau. Agron J 108:53–63. https://doi.org/10.2134/agronj15.0262

Gruda N, Bisbis M, Tanny J (2019) Influence of climate change on protected cultivation: impacts and sustainable adaptation strategies—a review. J Cleaner Product 225:481–495. https://doi.org/10.1016/j.jclepro.2019.03.210

Gupta D, Tiwari KN, Machavaram R (2019) Studies on structural design of greenhouse. PFDC IIT Kharagpur

Juroszek P, Von Tiedemann A (2011) Potential strategies and future requirements for plant disease management under a changing climate. Plant Pathol 60:100–112. https://doi.org/10.1111/j.1365-3059.2010.02410.x

Mo XG, Hu S, Lin ZH, Liu SX, Xia J (2017) Impacts of climate change on agricultural water resources and adaptation on the North China Plain. Adv Climate Change Res 8(2):93–98

Moller M, Assouline ÆS (2007) Effects of a shading screen on microclimate and crop water requirements 171–181. https://doi.org/10.1007/s00271-006-0045-9

Rajwade YA, Swain DK, Tiwari KN (2016) Drip irrigated rice production system for improving yield and resource use efficiency under climate change scenarios in subtropical India (Doctoral thesis). Indian Institute of Technology Kharagpur, India

Ray DK, Ramankutty N, Mueller ND, West PC, Foley JA (2012) Recent patterns of crop yield growth and stagnation. Nat Commun 3(1):1–7

Rosenzweig EE, Siebert S, Ewert F (2015) Intensity of heat stress in winter wheat—phenology compensates for the adverse effect of global warming. https://doi.org/10.1088/1748-9326/10/2/024012

Santosh DT, Tiwari KN, Singh VK (2017) Influence of different protected cultivation structures on water requirements of winter vegetables. Int J Agric Environ Biotechnol 10(1):93–103

Stamps RH (1994) Evapotranspiration and nitrogen leaching during leather leaf fern production in shade houses. SJRWMD Spec. Publ. SJ94-SP10. St. Johns River Water Management District, Palatka, F

Zimmermann A, Webber H, Zhao G, Ewert F, Kros J, Wolf J, Britz W, Vries WD (2017) Climate change impacts on crop yields, land use, and the environment in response to crop sowing dates and thermal time requirements. Agric Syst 157:81–92. https://doi.org/10.1016/j.agsy.2017.07.007

Chapter 16
Using Oxygen-18 and Deuterium to Delineate Groundwater Recharge at Different Spatial and Temporal Scales

Alan E. Fryar, Joshua M. Barna, Lahcen Benaabidate, Brett A. Howell, Sunil Mehta, and Abhijit Mukherjee

16.1 Introduction

Over the past five decades, stable isotopes of oxygen (^{18}O) and hydrogen (^{2}H, or deuterium [D]) have been used to delineate sources and timing of precipitation, identify effects of evaporation, and apportion end-member contributions in streamflow and groundwater (Darling et al. 2005). Equilibrium and kinetic fractionations cause these isotopes to be preferentially enriched in liquid water and depleted in water vapour relative to the lighter, more common stable isotopes ^{16}O and ^{1}H. As condensation and precipitation occur, the remaining water vapour becomes isotopically lighter; this process is promoted by decreasing temperature. During a storm, rainout can result in progressive depletion in the ^{18}O and ^{2}H contents of precipitation. Similarly, rainfall becomes progressively depleted with distance from the coast

A. E. Fryar (✉)
Department of Earth and Environmental Sciences, University of Kentucky, Lexington, KY 40506-0053, USA
e-mail: alan.fryar@uky.edu

J. M. Barna
ARM Group Inc., 9175 Guilford Rd., Suite 310, Columbia, MD 21046, USA

L. Benaabidate
Department of Environment, Faculty of Sciences and Techniques, University of Sidi Mohamed Ben Abdellah, P.O. Box 2202, 30000 Fès, Morocco

B. A. Howell
AECOM, 100 N. Broadway, 20th Floor, St. Louis, MO 63102, USA

S. Mehta
INTERA, 3240 Richardson Rd., Suite 2, Richland, WA 99354, USA

A. Mukherjee
Department of Geology and Geophysics, Indian Institute of Technology Kharagpur, Kharagpur 721302, India

© The Author(s), under exclusive license to Springer Nature Singapore Pte Ltd. 2021

A. Pandey et al. (eds.), *Hydrological Aspects of Climate Change*,
Springer Transactions in Civil and Environmental Engineering,
https://doi.org/10.1007/978-981-16-0394-5_16

in mid-latitude regions and with elevation as air masses move inland and upward (Darling et al. 2005). Isotopic analyses of precipitation from stations around the world show the following general relationship, known as the Global Meteoric Water Line (GMWL; Craig 1961):

$$\delta^2\mathrm{H} = 8\delta^{18}\mathrm{O} + 10 \tag{16.1}$$

where the relative abundance of stable isotopes is defined as

$$\delta = \left(\left(\frac{R_{\mathrm{sample}}}{R_{\mathrm{standard}}}\right) - 1\right) \times 1000 \tag{16.2}$$

and R refers to the isotopic ratio ($^{18}\mathrm{O}/^{16}\mathrm{O}$ or $^{2}\mathrm{H}/^{1}\mathrm{H}$). Both $\delta^{18}\mathrm{O}$ and $\delta^{2}\mathrm{H}$ are reported in per mil (‰) notation relative to Standard Mean Ocean Water (SMOW; Craig 1961) or the equivalent Vienna SMOW (VSMOW) (Kendall and Caldwell 1998). Local meteoric water lines (LMWLs), commonly with slopes <8, reflect seasonal variability in rainfall and moisture source areas. Partial evaporation can cause differential enrichment of $^{18}\mathrm{O}$ relative to $^{2}\mathrm{H}$ in residual soil moisture and surface water, resulting in $\delta^{2}\mathrm{H}$ versus $\delta^{18}\mathrm{O}$ trends sub-parallel to MWLs (Darling et al. 2005).

Variability in $\delta^{18}\mathrm{O}$ and $\delta^{2}\mathrm{H}$ over broad spatial and temporal scales facilitates the use of water isotopes in identifying sources and timing of groundwater recharge and flow. Recharge tends to be only slightly modified by evaporation (typically within ~0.5‰ in $\delta^{18}\mathrm{O}$ relative to bulk rainfall), but different sources of recharge (e.g. partly evaporated surface water or intruded seawater in coastal regions) can impart distinctive isotopic compositions to groundwater (Darling et al. 2005). In regional aquifer systems, groundwater residence times can be as long as 10^6 years (Sturchio et al. 2004), although actively circulating groundwater is commonly much younger (Darling et al. 2005). Consequently, deep groundwater can serve as a paleoclimatic archive, preserving evidence of recharge during glacial periods as indicated by depleted values of $\delta^{18}\mathrm{O}$ and $\delta^{2}\mathrm{H}$ (Jasechko et al. 2015). Stable isotopes of younger groundwater ($\lesssim 10^4$ years) show seasonality of recharge (i.e. during winter in arid and temperate climates and during the wet season in tropical regions; Jasechko et al. 2014). Although dispersion during groundwater recharge and flow dampens variability in $\delta^{18}\mathrm{O}$ and $\delta^{2}\mathrm{H}$, storm event-scale (hourly to daily) fluctuations in stable isotopes and other hydrochemical parameters can be evident in surficial aquifers with relatively rapid circulation. This is pronounced in karstified limestone, where solution-enhanced permeability can result in integrated surface and subsurface drainage networks linking sinkholes to springs (Darling et al. 2005). The development of isotope-ratio infrared spectroscopy (IRIS), such as cavity ring-down spectroscopy, during the past 20 years has simplified measurements of $\delta^{18}\mathrm{O}$ and $\delta^{2}\mathrm{H}$ relative to gas-source isotope-ratio mass spectrometry (IRMS) (van Geldern and Barth 2012). As a result, large sample sets, such as high temporal-resolution storm hydrographs, are amenable to stable isotope analyses (Tweed et al. 2016).

Fig. 16.1 Locations of study sites. HP = Southern High Plains (USA); MA = Middle Atlas plateau (Morocco); WB = western Bengal basin (India); H = Houzhai karst basin (China). Modified from www.freeusandworldmaps.com/html/World_Projections/WorldPrint.html (Copyright J. Bruce Jones 2019)

This paper reviews the use of $\delta^{18}O$ and $\delta^{2}H$ to constrain sources and timing of recharge in two regional sedimentary aquifer systems and two mountainous karst terrains. The study sites are located between 21°N and 36°N (Fig. 16.1) and span a variety of climatic settings. The regional aquifer systems include the unconfined High Plains aquifer and underlying confined aquifers in the northern part of the Southern High Plains (Texas, USA; continental, temperate, semi-arid climate) and the semi-confined Holocene–Pleistocene aquifers of the western Bengal basin (West Bengal, India; monsoonal, tropical climate). The karst terrains include the Liassic aquifer of the Middle Atlas plateau (Morocco; Mediterranean [dry-summer, sub-tropical] climate) and the Houzhai basin of the Southeast Asian karst region (Guizhou, China; monsoonal, sub-tropical climate). We focus on using stable isotopes to delineate spatial variability in regional aquifers, including paleorecharge to deep aquifers, diffuse versus focused recharge to surficial aquifers and sources of salinization. For mountainous karst aquifers, which may be sensitive to climate change (Hartmann et al. 2014), we focus on temporal variability in individual spring basins and identify recharge at event to seasonal time scales.

16.2 Materials and Methodology

Water samples were collected from water and oil wells in the Southern High Plains (HP) in July–August 1997; from water wells in the western Bengal basin (WB) in May 2003–2005 and November 2007; from Zerouka spring in the Middle Atlas (MA) daily from 19 March 2014 to 28 March 2015; and from Maoshuikeng spring in the Houzhai basin (H) hourly to bihourly on 23–25 June 2018 (Table 16.1). Stable

Table 16.1 Study sites, numbers of samples collected and water bodies sampled

Study site	Location	No. of samples	Water body
Southern High Plains	Carson and Gray Counties, Texas, USA	9 3 3	High Plains (Ogallala) aquifer Whitehorse Group (Permian) Wolfcampian and Upper Permian petroleum reservoirs
Western Bengal basin	Murshidabad district, West Bengal, India	43 27	East-bank (Sonar Bangla) aquifer West-bank aquifer
Middle Atlas plateau	Ifrane, Morocco	375	Zerouka spring, Liassic aquifer
Houzhai karst basin	Puding County, Guizhou, China	36	Maoshuikeng spring, Guanling Formation

isotopes were analysed by IRMS for HP and WB (2003–2005) samples and by IRIS for WB (2007), MA and H samples. Details of monitoring, including sample collection and analyses, are given in Mehta et al. (2000a) for HP, in Mukherjee et al. (2007b, 2018) for WB, in Howell et al. (2019) for MA and in Barna (2019) for H.

16.3 Results and Discussion

Southern High Plains

The High Plains aquifer is the largest in the USA. In the Southern High Plains, this aquifer occurs within the Ogallala Formation (Upper Tertiary), which consists of clayey to gravelly sediments overlying Triassic sandstones and mudstones (Dockum Group) and Permian evaporites, carbonates and clastic redbeds. The High Plains aquifer is extensively exploited for agriculture as well as public and industrial uses. In the northern half of the region, High Plains groundwater typically has total dissolved solids (TDS) < 400 mg/L. However, two saline plumes (maximum Cl^- concentration >500 mg/L and maximum TDS >2000 mg/L) of combined areal extent >1000 km^2 occur in the aquifer near its northeastern edge (Mehta et al. 2000b). The southern plume overlies the Panhandle oil and gas field, which produces petroleum from Pennsylvanian and Permian carbonate and clastic reservoirs with TDS typically 140–290 g/L (Mehta et al. 2000a). Identifying the mechanism of salinization of the High Plains aquifer (natural vs. anthropogenic) is important for regional water resources management.

A plot of δ^2H versus $\delta^{18}O$ (Fig. 16.2), which includes data from the previous regional studies, shows that four of seven groundwater samples from the southern plume are isotopically depleted ($\delta^{18}O$ −8.8 to −6.9‰, δ^2H −88 to −70‰) relative to

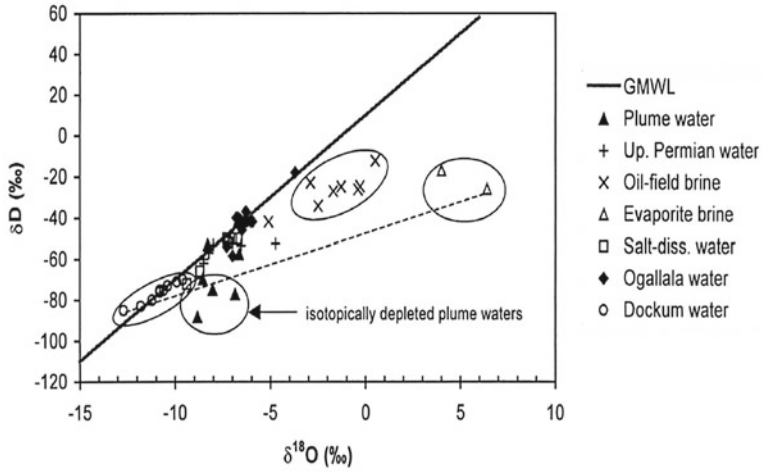

Fig. 16.2 δD (δ^2H) versus δ^{18}O relationship for end-member waters in the northern part of the Southern High Plains. Reprinted from *Applied Geochemistry*, Vol. 15, Mehta, S., Fryar, A. E., and Banner, J. L., Controls on the regional-scale salinization of the Ogallala aquifer, Southern High Plains, Texas, USA, pp. 849–864, Copyright 2000, with permission from Elsevier

upgradient High Plains groundwater, water from the salt-dissolution zone in Permian evaporites and oil-field brines. On the plot of δ^{18}O versus Cl^- (Fig. 16.3), the isotopic signatures of plume water can be explained by cross-formational mixing of depleted water from the confined Dockum aquifer with water from Permian evaporites and thence with High Plains groundwater. Consequently, petroleum production is not implicated in regional-scale salinization of the High Plains aquifer (Mehta et al.

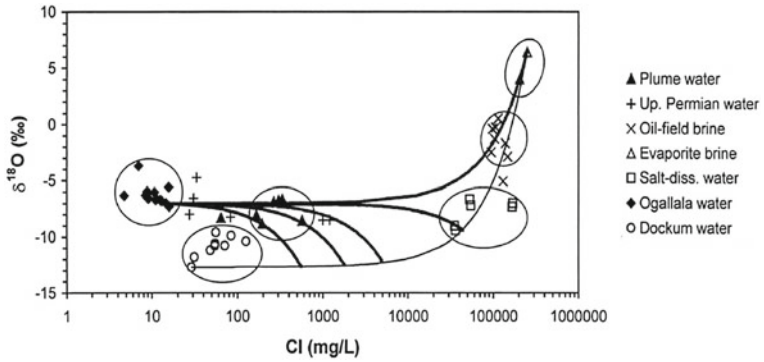

Fig. 16.3 δ^{18}O versus Cl^- relationship for end-member waters with selected mixing lines to explain the origin of salinity in the High Plains aquifer. Reprinted from *Applied Geochemistry*, Vol. 15, Mehta, S., Fryar, A. E., and Banner, J. L., Controls on the regional-scale salinization of the Ogallala aquifer, Southern High Plains, Texas, USA, pp. 849–864, Copyright 2000, with permission from Elsevier

2000a). Numerical modelling indicates that groundwater recharged during Pleistocene or earlier times flows laterally tens of km to >100 km within the Dockum and contiguous Upper Permian units. Salinization may result from relatively low rates (<1 L/day) of cross-formational discharge into the High Plains aquifer (Mehta et al. 2000b).

Western Bengal Basin

The Bengal (Ganges–Brahmaputra–Meghna) basin is the world's largest fluvio-deltaic basin. Its western margin is marked by the River Bhagirathi-Hooghly, the primary distributary of the River Ganges in India, which flows ~200 km south to the Bay of Bengal. East of the Bhagirathi-Hooghly, meandering and aggradation have created a sequence of channel sands that comprise the regional, semi-confined Sonar Bangla aquifer (Mukherjee et al. 2007a). This and other Holocene aquifers in the Bengal basin are marked by the widespread occurrence of As concentrations in groundwater >0.01 mg/L (the World Health Organization drinking-water guideline). Reductive dissolution of sedimentary Fe (oxyhydr) oxides appears to release adsorbed As to groundwater (Bhattacharya et al. 1997). Groundwater in surficial aquifers west of the Bhagirathi-Hooghly tends to have As concentrations <0.01 mg/L, even though total As in sediments does not systematically vary between areas with high and low As in groundwater (Mukherjee et al. 2018). Consequently, As mobilization from sediments into groundwater appears to depend upon local redox and groundwater flow conditions.

A plot of δ^2H versus $\delta^{18}O$ (Fig. 16.4) shows distinct differences between groundwater samples from east and west of the Bhagirathi-Hooghly in the northwest corner of the Bengal basin (Murshidabad district, West Bengal). With the exception of one sample that may have been affected by infiltration along the well casing, east-bank

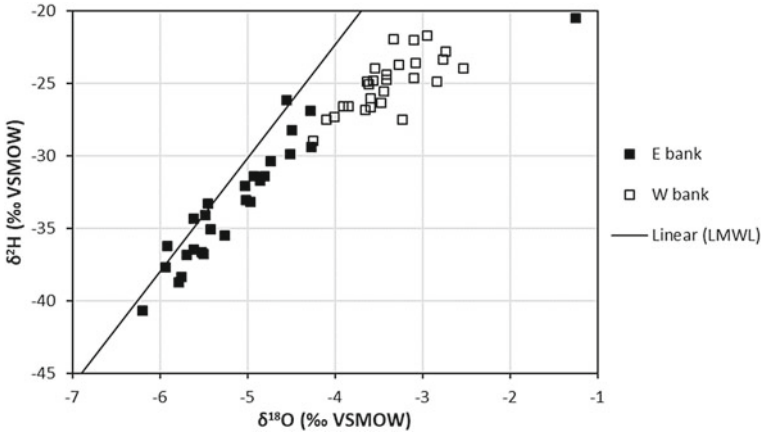

Fig. 16.4 δ^2H versus $\delta^{18}O$ relationship for east-bank (Sonar Bangla aquifer) and west-bank groundwater, Murshidabad district, West Bengal. Data from Mukherjee et al. (2007b, 2018); LMWL ($\delta^2H = 7.83\delta^{18}O + 9.01$) from Datta et al. (2011)

samples in the Sonar Bangla aquifer fell along the LMWL of Datta et al. (2011) and had lower $\delta^{18}O$ values than west-bank samples, which fell sub-parallel to the LMWL. Isotopically depleted east-bank values appear to reflect focused, minimally evaporated recharge through paleochannels that are incised through near-surface clays, whereas enriched west-bank values reflect diffuse recharge in upland areas (Mukherjee et al. 2018). Several previous studies in the area have noted a coincidence of paleochannels (as opposed to artificial ponds; Datta et al. 2011) with elevated As in underlying groundwater. We speculate that focused infiltration associated with monsoonal flooding introduces organic matter capable of mobilizing As.

Middle Atlas

Around the Middle Atlas plateau, springs in Jurassic (Liassic) dolomitic limestones and calcareous dolomites form the headwaters of Morocco's two largest rivers (the Sebou and Oum Er-Rbia). A series of SW–NE trending normal faults runs through the plateau and adjoining Saiss basin to the north. Development of preferential flowpaths and karst features is promoted by faulting and limited by the Mg content of the carbonate rocks. Recharge occurs at elevations $\gtrsim$800 m above mean sea level (amsl) and is associated primarily with cool-season (October–April) rainfall (Howell et al. 2019). Morocco is susceptible to droughts lasting years to decades, and the western Mediterranean region is projected to be a hotspot of climate change during the twenty-first century (Schilling et al. 2012). Understanding event scale to seasonal responses of springs to precipitation and air temperature is thus important for managing water supplies for municipal use, agriculture and environmental flows.

A 13-month time-series plot for Zerouka spring (Fig. 16.5) shows that hourly water temperature was nearly invariant (mean 12.54 °C, range 12.49–12.61 °C), in contrast to daily $\delta^{18}O$ fluctuations (mean −7.84‰, range −8.28 to −7.22‰). Temperature fluctuations appear to be dampened by flow circulating to depths >100 m below land

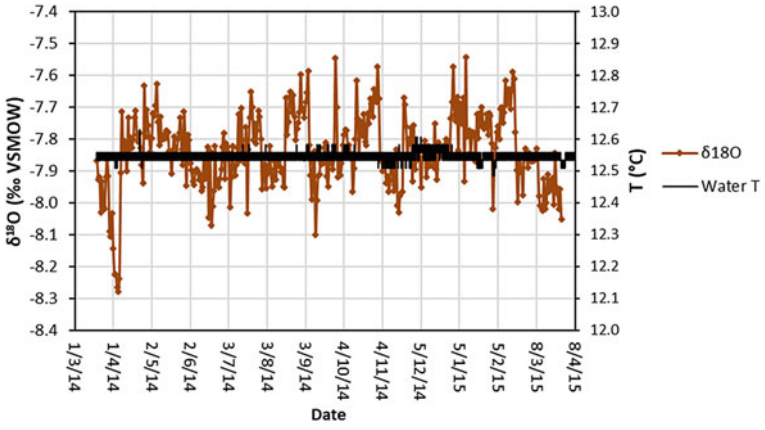

Fig. 16.5 Daily $\delta^{18}O$ and hourly water temperature for Zerouka spring, Middle Atlas plateau, March 2014–April 2015. Data from Howell et al. (2019)

surface at Zerouka (1664 m amsl). Howell et al. (2019) observed that Zerouka water samples from late winter–early spring tended to fall along the LMWL ($\delta^{18}O = 6.9\delta^{2}H + 6.9$; Benaabidate and Fryar 2010), whereas samples at other times were more scattered and sub-parallel to the LMWL. Similarly, 10-day moving averages of $\delta^{18}O$ and $\delta^{2}H$, which smoothed variability in daily signals, tracked together in March–April 2014 and February–March 2015 (Howell et al. 2019). The seasonal coincidence of smoothed $\delta^{18}O$ and $\delta^{2}H$ signals suggests that less-evaporated, focused recharge displaces more-evaporated, diffuse recharge as the aquifer refills. The insensitivity of water temperature to storm events indicates significant inertia and subsurface storage in the spring basin, perhaps because of limited karstification. Consequently, discharge may respond relatively slowly (over periods of years) to anticipated changes in recharge (Howell et al. 2019).

Houzhai Basin

The ~73.5-km^2 Houzhai basin is located on the Yunnan–Guizhou plateau near the centre of the South China karst region. The basin is marked by Neogene cockpit karst, comprised of conical hills and star-shaped valleys, developed in Triassic carbonates of the Guanling Formation. Elevation ranges from 1565 m amsl in the headwaters to 1218 m amsl at the basin outlet (Maoshuikeng spring; Zhang et al. 2017). The southern part of the basin is marked by a well-developed conduit network with multiple branches, whereas surface drainage is pronounced in the northern part of the basin, where dolomite and mudstones are more prevalent. Monsoon rains during summer cause the conduit network to fill and overflow passages to become active. As summarized by Zhang et al. (2017) and Barna (2019), numerous studies during the past three decades have investigated the hydrology and geochemistry of the Houzhai basin. However, the relative contributions of different branches of the conduit network to discharge at Maoshuikeng are still not completely understood.

A 46-h time-series plot (Fig. 16.6) shows responses of $\delta^{18}O$ and manually measured water temperature at Maoshuikeng following 60 mm of rainfall in the preceding 53 h. Sampling began 5 h after the stage peak. Temperature was marked by two distinct drops and an intervening rebound, each ~3 °C, which suggests the arrival of two successive storm pulses at the spring. In comparison, $\delta^{18}O$ data (and $\delta^{2}H$; Barna 2019) shows three drops, which may represent recharge from progressively farther up the watershed. This inference is consistent with relatively depleted values measured in the Chenqi sub-catchment near the headwaters of the Houzhai basin (Chen et al. 2018). The multiple pulses observed at Maoshuikeng could also represent fast- and slow-flow contributions from different branches of the conduit network, consistent with dye tracing (Barna 2019). The results of this study are useful for understanding the susceptibility of local water supplies to possible sources of contamination.

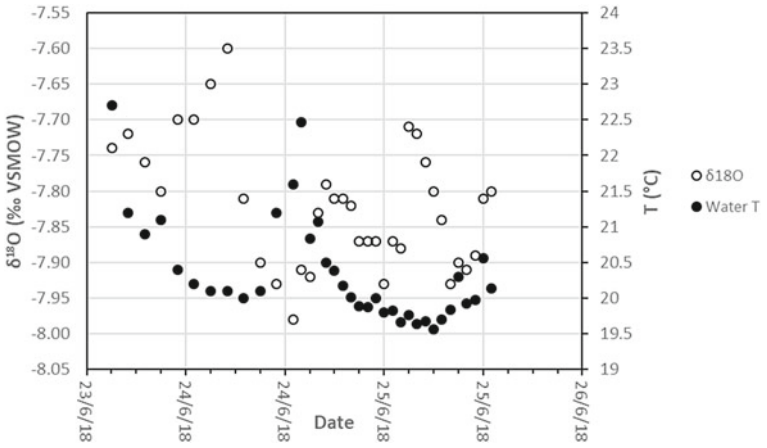

Fig. 16.6 Hourly to bihourly $\delta^{18}O$ and water temperature for Maoshuikeng spring, Houzhai Basin, 23–25 June 2018. Data from Barna (2019)

16.4 Conclusions

The case studies presented in this paper illustrate the utility of stable isotopes of water for constraining sources and timing of recharge over a range of spatial and temporal scales. In regional sedimentary aquifer systems, $\delta^{18}O$ and $\delta^{2}H$ values can indicate sources of paleorecharge and salinization (as in the High Plains aquifer) and differentiate between diffuse and focused recharge (as in the western Bengal basin). In karst terrains, where groundwater flow is relatively rapid, $\delta^{18}O$ and $\delta^{2}H$ values can indicate event scale to seasonal variability in recharge, as in the Houzhai basin and Middle Atlas plateau, respectively. In each of these cases, water isotopes complement other techniques, such as monitoring of other hydrochemical parameters (e.g. solutes and temperature), use of anthropogenic tracers and mathematical modelling of groundwater flow, in understanding the behaviour of groundwater flow systems in various settings. The development of IRIS, with its relatively low-cost, high-throughput analyses, should make the use of stable isotopes more routine in hydrologic studies.

References

Barna JM (2019) Variability in groundwater flow and chemistry in the Houzhai karst basin, Guizhou Province, China. M.S. Thesis, University of Kentucky, Lexington, Kentucky, USA. https://doi.org/10.13023/etd.2019.109

Benaabidate L, Fryar AE (2010) Controls on ground water chemistry in the central Couloir sud rifain, Morocco. Groundwater 48:306–319

Bhattacharya P, Chatterjee D, Jacks G (1997) Occurrence of arsenic-contaminated groundwater from the Bengal Delta Plain, Eastern India: options for a safe drinking water supply. Water Resour Dev 13:79–92

Chen X, Zhang Z, Soulsby C, Cheng Q, Binley A, Jiang R, Tao M (2018) Characterizing the heterogeneity of karst critical zone and its hydrological function: an integrated approach. Hydrol Process 32:2932–2946

Craig H (1961) Isotopic variations in meteoric waters. Science 133:1702–1703

Darling WG, Bath AH, Gibson JJ, Rozanski K (2005) Isotopes in water. In: Leng MJ (ed) Isotopes in palaeoenvironmental research. Springer, Dordricht, The Netherlands, pp 1–66

Datta S, Neal AW, Mohajerin TJ, Ocheltree T, Rosenheim BE, White CD, Johannesson KH (2011) Perennial ponds are not an important source of water or dissolved organic matter to groundwaters with high arsenic concentrations in West Bengal, India. Geophys Res Lett 38:L20404. https://doi.org/10.1029/2011GL049301

Hartmann A, Mudarra M, Andreo B, Marín A, Wagener T, Lange J (2014) Modeling spatiotemporal impacts of hydroclimatic extremes on groundwater recharge at a Mediterranean karst aquifer. Water Resour Res 50:6507–6521

Howell BA, Fryar AE, Benaabidate L, Bouchaou L, Farhaoui M (2019) Variable responses of karst springs to recharge in the Middle Atlas region of Morocco. Hydrogeol J 27:1693–1710

Jasechko S, Birks SJ, Gleeson T, Wada Y, Fawcett PJ, Sharp ZD, McDonnell JJ, Welker JM (2014) The pronounced seasonality of global groundwater recharge. Water Resour Res 50:8845–8867

Jasechko S, Lechler A, Pausata FSR, Fawcett PJ, Gleeson T, Cendón DI, Galewsky J, LeGrande AN, Risi C, Sharp ZD, Welker JM, Werner M, Yoshimura K (2015) Late-glacial to late-Holocene shifts in global precipitation $\delta^{18}O$. Clim Past 11:1375–1393

Kendall C, Caldwell E (1998) Fundamentals of isotope geochemistry. In: Kendall C, McDonnell JJ (eds) Isotope tracers in catchment hydrology. Elsevier, Amsterdam, pp 51–86

Mehta S, Fryar AE, Banner JL (2000a) Controls on the regional-scale salinization of the Ogallala aquifer, Southern High Plains, Texas, USA. Appl Geochem 15:849–864

Mehta S, Fryar AE, Brady RM, Morin RH (2000b) Modeling regional salinization of the Ogallala aquifer, Southern High Plains, TX, USA. J Hydrol 238:44–64

Mukherjee A, Fryar AE, Howell PD (2007) Regional hydrostratigraphy and groundwater flow modeling of the arsenic-affected western Bengal basin, West Bengal, India. Hydrogeol J 15:1397–1418

Mukherjee A, Fryar AE, Rowe HD (2007) Regional-scale stable isotopic signatures of recharge and deep groundwater in the arsenic affected areas of West Bengal, India. J Hydrol 334:151–161

Mukherjee A, Fryar AE, Eastridge EM, Nally RS, Chakraborty M, Scanlon BR (2018) Controls on high and low groundwater arsenic on the opposite banks of the lower reaches of River Ganges, Bengal basin, India. Sci Total Environ 645:1371–1387

Schilling J, Freier KP, Hertig E, Scheffran J (2012) Climate change, vulnerability and adaptation in North Africa with focus on Morocco. Agr Ecosyst Environ 156:12–26

Sturchio NC, Du X, Purtschert R, Lehmann BE, Sultan M, Patterson LJ, Lu Z-T, Müller P, Bigler T, Bailey K, O'Connor TP, Young L, Lorenzo R, Becker R, El Alfy Z, El Kaliouby B, Dawood Y, Abdallah AMA (2004) One million year old groundwater in the Sahara revealed by krypton-81 and chlorine-36. Geophys Res Lett 31:L05503. https://doi.org/10.1029/2003GL019234

Tweed S, Munksgaard N, Marc V, Rockett N, Bass A, Forsythe AJ, Bird MI, Leblanc M (2016) Continuous monitoring of stream $\delta^{18}O$ and $\delta^{2}H$ and stormflow hydrograph separation using laser spectrometry in an agricultural catchment. Hydrol Process 30:648–660

van Geldern R, Barth JAC (2012) Optimization of instrument setup and post-run corrections for oxygen and hydrogen stable isotope measurements of water by isotope ratio infrared spectroscopy (IRIS). Limnol Oceanogr Methods 10:1024–1036

Zhang Z, Chen X, Soulsby C (2017) Catchment-scale conceptual modelling of water and solute transport in the dual flow system of the karst critical zone. Hydrol Process 31:3421–3436